National Library
of Canada

Canadian Theses Division

Ottawa, Canada
K1A 0N4

Bibliothèque nationale
du Canada

Division des thèses canadiennes

51438

PERMISSION TO MICROFILM — AUTORISATION DE MICROFILMER

- Please print or type — Écrire en lettres moulées ou dactylographier

Full Name of Author — Nom complet de l'auteur

Donald William Blackadar

Date of Birth — Date de naissance

13/09/52

Country of Birth — Lieu de naissance

Canada

Permanent Address — Résidence fixe

139 Berkshire Place N.W. Calgary T3k 1Z7

Title of Thesis — Titre de la thèse

The Aristifats Diatreme; A Proterozoic Copper-Lead-Cobalt-Nickel-Silver Deposit Northwest Territories

University — Université

Alberta, Edmonton

Degree for which thesis was presented — Grade pour lequel cette thèse fut présentée

Master of Science (Geology)

Year this degree conferred — Année d'obtention de ce grade

1981

Name of Supervisor — Nom du directeur de thèse

Dr. R. D. Morton

Permission is hereby granted to the NATIONAL LIBRARY OF CANADA to microfilm this thesis and to lend or sell copies of the film.

The author reserves other publication rights, and neither the thesis nor extensive extracts from it may be printed or otherwise reproduced without the author's written permission.

L'autorisation est, par la présente, accordée à la BIBLIOTHÈQUE NATIONALE DU CANADA de microfilmer cette thèse et de prêter ou de vendre des exemplaires du film.

L'auteur se réserve les autres droits de publication; ni la thèse ni de longs extraits de celle-ci ne doivent être imprimés ou autrement reproduits sans l'autorisation écrite de l'auteur.

Date

April 6, 1981

Signature

DWBlackadar

NL-91 (4/77)

National Library of Canada
Collections Development Branch

Canadian Theses on
Microfiche Service

Bibliothèque nationale du Canada
Direction du développement des collections

Service des thèses canadiennes
sur microfiche

NOTICE

The quality of this microfiche is heavily dependent upon the quality of the original thesis submitted for microfilming. Every effort has been made to ensure the highest quality of reproduction possible.

If pages are missing, contact the university which granted the degree.

Some pages may have indistinct print especially if the original pages were typed with a poor typewriter ribbon or if the university sent us a poor photocopy.

Previously copyrighted materials (journal articles, published tests, etc.) are not filmed.

Reproduction in full or in part of this film is governed by the Canadian Copyright Act, R.S.C. 1970, c. C-30. Please read the authorization forms which accompany this thesis.

THIS DISSERTATION
HAS BEEN MICROFILMED
EXACTLY AS RECEIVED

AVIS

La qualité de cette microfiche dépend grandement de la qualité de la thèse soumise au microfilmage. Nous avons tout fait pour assurer une qualité supérieure de reproduction.

S'il manque des pages, veuillez communiquer avec l'université qui a conféré le grade.

La qualité d'impression de certaines pages peut laisser à désirer, surtout si les pages originales ont été dactylographiées à l'aide d'un ruban usé ou si l'université nous a fait parvenir une photocopie de mauvaise qualité.

Les documents qui font déjà l'objet d'un droit d'auteur (articles de revue, examens publiés, etc.) ne sont pas microfilmés.

La reproduction, même partielle, de ce microfilm est soumise à la Loi canadienne sur le droit d'auteur, SRC 1970, c. C-30. Veuillez prendre connaissance des formules d'autorisation qui accompagnent cette thèse.

LA THÈSE A ÉTÉ
MICROFILMÉE TELLE QUE
NOUS L'AVONS REÇUE

Ottawa, Canada
K1A 0N4

NL-339 (Rev. 8/80)

THE UNIVERSITY OF ALBERTA

THE ARISTIFATS DIATREME; A PROTEROZOIC COPPER-LEAD-COBALT-NICKEL-SILVER DEPOSIT, NORTHWEST TERRITORIES

BY

©
DONALD WILLIAM BLACKADAR

A THESIS

SUBMITTED TO THE FACULTY OF GRADUATE STUDIES AND RESEARCH
IN PARTIAL FULFILMENT OF THE REQUIREMENTS FOR THE DEGREE
OF MASTER OF SCIENCE

DEPARTMENT GEOLOGY

EDMONTON, ALBERTA
Spring, 1981

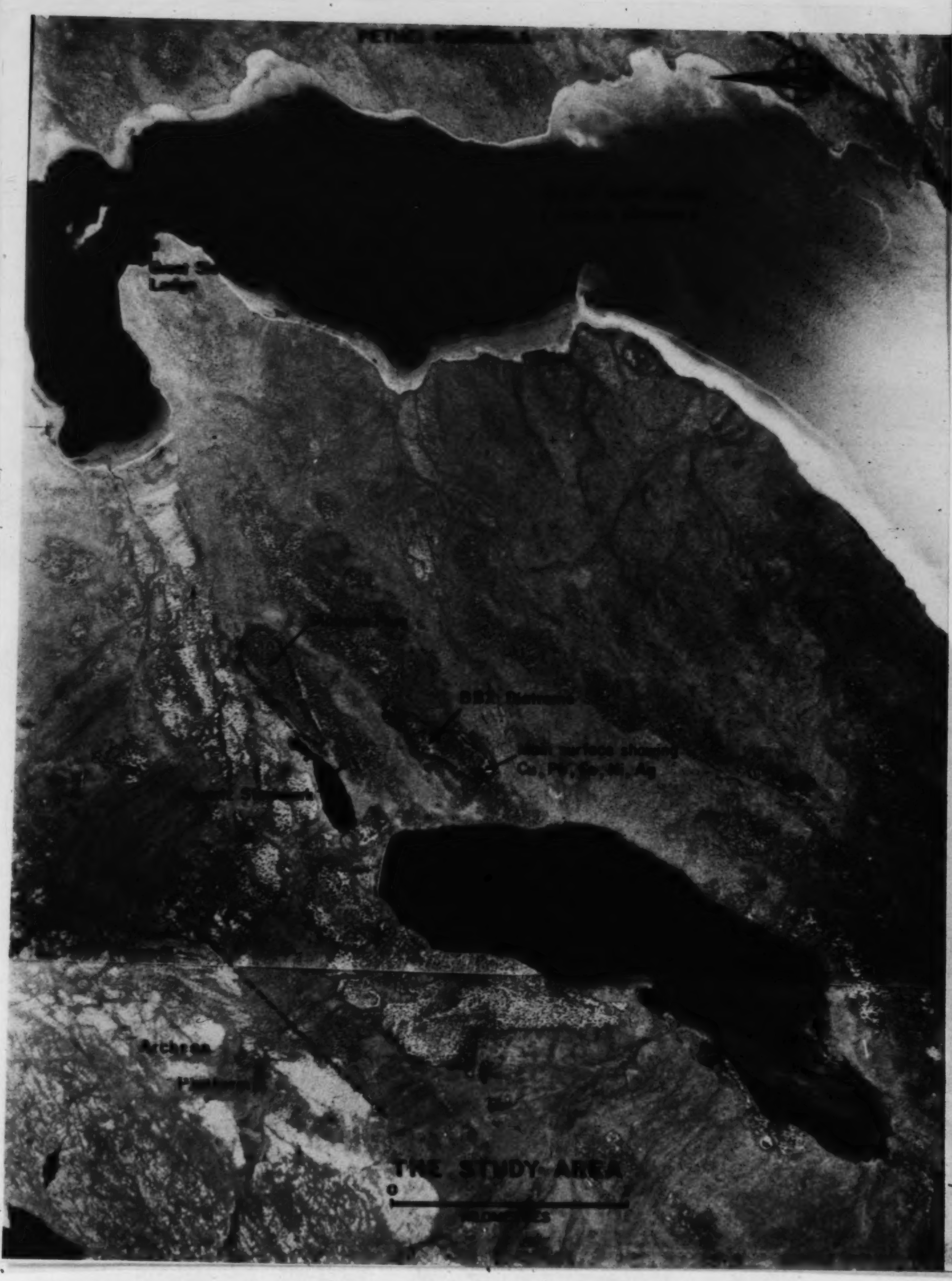

THE STUDY AREA

PETHEI PENINSULA
Lodge
BB2 Diamond
Main surface showing
Cu, Pb, Zn, Ni, Ag
Archean
0

m

THE UNIVERSITY OF ALBERTA

RELEASE FORM

NAME OF AUTHOR DONALD WILLIAM BLACKADAR

TITLE OF THESIS THE ARISTIFATS DIATREME; A PROTEROZOIC COPPER-LEAD-COBALT-NICKEL-SILVER DEPOSIT NORTHWEST TERRITORIES

DEGREE FOR WHICH THESIS WAS PRESENTED MASTER OF SCIENCE

YEAR THIS DEGREE WAS GRANTED 1981

Permission is hereby granted to THE UNIVERSITY OF ALBERTA LIBRARY to reproduce single copies of this thesis and to lend or sell such copies for private, scholarly or scientific research purposes only.

The author reserves other publication rights, and neither the thesis nor extensive extracts from it may be printed or otherwise reproduced without the author's written permission.

(Signed) D.W. Blackadar

PERMANENT ADDRESS:

139 Berkshire Place N.W.
Calgary, Alberta

DATED December 10 1980

THE UNIVERSITY OF ALBERTA

FACULTY OF GRADUATE STUDIES AND RESEARCH

The undersigned certify that they have read, and recommend to the Faculty of Graduate Studies and Research, for acceptance, a thesis entitled The Aristifats Diatreme: A Proterozoic Copper-Lead-Cobalt-Nickel-Silver Deposit, Northwest Territories submitted by Donald William Blackadar in partial fulfilment of the requirements for the degree of Master of Science

Supervisor

Bruce Nesbitt

R.E. Folinsbee

G.L. Cumming

External Examiner

Date: December 10, 1980

Abstract

The Aristifats diatreme is one of seven Seton age volcanic centres occurring in a linear belt between Taltheilei Narrows and Utsingi Point in the East Arm of Great Slave Lake, N.W.T. These diatremes cut Aphebian platform sediments and volcanics of the Great Slave Supergroup, and are controlled by a major basement fault trending 18° (az). The emplacement of the Aristifats diatreme into the Proterozoic succession was controlled by one of a set of shear fractures related to compressional folding in the East Arm orogen.

The vent agglomerate consists predominantly of mafic volcanic (basalt) fragments, with lesser, though locally significant, concentrations of sedimentary, diabasic and granitic rock. The volcanic fragments exhibit a variety of textures from highly vesicular-and pumiceous-lava to dark viscous lava. Much of the basalt is thought to represent accidental material from a pre-existing volcanic pile cut by the diatreme. Juvenile volcanic material appears to comprise a relatively small proportion of the total, possibly less than 25 percent. The volcanics have undergone incipient low grade regional metamorphism (prehnite-pumpellyite facies). Propyllitic, potassium and carbonate alterations are common. Silicification, hematitization and chloritization are less prominent.

The origin of the diatreme appears to have involved at least two pulses of volcanic activity. The final phase, which was explosive and possibly phreatomagmatic, was followed by collapse and subsidence within the vent. It can be inferred on the basis of sedimentary rock fragments in the diatreme, that it intruded as high as the basal part of the Pethei group. Model lead dating of galena from mineralized zones indicates an age of 1870 ± 15 m.y. for the diatreme. It is therefore associated with the middle Aphebian phase of intrusive/magmatic activity in the East Arm.

The diatreme hosts a complex mineral assemblage which has been related to four separate phases of mineralizing activity.

Phase I, which comprises primarily Fe-Co-Ni sulfides and sulfarsenides with minor U, Pb, Cu and Ag, is attributed principally to hydrothermal leaching of the mafic parent magma of the diatreme. U and Pb may have been introduced by gaseous transfer from the mantle.

Phase II is a sulfide phase consisting predominantly of chalcopyrite and galena with minor Cu-Ag sulfides. These minerals occur in zones which have undergone strong potassium alteration, and represent the only economically significant phase of mineralization.

Phase III comprises barite, specularite and possibly minor chalcopyrite.

Phase IV is represented by quartz-carbonate veins, and contains only minor quantities of chalcopyrite. Structural evidence suggests that these veins were deposited relatively near the surface.

Oxygen isotope, fluid inclusion and lead isotope studies suggest that phases III and IV and possibly phase II were deposited by connate brines. The metal content of these brines was derived from argillaceous sediments within the basin.

A model is proposed whereby late magmatic activity and tectonism propogated hydrothermal (connate) fluids from deep basinal areas into relatively porous and permeable host rocks such as the diatreme. The minerals were precipitated within the diatreme by chemical exhange between the fluid and the wall rock. The change from reducing (sulfide) fluids to those with high oxidation potential (specularite-barite) may have been related to tectonic unloading and mixing of the fluid with oxygenated surface waters. This change in chemistry may have been accompanied by a decrease in temperature as the system neared the surface. Corrected fluid inclusion temperatures for phase IV quartz veins range from 150°C to 179°C.

A second and tentative date of 1110 ± 20 m.y. has been established through model lead dating of galena from mineralized zones. This approximates the age of a series of major diabase sills in the East Arm, and it is suggested that this major magmatic event may have provided the heat necessary to drive the hydrothermal system responsible for at least part of the mineralization present in the diatreme.

Acknowledgements

I would like to acknowledge with thanks the continuous support and guidance of my supervisor, Dr. R. D. Morton.

This study would not have been possible without the permission of Norcen Energy Resources Limited of Calgary, Alberta, owners of the Aristifats property. I wish to acknowledge their kind support in expediting my field work and in drafting all figures and maps in this thesis. In particular, I would like to thank Mr. Don Sawyer, Manager-Minerals Department, for his co-operation and assistance.

I wish to thank the Department of Indian Affairs and Northern Development in Yellowknife, N.W.T. for their generous support in expediting my field work.

This thesis has benefited greatly from the contributions and helpful suggestions of several faculty and staff members at the University of Alberta. I would like to gratefully acknowledge Dr. H. A. K. Charlesworth for his assistance with structural geology, and Drs. K. Muehlenbachs and K. Hattori for their assistance in carrying out the oxygen isotope work. Thanks are also extended to Mr. S. Launspach who was of considerable assistance in carrying out microprobe studies of the metalliferous mineral assemblage. I am grateful to Dr. G. L. Cumming and Mr. D. Krstic of the department of Physics for their valuable assistance in carrying out the lead isotope work.

I wish to thank Mrs. Loretta Tetzlaff for her patience (and endurance) in typing the manuscript.

Finally, I would like to extend a special thanks to my wife Janet, for her patience, support and assistance during the preparation of this thesis.

TABLE OF CONTENTS

Page

Section I Background 1

Chapter 1. Introduction 2

- I. Scope of Study 3
- II. Location and Access 5
- III. Ownership 5
- IV. Exploration History 9
- V. Grades of Mineralization 12
- VI. Basis of Study 17

Chapter 2. Regional Geology and Tectonic Framework 18

- 1. Regional Geological Setting 19
  - A. Phanerozoic Rocks 19
  - B. Archean Basement Rocks 19
    - 1. The Slave Province 19
    - 2. The Churchill Province 21
  - C. Early Proterozoic Supracrustal Rocks 22
    - 1. The Coronation Geosyncline 22
      - (i) The Bear Province 25
      - (ii) The Great Slave and Goulburn Basins 26
- II. Geology of Great Slave Basin 27
  - A. General Remarks 27
  - B. Origin of Great Slave Basin 30
    - 1. The Aulacogen Model 30
    - 2. Permobile Tectonics 31
  - C. Geological History of Great Slave Basin 32
    - 1. Stratigraphy and Depositional History 32
    - 2. Structural Evolution 37
    - 3. Igneous Activity and Geochronology 39
- III. Local Geology: Hearne Channel and The Seton Volcanic Centres 42

Page

Section II Geology of the Study Area 45

Preface 46

Chapter 3. Geology Exclusive of the Diatreme 51

- I. The Sediments 52
- II. The Diabase 57
  - A. General 57
  - B. Form 57
  - C. Petrography 58
    - 1. Mineralogy 58
    - 2. Color Index 66
    - 3. Zonation 66
    - 4. Contact Phenomena 68
    - 5. Alteration 70
      - (i) Late Magmatic and Deuteric Alteration 70
      - (ii) Hydrothermal Alteration 70
    - 6. Late Veining 74
  - D. Affinity 74

Chapter 4. Petrography of The Diatreme 75

- I. Form 77
- II. General Description 78
  - A. Breccia Fragments 78
  - B. Matrix 80
- III. Petrography of Volcanic Fragments 86
  - A. Mineralogy 87
  - B. Types of Volcanic Fragments 88
    - 1. Light-colored Lava 89
    - 2. Pumiceous Lava 93
    - 3. Black Lava 96
  - C. Metamorphic Grade 100
- IV. Alteration of the Diatreme 101
  - A. General Remarks 101
  - B. Methodology 102

Page

1. Staining Techniques 102

(i) for Potassium 102
(ii) for Carbonate 105

2. X-ray Diffractometer Studies 105

C. Discussion of Alteration Assemblages 107

1. Deuteric Alteration 107

(i) Propyllitization 107

2. Hydrothermal Alteration 108

(i) Potassium Alteration 108
(ii) Carbonatization 111
(iii) Silicification 115

3. Other Alteration Types 116

(i) Hematitization 116
(ii) Chloritization 117

V. Affinity of the Diatreme 118

Chapter 5. Structural Geology 121

I. Purpose and Scope of Study 122
II. Results of Study 125

A. Bedding and Major Folds 125
B. Joints 128
C. Veins 130
D. Minor Folds 133
E. Shearing 137

III. Discussion of Results 137
IV. Structural Control of Igneous and Hydrothermal Activity 145

A. The Diatreme 145
B. The Diabase Plug 146
C. Quartz-Carbonate Veins and Stockworks 147

V. Chronology 150
VI. Conclusions 153

Page

Chapter 6. Nature and Origin of the Diatreme 155

I. General Remarks 156
II. Nature of the Diatreme 157

A. The Role of Fluidization 157

1. Volcanic Bed Forms 159
2. Matrix - Supported Lapilli 163
3. Tuffisite Apophyses 164
4. Thermal Metamorphism of Country Rocks 164
5. Attitude of Peripheral Sediments 165

B. The Role of Groundwater 166

1. Base Surge Deposits(?) 168
2. Accretionary Lapilli(?) 170
3. Structures Indicative of An Explosive Eruption 172

C. The Significance of Textural Varieties of Lava 176

1. Black Lava 176
2. Pumiceous Lava 177
3. Light-colored Lava 179

D. Venting of the Diatreme and Level of Intrusion 180
E. Relationship Between the Diatreme and the Diabase 184
F. Orientation of the Diatreme 185

III. Origin of the Diatreme 187
IV. Conclusions 193

Section III Geochemistry 194

Preface 195

Chapter 7. Fluid Inclusion Study 196

I. General Remarks 197
II. Instrumentation 198
III. Selection of Samples and Sample Descriptions 198
IV. Problems and Sources of Error 200
V. Fluid Inclusion Petrography 203

Page

VI. Low Temperature Studies 207

- A. Introduction 207
- B. Behavior Upon Freezing 212
- C. Statistical Treatment of Data 214
- D. Discussion of Results 217
  - 1. Determination of Salinity 217
  - 2. Clathrate Chemistry 220
  - 3. Geobarometry 229

VII. High Temperature Studies 233

- A. Introduction 233
- B. Statistical Treatment of Data 233
- C. Pressure Correction and Temperature of Formation 234

VIII. Implications 238

Chapter 8 Oxygen Isotope Study 242

- I. Introduction 243
- II. Theoretical Background 243
- III. Methodology 244
- IV. Discussion 245
- V. Conclusions 248
- Closing Remarks to Section III 250

Section IV Economic Geology 255

Preface 256

Chapter 9. Lead Isotope Study 262

- I. General Remarks 263
- II. Methodology 263
- III. Discussion of Results 265
- IV. Implications 269
  - A. The Seton Volcanics and Mineralization 269
  - B. Late Hydrothermal Activity 270
  - C. Zonation 271

Page

Chapter 10. The Mineralization 273

I. General Remarks 274
II. Mineralogy and Paragenesis 274

A. Phase I Ag, Co-Ni Mineralization 278

1. Introduction 278
2. Mineralogy 278
3. Mode of Occurrence of Mineralization 283
4. Paragenesis 290
5. Economic Significance 292

B. Phase II Cu-Pb Sulfides 293

1. Introduction 293
2. Mineralogy and Paragenesis 294
3. Controls of Mineralization 298
4. Economic Significance 301

C. Phase III Barite-Specularite 301

1. Introduction 301
2. Mineralogy and Paragenesis 302
3. Economic Significance 306

D. Phase IV Carbonate-Quartz 306

III. Remobilization of Hydrothermal Mineralization 307
IV. Changes in the Zone of Oxidation 308
V. Geochemical Inferences 313
VI. Zonation 315
VII. Origin of Mineralization 316

A. Mineralization Related to Emplacement of the Diatreme 316
B. Mineralization Related to Connate Brines 319

1. Source of Mineralization 319
2. Movement of Mineralizing Fluids 322

VIII. Deposition of Mineralization 326

A. Introduction 326
B. Theoretical Background 328
C. Occurrence and Affinity of Mineralization 331
D. Discussion 333

IX. Implications 336

Page

Section V. Closing Remarks 338

Chapter 11. Summary and Conclusions 339

I. Summary 340
II. Implications 343

A. Geotectonics 343
B. The Mineralizing Events 346
C. Economic Considerations 348

III. Suggestions for Further Work 353

* * *

References Cited 355

Appendix 1. Summary of Mining Exploration on the BBX Property 364

Appendix 2. Density Calculation for Mineralizing Fluid Based on Fluid Inclusion Data 370

LIST OF TABLES

Table Page

1. Compilation of "Epigene" Elements in Samples From the Main Surface Showing 13
2. Grades of Mineralization from the Main Surface Showing, BBX Diatreme 15
3. Average Copper Values of Mineralized Intervals from Diamond Drill Hole 76-1 16
4. Stratigraphic Column, East Arm of Great Slave Lake 33
5. Relationship Between Sedimentation and Structural Evolution, Great Slave Basin 35
6. Major Intrusive Events and Geochronology, Great Slave Basin 40
7. Platform Sediments of the Great Slave Supergroup 44
8. Summary of Structural Trends from Stereograms 140
9. Fluid Inclusion Data 201
10. Statistical Treatment of Freezing Temperature Data 215
11. Statistical Treatment of Homogenization Temperature Data 235
12. Oxygen Isotope Data For Quartz 246
13. a. Abundance of Lithium and Potassium in Natural Waters 252
    b. Abundance of Lithium and Potassium in Common Sediments and Sedimentary Rock Types 252
14. Major Element Chemistry of Selected Samples from Mineralized Zones in the BBX Diatreme 258
15. Accessory Element Chemistry of Selected Samples from Mineralized Zones in the BBX Diatreme 259
16. Pertinent Information on Chemically Analyzed Samples from Mineralized Zones 260

Table | Page

17. Major Element Chemistry of Relatively Unaltered Basaltic Rocks 261

18. Lead Isotope Data, BBX Deposit 264

19. Epigene Minerals Identified in the BBX Diatreme 275

20. Paragenetic Sequence of Mineralization in the BBX Diatreme 279

LIST OF FIGURES

Figure		Page
1.	Aristifats Property, Northwest Territories Location and Access	6
2.	Aristifats Property, Northwest Territories Local Access	7
3.	Aristifats Property, Northwest Territories Claim Distribution	8
4.	Tectonic Map of Northwestern Part of Canadian Shield, and Structural Cross Section of type Area of Coronation Geosyncline Near North End of Bear Province	20
5.	Aphebian Tectonic Elements of the Coronation Geosyncline	24
6.	Geologic and Tectonic Maps of East Arm of Great Slave Lake	28
7.	Stratigraphic Cross-Section of the Northwest Margin of Great Slave Basin Between Taltheilei Narrows and Hornby Channel	34
8.	Aristifats Property and Adjacent Areas, Northwest Territories, Airphoto Lineaments	123
9.	Aristifats Property, Northwest Territories Airphoto Lineaments	124
10.	Stereogram Showing Bedding	127
11.	Stereogram Showing All Joints	129
12.	Stereogram Showing Joints in Sediments	131
13.	Stereogram Showing Joints in Diatreme	132
14.	Stereogram Showing All Veins	134
15.	Stereogram Showing Veins in Sediments, except those in Bedding Joints	135
16.	Stereogram Showing Orientation of Minor Fold Axes	136
17.	Stereogram Showing Trend and Plunge of Slickensides	138

Figure Page

18. a. Structural Features Related to Compressional Folding Along 50° (Az) 142
    b. Structural Features Related to Minor Fold System along 16° (Az) 142

19. Histogram of Freezing Temperature VS % Frequency for Quartz 216

20. Phase Diagram for the System H_2O-CO_2 225

21. Methane Hydrate Decomposition Conditions for Various Sodium Chloride Brine Concentrations 227

22. Histogram of Homogenization Temperature VS % Frequency for Quartz 236

23. Plot of $^{207}Pb/^{204}Pb$ VS $^{206}Pb/^{204}Pb$ for the BBX Deposit, All data 266

24. Plot of $^{207}Pb/^{204}Pb$ VS $^{206}Pb/^{204}Pb$ for the BBX Deposit, Expanded Scale 267

MAPS (in Pocket)

Map

1. BBX Property and Adjacent Areas, N.W.T.: Geological Compilation

2. BBX Claims, N.W.T.: Geology and Structure

3. BBX Claims, N.W.T.: Diamond Drill Holes and Geology in Vicinity of Diatreme

LIST OF PLATES

Plate	Description	Page
1.	View of the JDA group looking to the NE.	10
2.	View of Hearne Channel from the BBX diatreme.	48
3.	View of the BBX group from Aristifats Lake.	48
4.	Typical glauconitic sandstone of the Akaitcho Formation (transmitted light).	53
5.	The olivine diabase (transmitted light, crossed polars).	60
6.	The olivine diabase (plane polarized transmitted light).	60
7.	Titaniferous magnetite with reticulate texture (transmitted light).	62
8.	Autobrecciated diabase (transmitted light).	62
9.	Propylitically altered diatreme breccia.	79
10.	Diatreme breccia with basalt fragments and olivine xenocrysts in a matrix of comminuted rock debris (transmitted light).	83
11.	Diatreme breccia with basalt fragments, feldspar xenocrysts and sulfides in a partially chloritized rock flour matrix (transmitted light).	83
12.	Carbonatized rock flour in the breccia matrix (transmitted light).	85
13.	Diatreme breccia with basalt fragments and olivine xenocrysts in a matrix of comminuted rock debris (transmitted light).	85
14.	"Light-colored lava" (transmitted light).	91
15.	Pumiceous lava (transmitted light).	91
16.	Highly vesicular pumiceous lava (transmitted light).	95
17.	Vesicular glassy lava and sideromelane (transmitted light).	95

Plate	Description	Page
18.	"Black lava" enclosing a feldspar xenocryst (transmitted light).	98
19.	"Black lava" enclosing a fragment of glauconitic sandstone (transmitted light).	98
20.	Potassium alteration of agglomerate showing potassic veinlets (transmitted light).	104
21.	Potassium alteration of the agglomerate showing altered feldspar xenocrysts and plagioclase microlites (transmitted light).	104
22.	Carbonatization of olivine. Alteration to talc and magnesite (transmitted light).	113
23.	Trench 2, showing horizontal "bed forms".	160
24.	Trench 1, showing base surge bed forms(?).	169
25.	Trench 2, showing shattercone structure(?) (diagonal view).	174
26.	Trench 2, showing shattercone structure(?) (view along axis).	174
27.	A typical three phase fluid inclusion from quartz (transmitted light).	205
28.	A typical three phase fluid inclusion from quartz (transmitted light).	205
29.	Pyrrhotite-pentlandite exsolution intergrowth (reflected light).	282
30.	Siegenite being replaced by chalcopyrite (reflected light).	282
31.	Layered intergrowth of chalcopyrite, glaucodot and galena (reflected light).	285
32.	Fine grained intergrowth of glaucodot and rutile (reflected light).	285
33.	Emulsion texture with gersdorffite in chalcopyrite (reflected light).	288

Plate	Description	Page
34.	Emulsion texture with gersdorffite in chalcopyrite (reflected light).	288
35.	Crystal skeletons of gersdorffite in galena (reflected light).	289
36.	Acanthite-jalpaite intergrowth (reflected light).	297
37.	Digenite replacing pyrrhotite (reflected light).	297
38.	Pyrite being replaced by galena. Anglesite veinlets (reflected light).	300
39.	Replacement of glass shards by galena (reflected light).	300
40.	Barite-specularite vein (transmitted light).	305
41.	Barite-chalcopyrite-specularite intergrowth (reflected light).	305
42.	Alteration of chalcopyrite to limonite (reflected light).	312

SECTION I

BACKGROUND

CHAPTER 1

INTRODUCTION

I. Scope of Study

The Aristifats deposit is a mineralized volcanic diatreme cutting Aphebian sediments and volcanics of the Great Slave Supergroup. The diatreme hosts significant concentrations of copper, with lesser lead and barium, and minor cobalt, nickel and silver. This mineralization occurs intermittently in the diatreme and is variable in grade. Deposition from hydrothermal fluids has been brought about by chemical exchange with the wall rock, and is primarily controlled by gross textural features related to the formation of the diatreme itself. These features are randomly distributed, and the locations of potential zones of interest cannot be readily predicted. These factors have made exploration difficult, and consequently the deposit remains an economically unproven but intriguing prospect.

The purpose of this study is to document the geology of the Aristifats deposit, through structural and geological mapping, and studies of petrography, mineralogy and chemistry. Based on these investigations, the nature, origin and affinity of both the diatreme and the associated mineralization, and the relationship of these features to the geologic and tectonic history of the East Arm Synclinorium will be discussed.

It is beyond the scope of this study to discuss certain aspects of geology which are of particular interest to the explorationist. Consequently, no attempt has been made to correlate or extrapolate drill hole data, to speculate on the configuration of the diatreme at depth, or to establish potential drill hole locations. Nevertheless, the study has three principal applications with respect to exploration and evaluation of the deposit.

(1) It defines the economic mineralogy and alteration assemblages.

(2) It defines a paragenetic sequence and establishes the relative economic importance of mineralizing events.

(3) It defines the factors controlling the distribution of mineralized zones in the diatreme.

As will become evident in the following chapters, the geology of the Aristifats deposit is complex. While this study has resolved many of the major questions, the interpretation of others must remain to some extent ambiguous.

II. Location and Access

The Aristifats deposit is located near Taltheilei Narrows, immediately north of the East Arm of Great Slave Lake, approximately one hundred air miles east of Yellowknife, N.W.T. The deposit lies in N.T.S. 75-L-12 at 62°35' north latitude and 111°33' west longitude (Figure 1).

The study area, which comprises the mineralized diatreme and adjacent environs is shown in figure 2. Access to the property is by float or ski-equipped aircraft to Aristifats Lake. In addition, a large airstrip operated by Great Slave Lodge lies approximately two thirds of a mile north of the diatreme (Figure 2).

III. Ownership

The Aristifats deposit is currently held as a mineral prospect by Norcen Energy Resources Limited of Calgary, Alberta. The company holds two principal blocks of claims in the area; the BBX Group, and the JDA Group (Figure 3).

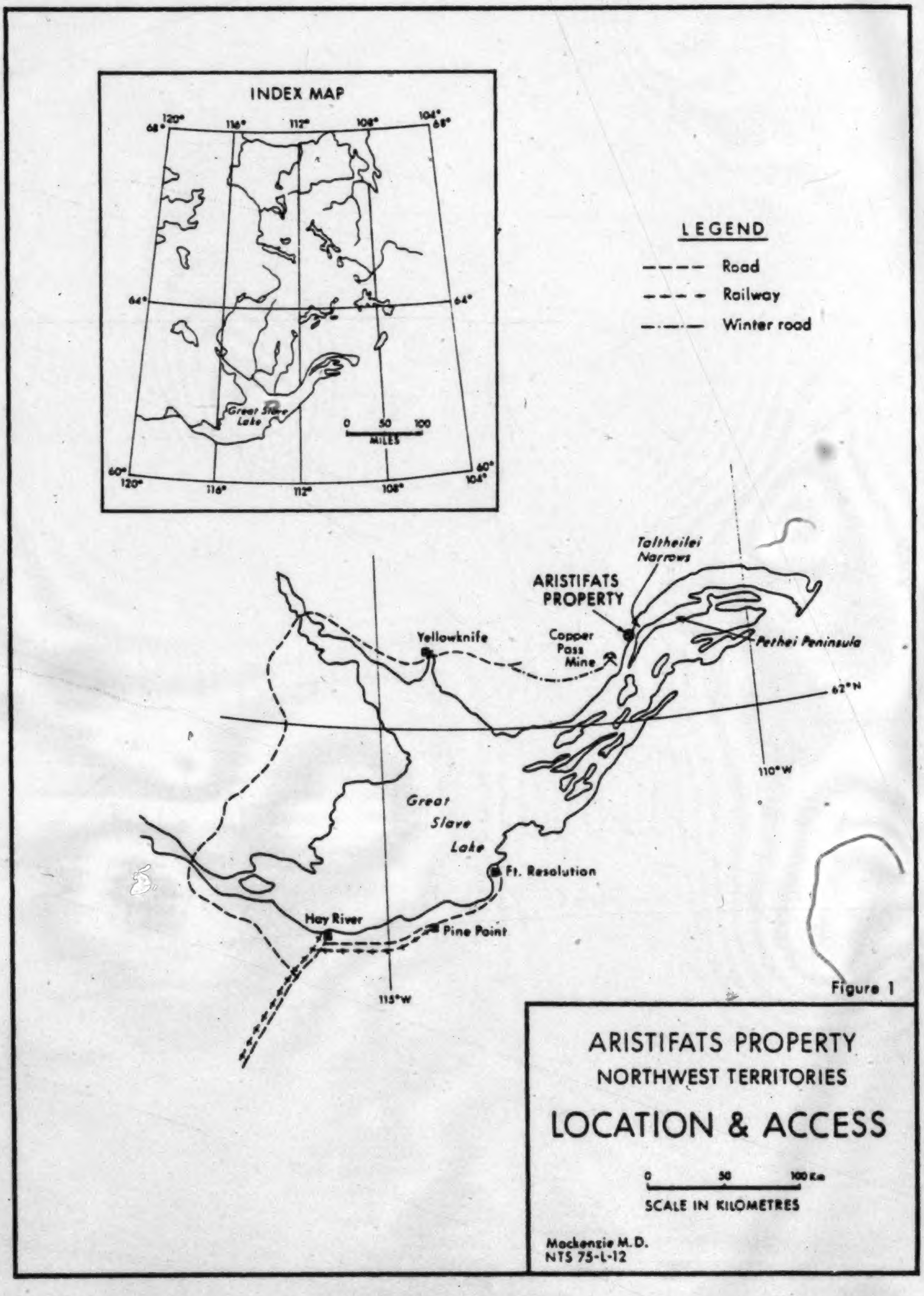
INDEX MAP
120°
116°
112°
108°
104°
68°
64°
60°
Great Slave Lake
0 50 100
MILES
LEGEND
Road
Railway
Winter road
Taltheilei Narrows
ARISTIFATS PROPERTY
Copper Pass Mine
Pethei Peninsula
Yellowknife
62°N
110°W
Great Slave Lake
Ft. Resolution
Hay River
Pine Point
115°W
0 50 100 Km
SCALE IN KILOMETRES

Figure 1

ARISTIFATS PROPERTY
NORTHWEST TERRITORIES

LOCATION & ACCESS

Mackenzie M.D.
NTS 75-L-12

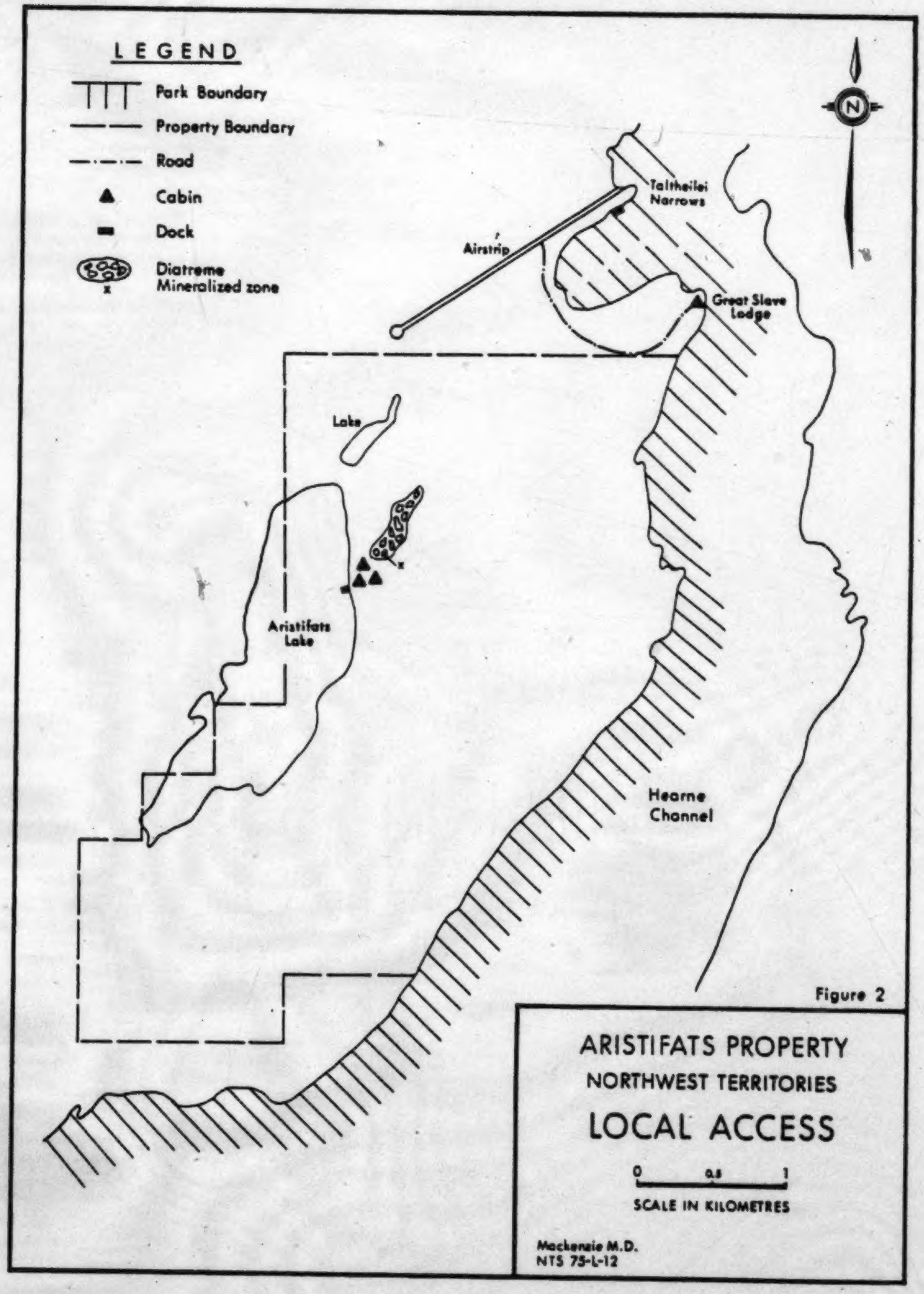
LEGEND
Park Boundary
Property Boundary
Road
Cabin
Dock
Diatreme
Mineralized zone
Taltheilei Narrows
Airstrip
Great Slave Lodge
Lake
Aristifats Lake
Hearne Channel
N
0
0.5
1
SCALE IN KILOMETRES

Figure 2

ARISTIFATS PROPERTY
NORTHWEST TERRITORIES
LOCAL ACCESS

Mackenzie M.D.
NTS 75-L-12

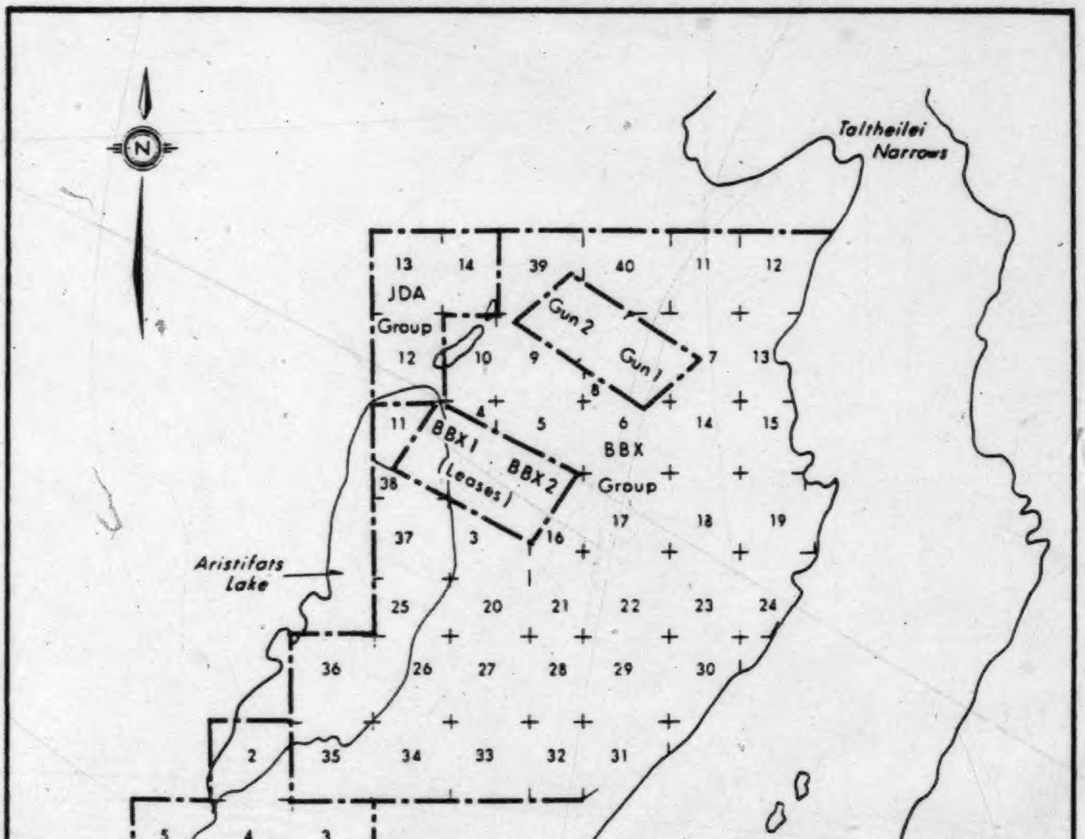
N
Taltheilei Narrows
13
14
39
40
11
12
JDA Group
12
10
9
Gun 2
Gun 1
7
13
8
11
4
5
6
14
15
BBX 1
BBX 2
(Leases)
BBX Group
38
37
3
16
17
18
19
Aristifats Lake
25
20
21
22
23
24
36
26
27
28
29
30
2
35
34
33
32
31
5
4
3
JDA Group
6
7
8
10
9
1
Hearne Channel
0
0.5
1
KILOMETRES
Mackenzie M.D.
NTS 75-L-12

Figure 3

ARISTIFATS PROPERTY
NORTHWEST TERRITORIES

CLAIM DISTRIBUTION

The BBX claims cover the mineralized diatreme which is the principal subject of this study. The name "Aristifats prospect" is used interchangeably with "BBX deposit" in this thesis.

The JDA group which was staked somewhat later than the BBX group, covers a minor copper showing associated with a diatreme southwest of Aristifats Lake (Plate 1).

IV. Exploration History

Copper and cobalt mineralization was noted in the vicinity of Taltheilei Narrows as early as 1899 (Bell, Robert, 1900, P. 108A), but the actual date of discovery of what is now the BBX deposit is unknown.

The main surface showing, located at the southwest end of the diatreme, was staked initally in 1948 by private interests. Since that time, exploration on the property has been carried out by several organizations, including the BBX Syndicate, Preston East Dome Mines Limited, Colby Mines, and Great Plains Development Company of Canada Ltd. (now Norcen Energy Resources Limited). Work carried out on the property to date includes geological mapping,

Plate 1 View of the JDA group looking to the N.E. Mafic Volcanic pile bordered on the west by a scarp approximately 20 metres high.

trenching, diamond drilling, and IP, magnetometer and soil geochemistry surveys. The salient aspects of this work, which is chronicled in Appendix 1 of this thesis, are discussed below.

Although records of some of the earlier work are limited, data are available for 36 diamond drill holes comprising a total drilled depth of approximately 7760 feet. These holes which range in depth from 53 feet to 800 feet, are shown on map 3 (in pocket).

Prior to the involvement of Colby Mines in 1972, the majority of drill holes were collared in the vicinity of the main surface showing, and in some cases intersected significant amounts of chalcopyrite and galena. Unfortunately, drill core from these programs has been lost, and core descriptions, which are not geologically oriented, are useful only as a general indication of the presence or absence of mineralization.

Diamond drilling undertaken by Colby Mines in 1972 was based on the assumption that the deposit was stratabound and dipping in a southerly direction (Nickerson, 1970, p. 4). This drilling program intersected relatively unmineralized volcanics and sediments, and was unsuccessful except as a general guide in delineating the boundaries of the diatreme.

Diamond drilling by Great Plains Development in 1975 and 1976 was based on the premise that the mineralization was hosted in a diatremic breccia pipe (Nutter and Sawyer, 1975, pp. 66 & 77). These programs were successful in that they further delineated the boundaries of the diatreme, and intersected vent agglomerate to depths of as much as 450 feet. Significant copper mineralization (chalcopyrite) was intersected in two drill holes (DDH 75-5 and DDH 76-1).

V. Grades of Mineralization

The BBX prospect is primarily a copper deposit, although significant concentrations of lead occur locally. Cobalt, nickel and silver are minor constituents which enhance the potential value of the mineralization. Barite is common as a gangue mineral in some zones, and concentrations of barium as high as 6.5% have been recorded.

In addition to the above, numerous other elements have been detected in very small quantities. This diversity is illustrated in Table 1 which is compiled from semiquantitative spectrographic analyses of selected samples from the main surface showing. This table clearly illustrates the relative importance of copper and lead. Although the

TABLE 1

Compilation of "Epigene" Elements in Samples from the Main Surface Showing[1]

Abundance	Elements
>1%	Ti, Cu, Ba, Pb
0.1 - 1.0%	Cr, Th
0.01 - 0.1%	Li, Bo, V, Co, Ni, Zn, Mo, Sn, W, Tl, Bi
<0.001%	Ga, Y, Cd, La, Ce, Au, U

---

[1] Data from Blackadar and McInnis, 1976, Appendix IX C-semiquantitative spectrographic analyses of mineralized samples. Elements in each group are arranged in order of increasing atomic number.

concentration of elements in the table may vary widely between samples, their relative order of magnitude remains constant. It should be noted that certain of these elements may occur as accessories in rock-forming minerals, and hence may have no implication with respect to epigenetic processes. Titanium for instance, is present both as leucoxene associated with basalt fragments, and as a hydrothermal phase associated with the mineralization.

The grades of mineralization which have been encountered in the deposit are briefly illustrated in Tables 2 and 3.

TABLE 2

Grades of Mineralization from the Main Surface Showing BBX Diatreme[1]

	Element	Abundance
(I) Channel Sample over 30 foot width	Cu	4.77%
	Ag	1.88 oz/ton
	Au	0.02 oz/ton
(2) Grab Samples	Cu	2.7 - 6.6%
	Pb	0.8 - 4.2%
	Co	0.7 - 2.1%
	Ni	0.04 - 1.23%
	Ag	0.1 - 7.5 oz/ton
	Au	Trace - 0.2 oz/ton

[1] Data compiled from (a) Blackadar and McInnis, 1976
pp. 24 & 25.
(b) This Thesis, Table 15.

TABLE 3

Average Copper Values of Mineralized Intervals from Diamond Drill Hole 76-1[1]

Interval	Length	% Cu
114'8"-123'6"	8'10"	1.23
158' - 160'	2'	1.61
172' - 178'4"	6'4"	1.71
262'6"-300'6"	38'	2.24
335' - 350'	15'	1.28

[1] Data from Blackadar and McInnis, 1976, p.15.

VI. Basis of Study

This study is based on geological mapping, structural mapping, and sample collection undertaken by the author between June 3 and July 2, 1978. This work was focused mainly on the BBX diatreme, and immediately adjacent areas. The volcanic rocks of the JDA group were examined briefly, as were sediments in the vicinity of Great Slave Lodge. In addition, geological reconnaissance of selected areas of that part of Pethei Peninsula (Figure 1) south of Taltheilei Narrows was undertaken for comparative purposes.

Diamond drill core from exploration programs carried out by Great Plains Development in 1975 and 1976 (particularly DDH 76-1) was examined in detail and was an invaluable source of information on volcanic textures, alteration and hydrothermal mineralization.

CHAPTER 2

REGIONAL GEOLOGY AND TECTONIC FRAMEWORK

I. Regional Geological Setting

The geology of the Great Slave Lake are has been summarized by Hoffman and Henderson (1972), Hoffman (1973) and Hoffman et al, (1974). The prominent geological features of the area, shown in figure 4 are discussed below.

(A) Phanerozoic Rocks

The Phanerozoic cover west of Great Slave Lake comprises relatively thin, subhorizontal Paleozoic and Mesozoic sedimentary rocks.

(B) Archean Basement Rocks

1. The Slave Province

The Slave Province comprises weakly north-trending synclinal belts of Archean supracrustal rocks of the Yellowknife Supergroup, separated by sialic batholiths. These intrusives range in age from 2300 to 2600 m.y.

The supracrustal belts generally contain several thousand metres of basic, submarine lava flows. These are overlain by a thick succession of pelitic sediments with greywacke turbidites, and in places by minor amounts of cross-bedded sandstone, conglomerate, cherty carbonate, and acid volcanics. These rocks are pervasively

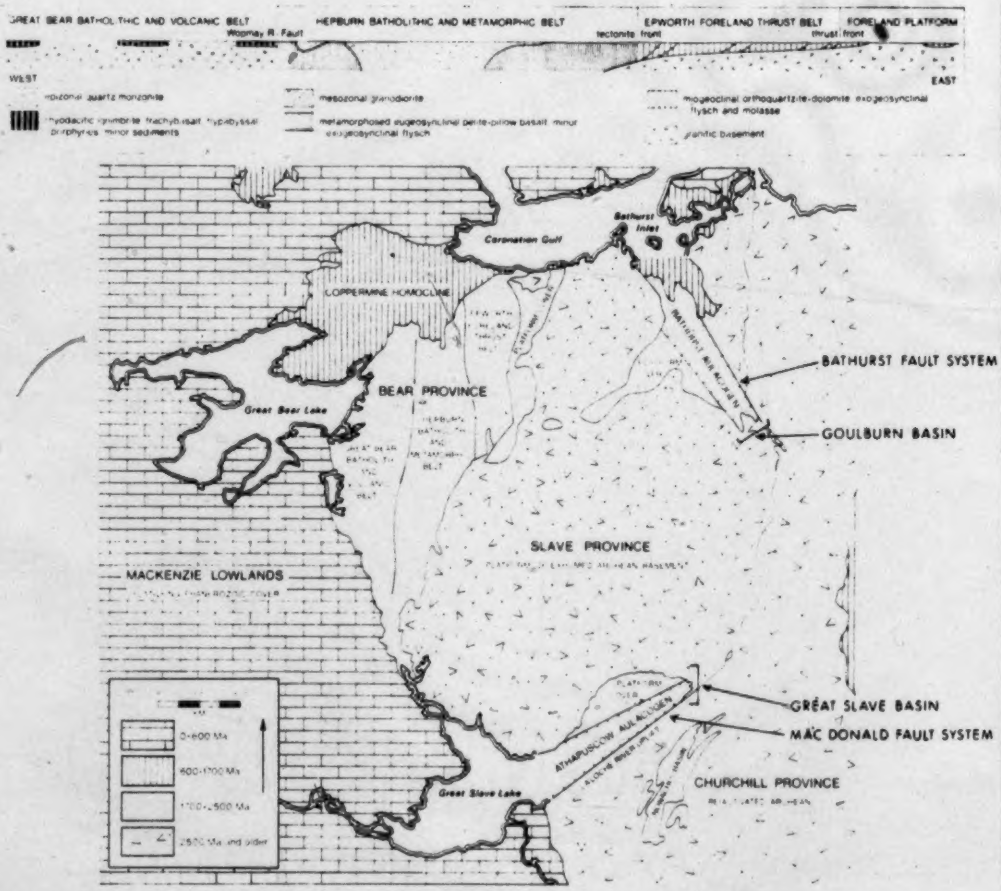
GREAT BEAR BATHOLITHIC AND VOLCANIC BELT
HEPBURN BATHOLITHIC AND METAMORPHIC BELT
EPWORTH FORELAND THRUST BELT
FORELAND PLATFORM
Wopmay R. Fault
tectonite front
thrust front
WEST
EAST
epizonal quartz monzonite
rhyodacitic ignimbrite trachybasalt hypabyssal porphyries minor sediments
mesozonal granodiorite
metamorphosed eugeosynclinal pelite-pillow basalt minor exogeosynclinal flysch
miogeoclinal orthoquartzite-dolomite exogeosynclinal flysch and molasse
granitic basement
Coronation Gulf
Bathurst Inlet
COPPERMINE HOMOCLINE
BEAR PROVINCE
Great Bear Lake
SLAVE PROVINCE
MACKENZIE LOWLANDS
ATHAPUSCOW AULACOGEN
Great Slave Lake
CHURCHILL PROVINCE
BATHURST FAULT SYSTEM
GOULBURN BASIN
GREAT SLAVE BASIN
MAC DONALD FAULT SYSTEM
0-600 Ma
600-1700 Ma
1700-2500 Ma
2500 Ma and older

Figure 4 : Tectonic map of Northwestern Part of Canadian shield and Structural Cross-section of type area of Coronation Geosyncline near north end of Bear Province

(adapted from Hoffman et al , 1974, fig. 3) metamorphosed to greenschist facies. The sedimentary rocks exhibit penetrative cleavage, and commonly, refolded isoclinal folds.

It has not been conclusively shown whether the belts of supracrustal rocks represent individual depositional troughs, or are part of a much larger basin which has been tectonically fragmented.

2. The Churchill Province

That part of the Churchill Province adjacent to Great Slave Lake comprises Archean metamorphic rocks which have generally attained a higher degree of metamorphism than is typical of the Slave Province. This suggests that these rocks have undergone greater subsequent uplift.

The Churchill Province rocks have also experienced intense cataclastic and retrogressive metamorphism which has resulted in a regional northeast-southwest foliation.

The complex history of these rocks is indicated by the wide range in radiometric ages, from 1695 to 2460 m.y. (Hoffman and Henderson, 1972, p. 7). These dates generally reflect deformational (i.e. shearing) rather than intrusive events.

(C) Early Proterozoic Supracrustal Rocks

It is probable that Early Proterozoic supracrustal rocks once covered the entire northwestern part of the Canadian Shield (figure 4), but they are now preserved in three main structural basins. These are the Epworth Basin, southwest of Coronation Gulf, the Great Slave Basin, around the East Arm of Great Slave Lake, and the Goulburn Basin, around Bathurst Inlet. The latter two basins are associated with regional high-angle fault systems - the Bathurst fault system of Bathurst Inlet, and the MacDonald fault system of Great Slave Lake.

1. The Coronation Geosyncline

During the early part of the Proterozoic Era, the Archean rocks of the northwestern Canadian Shield formed an extensive continental platform.

The Coronation Geosyncline (Hoffman, 1973) formed along the western margin of this platform. The Slave and Bear Provinces represent the foreland, and the orogenic/batholithic belt of this geosyncline respectively. The Churchill Province also formed part of the foreland platform during the evolution of the Coronation Geosyncline. Shortly thereafter however, it was uplifted and dextrally displaced relative to the Slave Province (Hoffman et al, 1974, p. 39).

The Slave Province was overlain by a thin, relatively little deformed cover of Proterozoic sedimentary rock. Thick successions of sediments accumulated only in the Coronation Geosyncline, and in the Great Slave and Goulburn Basins. Deposition in the geosyncline is assumed to have occurred in Aphebian times, between 2200 and 1700 million years ago (Hoffman et al, 1974, p.42).

The prominent tectonic elements of the Coronation Geosyncline are shown in figures 4 and 5, and are discussed below.

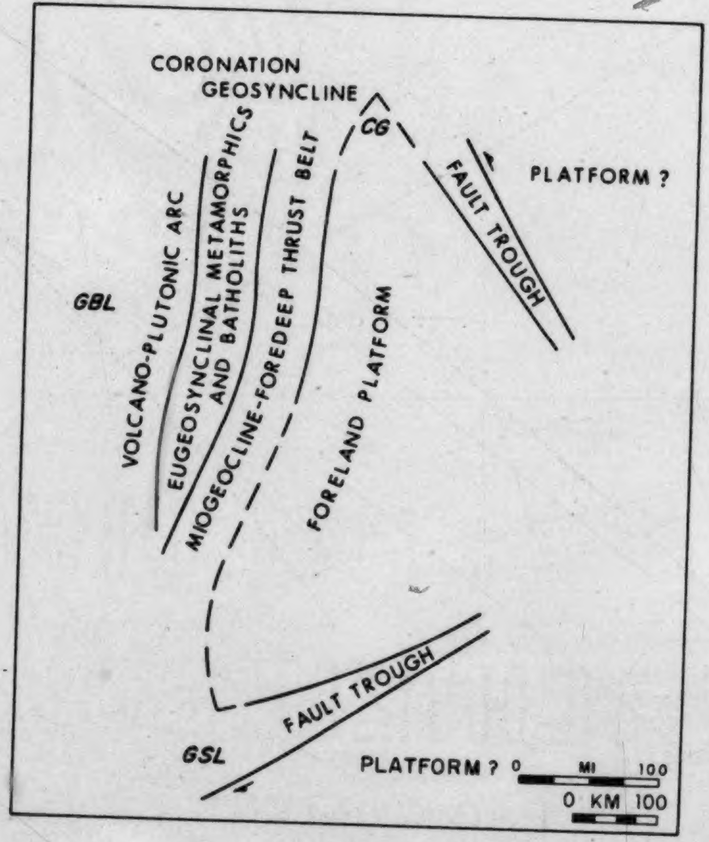
CORONATION
GEOSYNCLINE
CG
VOLCANO-PLUTONIC ARC
EUGEOSYNCLINAL METAMORPHICS AND BATHOLITHS
MIOGEOCLINE-FOREDEEP THRUST BELT
FORELAND PLATFORM
FAULT TROUGH
PLATFORM ?
GBL
FAULT TROUGH
GSL
PLATFORM ?
0 MI 100
0 KM 100

Figure 5: Aphebian tectonic elements of the Coronation Geosyncline. Locations are GSL, Great Slave Lake; GBL, Great Bear Lake; CG, Coronation Gulf.

(After Hoffman and Henderson, 1972, Fig. 3)

(i) The Bear Province

The Bear Province is divisible into three principle belts: (Hoffman et al, 1974 p. 39).

(a) Great Bear Batholith and Volcanic Belt

This westernmost belt comprises a broadly folded, locally metamorphosed series of acid to intermediate welded ash-flow tuff and andesite flows, with interstratified mudstone, sandstone and porphyry-pebble conglomerate. These rocks are intruded by porphyritic granophyric dyke and sill swarms related to epizonal plutons of the Great Bear Batholith. These plutons are co-magmatic with the ash-flow tuffs and range in age from 1700 to 1780 m.y.

(b) Hepburn Batholith and Metamorphic Belt

These rocks are separated from the Great Bear Batholith by the north-trending 400 km long Wopmay River fault, of unknown displacement. This belt comprises metamorphosed and penetratively deformed pelites, turbidites and pillow basalts which are the eugeosynclinal facies equivalents of the Epworth Group (Hoffman and Henderson, 1972, p. 8). These rocks are intruded by porphyroblastic granodiorites of the Hepburn Batholith, ranging in age from 1700 to 1870 million years (op. cit. p. 8).

(c) Epworth Foreland Thrust Belt

This belt comprises miogeosynclinal orthoquartzite and dolomite overlain by eugeosynclinal flysch. These rocks have been broadly folded and thrust eastward over granitic basement.

(ii) The Great Slave and Goulburn Basins

The rocks of the Great Slave and Goulburn Basins are broadly correlative with the Epworth Group, but are deposited in a different tectonic setting (Hoffman and Henderson, 1972, p. 8). These basins have been interpreted as aulacogens related to the Coronation geosyncline (Hoffman, 1973), and as grabens generated by transcurrent faulting (Badham 1978b p. 213).

II. Geology of Great Slave Basin

The geology of Great Slave Basin has been described and discussed by Hoffman (1968, 1969 and 1973) and Hoffman et al (1977). The geology of the basin has been mapped in detail by Hoffman (1977). Alternate theories on its origin have been proposed by Hoffman et al (1974) and Badham (1978b).

A. General Remarks (refer to figure 6)

The East Arm of Great Slave Lake is occupied by more than 50,000 feet of unmetamorphosed sedimentary and volcanic rock (Hoffman, 1968, p. 1), which accumulated in a tectonic basin produced by the MacDonald fault system. The sedimentary rocks of the East Arm were deposited predominantly in fluviatile, coastal and shallow marine environments between approximately 2400 and 1600 m.a. (Badham and Stanworth, 1977, p 516).

The Great Slave Basin consists of a deeply subsiding fault-controlled trough in the south, and the adjacent Slave platform to the north. Sedimentary and

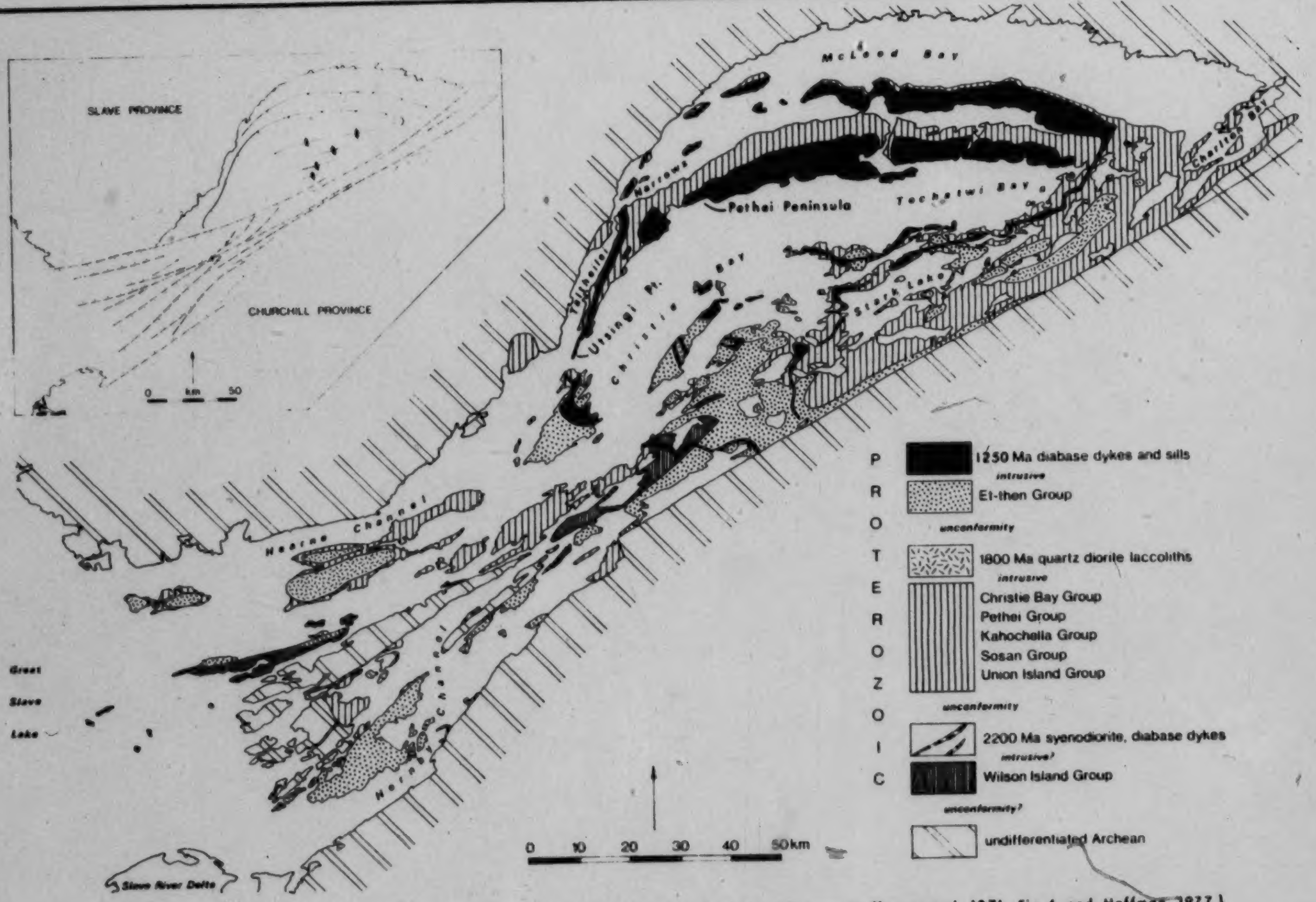
SLAVE PROVINCE
CHURCHILL PROVINCE
0 km 50
McLeod Bay
Narrows
Pethei Peninsula
Tochatwi Bay
Charlton Bay
Taltheilei
Utsingi Pt.
Christie Bay
Stark Lake
Hearne Channel
Hornby Channel
Great Slave Lake
Slave River Delta
0 10 20 30 40 50km
P R O T E R O Z O I C
1250 Ma diabase dykes and sills
intrusive
Et-then Group
unconformity
1800 Ma quartz diorite laccoliths
intrusive
Christie Bay Group
Pethei Group
Kahochella Group
Sosan Group
Union Island Group
unconformity
2200 Ma syenodiorite, diabase dykes
intrusive?
Wilson Island Group
unconformity?
undifferentiated Archean

Fig 6: Geologic and tectonic (inset) maps of east arm of Great Slave Lake (adapted from Hoffman et al, 1974, Fig 6 and Hoffman, 1977)

volcanic rocks in the basin reached a great thickness in the trough, but thinned considerably towards the platform. Changes in sedimentary facies and thickness across the basin were controlled by prolonged subsidence in the trough. The geological history of the East Arm is dominated by intermittent movements on various splays of the MacDonald fault system (Figure 6, inset). These movements controlled deposition, deformation and preservation of sedimentary and volcanic rocks and acted as the locus for intrusion of alkaline magma throughout the Aphebian (Badham, 1978b, p. 201).

The supracrustal rocks within the trough itself thicken toward the southwest and are broadly folded about northeast-trending axes and cut by a complex system of high angle faults that parallel the folds. The overall structural configuration of the basin is that of an asymetric synclinorium. On the north side of the synclinorium, gently dipping Aphebian strata overlie Archean rocks of the Slave Province. On the south side however, Aphebian and possibly Paleohelikian strata are tightly folded and faulted and abut against the Churchill Province along the MacDonald fault.

B. Origin of Great Slave Basin

1. The Aulacogen Model

The possibility that the Great Slave and Goulburn Basins are aulacogens related to the Cornation Geosyncline was proposed by Hoffman (1973). This model was revised slightly by Hoffman et al (1974). The name Athapuscow Aulacogen, which derives from the aboriginal name for Great Slave Lake, was proposed by Hoffman (1973, p. 560) for the Great Slave Basin.

Aulacogens are defined as:

> "long-lived, deeply subsiding troughs, at times fault-bounded, that extend at high angles from geosynclines far into adjacent foreland platforms. They are generally located where geosynclines make reentrant angles at the margins of the platforms, and they gradually die out towards the interiors of the platforms. Their fill is contemporaneous with, and lithologically similar to the foreland sedimentary wedge of the geosyncline".
>
> (Hoffman et al, 1974, p. 38)

Based predominantly on structural, geochemical and geophysical considerations, Hoffman et al (1974, p. 51) proposed that aulacogens represent failed arms of triple rift systems. Essentially, this model involves the formation of domal uplifts related to plumes of hot material beneath continents that are stationary with respect to the plumes. These domal uplifts break into three-armed crestal rift systems dominated by alkalic volcanism. Assuming that continental separation occurs along a belt formed by two of these arms, the third will remain as a transverse trough located at a reentrant on a new continental margin.

2. Permobile Tectonics

Based primarily on structural considerations, Badham (1978b, p. 210), suggested that the East Arm graben was in existence long before its supposed genesis at a triple junction, and hence argued against the failed arm model of Hoffman et al. He proposed instead, that the East Arm and Bathurst grabens are the result of a northwesterly-directed compression between the Superior and Slave cratons, and deflection of this compression along the rigid Slave craton. This deflection caused intermittent and variable transcurrent faulting and resulted in formation of the grabens (op. cit. p. 213).

C. Geological History of Great Slave Basin

1. Stratigraphy and Depositional History

The stratigraphy of the Great Slave Basin has been divided into seven principle groups by Hoffman (1969). These groups are shown with lithologic descriptions in Table 4 and their stratigraphic and facies relationships are illustrated in Figure 7.

The Great Slave Basin has undergone eight major phases of sedimentation; pre-quartzite, quartzite, dolomite, pre-flysch, flysch, calc-flysch, molasse and fanglomerate (Hoffman, 1973). These phases are broadly correlative with those in the Coronation Geosyncline. Their relation to geological formations in the East Arm is illustrated in Figure 7 and Table 5.

The Wilson Island Group is limited in distribution (Badham, 1978b, p. 205) and its precise significance is unknown. It is younger than the Archean, and has attained a significantly greater degree of metamorphism than the Great Slave Supergroup which it unconformably underlies (Hoffman et al, 1977, p. 119). It has been proposed

TABLE 4

STRATIGRAPHIC COLUMN[1]
EAST ARM OF GREAT SLAVE LAKE

Age		Group	Description
Helikian		Et-Then Group	A nearly flat-lying sequence of coarse-grained terrigenous sedimentary rocks comprises flaglomerate overlain by sandstone.
		Unconformity	
Late Aphebian	Great Slave Supergroup	Christie Bay Group	A complex assemblage of red beds - includes red mudstone with stromatolitic mega-breccia, red laminated and cross-bedded sandstone with carbonate-pebble conglomerate, red mudcracked mudstone with buff siltstone beds, and columnar basalt flows.
		Pethei Group	Stromatolitic and oolitic limestone and dolomite, thin bedded argillaceous limestone and mudstone, stromatolite mounds and graded greywacke beds.
		Kahochella Group	Red and green fissile mudstone, granular hematitic ironstone and spherulitic limestone, flat pebble intraformational conglomerate and red concretionary mudstone.
		Sosan Group	Pebbly crossbedded subarkose, stromatolitic limestone and basalt ash and lapilli-fall tuff fine cross bedded quartzite and red platy siltstone.
		Unconformity	
	?	Union Island Group	Arkose and granite rubble, non-stromatolitic dolomite, black mudstone, pillow basalt and gabbro sills, and cherty dolomite.
		Unconformity	
Early Aphebian		Wilson Island Group	Basalt and rhyolite flows, conglomerate containing basement clasts, cross bedded quartzite, feldspathic quartzite, dolomitic quartzite, impure dolomite, argillaceous quartzite and argillite, porphyritic basalt flows.
		Unconformity	
Archean			Basement Rocks.

---

[1] Column adapted from Hoffman, 1969, 1973 and 1977 and Badham 1978b.

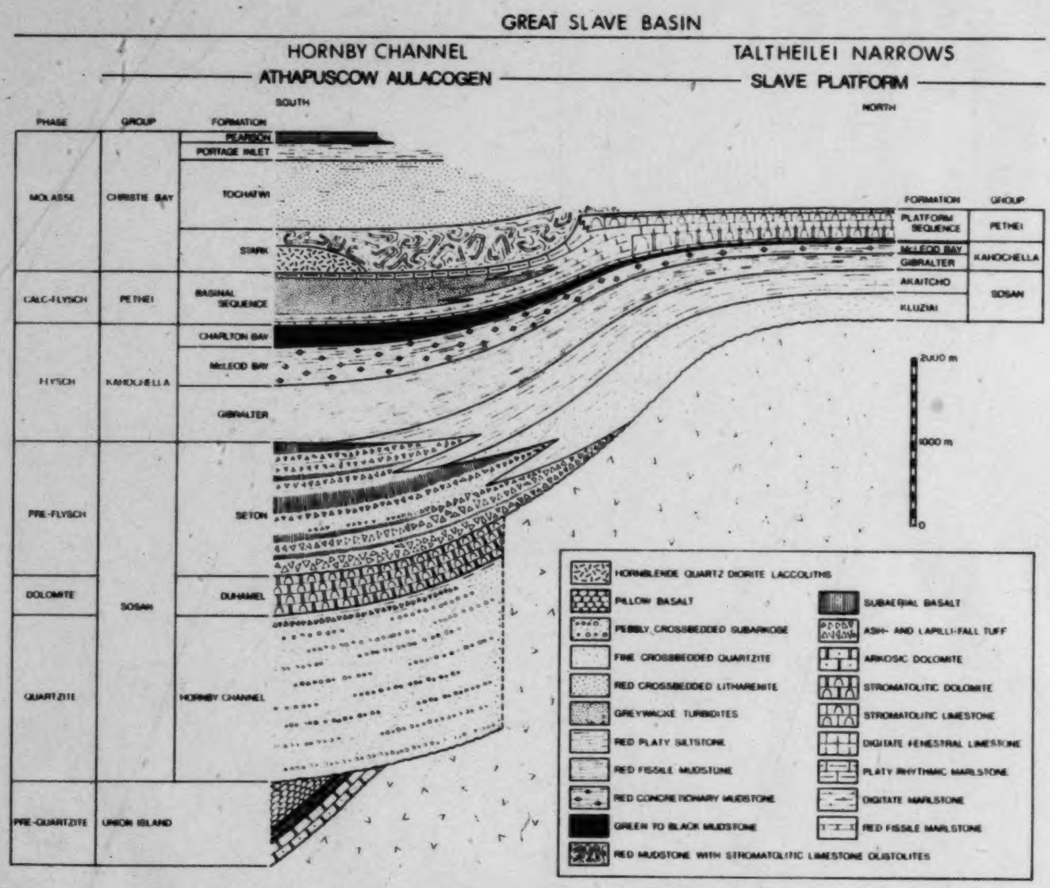
GREAT SLAVE BASIN
HORNBY CHANNEL
ATHAPUSCOW AULACOGEN
TALTHEILEI NARROWS
SLAVE PLATFORM
SOUTH
NORTH
PHASE
GROUP
FORMATION
MOLASSE
CHRISTIE BAY
PEARSON
PORTAGE INLET
TOCHATWI
STARK
CALC-FLYSCH
PETHEI
BASINAL SEQUENCE
FLYSCH
KAHOCHELLA
CHARLTON BAY
McLEOD BAY
GIBRALTER
PRE-FLYSCH
SETON
DOLOMITE
SOSAN
DUHAMEL
QUARTZITE
HORNBY CHANNEL
PRE-QUARTZITE
UNION ISLAND
FORMATION
GROUP
PLATFORM SEQUENCE
PETHEI
McLEOD BAY
GIBRALTER
KAHOCHELLA
AKAITCHO
KLUZIAI
SOSAN
2000 m
1000 m
0
HORNBLENDE QUARTZ DIORITE LACCOLITHS
PILLOW BASALT
PEBBLY CROSSBEDDED SUBARKOSE
FINE CROSSBEDDED QUARTZITE
RED CROSSBEDDED LITHARENITE
GREYWACKE TURBIDITES
RED PLATY SILTSTONE
RED FISSILE MUDSTONE
RED CONCRETIONARY MUDSTONE
GREEN TO BLACK MUDSTONE
RED MUDSTONE WITH STROMATOLITIC LIMESTONE OLISTOLITES
SUBAERIAL BASALT
ASH- AND LAPILLI-FALL TUFF
ARKOSIC DOLOMITE
STROMATOLITIC DOLOMITE
STROMATOLITIC LIMESTONE
DIGITATE FENESTRAL LIMESTONE
PLATY RHYTHMIC MARLSTONE
DIGITATE MARLSTONE
RED FISSILE MARLSTONE

Figure 7: Stratigraphic Cross - section of the Northwest Margin of Great Slave Basin between Taltheilei Narrows and Hornby Channel.
(adapted from Hoffman et al 1974, fig. 7 and Hoffman, 1973 b Figure 1)

TABLE 5

Relationship Between Sedimentation and Structural Evolution Great Slave Basin

Geological Group	Phase of Sedimentation	Stage of Structural Evolution
Et-Then	Fanglomerate	V. Postgeosynclinal
		IV. Compressional Deformation
Christie Bay	Molasse	
Pethei	Cal-flysch	III. Downwarping
Kahochella	Flysch	
	Pre-flysch	II. Transitional
Sosan	Dolomite	
	Quartzite	I. Graben
Union Island	Pre-quartzite	

that the Wilson Island Group was deposited in a precursor trough coincident with the Athapuscow Aulacogen. This early rifting was separated from the main development of the aulacogen by intense mylonitization and perhaps thermal metamorphism of mid-Aphebian age (op. cit. p. 119).

The majority of rocks which outcrop in Great Slave Basin belong to the Great Slave Supergroup, which comprises the Sosan, Kahochella, Pethei and Christie Bay Groups, and possibly the Union Island Group.

The Union Island Group, which represents the pre-quartzite phase of deposition, contains the oldest supracrustal rocks in the aulacogen that can be correlated with rocks in the Coronation Geosyncline (Hoffman et al, 1977, p. 120). The group outcrops only around Union Island, where it is gently folded and preserved in fault blocks (Badham, 1978b, p. 208). It is overlain unconformably by the Sosan Group (Hoffman et al, 1977, p. 120) and bears little lithologic or genetic resemblance to younger rocks (Hoffman, 1969, p. 444). The significance of the Union Island Group remains speculative, but it has been included in the Great Slave Supergroup (Badham, 1978b, Table 1).

The rocks of the Sosan and Kahochella Groups are regarded as pre-orogenic phases of sedimentation within the Coronation Geosyncline, while those of the Pethei and Christie Bay Groups are thought to be syn-orogenic (Olade and Morton, p. 1111).

The Helikian rocks of the Et-Then Group lie unconformably on folded rocks of the Great Slave Supergroup, and are thought to represent post orogenic sedimentation (op. cit., p. 1111).

2. Structural Evolution

The structural evolution of Great Slave Basin has been divided into five stages (Hoffman, 1973, Hoffman et al 1974), which are briefly discussed below. The relationship between these stages and depositional phases is summarized in Table 5.

(i) Graben Stage

During this stage, which includes sedimentation in the pre-quartzite through dolomite phases, the aulacogen was a narrow fault-bounded rift valley or graben. Because the first three phases of deposition are absent from the northern periphery of the basin, the graben is assumed to have had elevated margins. Sediments were shed into the trough from these margins.

(ii) Transitional Stage

At the beginning of the pre-flysch phase, the aulacogen began to change character with the margins sagging in towards the centre.

(iii) Downwarping Stage

During this stage, the flysch, calc-flysch and molasse phases accumulated in a broad synclinal depression centred over the aulacogen.

(iv) Compressional Stage

Following deposition of the Great Slave Supergroup, the aulacogen underwent mild transverse compression. Sediments on the Slave platform tilted toward the aulacogen, while those in the aulacogen were compressed into broad folds.

(v) Post Geosynclinal Stage

During the Fanglomerate phase of deposition, the aulacogen again became an active fault zone. These faults formed a braided network having dextral transcurrent and vertical movement. Fanglomerate sedimentation of the Et-Then Group, which unconformably overlies the Great Slave Supergroup, was controlled by a complex pattern of uplifted and downdropped blocks separated by these faults. Sediments were shed into the aulacogen mainly from the La Loche River uplift to the south.

3. Igneous Activity and Geochronology

The major igneous events in the East Arm, summarized in Table 6, are as follows (refer to Figure 6).

(i) The Sosan Group is intruded by mafic alkaline dykes and diatremes having ages of approximately 2200 m.y. (Badham 1978b, p. 209). These are emplaced along or at intersections of major faults, and are related to intrusions along the north shore.

TABLE 6

Major Intrusive Events and Geochronology Great Slave Basin[1]

		Group	Dated Events	Age (m.y.)
Helikian		Mackenzie dykes	diabase dykes	1315
			diabase dykes	1295
			diabase dykes	1250
		Diabase Sills	diabase sill	1020
		Et-Then Group		
APHEBIAN			Alkaline Diorites	1630 1795 1845 1785
	Great Slave Super-group.	Christie Bay Group		
		Pethei Group		
		Kahochella Group	Seton volcanics	1872[2]
		Upper Sosan Group	Mafic alkaline intrusions	2170 2057 2200
		Lower Sosan Group		
		Union Island Group		
		Wilson Island Group		

---

[1] After Badham, 1978b, Table I

[2] Revised to 1833 m.y. (refer to text, p.41).

(ii) The Seton Formation comprises a variety of rock types including volcanics, iron formation, and marine epiclastic sediments (Olade and Morton, p. 1111). In the type area on Seton Island, the volcanics have a spilitic to keratophyric affinity (op. cit. p. 1110). and have been dated at 1872 ± 10 m.y. (Baadsgaard et al, p. 1580). This age has been recalculated to 1833 ± 28 m.y. using a revised value for λ^{87}Rb (Cumming, 1980, pers. com.). Other ages of Seton volcanics are 1804 ± 23 m.y. (Cumming, 1980) and 1805 ± 16 m.y. (Loveridge).

Although rocks of the Seton Formation are the main volcanics in the East Arm, alkaline volcanic activity occurred intermittently throughout the deposition of the Great Slave Supergroup.

(iii) Diorite laccoliths yielding ages of 1845, 1795, 1785 and 1630 m.y. (Hoffman, 1969, p. 444), were intruded contemporaneously with, or after deposition of the Christie Bay and Pethei Groups. These high level alkaline intrusions are overlain unconformably by the Et-Then Group.

(iv) Rocks of the Et-Then Group are intruded by diabase dykes and sills. The northwest-trending dykes are classified as part of the MacKenzie Dyke Swarm (Hoffman, 1969, p. 444), and show ages of 1315, 1295 and 1250 m.y. One of the sills in the East Arm has been dated at 1020 m.y. (Hoffman, 1969, p. 444). This date provides a minimum age for the Et-Then Group, although considerations of regional geology suggest that the minimum age may be closer to 1600 - 1700 m.y. (Hoffman, 1969, p. 446).

III. Local Geology: Hearne Channel and the Seton Volcanic Centres

Volcanic rocks occurring in both the Sosan and Kahochella Groups are known collectively as the Seton Formation (Hoffman et al, 1977, p. 122). These rocks are found over a wide geographical area, but are concentrated along the MacDonald - Wilson Island Fault (Goff and Scarfe, 1978, p. 129), and along the northwest margin of the East Arm (Op. Cit., p. 129). In the latter location, a series of six, possibly seven, basalt breccia pipes extend in a linear south-southwest-trending belt from Taltheilei Narrows to Utsingi Point. These pipes occur along an old fault line bordering the basement high east of Taltheilei Narrows (Hoffman et al, 1977, p. 122). This fault trends approximately N18°E (op. cit., Figure 25.3).

The southern four basalt pipes all intrude the Gibralter Formation (Table 7), which includes basalt flows at its base. At the top of the formation, beds of lapilli tuff are associated with green shale and beds of red granular ironstone. It has been suggested that these basalt pipes may have acted as feeders to the upper tuffs (Hoffman et al, 1977, p. 125). This may not be true in all cases however, as at least two of these pipes also intrude the McLeod Formation (Hoffman, 1977, sheet 475J).

The BBX diatreme, which is the subject of this study, is the northernmost of these Seton pipes, and intrudes sediments of the Akaitcho Formation. On the JDA Group to the south, a poorly-defined basalt pipe comprises part of a large mafic volcanic pile, and is also inferred to have cut the Akaitcho Formation, although rocks of this formation do not outcrop in the immediate vicinity. If these pipes are the same age as those farther south, they are more deeply eroded (Hoffman et al, 1977, p. 123).

TABLE 7

PLATFORM SEDIMENTS OF THE GREAT SLAVE SUPERGROUP[1]

Group	Formation		Lithology
Pethei	Hearne	(Ph)	LS, pale gy, v thk bdd, fenestrate, thn stromlt dol bd at top.
	Wildbread	(Pw)	LS, pale gy, thk fenestrate bd at base, alternating stromlt and ool bds in middle, thk columnar stromlt bd at top.
	Utsingi	(Pu)	LS, pale gy/bn dol mot, thk bdd, fenestrate, p lam digitate to columnar stromlts.
	Taltheilei	(Pt)	Dol, pale bn, chty, thk mounded stromlts at base, m bdd columnar and undulatory stromlts in middle, thk columnar stromlt bd at top.
	Douglas	(Pd)	Mrlst, rd, fis, v thn calc lenticles, sh ptgs.
Kahochella	Charlton	(kc)	Sh, dk gy gn, lam, large calc conc, thn grd sltst bds, locally tuf, bd of coalesced conc at top.
	McLeod	(km)	Sh, rd, lam, s calc conc, thn bds of gran hem ironstone at top.
	Gibralter	(kg)	Sh, rd, lam, locally tuf.
	Ogilvie	(ko)	Sh, dk gy gn, lrg calc conc, locally tuf.
Sosan	Akaitcho	(Sa)	SS, rd, mica, low-angle planar xbdg, mudcracked, glau, locally tuf, in pt intertongued/kluziai fm.
	Kluziai	(Sk)	Qtzt, pk to pale gy, m trough xbdg, heavy mnrl bnds, mud chip cgl, locally tuf.

[1] Adapted from Hoffman, 1977 (common legend and sheets 475D and 475 J) and Hoffman et al, 1974 (fig. 7)

N.B. Lithologic abbreviations are those used by Canadian Stratigraphic Service Ltd.

SECTION II

GEOLOGY OF THE STUDY AREA

PREFACE

(1) Mapping Procedure

The study area is situated on an isolated block of Proterozoic volcanics and platform sediments of the Great Slave Supergroup. These rocks are bounded on the west by Archean Basement (Slave Province) and on the east by Taltheilei Narrows and Hearne Channel (Plate 2). This Proterozoic block has been mapped from airphotographs at a scale of approximately 1 cm = 0.2 km (Map 1, in pocket).

The mineralized diatreme and immediately adjacent parts of the BBX property were geologically mapped on a larger scale of 1" = 30 m along a northeast-trending grid (baseline azimuth 44°) which parallels the dominant geological trend (Map 2, in pocket). Grid lines were established perpendicular to the baseline every 60 metres.

(2) Overview of Geology

The area of interest (Map 2) is dominated by two prominant northeast-trending ridges which rise up to 50 metres above the surrounding muskeg (see frontispiece and plate 3). The northernmost ridge comprises medium red to maroon-coloured siltstone and very fine grained sandstone in the west, and a diabase plug in the east. The more elongate

Plate 2 View of Hearne Channel and Pethei Peninsula (background) looking SSW from the BBX diatreme (top of ridge). Aristifats Lake is in the right foreground. Low-lying wooded areas are underlain by muskeg.

Plate 3 View of the BBX group looking NNE from Aristifats Lake. The ridge on the left is the surface expression of an olivine diabase plug. That on the right is the diatreme.

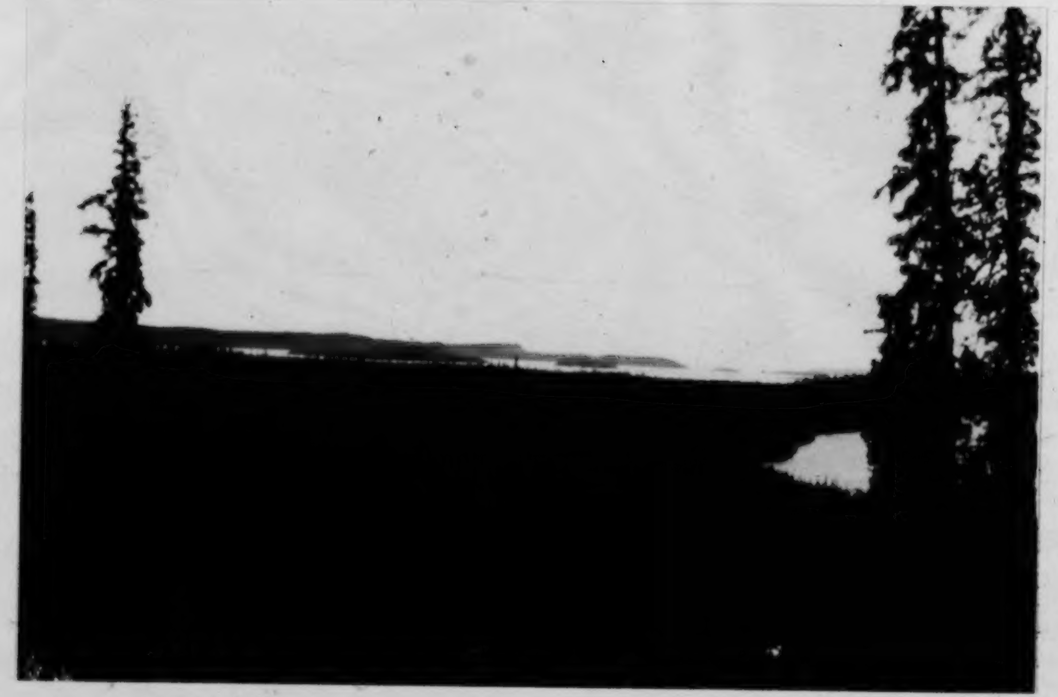

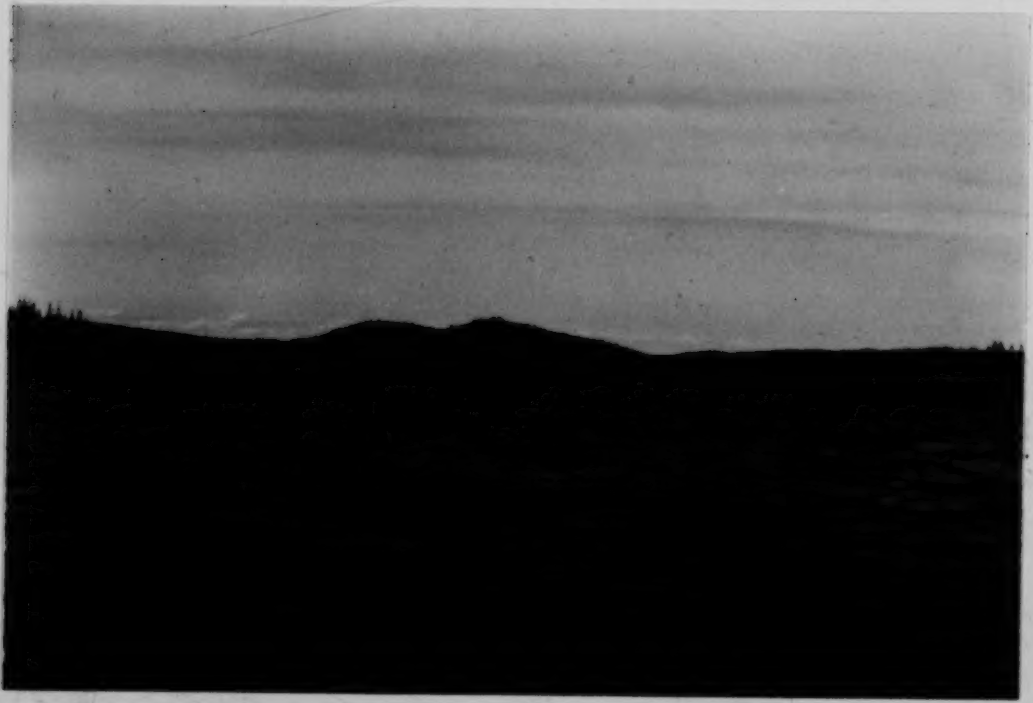

southerly ridge is dominated by the BBX diatreme and immediately adjacent outcrops of shale, silty shale, and micaceous and argillaceous siltstone. East of the diatreme, this ridge is largely covered with overburden, but local exposures of mafic tuff and lapilli tuff are evident. The volcanic rocks and the diabase stand out in marked relief relative to the sediments which are more recessive.

All rock types on the BBX property are cut by a variety of quartz-carbonate veins. These range in size from less than 1 mm to large quartz veins up to one metre wide (locations N-3, 45 and 31, Map 2). In addition, a large quartz and quartz-carbonate stockwork occupies a linear zone in the sediments which parallels the south margin of the diabase (locations 28 and 38, Map 2). Narrow carbonate and quartz-carbonate veins have been encountered at depth during diamond drilling programs. These veins, which are generally less than 2 cm in width, occur throughout the diatreme, and at depths of as much as 800 feet in the sediments (DDH 76-1). The formation of quartz veins results in silicification of the adjacent wall rock. This is particularly evident in sedimentary rocks, where red hematitic siltstones are bleached to pink and light grey.

Outcrop exposure is generally restricted to the ridges where it may be as much as 15% - 20% on the average. Outcrop exposure elsewhere is minimal due to the extensive cover of muskeg in areas of low relief, and occasional glacial drift (Map 1). Glacial debris is concentrated particularly along the base of the Archean platform (Map 1) where it consists predominantly of hummocky deposits of sand. East of Aristifats Lake, deposits of boulder till and sand form small elongate ridges.

The geology of the BBX property, shown on Maps 1, 2 and 3 is discussed in detail in the following chapters.

CHAPTER 3

GEOLOGY EXCLUSIVE OF THE DIATREME

I. The Sediments

The geology of sedimentary rocks in the study area is complex, and a detailed description of these rocks is beyond the scope of this study. The important lithological features of these rocks however, are summarized on Maps 1 and 2.

It is assumed that the majority of sedimentary rocks exposed on the BBX property belong to the Akaitcho Formation. This assumption is based on regional mapping carried out by the GSC (Hoffman, 1977, Map 475J), during which outcrops of red siltstone near Great Slave Lodge (Location R3, Map 1), and red, very fine grained glauconitic sandstone at the northeast end of Aristifats Lake (Location 37, Map 2, Plate 4) were assigned to the Akaitcho Formation. On the basis of this assumption, the nature and occurrence of the Akaitcho Formation in the study area is described below.

(A) Sediments which outcrop between the diatreme and the diabase plug (Map 2) consist of red hematitic slightly micaceous siltstones. These grade occasionally into shales and very fine grained sandstones.

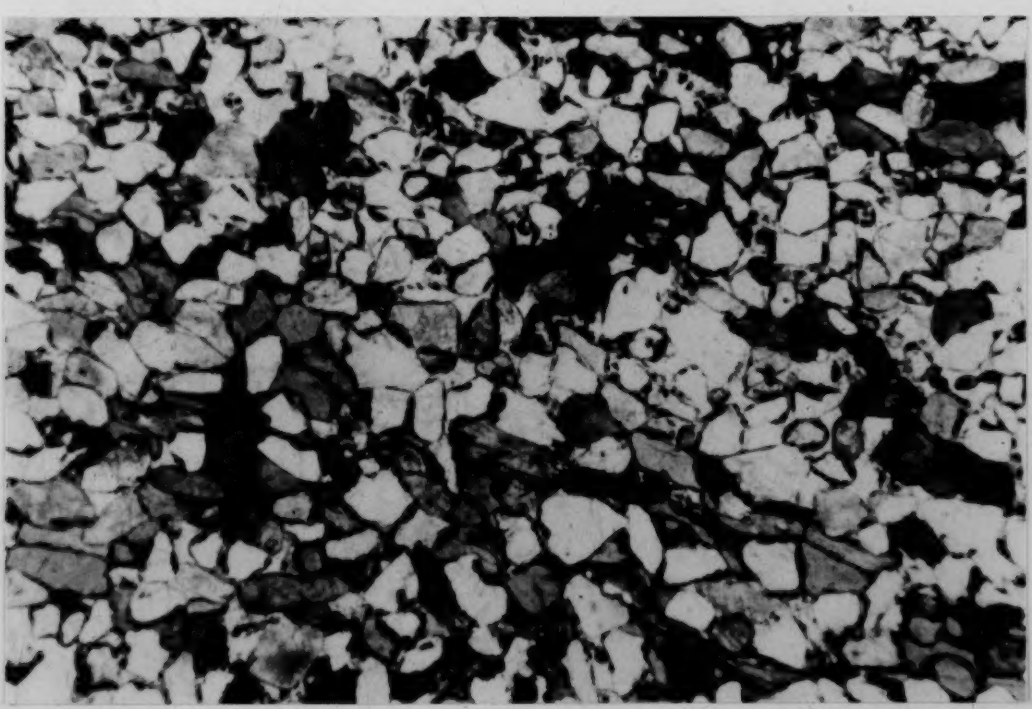

Plate 4 Photomicrograph showing a typical glauconitic sandstone of the Akaitcho Formation. The sandstone is very fine grained, and contains quartz (white), glauconite (Khaki green and brown) and hematite (black). (Transmitted light).

(B) South of the JDA Group, an extensive subcrop of large angular sandstone boulders occurs along the lake shore bordering Hearne Channel (Location R9, Map 1). This sandstone is a white to buff coloured very fine grained, medium bedded quartzite with occasional glauconite and minor muscovite. It shows abundant ripple marks and sole markings and occasional flat shale pebble horizons. This subcrop may represent the basal part of the Akaitcho Formation according to the description of Hoffman (1968, p. 13).

(C) Sediments of the Akaitcho Formation were encountered to depths of as much as 800 feet during diamond drilling programs. These generally comprise red slightly to moderately micaceous siltstones and shales, and green to greenish-grey fissile shales. These rocks are thinly bedded and are interbedded on both a large and a small scale. Occasional narrow horizons of granular and oolitic hematite occur with the red siltstone and shale. The hematitic horizons are frequently associated with pisoliths (Dunham, 1969, p. 183) of hematite, calcite and quartz as much as 2 cm in diameter. The more hematite-rich horizons are cut cut by narrow veinlets of specularite. Similar hematitic horizons outcrop on the west side of

Pethei peninsula, approximately three miles south of of Taltheilei Narrows. Here, these hematitic sediments are overlain by grey shales and are assigned to the Ogilvie Formation (Hoffman, 1977, Map 475D).

Although the majority of sediments which outcrop in the study area are siltstones and shales of the Akaitcho Formation, other lithologies are present around the perimeter of the diatreme and include grey fissile shale and siltstone, black shale and red concretionary shale and silty shale. These lithologies are not consistent with published descriptions of the Akaitcho Formation (Hoffman, 1968, p. 13, and 1977 "Table of Formations") and are tentatively interpreted as large blocks of sediment from up section, which have subsided within the diatreme during its formation. The significance and implications of this phenomenon are discussed at a later point in the thesis (Chapter 6, p. 165).

Outcrops in question are as follows:

(A) Locations 19 and 49 (Map 2)

These rocks comprise red shales and silty shales which generally exhibit massive irregular bedding, but are occasionally thinly bedded and fissile, with ripple marks and desiccation cracks. Lenticular shale concretions up to approximately 5 cm across, occur in the more massive zones. These outcrops are tentatively assigned to the McLeod Formation. Outcrops of similar rock, belonging to the McLeod Formation occur on a small island in Hearne Channel, approximately seven miles south of Taltheilei Narrows (Hoffman, 1977, Map 475J).

(B) Locations 16, 18 and 21 (Map 2)

The large outcrop of grey fissile shale at location 21 is tentatively assigned to the Ogilive Formation (Hoffman, 1978, personal communication). Small outcrops of grey micaceous siltstone and shale at the southwest end of the diatreme (locations 16 and 18) may also belong to this formation.

At the northeast end of the diatreme, red thinly bedded shale and silty shale overlie grey shale (locations 44, 45 and 47). At location 48, a minor exposure of grey and black shale occurs at the base of a large outcrop of red shale. The significance of these outcrops is unknown, but they are assumed to belong to the Akaitcho Formation.

II. The Diabase

(A) General Remarks

The mafic intrusion which occupies the northwest section of the BBX property (Map 1) is variable in composition and texture, but can be generally described as a phaneritic, medium grained (average 3 mm) olivine diabase. This diabase which is dark green in color, consists mainly of plagioclase, clinopyroxene, serpentine (after olivine), chlorite and opaque minerals. The intrusion exhibits a crude primary zonation related to its cooling history, which results in variations in texture, grain size and mineralogy. Late-stage deuteric and hydrothermal fluids have altered the rock to varying degrees and have further complicated its petrography.

(B) Form

The diabase, as shown on Map 1, is a roughly wedge shaped or teardrop shaped plug. Because geological contacts are not exposed in outcrop however, the configuration of the intrusion must be inferred. The south boundary of the diabase is represented by a linear ridge trending 71° (az.), on which outcrop is exposed more or less continuously for 330 metres. Adjacent outcrops of sediment help to define this boundary (Map 2). The northern margin of the intrusion is thought to approximate the base of a steep slope, perhaps 50 metres high, on which several small outcrops of diabase occur. The rounded eastern contact is not exposed, and is interpreted entirely from airphotographs.

(C) Petrography

1. Mineralogy

The following descriptions pertain to the relatively unaltered central part of the intrusion (refer to Plates 5, 6 and 7).

(i) Plagioclase

Plagioclase occurs in euhedral unzoned laths which exhibit well defined lamellar twinning (albite). These are locally intergrown and lie in subparallel orientation. The feldspar frequently has a brownish tint imparted by finely divided hematite. Most of the plagioclase has undergone some alteration to sausserite, which is controlled by cleavage planes, and locally occurs as

Plate 5 Photomicrograph showing typical olivine diabase (crossed polars). The minerals are plagioclase (p), clinopyroxene (c), serpentine after olivine (s) and titaniferous magnetite (black). Note the mesh texture in serpentine grains. (Transmitted light.)

Plate 6 Photomicrograph showing typical olivine diabase (plane polarized light). The minerals are plagioclase (p), clinopyroxene (c), serpentine (s) and titaniferous magnetite (opaque). (Transmitted light.)

c

Plate 7 Photomicrograph showing titaniferous magnetite with reticulate texture. Phases are magnetite (black) and ilmenite which has altered to leucoxene (dark brown). (Transmitted light.)

Plate 8 Photomicrograph showing autobrecciated diabase. Medium green lava (L) occupies the interstices between hematitically altered diabase fragments (D). The rock is cut by a carbonate vein (vertical, C) related to late hydrothermal activity. (Transmitted light.)

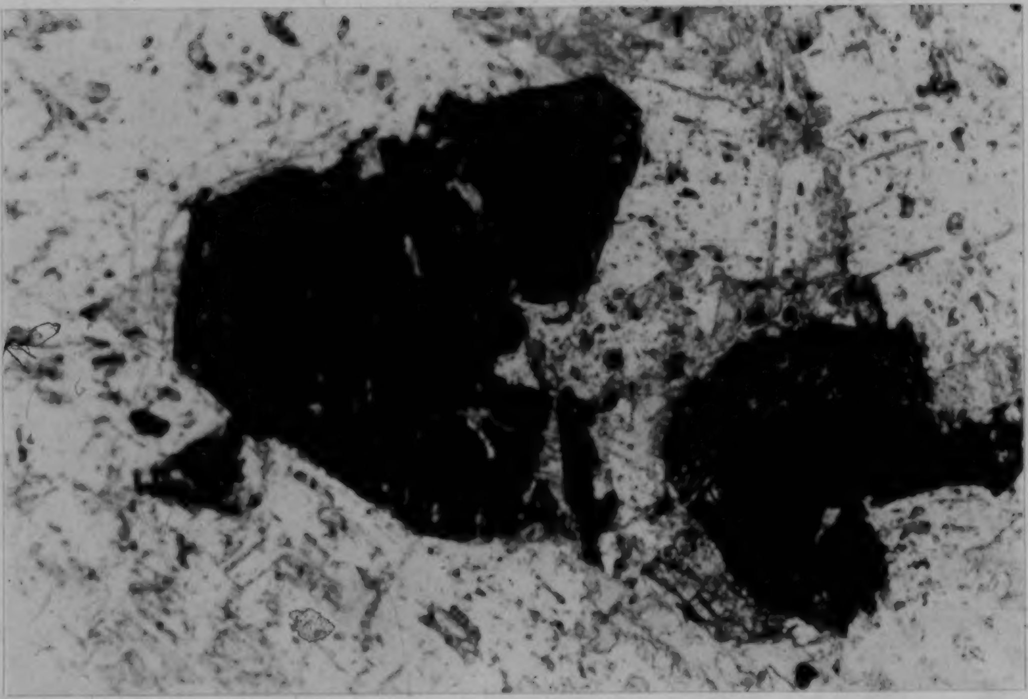

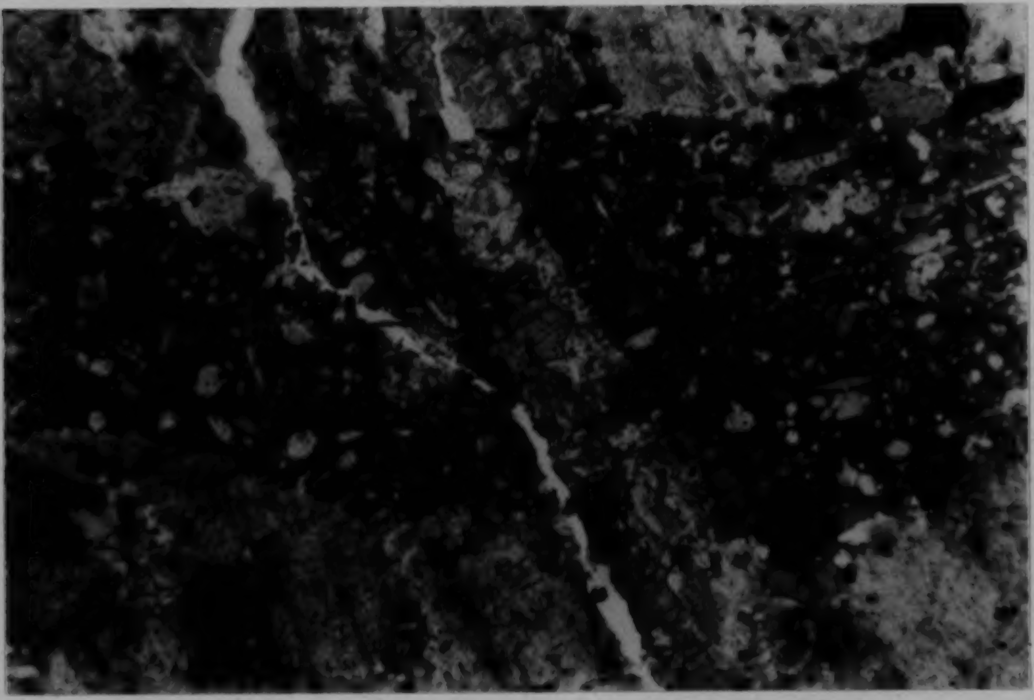

minute fibrous radiating aggregates. Sericite is developed locally. The composition of the plagioclase has been determined as An 39 by the Michel Levy method.

(ii) Clinopyroxene

The clinopyroxene is colorless to very pale brown in color, and is tentatively identified as augite. The perimeter of some grains has undergone incipient alteration to uralite. The pale brown color may suggest the presence of trace amounts of titanium, but may also be due to ferric iron (Moorehouse, 1959, p. 233). The pyroxene tends to occur as isolated subhedral stumpy prisms and square grains in the interstices between plagioclase laths. It also occurs in clusters which may partially to completely rim altered olivine crystals. Locally, it exhibits a subophitic texture with plagioclase.

(iii) Olivine (now altered to serpentine)

Olivine generally occurs as altered,

ovoid to rounded anhedral grains in the interstices between plagioclase laths. A few relic six sided grains were also noted. The olivine is pervasively altered to a variety of minerals, of which serpentine is the most important. Serpentine commonly exhibits a well-developed mesh structure along relic curving fractures in the olivine. Iddingsite is generally associated, and occurs as granular dark rims of high relief around the perimeter of the grains. This may imply that the original olivine was zoned, with iron-rich rims (Kerr, 1977, p. 382). In some instances, the perimeter of the serpentine grains has an orangy brown iron-oxide stain. Magnetite occurs locally as an alteration product along relic cracks in the serpentine. Bowlingite was also tentatively identified in one instance.

(iv) Chlorite

Chlorite occurs in elongate irregular to interstitial patches, which suggests it is an alteration product of glass.

(v) Opaques

Titaniferous magnetite occurs as irregular and subhedral tabular grains which appear to be preferentially associated with serpentine and clinopyroxene. In most instances, it occurs as reticulate grains exhibiting triangular or rhombic patterns. These are exsolution features suggestive of slow cooling, during which the original mineral exsolved into an intergrowth of magnetite and ilmenite. The ilmenite has subsequently altered to leucoxene (Plate 7).

(vi) Other Minerals

Trace amounts of biotite and possibly apatite, and minor orthoclase were identified in the diabase. Biotite occurred as a single slightly elongate ragged grain which was highly corroded, and clearly out of equilibrium with the surrounding rock. Orthoclase is probably related to a late hydrothermal event, and is described at a later point in this chapter (p. 71).

2. Color Index[1]

Two point counts were carried out on a sample from the central part of the intrusion and are tabulated below.

	Plagioclase	Clinopyroxene	Serpentine	Chlorite	Opaques	Orthoclase
(i)	59	19	8	8	4	2
(ii)	61	12	15	5	5	2

These indicate that the ratio of feldspar to mafics plus opaques is approximately 60:40, and suggest a color index of 40.

3. Zonation

The diabase exhibits a crude zonation which is related to its cooling history. This zonation is expressed through textural and mineralogical changes between the chilled margins and the more slowly cooled inner parts of the intrusion.

Texturally, the centre of the plug can be described as holocrystalline diabasic, and locally subophitic. Plagioclase crystals are generally well developed and crudely aligned. Towards the south

[1] Color index is defined as the percentage of dark minerals in a rock (Williams, Turner and Gilbert, 1954 p. 33).

contact of the intrusion however, the texture becomes intersertal to hyalo-ophitic, with phenocrysts of plagioclase and olivine in a very fine grained to glassy groundmass which has altered largely to chlorite. Plagioclase in these zones is generally in random orientation and is less euhedral. These features are consistent with rapid chilling of the diabase. In general, ferromagnesian minerals are less abundant in chilled zones due to the lack of pyroxene which was apparently late to crystallize and is therefore quenched in the glass.

Titaniferous magnetite is generally more abundant in the chilled margins, and may comprise as much as 10% to 15% of a given sample. These opaques tend to be more euhedral and generally non reticulate in chilled zones. This further attests to rapid cooling along the margins, during which magnetite-ilmenite phases were not able to exsolve.

Plagioclase crystals in border zones exhibit at least weak alteration to chlorite which replaces them both externally and along cleavage planes.

To a lesser extent, this primary zonation is expressed in samples which approach the postulated northern margin of the intrusion. Texturally, these samples are somewhat porphyritic to intersertal, with phenocrysts of plagioclase and altered olivine in a very fine grained groundmass of plagioclase and chlorite. Poorly developed tabular to stubby grains of chlorite are probably after pyroxene, and are often associated with altered olivine. As at the south margin, opaques are relatively abundant, and exsolution textures are not developed.

4. Contact Phenomena

Immediately along its south margin, the diabase exhibits a well-defined brecciated texture, with angular blocks of reddish diabase in a featureless dark green chloritic matrix. The diabase owes its red color to a fine dusting of iron oxides, particularly around the edges of feldspar grains (Plate 8).

In thin section, the chloritic matrix between the diabase fragments is a porphyritic lava containing abundant microlites of untwinned plagioclase in a groundmass of patchy chlorite. The feldspar microlites are arranged in subparallel orientation (trachytic texture) and exhibit minor alteration to chlorite and sausserite. Using the microlite method for plagioclase determination (Moorehouse, 1959, p. 55), the plagioclase was found to be An 39 which is identical to the composition of plagioclase in the diabase itself.

Opaques are present in minor amounts. These have anhedral to square or rhombic outlines and are thought to be mainly magnetite.

The model which best explains these features is autobrecciation. Conceivably, stresses related to emplacement of the diabase, or convection currents within the magma, caused brecciation of the chilled and solidified marginal part of the intrusion. Immediately following this brecciation, molten magma from adjacent parts of the intrusion filled these fractures. Autobrecciation suggests that the parent magma was highly volatile (Badham 1979, p. 69).

The restriction of hematitic alteration to the south margin of the diabase suggests that it is a contact phenomenon related to the adjacent hematitic sediments.

5. Alteration

(i) Late Magmatic and Deuteric Alteration

The alteration of olivine to serpentine, iddingsite and magnetite is probably a late magmatic event (Moorehouse, 1959, p. 179). Subsequent deuteric alterations probably include the development of uralite, chlorite, saussurite and leucoxene.

(ii) Hydrothermal Alteration

The diabase has undergone potassium and carbonate alterations which are almost certainly related to a late hydrothermal event. These alteration types are strongly developed in the BBX diatreme where potassium alteration is intimately associated with mineralized zones (refer to Chapter 4, p. 108).

In the diabase, potassium and carbonate alterations are strongly developed along the south margin, but are absent from the interior of the intrusion. Incipient carbonate alteration is also evident in outcrops which approach the postulated northern margin of the diabase. These features suggest that late hydrothermal fluids migrated from depth along the relatively pervious contact between the intrusion and the country rock.

(a) Potassium Alteration

Potassium alteration has been identified through thin section studies and sodium cobaltinitrite staining of hand-specimens. Staining indicates that this alteration is related to migration of fluids along fractures in the diabase, and is therefore relatively localized. Altered zones contain othoclase, sericite and quartz as significant phases.

Orthoclase occurs as well developed rims around plagioclase crystals. These rims contain abundant finely divided iron oxide. Internal replacement of plagioclase by orthoclase is very regular and occurs along crystallographic directions. Locally, replacement antiperthite textures are developed.

Sericite is formed at the expense of chlorite and plagioclase, where it is best developed along cleavage planes.

Quartz and minor orthoclase occur as small rounded grains in the angular interstices between plagioclase laths. These grains are generally very fresh, and represent a later phase which veins and replaces, metasomatically altered feldspar.

These features suggest that the hydrothermal event commenced with the introduction of potassium-rich fluids which sericitized chlorite and plagioclase, and metasomatically altered plagioclase to orthoclase. As alteration proceeded, quartz and orthoclase crystallized as discrete phases in the chloritic interstices between plagioclase laths.

Minor chalcopyrite and pyrite occur in the diabase and are associated with potassium alteration.

(b) Carbonate Alteration

Carbonatization postdates potassium alteration, and by comparison is continuous and pervasive along the south margin of the diabase. It is developed to a lesser extent along the north margin.

Carbonate is particularly evident in the chloritic groundmass, but is also developed to some extent in plagioclase. The addition of CO_2 has altered serpentine (after olivine) to a mixture of talc and minor magnesite (Deer Howie and Zussman, 1970, p. 5). Carbonate also replaces earlier hydrothermal orthoclase and quartz.

Staining of selected samples indicates that the carbonate ranges from iron-free to iron-rich calcite.

This phase of alteration does not appear to be associated with mineralization.

6. Late Veining

A final pulse of hydrothermal activity is indicated by late quartz and quartz-carbonate veins, generally less than two cm in diameter, which occur occasionally near the south margin of the diabase. Trace amounts of pyrite and chalcopyrite are associated with these veins (Plate 8).

D. Affinity

The diabase plug appears to be slightly anomalous in composition. In particular, the association of andesine which is typical of andesitic rocks, with olivine, more typical of basalts is unusual. Also, the presence of apatite (?) with olivine and pyroxene is uncommon. Biotite is generally not found in mafic rocks, although it may be quite common in altered basalts (Moorehouse, 1959, p. 167).

The diabase has not been mapped by the GSC, but may represent an intrusion of "Jackson Gabbro (Jg)" (Hoffman, 1977). These irregular intrusions, which are highly variable in grain size and texture, occur in all formations of the Sosan and Kahochella Groups, around discrete volcanic centres (op. cit., "Table of Formations").

CHAPTER 4

PETROGRAPHY OF THE DIATREME

"Diatremes are pipe-like structures filled with brecciated country rocks that are almost invariably admixed with juvenile, magmatic materials. They are formed chiefly by fluidized gas-solid systems that initially rise along fissures, joints, and newly opened fractures. Enlargement of these initial channels into approximately cylindrical pipes results from spalling and slumping of the walls, abrasion and comminution, and various kinds of subsidence."

Lorenz et al, 1975, p. 12.

"Diatremes ----- a general term for a volcanic vent or pipe drilled through enclosing rocks (usually flat-lying sedimentary rocks) by the explosive energy of gas-charged magma."

American Geological Institute, 1962
Dictionary of Geological Terms

I. Form

The surface expression of the BBX diatreme is an elongate resistant ridge trending 35° (az.) and rising up to approximately 50 metres above the adjacent landscape. Because of limited outcrop, the precise boundaries of the diatreme are not well-defined. Topography, drill hole data (Map 3) and distribution of adjacent sediments however, suggest that the diatreme has a somewhat lobate plan. The vent pinches to 75 metres in the centre and forms two lobes of approximately equal size. The more northerly lobe has a maximum width of approximately 145 metres, and that in the south is inferred to be approximately 165 metres wide. The overall plan of the diatreme is an elongate lobate structure whose length (450 metres) is approximately four times its average width.

The diatreme is a transgressive pipe-like body of vent agglomerate, but its precise configuration at depth cannot be inferred from limited drill hole data. It appears however, that the pipe tapers with depth and that lobate plan is continuous in the subsurface (Map 3). The possibility that these data reflect local irregularities in the vent wall must also be considered.

II. General Description

Lithologically, the diatreme is a heterogeneous volcanic breccia, consisting predominantly of mafic volcanic fragments which are juvenile, accessory and accidental in origin. Accidental fragments of sedimentary rock and granitic and diabasic intrusive, derived from the adjacent country rock during formation of the diatreme are present in varying amounts (Plate 9). Breccia fragments lie in a matrix which varies widely in both composition and abundance. The variety and complexity of both breccia fragments and matrix are briefly illustrated in the following discussion.

(A) Breccia Fragments

Volcanic fragments include glassy lava, more coarsely crystalline lava, pumiceous lava and vitric tuff. The edges of the fragments tend to be quite rounded, although their shapes vary widely from almost spherical to blocky and irregular or tabular. They range in size from a few millimetres to several centimetres. The petrography of these fragments is dicussed in detail in section III of this chapter.

Sedimentary fragments include red and grey shale, red siltstone and sandstone, granular and pisolithic hematite, grey chert, and light grey bedded dolomitic marlstone. These fragments tend to be roughly tabular,

Plate 9 Propyllitically altered diatreme breccia. Volcanic fragments (dark green) and fragments of maroon shale and granular hematite (red) are set in a carbonate matrix (brown).

with rounded edges. This reflects original bedding. Harder fragments tend to be more angular because of their more brittle nature. Sedimentary fragments range considerably in size, but on the average tend to be slightly larger than the volcanic fragments. Red shale and siltstone are particularly abundant, and locally may give the rock a reddish tinge.

Granitic fragments from the Archean basement are locally abundant, and are commonly equidimensional and rounded.

Fragments of mafic intrusive are relatively minor. These consist primarily of medium grained plagioclase-rich rocks similar to the border phases of the olivine diabase to the north. Other fragments comprise coarse grained plagioclase phenocrysts set in a dark chloritic matrix.

(B) Matrix

The matrix, which comprises up to approximately 60% of the breccia, can be divided into two major groups.

1. Primary Matrix

The original matrix in the diatreme is finely comminuted rock debris or "rock flour" generated by abrasion of volcanic and other fragments during formation of the diatreme. This material is a pale brown color in thin section, where it has not been extensively altered (Plate 10). In hand specimen it has a waxy texture and a flesh to pale pink color.

2. Secondary Matrix

Following formation of the diatreme, the agglomerate underwent a variety of alterations related to deuteric and hydrothermal processes (refer to section IV, this chapter). Rock flour is particularly susceptible to alteration, and hence occurs rarely in its original form. It is frequently chloritized (Plate 11) and carbonatized (Plate 12), and to a lesser extent hematitized, sericitized and silicified. Minerals formed in this way are generally very finely crystalline and microcrystalline and give the matrix a waxy texture.

In addition to the above a variety of minerals of hydrothermal origin have crystallized as primary phases between breccia fragments. These minerals are generally finely crystalline (approximately 1 to 3 mm), and include carbonate, quartz and minor potassium feldspar.

Plate 10 Photomicrograph of diatreme breccia showing basalt fragments (black) and olivine xenocrysts (green) in a matrix of comminuted rock debris (brown). Rock flour is relatively unaltered. (Transmitted light.)

Plate 11 Photomicrograph of diatreme breccia showing basalt fragments, feldspar xenocrysts (white) and sulfides (S) in a partially chloritized rock flour matrix (green). A late quartz veinlet (Q) with associated sulfides extends from the left to the right of the picture. (Transmitted light.)

Q

Plate 12 Photomicrograph showing carbonatization of rock flour in the matrix. The basalt fragment (at left) and the olivine grain, now altered to talc (T) are set in a matrix of comminuted rock debris. The matrix becomes increasingly more carbonatized away from the fragments; i.e. unaltered rock debris (1), carbonatized rock flour with abundant impurities (2), relatively clean carbonate (3). (Transmitted light.)

Plate 13 Photomicrograph showing basalt fragments (black) and olivine xenocrysts (green) in a matrix of comminuted rock debris. Note the late tongue of carbonate (C). The abrupt contact between carbonate and rock flour suggests that carbonate has infilled open spaces. (Transmitted light.)

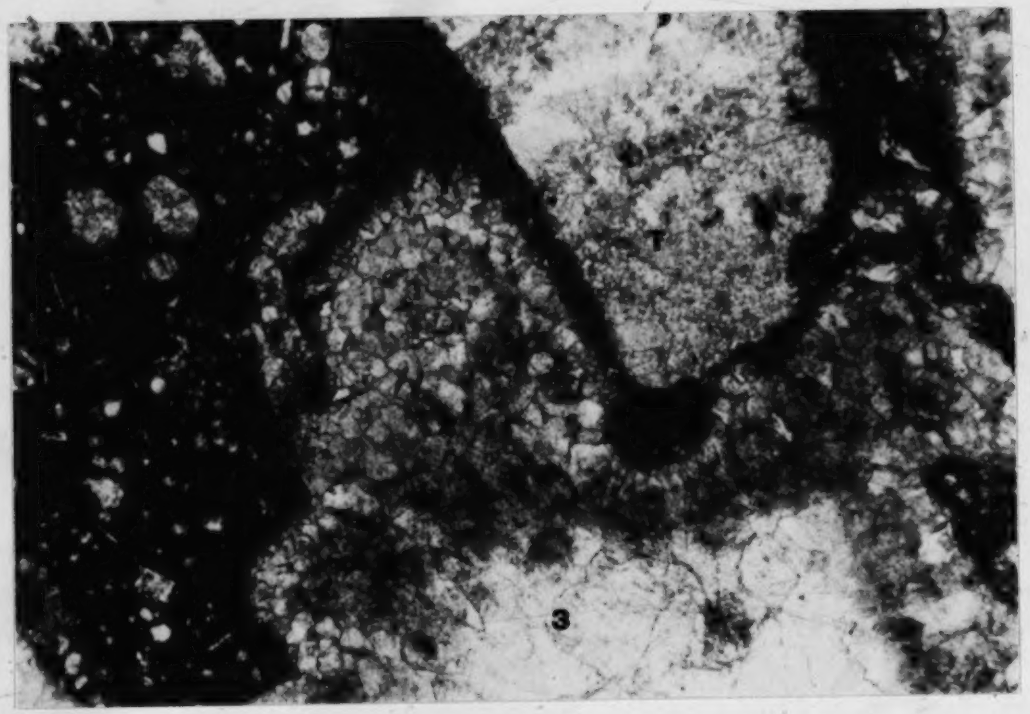
3

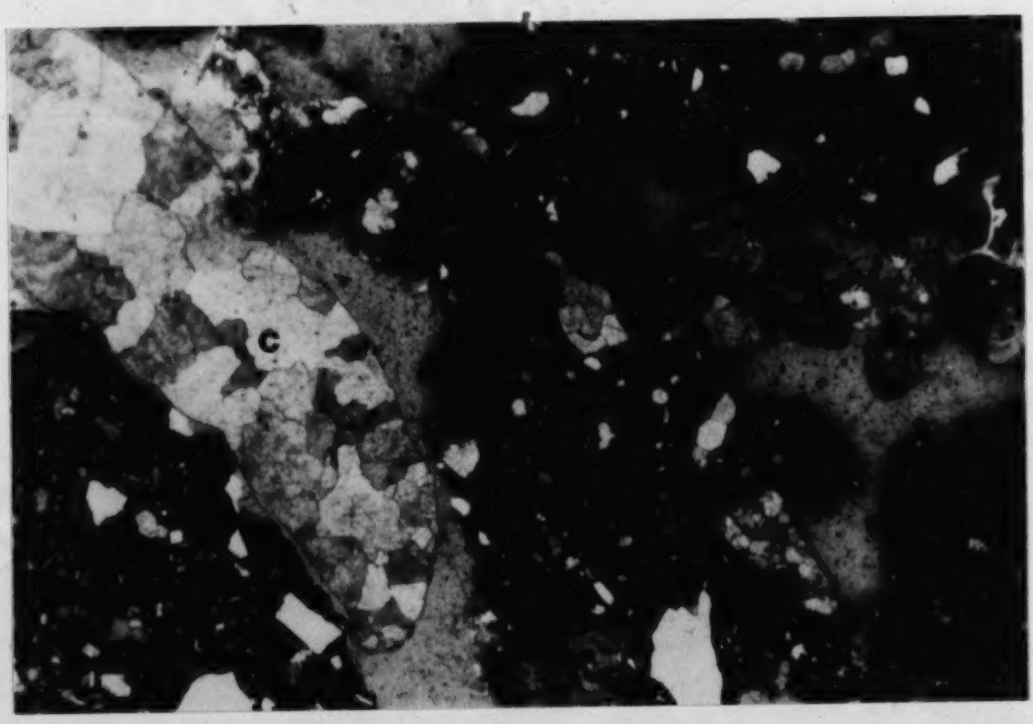
C

Carbonate is by far the major component of the matrix (Plate 13), and varies widely in composition, with iron-poor and iron-rich calcite predominating (this chapter, section IV B 1(ii).

Quartz may be clear and colourless, or tinted by iron impurities, possibly through reaction with adjacent basalt fragments. Locally, it occurs as hexagonal crystals.

Occasionally, the matrix is microcrystalline, and has a poorly defined ribbon structure, with bands of clear quartz and pink carbonate.

Chalcopyrite, galena and barite occur in the matrix in mineralized zones.

III. Petrography of Volcanic Fragments

The volcanic fragments in the diatreme are basaltic in composition and range from glassy, rapidly-chilled dark lava to a more coarsely crystalline, lighter colored lava. These volcanics are porphyritic and contain plagioclase microlites and olivine phenocrysts set in a cryptocrystalline to felsitic groundmass. The petrography of the volcanics is complicated by the effects of devitrification and deuteric and hydrothermal alterations which have obscured original textures and mineralogy to varying degrees. The petrography of the lava is further complicated by the incorporation of abundant xenocrysts; particulary quartz and microcline, and occasionally plagioclase and olivine. Many xenocrysts are readily identifiable by their irregular fragmentary shape. In other cases however, they are difficult or impossible to distinguish from juvenile magmatic material.

A. Mineralogy

1. Plagioclase

Plagioclase is generally euhedral and untwinned and ranges from 50 to 450 microns in size, with an average of approximately 120 microns. The plagioclase composition was determined by the microlite method (Moorehouse, 1959, p. 57) from a population of 18 grains, as An 53.

Plagioclase crystals exhibiting lamellar twinning are commonly irregular and may be corroded by the lava. These grains are interpreted as xenocrysts. Compositions of several of the more euhedral twinned crystals were determined using the Michel Levy method (Deer, Howie and Zussman, 1970, p. 333, Fig. 123) as An 38. This composition is very close to that of plagioclase from the adjacent diabase plug. The implications of this will be discussed in Chapter 6.

2. Olivine

Olivine has invariably undergone deuteric alteration to serpentine pseudomorphs. In many instances, iddingsite occurs along relic curving fractures, or rimming the phenocrysts. Occasionally, the perimeter of the phenocrysts is stained an orangy brown color by finely divided iron oxides. Secondary magnetite also occurs as an alteration product in some cases.

3. Quartz and Microcline

Quartz and microcline are generally irregular in shape and are thought to be mainly xenocrysts incorporated from adjacent granitic and sedimentary rocks. In many cases however, quartz occurs as rounded grains and is hydrothermal in origin. Quartz occasionally occurs as regular lath-shaped grains which suggests that it has replaced plagioclase. Quartz frequently exhibits undulose extinction.

B. Types of Volcanic Fragments

The volcanics exhibit a wide variety of textures which can be divided into three principle groups. It will become evident in the following discussion that a continuum exists between these extremes.

1. Light Colored Lava (Plate 14)

This lava is a light to medium greyish brown color and generally occurs as rounded to oblong fragments of various sizes. These fragments are often so highly altered that original textures are difficult to discern.

The lava is primarily a very finely crystalline mosaic of optically irresolvable grey birefringent material (mainly feldspar and chlorite) and finely divided iron oxides and leucoxene. Randomly oriented plagioclase microlites can be recognized only occasionally in this felsitic groundmass. Poorly defined squarish chlorite patches, possibly after pyroxene are present locally.

The texture of this lava is best described as hyalopilitic. A series of interconnected rounded and polygonal structures occur in the matrix. These structures contain radial or concentric masses of colorless feebly birefringent material which is probably an intergrowth of plagioclase and possibly chalcedony. This variolitic texture may be the result of devitrification of glass around scattered nuclei or may have been formed by rapid crystallization

Plate 14 Photomicrograph showing "light-colored lava" (bottom right). The matrix (yellow-brown) comprises very slightly chloritized rock flour. (Transmitted light.)

Plate 15 Photomicrograph showing pumiceous lava. Note glass shards (G) and sideromelane (medium brown). The matrix is carbonatized rock flour. (Transmitted light.)

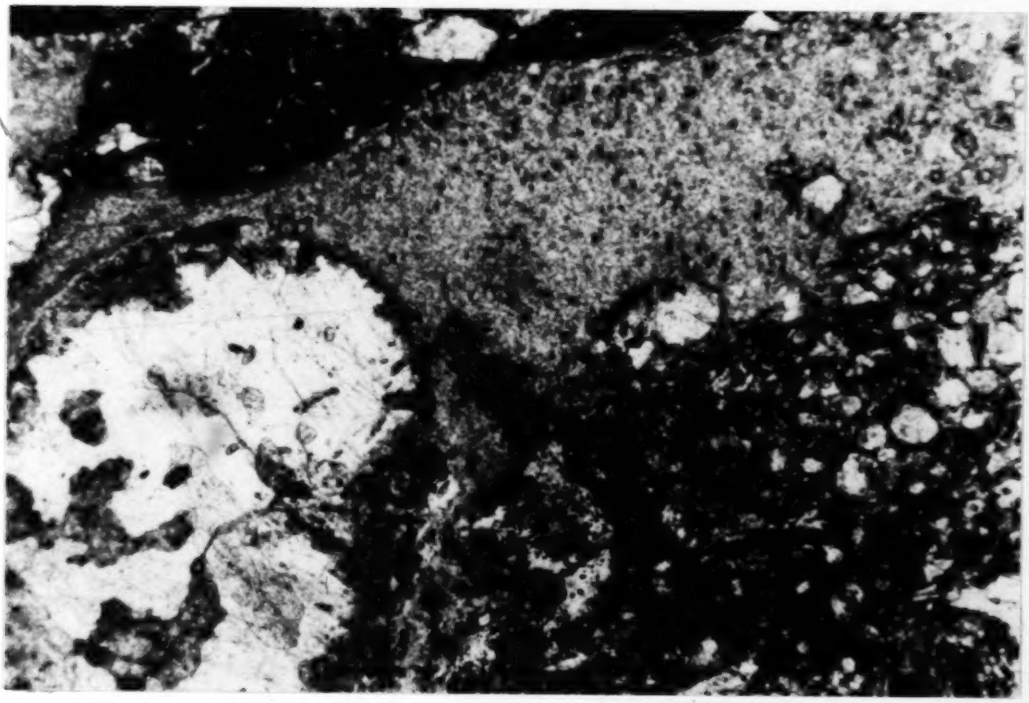

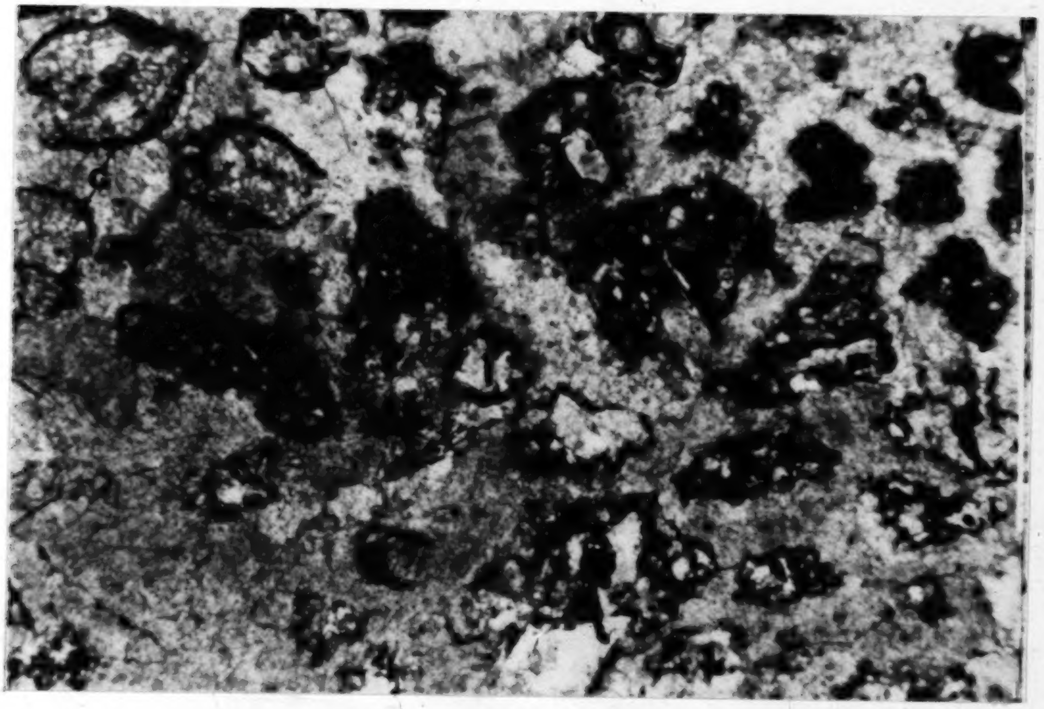

of viscous magma (Williams, Turner and Gilbert, 1954, p. 24). These structures are generally free of iron and titanium oxides.

Similar rounded and polygonal structures are filled with carbonate and weakly colored chlorite. The boundaries of these structures vary from diffuse and irregular to abrupt, and their precise origin is unknown. They may represent varioles which have been preferentially replaced by chlorite and carbonate or gas vacuoles which have been infilled by these minerals.

Some basalt fragments have a medium khaki color. The groundmass in these fragments is semi-opaque and non birefringent and is probably palagonite formed by devitrification of volcanic glass (Hatch Wells and Wells, 1972, p. 458).

The light colored lava is generally more coarsely crystalline than other lava types in the diatreme.

2. Pumiceous Lava (Plates 15, 16 and 17)

Pumiceous, highly vesicular lava and glass shards are present locally in the diatreme. These fragments are generally light to medium brown in color (Plate 15) and have a refractive index greater than 1.54. This suggests that the glass is sideromelane and is therefore nearly anhydrous (Williams, Turner and Gilbert, 1954, p. 39).

In some instances, pumice fragments may be quite angular (Plate 17) and are interpreted as accidental or accessory fragments from rocks intruded by the diatreme. Generally however, the pumice fragments are small highly abraded grains, and are thought to be juvenile in origin. These grains are particularly susceptible to hydrothermal alteration (carbonatization), and are more readily abraded during formation of the diatreme. This is evidenced by the fact that they often occur supported in a matrix of rock flour which has been subsequently carbonatized.

Plate 16 Photomicrograph showing highly vesicular to pumiceous lava. Basalt is oxidized (brown). (Transmitted light.)

Plate 17 Photomicrograph showing vesicular glassy lava set in a matrix of carbonatized rock flour. Basalt glass is altered to sideromelane (light brown). The angular shape may suggest it is an accidental fragment from a pre-existing volcanic pile. Note sulfides (black). (Transmitted light.)

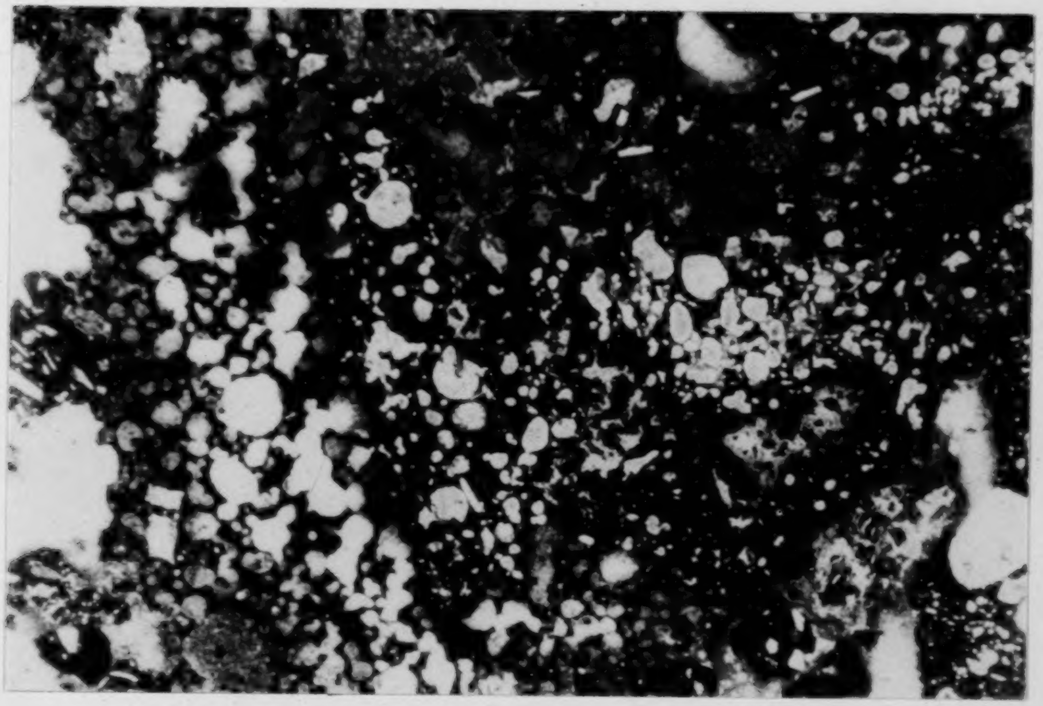

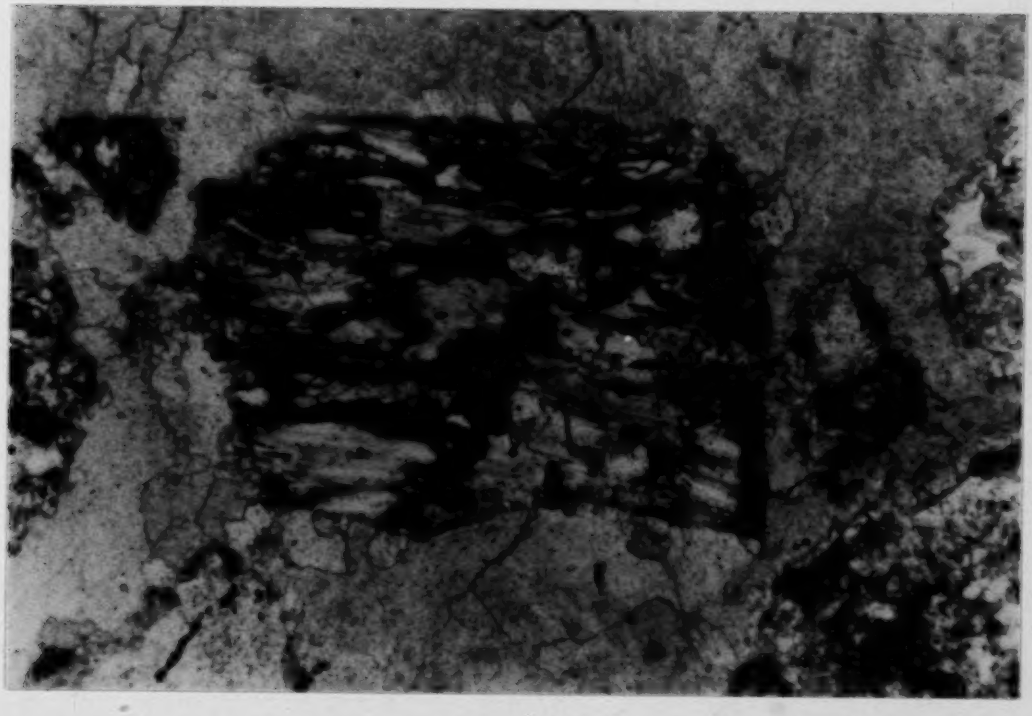

In some instances, more massive porphyritic black lava fragments (refer to section 3 below) may have pumiceous and highly vesicular appendages or fringes which are altered to brown sideromelane.

Locally, tabular fragments of vitric tuff with angular corners occur in the diatreme. These are composed almost entirely of glass shards which are flattened and compressed parallel to the long axis of the fragment. These almost certainly represent bedded tuffs which were incorporated into the diatreme from an existing volcanic pile. Although they are now largely altered to chlorite, sericite and pumpellyite, their shape suggests that these tuffs were well indurated prior to their incorporation in the diatreme.

3. Black Lava (Plates 18 and 19)

Black lava is a relatively minor constituent, and tends to occur as elongate sinuous bodies which frequently surround and embay other

Plate 18 Photomicrograph showing black lava (B) enclosing a feldspar xenocryst (F). Note pumiceous lava and matrix of comminuted rock debris. The light green mineral occupying vacuoles in the pumiceous lava is pumpellyite. (Transmitted light.)

Plate 19 Photomicrograph showing black lava (B) enclosing a fragment of glauconitic sandstone (bottom of picture). The matrix of the agglomerate is carbonatized rock flour (medium brown). (Transmitted light.)

B

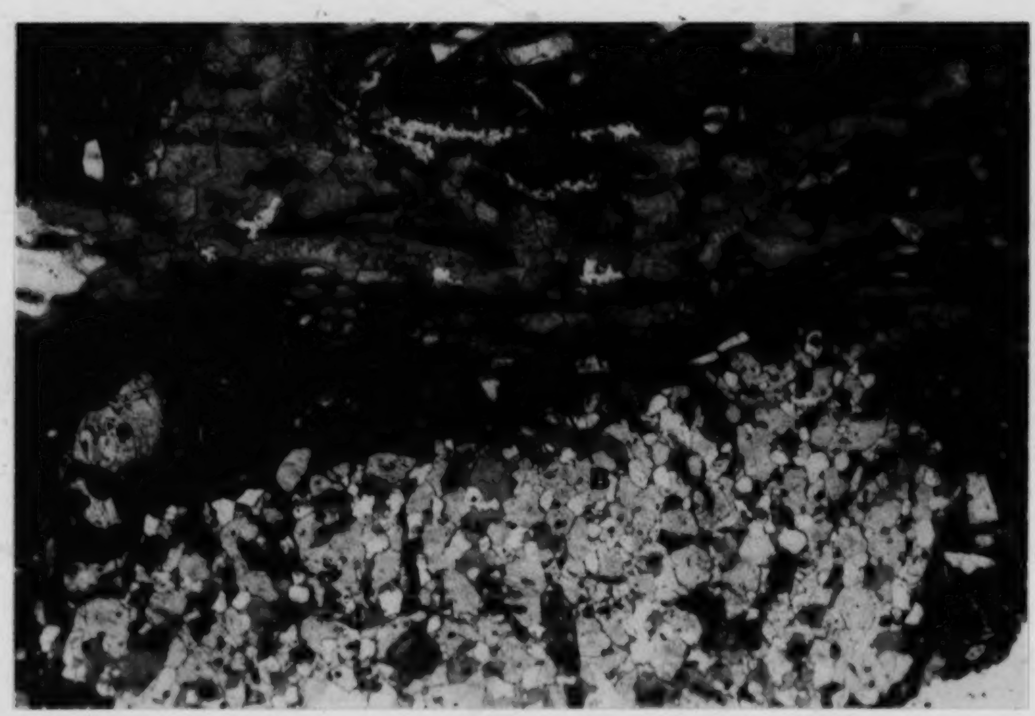
B

fragments including granite, shale, sandstone, light colored lava and pumiceous lava.

The lava consists of plagioclase microlites set in a black opaque microcrystalline matrix. In addition to an hyalopilitic texture, the lava can be described as trachytic because of the alignment of feldspar laths. Also, gas vacuoles, now filled with secondary chlorite, calcite and chalcedony are elongated parallel to the feldspar laths. Both the vacuoles and the feldspar laths are oriented parallel to the elongation of the basalt or to contacts between the lava and the enclosed fragments. In some instances these features are paralleled by elongate sinuous bodies of chlorite within the lava mass. This probably represents altered rock flour incorporated during formation of the diatreme.

The above features suggest that the black lava is a predominantly late molten phase which incorporated accessory and accidental fragments of vent and wall rock during formation of the diatreme. That it is more finely crystalline that the light colored lava implies that the magma was rapidly chilled. The dark color of this lava results mainly from its relatively fine grain size, but may reflect in part the failure of ilmenite to break down to leucoxene.

C. Metamorphic Grade

Pumpellyite has been identified locally filling vacuoles in fragments of vesicular basalt (Plate 18). It also occurs with pumiceous fragments and is well developed in fragments of vitric tuff. Prehnite was identified in one instance.

The association of prehnite and pumpellyite is characteristic of low grade metamorphism of mafic volcanic rocks at low pressures (Winkler, 1979, p. 180, 181). The rocks have been only partially reconstituted and have not yet reached greenschist facies metamorphism as evidenced by the presence of prehnite and pumpellyite (Turner, 1968, p. 268). The assemblage chlorite-prehnite-pumpellyite most closely resembles the prehnite-pumpellyite-metagreywacke facies (op. cit., p. 266).

IV. Alteration Of The Diatreme

A. General Remarks

At the surface, the agglomerate is generally dark green in color. In the subsurface however, it may be pale to dark green, yellow-brown, medium brown, khaki, off-white, red or purple. This variation is primarily a function of the alteration type, the intensity of alteration and the degree to which alteration types are superimposed.

The study of alteration assemblages in the diatreme is complicated by the difficulty in distinguishing hydrothermal alteration products from those related to deuteric and metamorphic processes. Minerals such as carbonate and chlorite are readily formed in a variety of environments and are difficult to relate with certainty to a particular event. It is apparent from a variety of studies that the principle alteration types are propyllitization, potassium alteration and carbonatization. Minor alterations are hematitization, silicification and chloritization.

Alteration in the diatreme is generally restricted to basalt fragments and finely comminuted rock debris in the matrix. Accidental fragments of granitic and sedimentary rock are relatively unaltered.

B. Methodology

Alteration assemblages have been determined primarily through staining techniques and X-ray diffractometer studies, supplemented by thin section examination.

1. Staining Techniques

(i) For Potassium (Plates 20 and 21)

A representative suite of hand specimens and thin sections was stained with a saturated solution of sodium cobaltinitrite to test for the presence of potassium feldspar and sericite. Most basalt fragments exhibit at least some degree of potassium alteration, although some are notably unpotassic. Mineralized and visibly altered portions of the diatreme however, are highly potassic. This alteration appears to be related to narrow fractures cutting breccia fragments. Alteration decreases in intensity away from these fractures (Plate 20).

Plate 20 Photomicrograph showing potassic alteration of the agglomerate. Note the narrow potassic veinlets (yellow), and alteration around the perimeter of feldspar xenocrysts (F). The yellow color is sodium cobaltinitrite stain. (Transmitted light.)

Plate 21 Photomicrograph showing potassic alteration of basalt fragments. Note potassic alteration (yellow) of the perimeter of feldspar xenocrysts (f), and of the plagioclase microlites in the lava. (Transmitted light.)

F

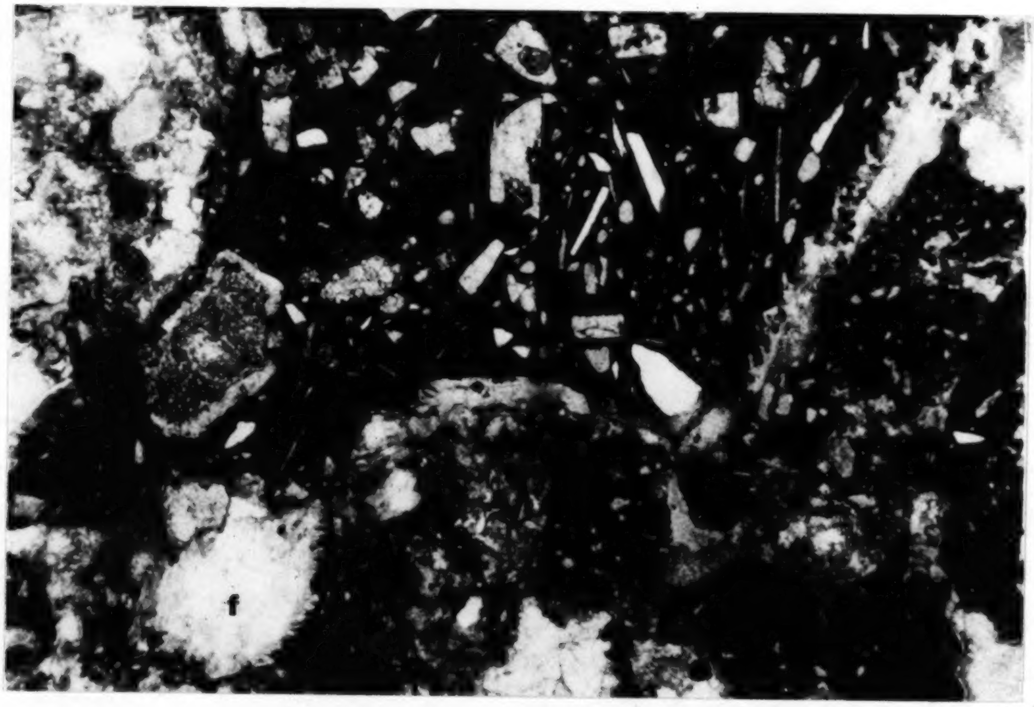
f

(ii) For Carbonate

A total of 26 carbonate samples were selected from the diatreme and stained to determine their composition. The results are tabulated below.

Mineral	Formula	Abundance (%)	
Iron-free Calcite	$CaCO_3$	1.9	
Iron-poor Calcite	$CaCO_3$ with Fe	32.7	Calcite Group
Iron-rich Calcite	$CaCO_3$ with Fe	38.5	73.1%
Iron-free Dolomite	$Ca\,Mg\,(CO_3)_2$	1.9	
Ferroan Dolomite	$Ca\,Mg\,(CO_3)_2$ with Fe	15.3	Dolomite Group
Ankerite	$Ca(Mg,Fe)(CO_3)_2$	9.6	26.8%

2. X-Ray Diffractometer Studies

X-ray powder diffractograms were run for four basalt samples representing mineralized and unmineralized zones. Phyllosilicate identification was made according to the system of Hathaway, in which each sample is run four times; untreated, glycolated overnight, heated to 400°C for one half hour, and heated to 550°C for one half hour.

The following minerals have been identified.

(i) Chlorite

In the two samples in which it was identified, the mineral was found to be a trioctahedral chlorite, but the specific isomorph is not well defined.

The petrography of chlorite in the diatreme is sufficiently complex that it would be unrealistic to assume a specific composition for this mineral.

(ii) Muscovite (Sericite)

Muscovite is restricted to samples from potassically altered and mineralized zones. The best fitting isomorph of this mineral is lithian muscovite (ASTM #14-11)

In normal muscovite, lithium substitutes for aluminum in the octahedral site. Up to approximately 3.5% Li_2O may enter the mineral without altering its structure to lepidolite (Deer, Howie and Zussman, 1970, p. 202). This mineral may account for the presence of small but varying amounts of lithium in the diatreme (Table 1).

(iii) Silicates and Carbonate

Other minerals identified by X-ray diffraction are ferroan dolomite, plagioclase, potassium feldspar and low quartz. The precise identity of the potassium feldspar is not clear from these studies, which show it to be either iron-bearing orthoclase [K(Al, Fe^{3+}) Si_3O_8] or microcline.

C. Discussion of Alteration Assemblages

1. Deuteric Alteration

(i) Propyllitization (Plate 9)

The process of propyllitization is generally associated with andesitic rocks (Williams, Turner and Gilbert, 1954, p. 96) where it is ascribed to hydrous carbon dioxide-rich deuteric solutions. Propyllites, in their early stages of formation are characterized by a drab green color in hand specimen, and the presence of secondary chlorite, calcite, sphene, iron oxides and serpentine (Williams, Turner and Gilbert, 1954, p. 97). Although the diatreme volcanics are basaltic in composition, the presence of chlorite, serpentine and iron and titanium oxides is certainly suggestive of a propyllitic assemblage. At least some carbonate may also be related to this alteration.

The petrography of chlorite in the diatreme is complex. It develops in the matrix at the expense of finely comminuted rock debris (Plate 11), and occurs rimming basalt fragments, and infilling vacuoles in basalt fragments. It also occurs with volcanic glass in the matrix of basalt fragments.

2. Hydrothermal Alteration

(i) Potassium Alteration

The term potassium alteration refers to all processes in which new minerals are formed by the introduction of potassium. Included under this heading are potassic alteration and sericitic alteration. Within the limited scope of this study however, these alterations have not been specifically distinguished.

The potassium alteration assemblage includes potassium feldspar, muscovite [sericite, ± lithium (?)], and fine grained pyrite. Potassium feldspar is developed both as a primary phase and as a product of metasomatic replacement of plagioclase.

In the incipient stages of alteration, plagioclase is replaced metasomatically by potassium feldspar. Plagioclase phenocrysts exhibit varying degrees of alteration (Plate 21).

As alteration proceeds, the chloritic groundmass of basalt fragments, and the chloritic matrix between basalt fragments is sericitized. This alteration is illustrated in the following schematic reaction:

chlorite + Al + Si + K + H^+ $\rightarrow$
muscovite + Fe^{2+} + Mg^{2+} + H_2O (Meyer and Hemley, 1967, p. 207).

Varying amounts of lithium are probably incorporated into the sericite lattice at this time. Sericite is also developed occasionally in plagioclase phenocrysts.

In advanced stages, potassium alteration is characterized by pervasive sericitization and by the formation of pyrite. Original textures are largely destroyed. In thin section, these basalt fragments are drab khaki green and brown in color, and appear as semi-opaque, homogeneous, optically irresolvable masses. The fragments have been completely reconstituted to a very fine grained intergrowth assumed to consist of sericite, potassium feldspar, quartz, and iron and titanium oxides.

In intensely altered zones, where original phases are completely modified, potassium feldspar crystallizes as a primary mineral in the matrix, around the perimeter of basalt fragments, and in narrow veinlets crosscutting the breccia.

In hand specimen, basalt fragments change in color from dark green (Propyllites) to drab shades of light green, light brown, and ultimately medium brown as potassium alteration increases in intensity. Basalt fragments in the more highly altered zones have a powdery to somewhat foliated texture.

Most basalt fragments in the diatreme exhibit at least weak potassium alteration. Basalt fragments in mineralized zones however, have undergone moderate to strong potassium alteration. This alteration is therefore intimately associated with and characteristic of mineralized zones in the diatreme. In general, the intensity of potassium alteration is directly proportional to the concentration of mineralization. This relationship is discussed further in Chapter 10.

(ii) Carbonatization

Carbonate is a common alteration product, and may be associated with a variety of alteration types, including propyllitization and potassium alteration. In the BBX diatreme however, carbonate is generally a late phase, and is so quantitatively important that it has been established as a separate alteration type.

Carbonatization is related to a late, non-mineralizing phase of hydrothermal activity. This alteration postdates potassium alteration and the main pulse of mineralization, and predates the formation of quartz and quartz-carbonate veins.

Carbonate alteration affects mainly the basalt fragments and finely comminuted rock debris in the matrix. Accidental fragments of granitic and sedimentary rock are also altered though to a lesser degree. Zones which have undergone pervasive potassium alteration are generally very resistant to carbonatization.

Carbonate alteration varies in intensity, and locally may be so pervasive that basalt fragments are barely recognizable. Pumice fragments are particularly susceptible to carbonate alteration. In fragments of porphyritic basalt, carbonate develops first in vacuoles and replacing feldspar phenocrysts, and ultimately affects the entire rock. Serpentine in carbonatized zones is altered to a mixture of talc and carbonate (presumably magnesite, Deer, Howie and Zussman, 1970, p. 5) (Plate 22).

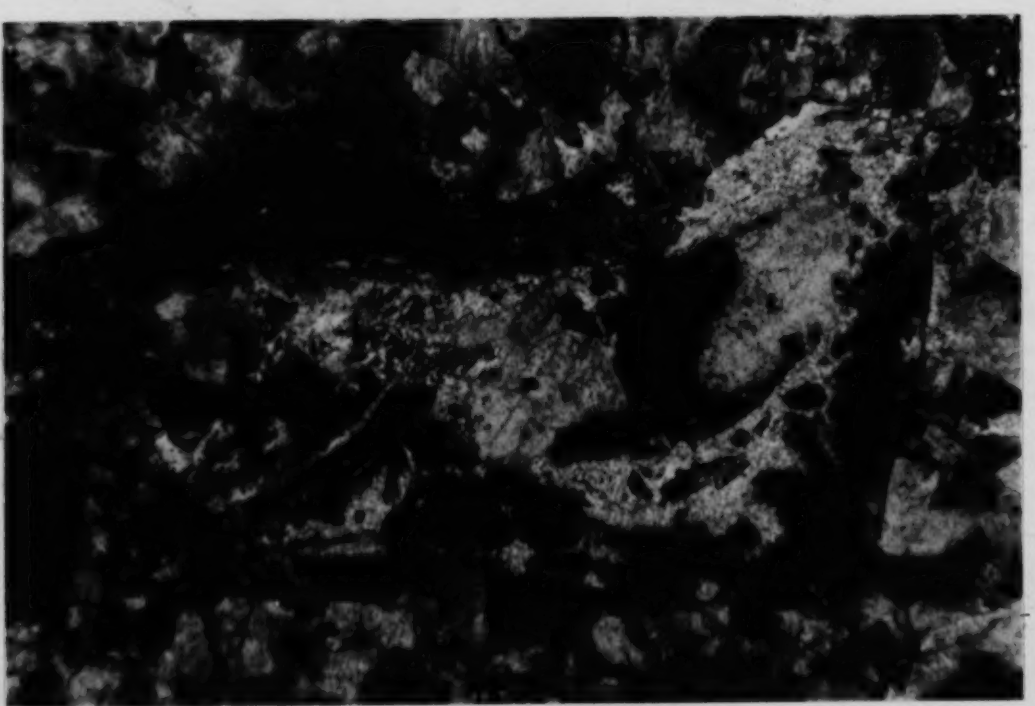

Plate 22 Photomicrograph showing carbonatization of olivine. The olivine grain has been altered to serpentine (dark green) by deuteric processes. Strong carbonatization has subsequently altered serpentine to a mixture of talc (t) and minor magnesite. (Transmitted light.)

Finely comminuted rock debris is usually highly carbonatized. Carbonate in these zones is generally very finely crystalline, tends to have abundant finely divided impurities, and is only semi-transparent (Plates 12 and 19). Matrix carbonate is occasionally fine or medium crystalline, in which case it is relatively clean and transparent. Vuggy carbonate is developed locally. These features suggest that carbonatization commenced with alteration of rock flour and breccia fragments. As alteration proceeded, carbonate precipitated as more coarsely crystalline primary phases in the interstices between breccia fragments.

The presence of CO_2 in an aqueous solution gives rise to varying proportions of carbonic acid, H_2CO_3 (Barnett and Wilson, 1958, p. 319). Although H_2CO_3 is a weak acid, it is probable that it results in breakdown of basalt fragments, and in release of Ca^{2+}, Fe^{2+} and Mg^{2+}. The combination of Ca^{2+} and varying amounts of Fe^{2+} and Mg^{2+} with CO_3^{-2} results in the formation of the variety of carbonates present in the diatreme (see Table, p. 105).

There is a possibility that the change from iron-poor to iron-rich calcite is controlled by the degree of carbonatization of adjacent basalt fragments. The more highly altered fragments tend to be associated with iron-rich calcite, while less altered volcanics are associated with iron-poor calcite.

(iii) Silicification

The BBX diatreme is cut by numerous quartz-carbonate veins and occasional quartz veins averaging 1 or 2 centimetres in width. Large quartz veins up to 1 metre wide occur at several locations on the property (Map 2), and one of these cuts the northeast margin of the diatreme (location 45). These veins contain minor chalcopyrite and pyrite, postdate carbonatization of the diatreme and represent the final pulse of hydrothermal activity. Wall rock surrounding these veins has been silicified to the point where it is either unidentifiable, or occurs only as remnants. Where these veins cut the Akaitcho Formation, the sediments are bleached.

3. Other Alteration Types

(i) Hematitization

Hematitic alteration is localized in the diatreme, and is particularly well-developed in the matrix of comminuted rock debris, and to a lesser extent in basalt fragments, especially along their margins. Where it is well developed, this alteration gives the rock a pronounced reddish color.

The origin of hematite in the diatreme is speculative. Because hematite is not spatially related to mineralization in the diatreme, a hydrothermal origin is not considered probable. A late oxidizing phase of hydrothermal activity has affected the diatreme (Chapter 10), but these zones are not hematitically altered.

The mode of occurrence of hematite, described above, suggests that it may be the result of oxidation of pyroclastic ejectamenta by steam during formation of the diatreme. Oxidation of magnetite to form hematite in this way is known as martitization (Ramdohr, 1969, p. 907). Implicit in this postulate is that the diatreme was vented at the surface during its formation.

The present limited distribution of hematitization is thought to be in part original, but it may also represent zones which for various reasons have not undergone deuteric or hydrothermal alteration.

(ii) Chloritization

Several features suggest that the occurrence of chlorite in the diatreme is not due solely to deuteric process.

(a) Chlorite lines narrow dilatant fractures which are generally filled with medium crystalline (1-3 mm) carbonate, and occasionally rims basalt fragments in zones where the matrix is predominantly carbonate. The occurrence of chlorite adjacent to carbonate suggests that it is a contact phenomenon developed in the presence of carbonatizing solutions.

(b) The diatreme is cut by abundant chlorite slips and shears (slickensided) which crosscut both the matrix and the basalt fragments in zones of propyllitic, potassium, hematitic and carbonate alteration. Most of this chlorite probably postdates the main mineralizing event as evidenced by the fact that these shears cut basalt fragments which have undergone potassium alteration.

V. Affinity Of The Diatreme

Determination of the composition and affinity of the diatreme is complicated by the following factors:

(A) Deuteric and hydrothermal solutions have altered the original chemistry, mineralogy and textures of the rock. This makes classification on the basis of chemistry or mineralogy unreliable. Carbonatization is generally so intense that even relatively stable trace elements such as Ti, Zr and Y would not be reliable indicators.

(B) The petrography of the diatreme is complicated by the presence of abundant xenocrysts which in some cases cannot be distinguished with certainty from juvenile volcanic material. Moreover, the significance of different lava types in the diatreme is uncertain. To some extent, these may be interpreted as accessory and accidental fragments incorporated into the diatreme from adjacent country rock, but they may also represent textural varieties of lava from a single volcanic event. These uncertainties make selection of reliable samples for chemical analysis difficult.

In spite of these uncertainties however, the basaltic composition of the diatreme is well established.

The modal composition of the lava was determined from two point counts carried out on relatively unaltered basalt fragments. The results, which are tabulated below, were determined by subtracting identifiable xenocrysts from the total, and normalizing the remainder of 100%.

	Point Count #1		Point Count #2	
	Total (%)	Normalized (%)	Total (%)	Normalized (%)
Groundmass	43	49.43	44	46.81
Plagioclase Microlites	24	27.59	25	26.60
Olivine Phenocrysts	15	17.24	17	18.09
Xenocrysts	13	-----	6	-----
Spherulites, Vacuoles	5	5.75	8	8.51
	100%	100%	100%	100%

This composition is consistent with that of a typical olivine basalt, which contains 20% olivine phenocrysts and 25% plagioclase phenocrysts by volume (Williams, Turner and Gilbert, 1954, p. 40).

The possibility that this basalt has an alkaline affinity can only be inferred. In the type area on Seton Island, the Seton volcanics are chemically alkaline (Olade and Morton, 1972, p. 1110).

Alkaline magmatism is characteristic of deep continental fracture zones, of which the East Arm graben is an example (Badham, 1979, p. 60). The emplacement of basaltic breccia pipes (Seton volcanic centres) in the vicinity of Taltheilei Narrows was controlled by a major deep-seated fault (p. 42, this thesis). That this fault cuts basement rocks is evident from the presence of granitic fragments in the diatreme. It is probable therefore, that these diatremes have a deep-seated origin. Most large clusters of diatremes are related to the rise of alkaline ultramafic and carbonatite magmas (Lorenz et al, 1975, p. 23). The juvenile fraction of the fragmental deposits of diatremes is most commonly related to ultramafic and alkali-basaltic magma (op. cit., p. 52).

CHAPTER 5

STRUCTURAL GEOLOGY

I. Purpose and Scope of Study

The primary purpose of this study is to identify major structures and to determine the factors which control significant geologic features; particularly the diatreme, the diabase plug, and quartz-carbonate veins and stockworks. It is possible on this basis to propose a tentative chronology of structural events in the area.

The analysis is based on measurement of all well-defined structures on the BBX property and immediately adjacent areas, with the exception of the Archean platform. These structures include bedding planes and joints, veins, minor folds, shear zones and slickensides. Many of these data have been plotted on stereograms, and the resultant structural trends have been interpreted in conjunction with major airphoto lineaments shown in Figures 8 and 9.

Structural mapping was governed by two principle limitations.

A. Because of the paucity of outcrop, structural measurements were not taken uniformly across the property. Also, structures are well-developed at some outcrops and almost absent at others. The resultant sampling bias, and the small populations

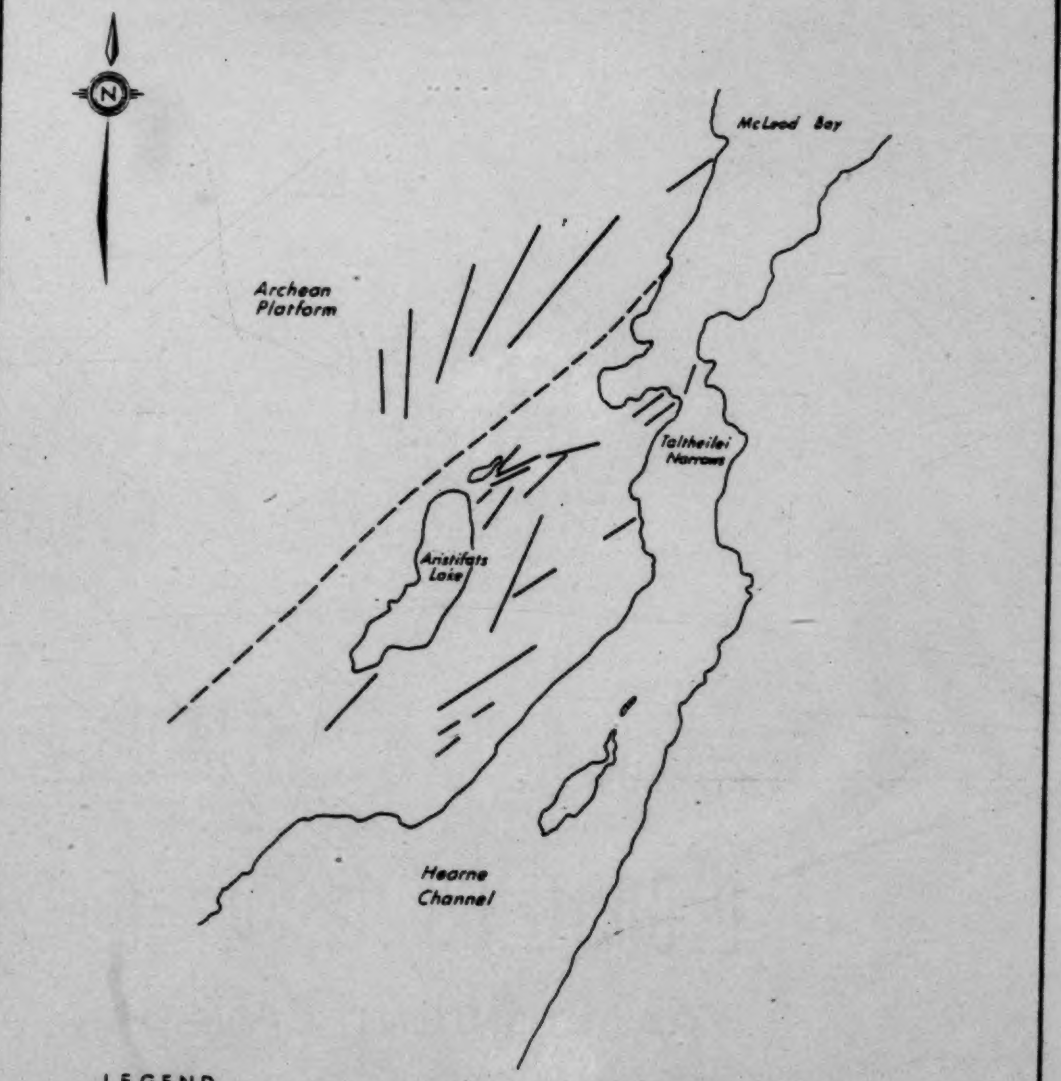
N
McLeod Bay
Archean Platform
Taltheilei Narrows
Aristifats Lake
Hearne Channel

LEGEND

—— LINEAMENT
– – – GEOLOGICAL CONTACT

Figure 8

ARISTIFATS PROPERTY
AND ADJACENT AREAS
NORTHWEST TERRITORIES

AIRPHOTO LINEAMENTS

0 1 2
KILOMETRES

Mackenzie M.D.
NTS 75-L-12

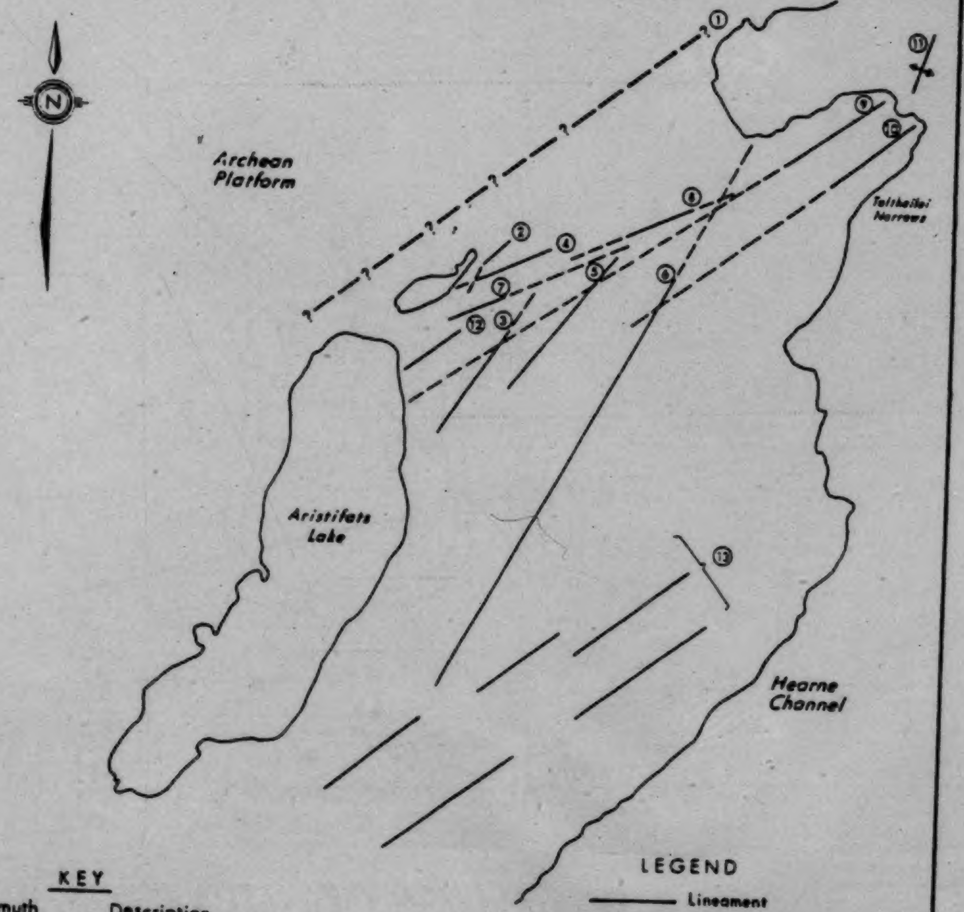
N
Archean Platform
Aristifats Lake
Tsitheilei Narrows
Hearne Channel
①
②
③
④
⑤
⑥
⑦
⑧
⑨
⑩
⑪
⑫
⑬
?

KEY

No	azimuth	Description
①	55°	Archean - Proterozoic contact
②	50°	Diabase plug - north margin
③	35°	Diatreme, surface trend
④	71°	Diabase plug - south margin
⑤	40°	Outcrop trend, basalt tuff, cut by giant qtz vein
⑥	29°	Elongate ridge, boulder till
⑦	69°	Outcrop trend Akaitcho fm, cut by qtz-carb stockwork
⑧	69°	Irregular drift-covered ridge
⑨	52°	Outcrop trend, Akaitcho fm, cut by qtz stockwork
⑩	55°	Outcrop trend Akaitcho fm.
⑪	21°	Anticlinal axis inferred from bedding plane measurements
⑫	57°	Outcrop trend Akaitcho fm.
⑬	54°	Low ridges assumed to be glacial drift

LEGEND

———	Lineament
- - - -	Lineament Extrapolated
— — —	Geological contact

Figure 9

ARISTIFATS PROPERTY
NORTHWEST TERRITORIES
AIRPHOTO LINEAMENTS

0 0.5 1
SCALE IN KILOMETRES

Mackenzie M.D.
NTS 75-L-12

being studied, limit the use of stereograms for detailed analysis.

B. In general, structural interpretations are based on data from sediments of the Akaitcho Formation, where structures are relatively well-developed and well-defined.

Mapping of the diatreme was limited by the difficulty in differentiating a wide variety of poorly-defined structures, including joints, fractures, small faults, and various features related to the formation of the vent iteself. Structural mapping of the diabase was limited to the measurement of a few joint planes, fractures and veins. In general, data from these intrusive bodies are used only to complement interpretations based on measurement of structures in adjacent sediments.

II. Results of Study

A. Bedding and Major Folds

The sedimentary rocks discussed in this study include those just north of the diatreme, those around the perimeter of the diatreme (Map 2), and those in the vicinity of Great Slave Lodge (Map 1).

On the scale of a single outcrop, these rocks are generally not highly deformed, although bedding ranges from steeply dipping to nearly horizontal. Occasionally, the rocks are plastically deformed and exhibit small crenulations and drag folds, in addition to the common presence of vertical joints and small quartz-carbonate veins.

The structure of the sediments is occasionally complicated by the presence of large quartz veins and quartz-carbonate stockworks (p. 49, this thesis). Sedimentary rocks in these locations are commonly brecciated, bleached and silicified.

Figure 10 is a contoured stereogram contructed using 40 bedding measurements. The diagram shows one well-defined and one poorly-defined great circle labelled "A" and "B" respectively.

Great circle A defines a rounded isoclinal fold, the axis of which trends 50° (az) and plunges 15°. A small anticline paralleling this trend can be inferred from bedding measurements at location 37, immediately east of Aristifats Lake (Map 2). Great

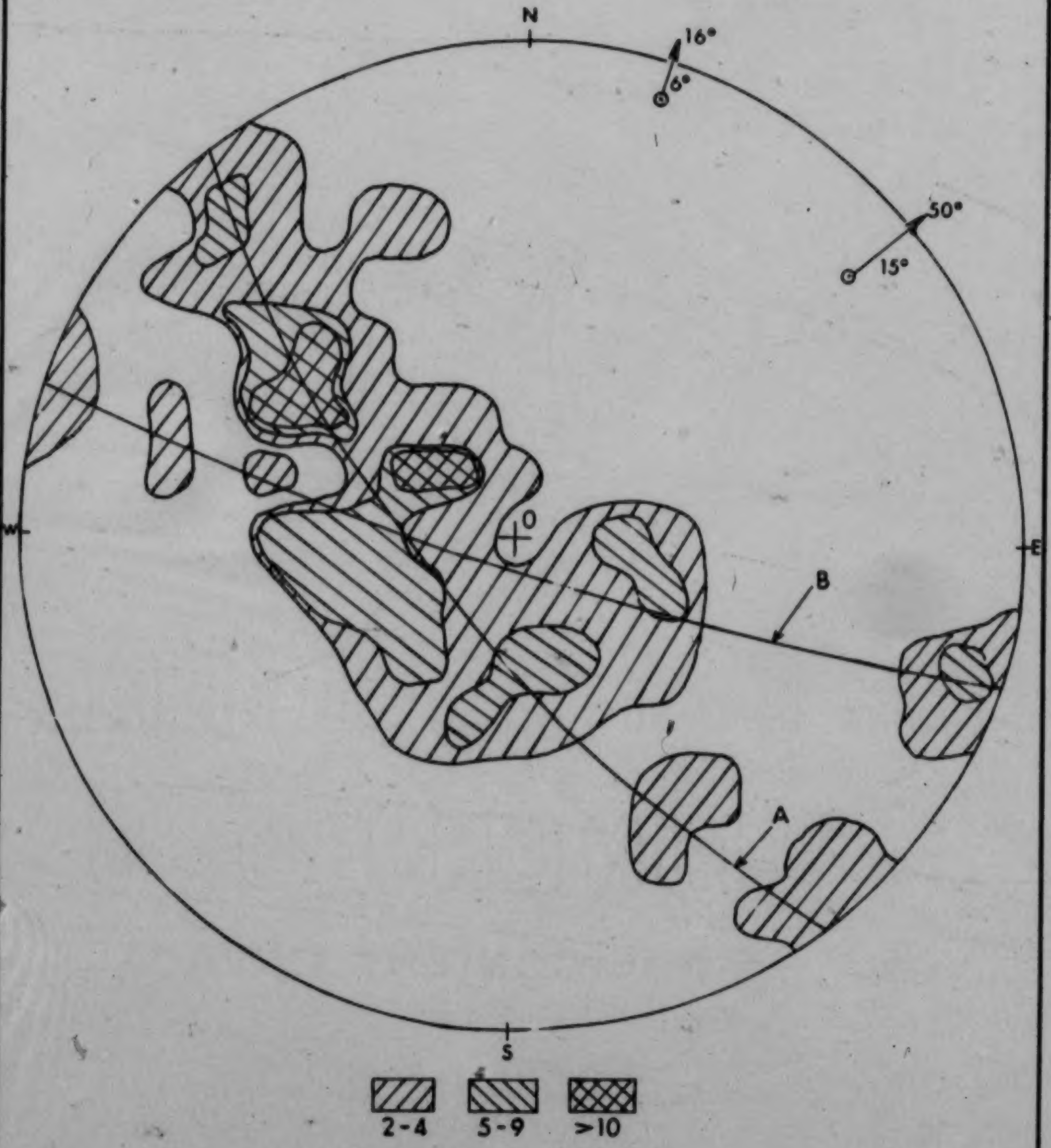
N
16°
6°
50°
15°
W
E
0
B
A
S
2-4
5-9
>10
Percentage of points per
1% area of projection

Figure 10 Stereogram showing Bedding (40 points)

circle B is less well-defined and somewhat discontinuous, but shows a fold trending 16° (az), and plunging 6°. A small anticline paralleling this axis can be inferred from bedding measurements in the vicinity of Great Slave Lodge (Map 1). It is interesting to note that this fold axis closely parallels the major (basement?) fault (trend 18° (az)) controlling the emplacement of diatremes in the vicinity of Taltheilei Narrows (p. 42, this thesis).

B. Joints

Figure 11 (53 points) shows all joints measured in the study area, including those on the BBX and JDA Groups, and those in the vicinity of Great Slave Lodge. Measurements were taken from sediments, both diatremes, and the diabase plug. It can be inferred from this plot that the majority of joints have a vertical dip. The strike of the joints varies widely, but maxima occur at 132° and 144° (approximately southeast). Less well-defined joint sets occur at 77°, 103°, 116°, 124° and 168°.

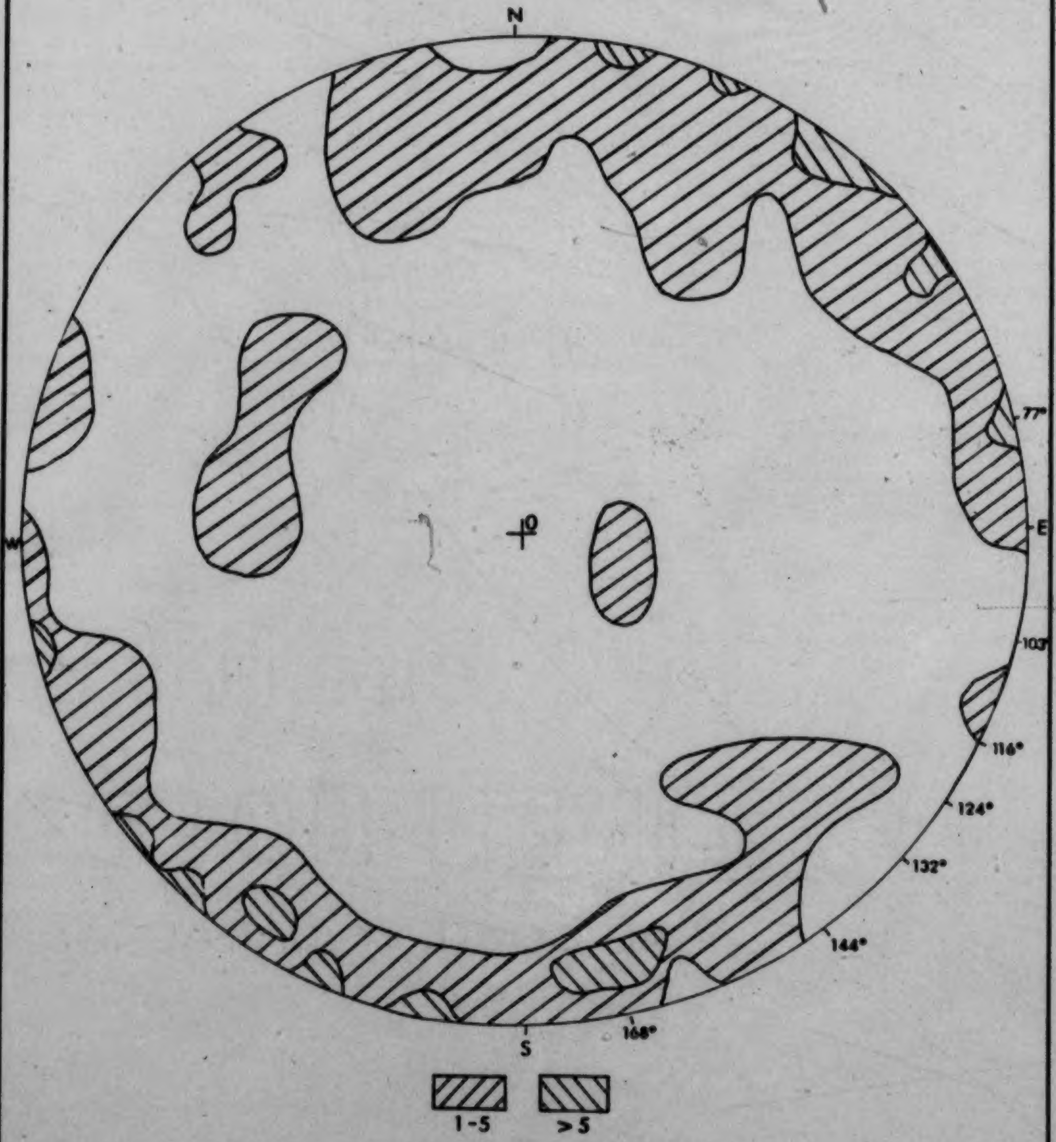
N
77°
E
W
O
103°
116°
124°
132°
144°
S
168°
1-5
>5

Percentage of points per
1% area of projection

Figure 11 Stereogram showing all Joints (53 points)

Figure 12 (26 points) represents only those joints measured from sediments on the BBX property and in the vicinity of Great Slave Lodge. As in the previous case, maxima occur in a generally southeast direction at 103° - 90°, 122° - 90° and 132° - 90°. In addition, three minor joint sets occur at 55° - 90°, 79° - 70° NNW and SSE, and 14° - 18° W. Bedding joints, which occur occasionally in the sediments, are not shown on this stereogram. These joints are commonly dilatant and conform precisely to bedding planes. Hence their orientation and configuration (planar versus curved) is dependent on the intensity of deformation of the host rock.

Figure 13 (15 points) represents only those points measured from the BBX diatreme. It shows a well-defined maxima at 147° - 90°, and two less well-defined joint sets at 79° - 90° and 168° - 90° which are mutually perpendicular.

C. Veins

Quartz-carbonate veins are frequently dilatant, particularly where they occupy narrow bedding joints.

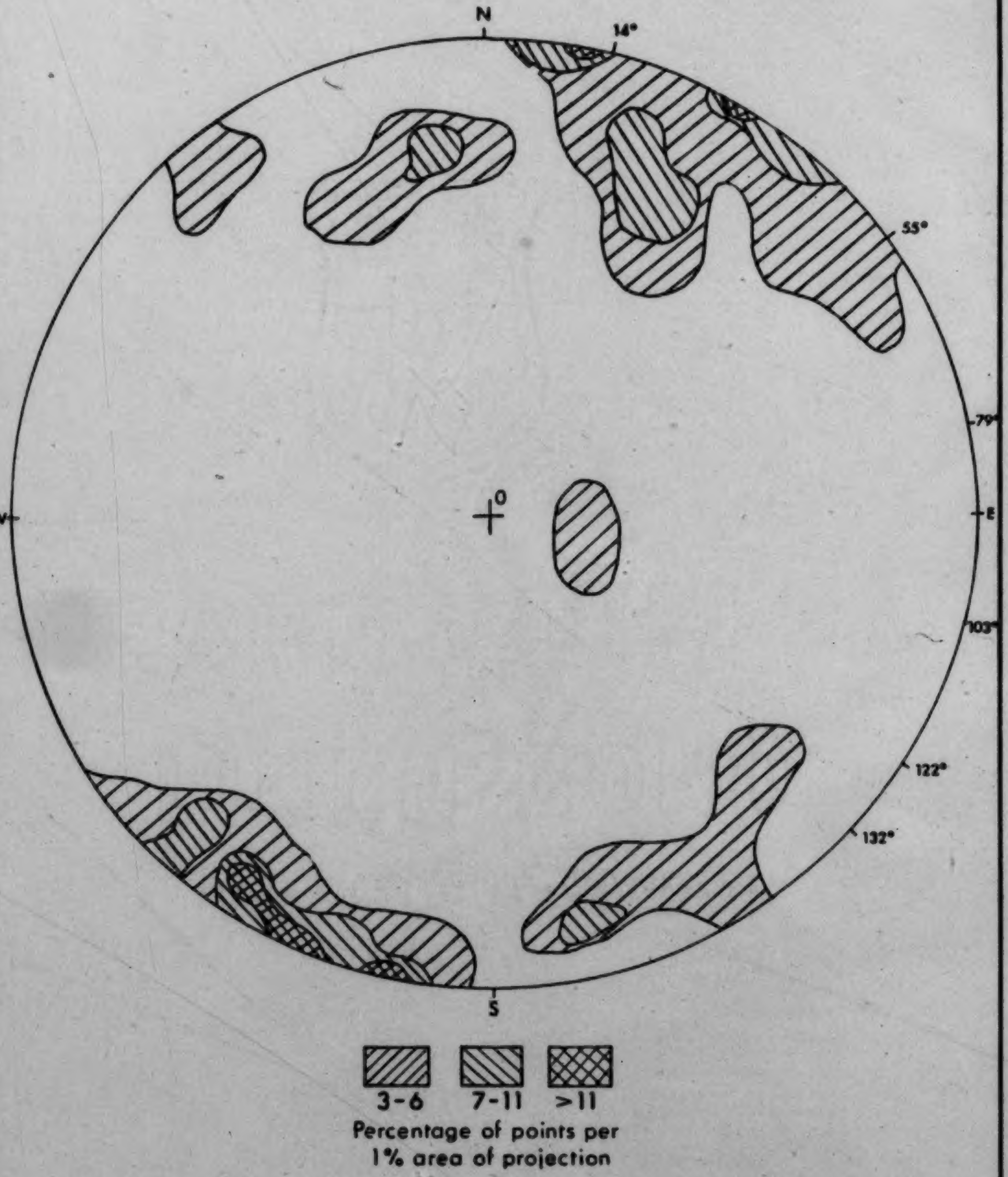
N
14°
55°
79°
W
0
E
103°
122°
132°
S
3-6
7-11
>11
Percentage of points per
1% area of projection

Figure 12 Stereogram showing Joints in Sediments (26points)

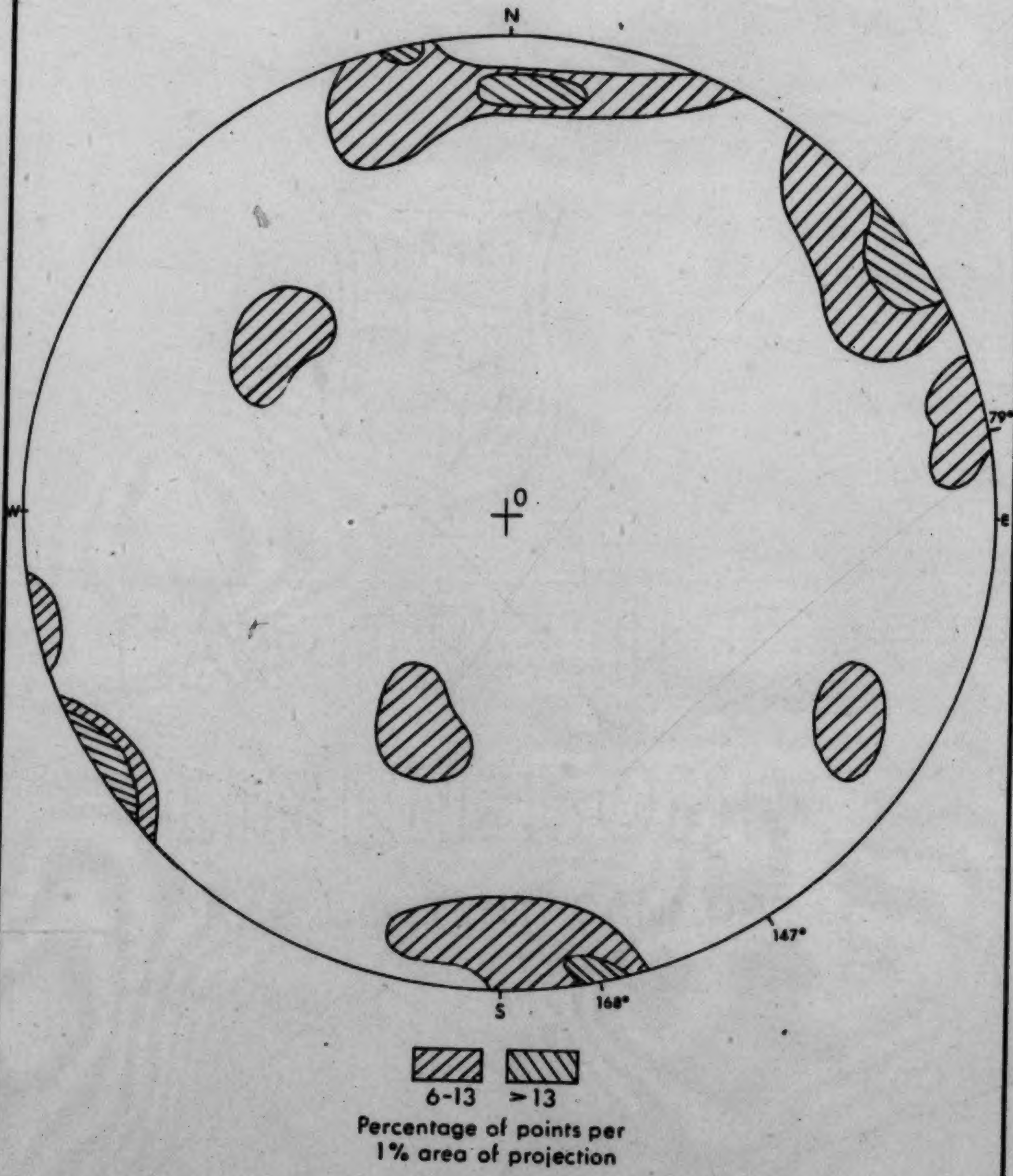
N
W
E
S
0
79°
147°
168°
6-13
>13
Percentage of points per
1% area of projection

Figure 13 Stereogram showing Joints in Diatreme (15 points)

Figure 14 (24 points) shows vein measurements from all rock types in the study area. Five directions of veining are evident at 28° - 90°, 45° - 80° SE, 71° - 90°, 98° - 90° and 130° - 90°, with maxima at 45° - 80° SE, 71° - 90° and 98° - 90°.

Figure 15 (15 points) shows all veins in sediments on the BBX Group and in the vicinity of Great Slave Lodge, exclusive of those between bedding planes. This figure, which is very similar to figure 14, shows five directions of veining at 27° - 90°, 70° - 90°, 98° - 90° (maxima), 121° - 90° and 142° - 90°.

D. Minor Folds

Minor folds occur occasionally in the study area. The seven fold axes which were measured are plotted on a stereogram in Figure 16. Although these points show a wide scatter consistent with the structural complexity of the area, two tentative great circles can be constructed defining planes as follows:

1. St. 154° dip 42° NE
2. St. 32° dip 63° SE

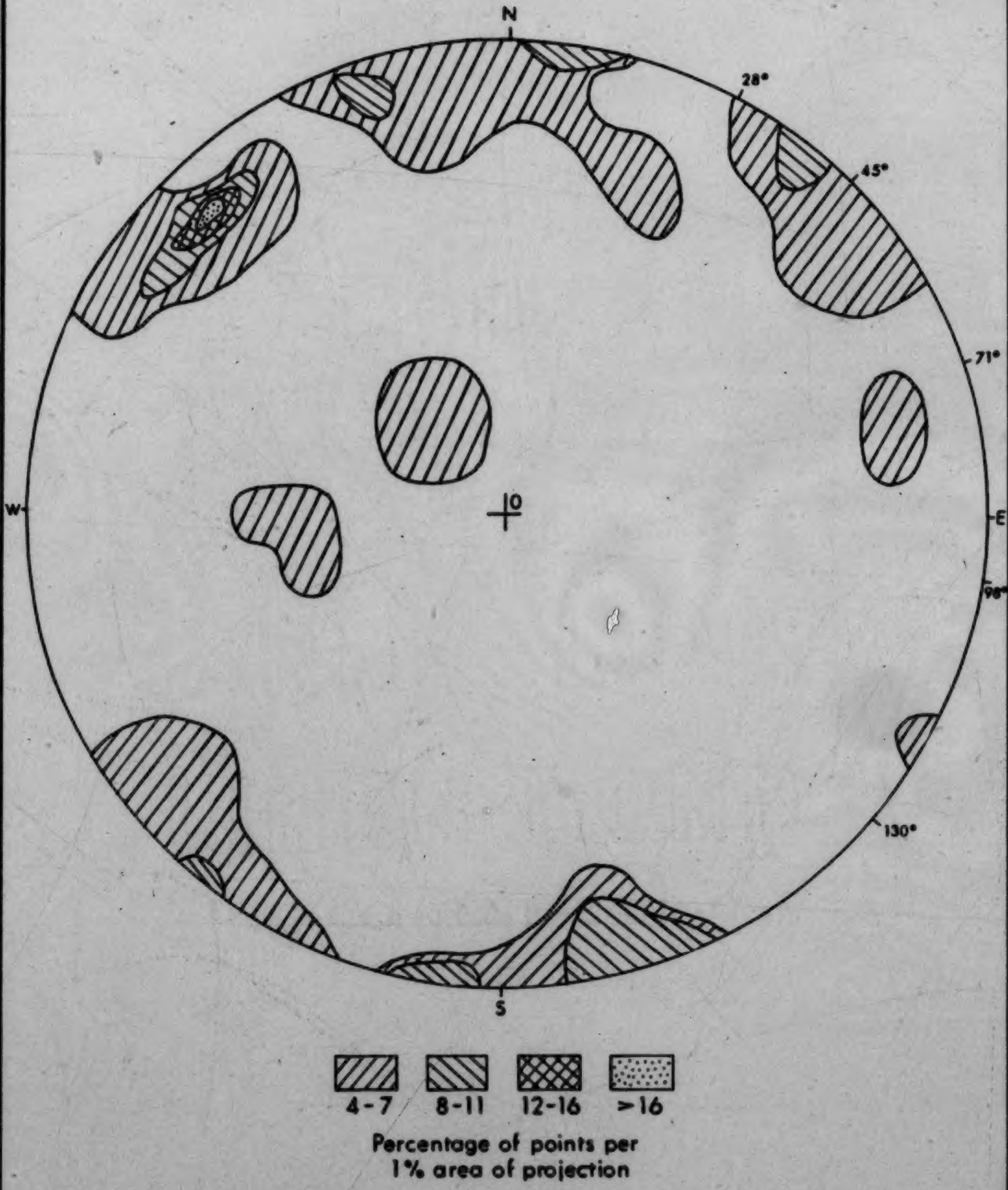
N
28°
45°
71°
W
0
E
98°
130°
S
4-7
8-11
12-16
>16
Percentage of points per
1% area of projection

Figure 14 Stereogram showing all Veins (24 points)

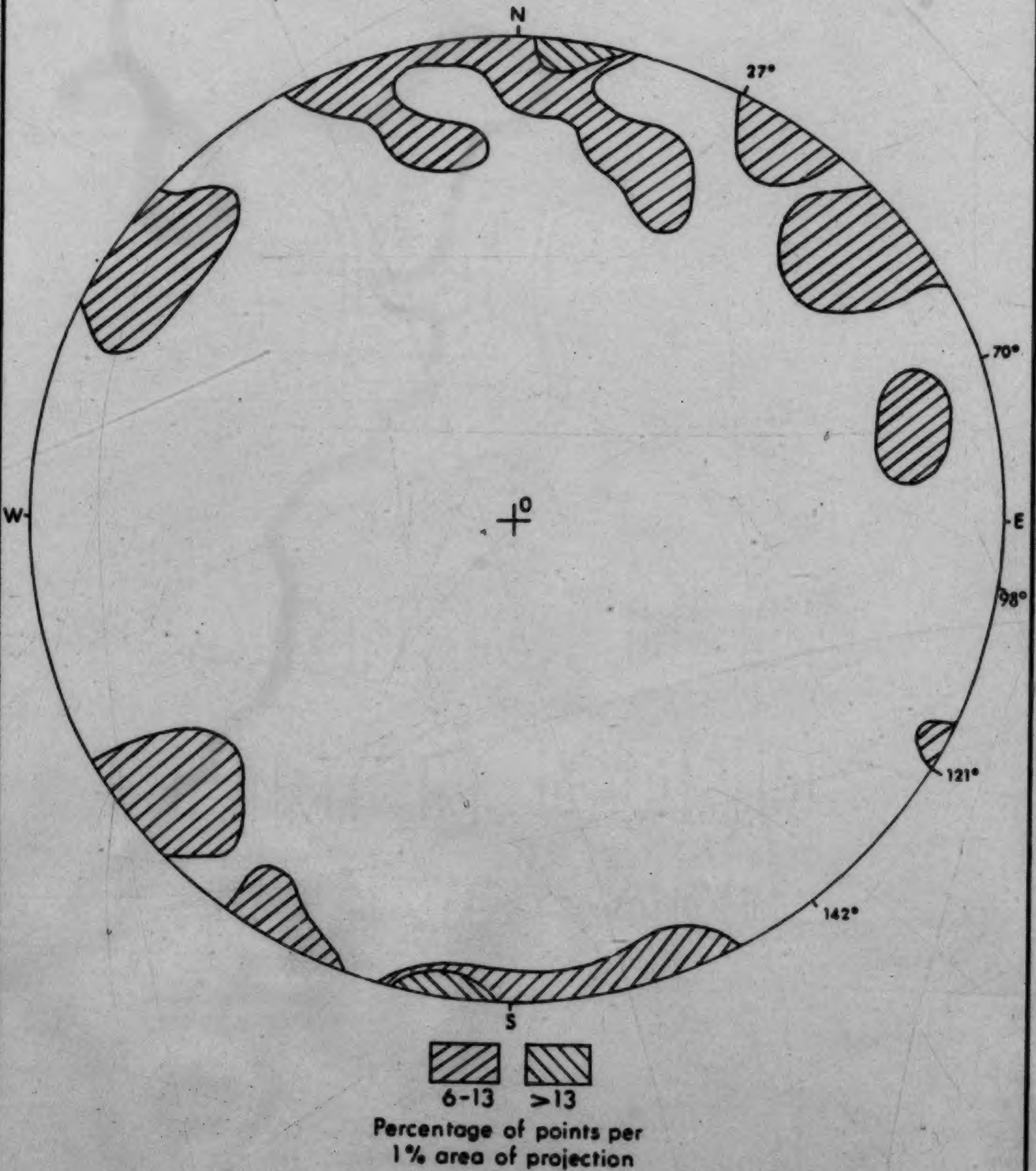
N
27°
70°
W
0
E
98°
121°
142°
S
6-13
>13
Percentage of points per
1% area of projection

Figure 15 Stereogram showing Veins in Sediments, except those in Bedding Joints (15 points)

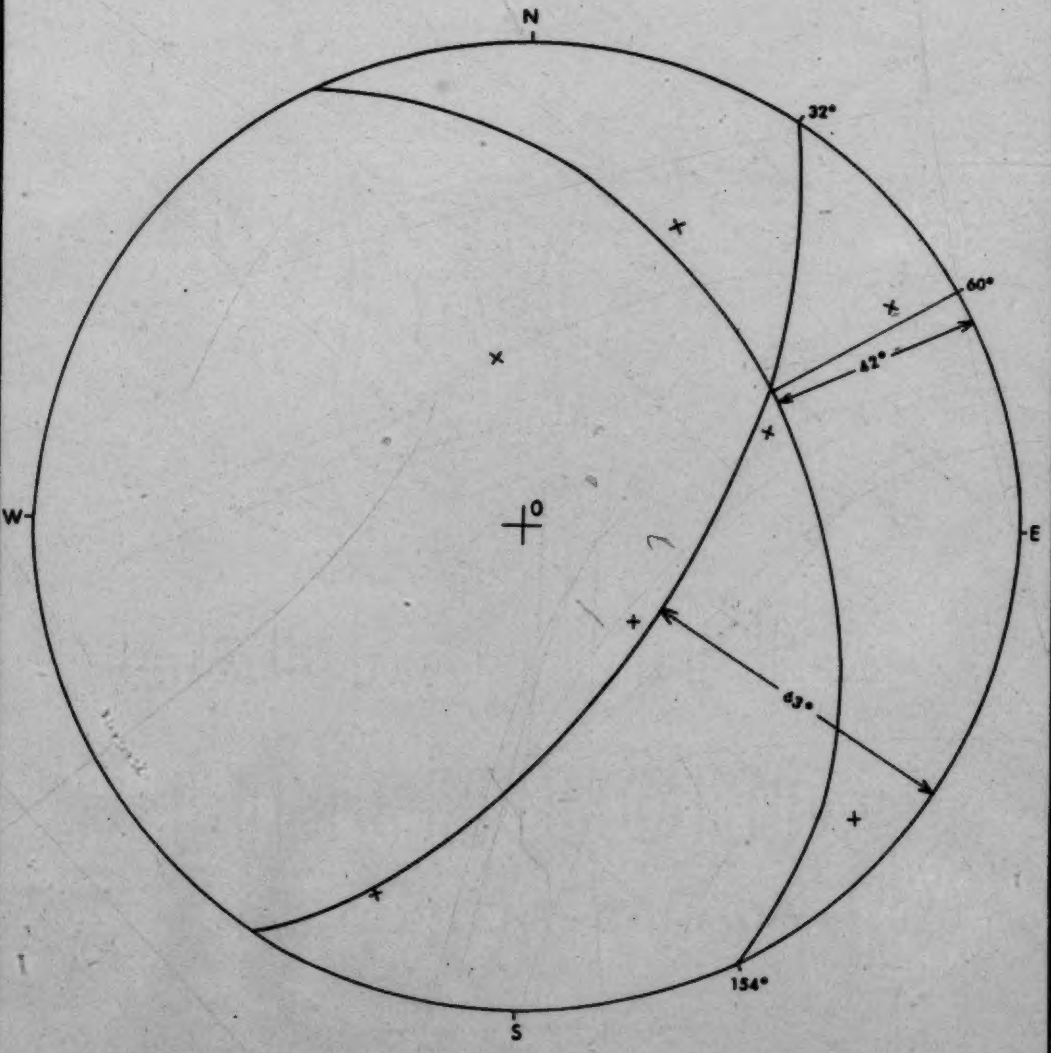
N
32°
60°
42°
W
0
E
43°
154°
S

Figure 16 Stereogram showing orientation of Minor Fold Axes (7 points)

These planes are not well-defined, but it is interesting to note that their strikes are roughly parallel to other structural features in the study area. Moreover, the intersection of these planes trends 60° (az) and hence very roughly parallels the orientation of the major fold axis. In view of the structural complexity of the area, it can be tentatively suggested that these minor folds are related to the major folding event, but that later structural modifications have resulted in a certain amount of scatter.

E. Shearing

Slickenside data are plotted on a sterogram in Figure 17, and show a moderately well-defined east-west trend, although some scatter is evident.

II. Discussion of Results

The study area is structurally complex, and shows evidence of several periods of deformation. The structures which have been observed can be explained in terms of episodic folding and related jointing. These structures have been subsequently modified by the emplacement

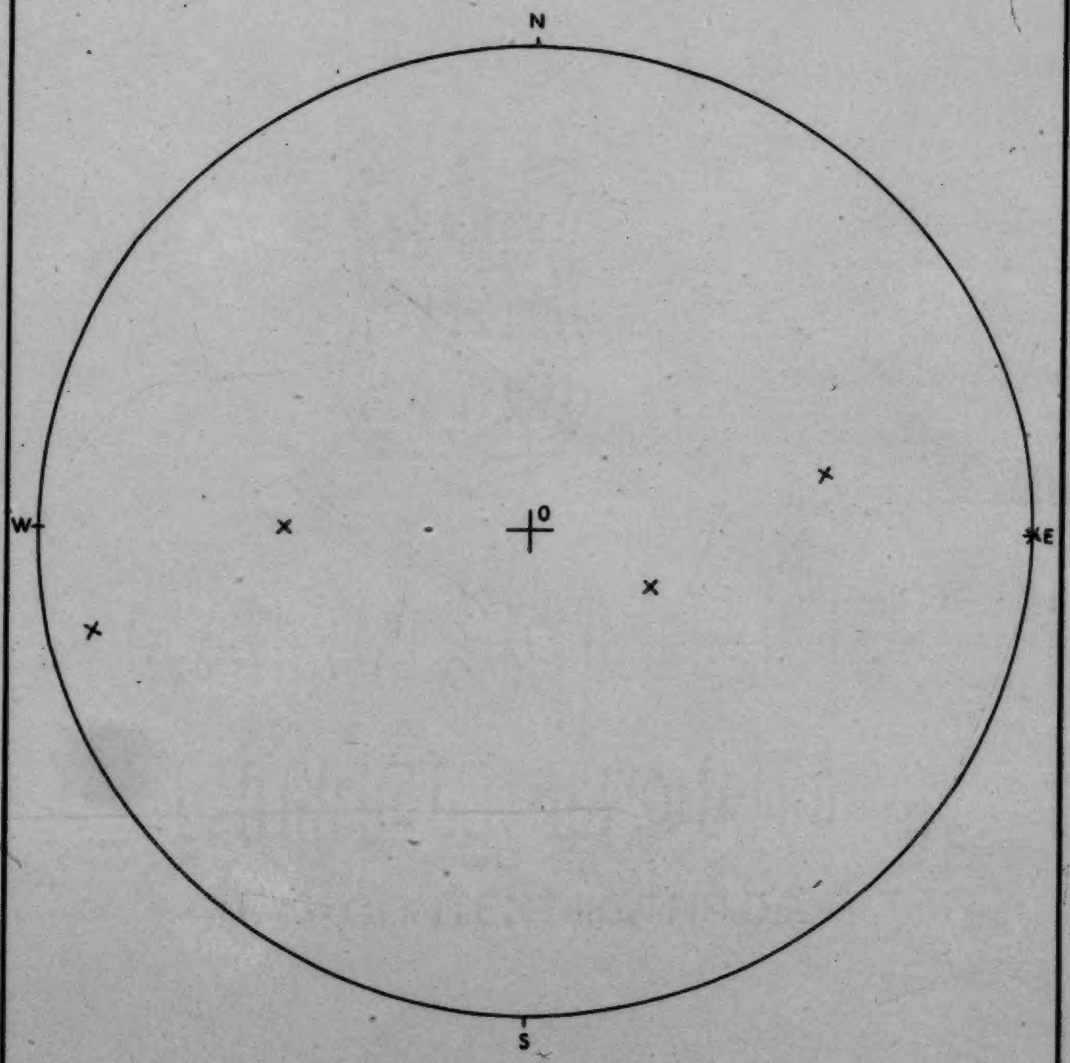

Figure 17 Stereogram showing Trend and Plunge of Slickensides (5 points)

of the diatreme, and by late small-scale faulting and shearing.

The major structural trends gleaned from sterograms are summarized in Table 8 and their relation to major lineaments is noted. In constructing this table, structural entities having the same, or very nearly the same strike were included in the same row. The small variations which do exist are ascribed to errors inherent in field measurements and in interpreting stereograms. This table should be examined in conjunction with Figure 9 which shows major airphoto lineaments.

It is apparent from these data that structural trends determined from stereographic plots of minor structures are remarkably consistent with major lineaments evident on air photographs. The majority of these structures are either approximately parallel to, perpendicular to, or symetrically disposed about fold axes. The following observations and conclusions are based on this fundamental relationship.

A. Folding along 50° (az) appears to be the major structural feature in the area, and many of the lineaments in Figure 9 parallel this trend. The fold axis roughly parallels the trend of the East Arm

TABLE 8

SUMMARY OF STRUCTURAL TRENDS FROM STEROGRAMS

*Maxima

Joints (Strike + Dip°)			Veins (Strike + Dip°)						
All Joints (Fig.11)	Joints in Sediments (Fig.12)	Joints in Diatreme (Fig.13)	All Veins (Fig.14)	Veins in Sediments (Fig.15)	Fold Axes (Trend + Plunge°) (Fig.10)	Shears (Strike°) (Fig.17)	Planes Defined by Minor Folds (Strike + Dip°) (Fig.16)	Comments	Interpretation
	14-18W				16- 6			Minor folding	Shear joints related to minor fold system
			28-90	27-90				Approx. parallels diatreme axis	Veins in shear fractures related to major fold system (?)
							32-63SE	Closely parallels diatreme axis	
	55-90		*45-80SE		50-15			Parallels major fold axis and Archean -Proterozoic contact	Major fold axis with release joints and veins
			*71-90	70-90				Parallels south margin of diabase	Shear fractures related to major fold system
77-90	79-70	79-90						Approx. parallels south margin of diabase	Jointing related to late shearing
						≈ 90			
103-90	*103-90		*98-90	*98-90				Approx. perpendicular to minor fold axis	Extension joints related to minor fold system
						≈ 110			
116-90 124-90	*122-90			121-90				Nearly perpendicular to diatreme axis	Fractures related to formation of diatreme (?) + late veining
*132-90	*132-90		130-90					Approx. perpendicular to diatreme	Fractures related formation of diatreme
*144-90		*147-90		*142-90				Nearly perpendicular to major fold axis	Extension joints related to major fold system
							154-42NE		
168-90		168-90						Approx. perpendicular to south margin of diabase	Jointing related to late shearing

Synclinorium (Figure 6), and closely parallels the Archean-Proterozoic contact north of Aristifats Lake (Figure 8). This suggests that folding has taken place parallel to the basement edge. This folding has given rise to several related structures (Figure 18a).

1. Shear Fractures

Major lineaments trending at approximately 71° and 35° (az) are symetrically disposed about the fold axis and are interpreted as conjugate shear fractures. The strain axes resulting in these shears would be oriented as follows (Billings, 1972, p. 166):

(i) Greatest Strain Axis - ∇_1 - NW-SE.
(ii) Intermediate Strain Axis - ∇_2 - vertical.
(iii) Least Strain Axis - ∇_3 - NE-SW.

Shear fractures may form in several ways (op. cit., p. 166), but in the present case their symetrical orientation about the fold axis suggests that they were formed by compression along ∇_1, or perpendicular to the axis of the East Arm Orogen.

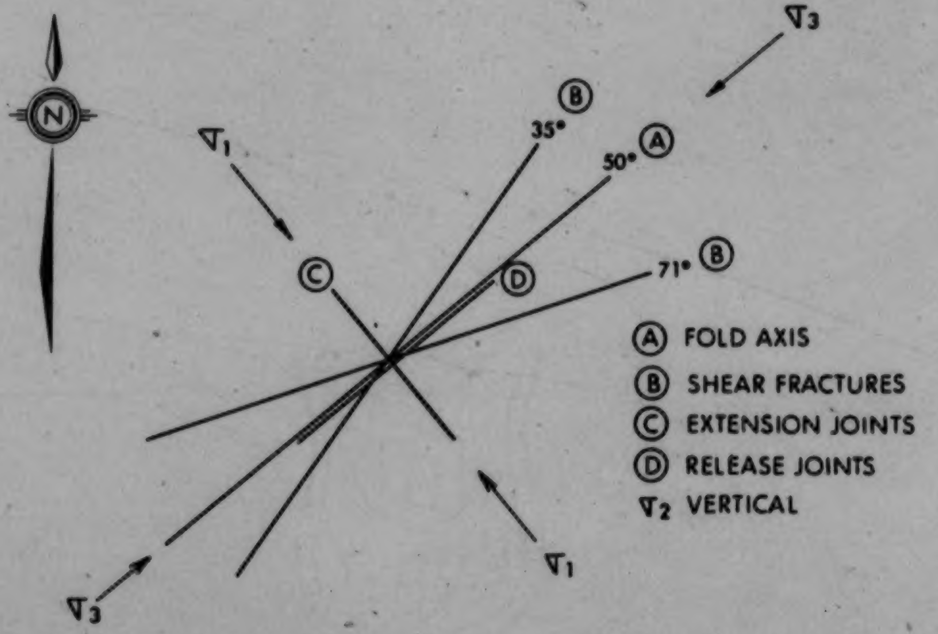
N
∇3
Ⓑ
35°
Ⓐ
50°
∇1
Ⓒ
Ⓓ
71° Ⓑ
Ⓐ FOLD AXIS
Ⓑ SHEAR FRACTURES
Ⓒ EXTENSION JOINTS
Ⓓ RELEASE JOINTS
∇2 VERTICAL
∇1
∇3

Fig. 18a. Structural Features Related to Compressional Folding along 50° (Az)

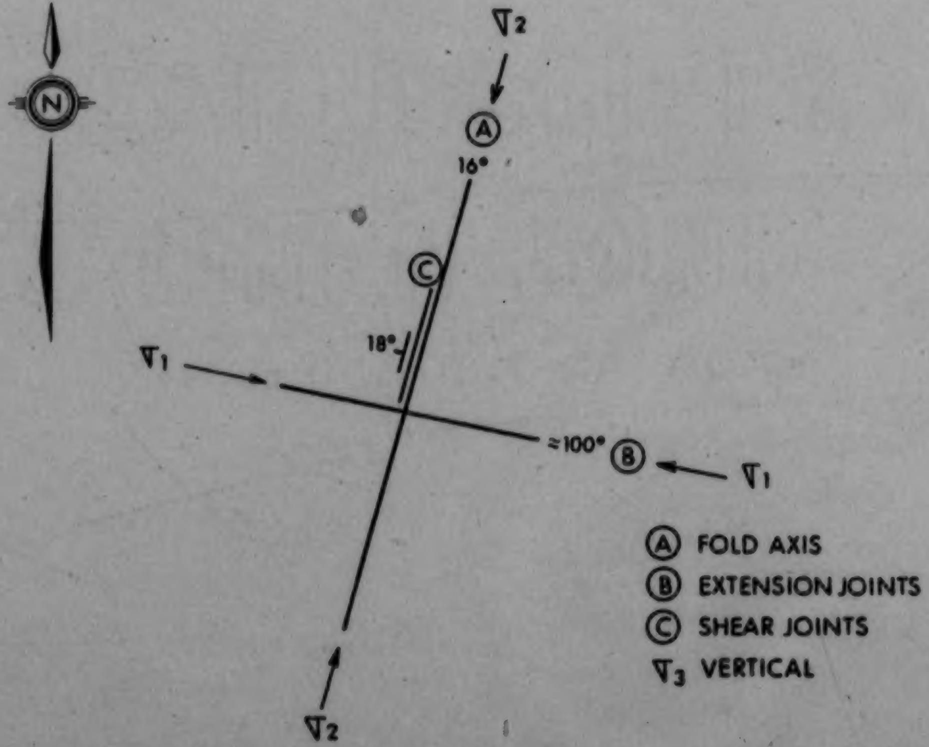
N
∇2
Ⓐ
16°
Ⓒ
18°
∇1
≈100° Ⓑ
∇1
Ⓐ FOLD AXIS
Ⓑ EXTENSION JOINTS
Ⓒ SHEAR JOINTS
∇3 VERTICAL
∇2

Fig. 18 b. Structural Features Related to Minor Fold System along 16° (Az)

2. Extension Joints

A series of veins and joints (≈144°-90°) which are approximately perpendicular to the fold axis are interpreted as extension joints. These joints are common in orogenic belts and result from slight elongation parallel to the axis of folds (Billings, 1972, p. 168).

3. Release Joints

Minor joints (55°-90°) roughly parallel to the fold axis are interpreted as release joints formed perpendicular to the axis of compression when the load is released.

B. A lesser system of folds trends 16° (az) (Figure 18b). Joints and veins trending 103°-90° and 98°-90° are approximately perpendicular to this trend and are interpreted as extension joints. A minor set of shallow-dipping joints (14°-18°W) which strike approximately parallel to the fold can be interpreted as shear joints developed during folding, under conditions where the easiest relief was upwards (Billings, 1972, p. 169). This suggests that the least principle stress is vertical, and that folding along 16° (az) took place relatively near the surface. The fact that this comparatively minor phase of folding parallels a major (basement?) fault (p. 128, this thesis), suggests that it is related to movement along this fault. It is tentatively proposed that this folding followed a period of uplift, and postdated major folding along 50° (az).

C. Joints and veins ranging from 116°-90° to 132°-90° are roughly perpendicular to the axis of the diatreme. These fractures also occupy an intermediate zone between extension joints related to folding along axes of 50° and 16°. These features may be interpreted as extension joints related to folding, or as fractures related to the formation of the diatreme by an explosive mechanism. Because of the elongate form of the diatreme, these fractures would tend to extend away from the source at approximately 90°, rather than in a radial pattern.

D. Joint sets at 79° and 168°, which are mutually perpendicular, may have been developed in response to a shearing couple established approximately parallel to the major shear fracture formed along 71° (az).

In support of this hypothesis is the fact that large quartz veins in trench 5 are slickensided, with a plunge of approximately 11°W. These slickensides are consistent with shearing in a lateral rather than a vertical sense, and indicate that shearing postdated the formation of the large quartz veins at this location.

IV. Structural Control of Igneous and Hydrothermal Activity

Having tentatively determined the nature of prominent structures in the study area, it is possible to discuss the factors controlling major geological features. Of particular interest are the diatreme, the diabase plug, and quartz-carbonate veins and stockworks.

A. The Diatreme

The BBX diatreme is one of several Seton volcanic centres occurring along a major fault trending 18° (az) (p. 42, this thesis). This fault presumably controlled the movement of alkaline magma beneath the Archean-Proterozoic unconformity. Above this unconformity however, the emplacement of the diatreme (axis trend 35° az) was evidently controlled by one of a conjugate set of shear fractures related to a major phase of compressional folding (axis 50° az). This is consistent with the observation that the major diameters of diatremes generally follow lines of structural weakness in the roof rocks (Lorenz et al, 1975, p. 57). The following implications arise from this assumption.

1. The shear fractures are major structural features, presumably extending to basement.

2. The diatreme was emplaced prior to movement along the basement fault, and hence preceded the minor phase of folding (axis 16° az) related to this movement. If this were not the case, and the fault did affect the Proterozoic succession, it is probable that the diatreme would have been emplaced along zones of weakness related to the fault (i.e. 18° az).

B. The Diabase Plug

The northern margin of the diabase is not well defined (p. 58, this thesis), but its abrupt linear south margin corresponds to the major shear fracture trending 71° az. This fracture and its conjugate (35°

az) have controlled the emplacement of the diabase and the diatreme respectively. The north margin of the diabase is presumably controlled by the Archean-Proterozoic contact.

C. Quartz-Carbonate Veins and Stockworks

The occurrence of quartz-carbonate veins in the study area is complex. Although they are a predominantly late feature, there is no reason to suggest that they were all formed contemporaneously. Indeed, structural evidence suggests that their formation may have been episodic. This observation is supported to some extent by the wide range in the composition of the veins and stockworks along a continuum between pure quartz and pure carbonate. Attempts to determine the order in which quartz and carbonate were deposited, on the basis of their relationship in outcrop, were unsuccessful and the results ambiguous. Several stages of carbonate veining, separated by intervals of brecciation, can be inferred from drill core, particularly where these veins cut sedimentary rocks (DDH 76-1).

In spite of these complexities, the structural control of veins and stockworks is well-defined. Examples of this control, and implications regarding the structural history of the area are discussed below.

1. It can be inferred from Table 8 that minor quartz-carbonate veins preferentially occupy joints and fractures trending in a NW-SE direction. These features are extension joints related to folding, and fractures related to the formation of the diatreme. It is probable that this preferential veining is the result of better access to these zones by hydrothermal fluids. It is proposed that this access was affected through late tectonism which caused the folds to plunge to the northeast, and exerted tensions which dilated these joints. In support of this postulate is that the major joint set in the diatreme (147° az) parallels one of these extension joints, and presumably developed parallel to an existing zone of weakness in response to a late tectonic event.

2. A prominent set of steeply dipping quartz-carbonate veins (45°-80° SE) closely parallels the major fold axis, and is probably controlled by release joints related to this structure.

3. Major quartz-carbonate stockworks immediately south of the diabase plug have an overall trend of 71°, which suggests that they are controlled by a shear fracture associated with the major phase of folding. Within these stockworks however, quartz veins show a variety of orientations, and in some cases parallel known directions of jointing. These features suggest that the shear fracture is the major factor controlling formation of the stockwork, but that the veins themselves are controlled by smaller features such as joint planes. It can be inferred from this, that the shear fracture is a major, probably deep-seated structure which has acted as the principle locus of movement for hydrothermal fluids.

4. Giant quartz veins exhibiting a meandering or irregular trend occur in two locations to the northeast of the diatreme. These unusal features appear to be controlled by the intersection of existing zones of weakness. The large vein cutting tuffs northeast of the diatreme for example, fluctuates between approximately 30° and 50°, and is presumably controlled variously by shear fractures and release joints related to the major fold system.

5. The occurrence of dilatant quartz veins in bedding joints is of considerable interest. These joints were presumably formed during tectonic uplift in response to residual stresses generated during deformation at deep levels. Implicit in this model is that the quartz veins occupying these joints were formed relatively near the surface.

6. Pronounced quartz veining in the vicinity of Great Slave Lodge, and small quartz-carbonate veins cutting volcanics of the JDA group have an east-west orientation, and are probably controlled by late shear planes having this attitude.

V. Chronology

Based on the foregoing discussion, it is possible to propose a tentative chronology of structural events. Although some events cannot be placed with certainty, and the chronology is somewhat intuitive, it conforms generally to the deformational history of the Great Slave Basin. This deformation involved compression of sediments into broad folds, followed by uplifting and down-dropping of blocks, and transcurrent faulting (pp. 37, this thesis).

The proposed structural history of the study area is as follows:

A. Compressional folding parallel to the basement edge (axis 50° az).

This major event probably corresponds to the Compressional Stage of structural evolution of the Great Slave Basin (p. 38, this thesis).

B. Emplacement of the diatreme and the diabase along major zones of weakness; specifically, shear fractures related to major compressional folding.

[The temporal relationship between the diabase and the diatreme is discussed at a later point in this thesis (p. 184)].

C. Uplift related to movement along a major deep-seated (basement?) fault (18° az), and related minor folding (axis 16° az).

D. Continued uplift and slight tilting to the northeast.

Dilatant zones opened along extension joints in response to this tilting. The relief of sufficient overburden pressure resulted in the dilation of bedding joints.

E. Quartz-carbonate Veining

Hydrothermal activity resulted in the formation of minor quartz-carbonate veins in dilatant zones, particularly bedding joints and extension joints. Major quartz veins and quartz-carbonate stockworks on the BBX property were also formed at this time.

F. Small Scale Shearing

This shearing took place along two principle directions; approximately 90° (az), and approximately 78° (az) [roughly parallelling the major shear fracture at 71°(az)]. This event postdated major quartz veins at locations 31 and 45 (Map 2), as evidenced by the presence of slickensides on these veins. Although no major movement is indicated, strain was sufficiently large to cause two mutually perpendicular vertical joint sets at 79° and 168°.

G. Renewed Hydrothermal Activity

This resulted in the formation of quartz-carbonate veins, predominantly in an east-west direction. Veins having this orientation occur in the vicinity of Great Slave Lodge and cutting volcanics of the JDA group south of Aristifats Lake.

H. Minor Shearing

The effect of late small scale shearing is particularly evident in the diatreme, where numerous chloritic slips and shears are developed. These are presumably formed on a local scale in response to late tectonic stresses (p. 118, this thesis).

VI. Conclusions

1

The postulated control of the diabase, the diatreme, and major quartz-carbonate stockworks by shear fractures related to compressional folding at deep levels, suggests that these features are of fundamental importance to our understanding of the geologic history of the study area. Presumably, these are major zones of structural weakness which extend to the basement. The conjugate fractures have acted as the major locus for emplacement of volcanic and hypabyssal rocks, and appear to have been a major factor controlling the migration of hydrothermal fluids. This is evidenced by the following features:

A. Significant mineralization, associated with strong potassium alteration occurs in the diatreme (Chapter 10, this thesis).

B. Minor chalcopyrite associated with incipient potassium alteration occurs along the south margin of the diabase plug (71° az) (p. 72, this thesis).

C. A late stage of carbonatization has strongly affected both the diatreme, and the south margin of the diabase plug.

D. Major quartz-carbonate stockworks occur along 71° (az) - trending shear fractures.

CHAPTER 6

NATURE AND ORIGIN OF THE DIATREME

I. General Remarks

The volcanics in the diatreme exhibit a variety of textural and structural features which provide clues as to its origin. The purpose of this chapter is to describe these features and to discuss their implications regarding the formation of the diatreme.

It is evident that the BBX diatreme has undergone a complex eruptive history, involving at least two pulses of volcanism. The process of fluidization played an important role in formation of the diatreme, and resulted in a variety of textures and structures both within the volcanics and in the adjacent sediments.

Several textures in the diatreme suggest that it originated primarily by way of a phreatomagmatic eruption, brought about by contact of magma with water-saturated sediments or sea water. The precise mechanism by which this occurred is complex. Structural and stratigraphic considerations suggest that while groundwater may have played an important role in the eruption, the initial conduit must have been formed either by opening of fractures by tectonism, or by drilling by high pressure gases exsolved from the underlying magma.

Because the significance of certain textures is not known with certainty, interpretation of the origin of the diatreme is complicated and to some extent ambiguous.

II. Nature of the Diatreme

A. The Role of Fluidization

Fluidization includes all processes in which denser particles are distributed within a rising liquid or gas phase, and comprises gas-solid, gas-liquid, gas-liquid-solid, and liquid-solid systems (Lorenz et al, 1975, p. 30). Fluidization results in three main types of particle distribution:

1. Fixed beds, in which gas rises through particles at rest.
2. Fluidized beds, in which particles are supported and agitated by gas.
3. Pneumatic transport, in which particles are entrained in the gas flow.

Fluidized systems are complex. The rate of flow in a volcanic vent may change with time, from the bottom upward, or from the margins inward (op. cit., p. 32). At a given location, a fluidized bed or a fixed bed may form, or pneumatic transport may occur.

Mixing of fragments is a very important characteristic of fluidized beds, and to a lesser extent of pneumatic transport. It may be so thorough that complete homogenization has occurred, and fragments from different stratigraphic levels occur together. Mixing results in abrasion and grinding of the solid phase, so that angular fragments tend to become spherical (op. cit., p. 31). Rounding may also result from thermal spalling.

Textures in fluidized systems may be further complicated by the presence of counter currents. These develop particularly in pipes with tapering walls, such as the BBX diatreme. Close to the walls of the pipe, gas rises more slowly than it does in the centre. Granular material here may subside, be picked up at depth, carried upward in the central parts and subside again near the margins (op. cit., p. 32).

Fluidization is active during every phase of gas flow. Mature stages of fluidization are indicated by grain size distribution, rounding of blocks, and homogenization of vent contents. Maturation may be reached at the close of short-lived activity, or during the main eruptive phase.

In the BBX diatreme, a variety of features are indicative of fluidization. These are described below, and their implications regarding other aspects of the formative process of the diatreme are discussed.

1. Volcanic Bed Forms

Texturally, the diatreme ranges from zones of well-defined breccia showing no preferred orientation, to zones which exhibit planar features somewhat reminiscent of bedding (Plate 23). The volcanic fragments in these zones are generally tightly packed and elongate, and lie with their long axes in parallel or subparallel alignment. These "bed forms" may comprise small angular fragments, larger fragments with embayed contacts, and in some cases, elongate undulating forms (this thesis, p. 96). The precise origin of these features is not known with certainty, but they are generally thought to be the result of "flow banding" or "chain stratification" (Lorenz et al, 1975, p. 38). This feature is common in diatremes, where it tends to occur near the contact between homogeneous pyroclastic debris, and either wall rocks or xenoliths. Flow banding takes two main forms, both of which occur in the BBX diatreme.

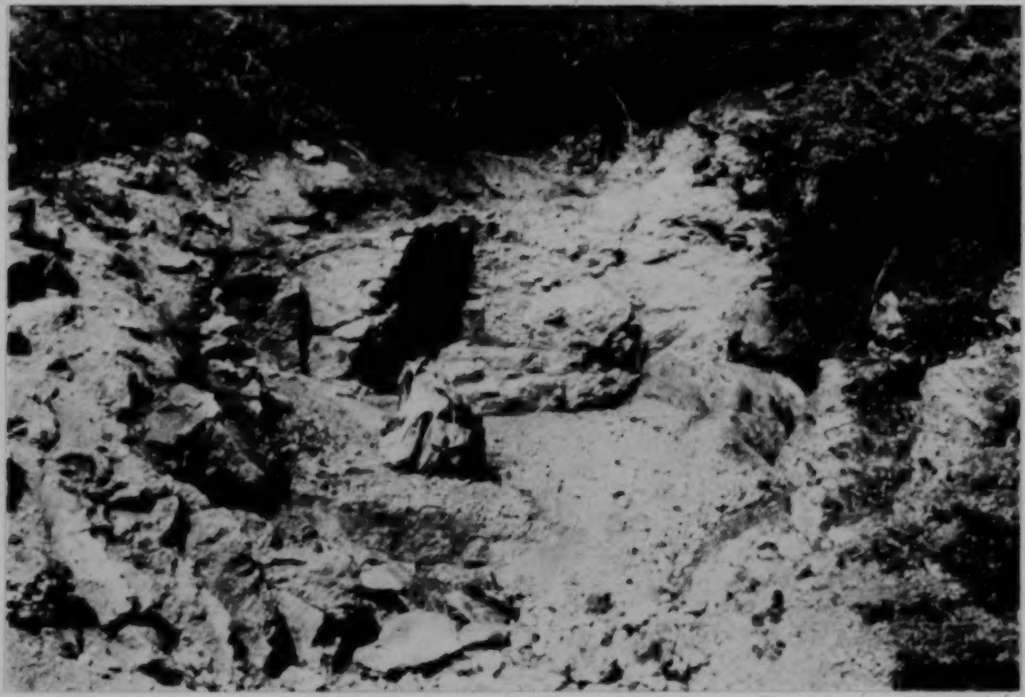

Plate 23 Trench 2, showing horizontal "bed forms" (behind packsack). Note strong potassium alteration (light brown) which is in marked contrast to propyllitically altered basalt (Plate 9). Malachite stain (light green) and wad (black) are present on the outcrop surface.

(i) Variations in grain size, with relatively fine pyroclastic debris grading into coarser debris away from the walls.

(ii) The alignment of elongate fragments of country rock, juvenile lapilli and platy minerals parallel to the walls.

Flow banding in diatremes is usually retricted to zones less than one metre wide (op. cit., p. 39). This is consistent with the occurrence of these features in the BBX diatreme.

It can be assumed that flow banding is attributable to pneumatic transport.

The variety of textures in "bed forms" is sufficiently complex that they may have resulted, at least in part, from processes other than flow banding. These processes include base surge deposition (this thesis, p. 168), and fallback of ejecta from successive eruptions (Lorenz et al, 1975, p. 50). This latter feature is generally restricted to the crater or the upper parts of the underlying conduit (op. cit., p. 50). Compaction of the ejecta may account in part for the relatively tight packing of fragments in these zones. Packing may also result from the process of defluidization (op. cit., p. 33). This occurs when gas flow diminishes markedly, or ceases.

"Bed forms" in the BBX diatreme exhibit a wide range in orientation from horizontal to almost vertical, and abrupt changes in attitude over short intervals (i.e. one metre) are common. This variation is attributable to slumping of bedded ejecta along the margin of the conduit, and to subsidence within the vent, possibly related to the withdrawal of magmatic support at depth (op. cit., p. 50). Similar subsidence structures, accompanied by differential rotation of bedding planes without disruption of bedding, have been noted in the Permian diatremes of southwest Germany (op. cit., p. 51).

Vertical or near vertical bed forms may also be attributed to the plastering of fine grained wet ejecta against the walls of the vent during a phreatomagmatic eruption (op. cit., p. 50).

2. Matrix-Supported Lapilli

In contrast to tightly packed zones ("bed forms") with very little matrix, are intervals containing as much as 60% matrix, usually carbonate. In these zones, the fragments tend to be relatively small and well rounded. These fragments are rarely in contact, and may be quite widely spaced. Prior to the introduction of carbonate, they were supported in a matrix of comminuted rock debris.

These features can be readily understood in terms of the various processes involved in fluidization (this Chapter, p.157). In particular, they may represent fluidized beds where particles were supported and agitated by gas. Mixing in these zones resulted in abrasion and rounding of solid ejecta. Rounded fragments in fluidized breccias may also suggest that they vented effectively at the surface (Bell, R. T., 1978, p. 320).

3. Tuffisite Apophyses

The term tuffisite refers to the composite juvenile, accessory and accidental filling of diatremes. It resembles tuff, but is differentiated by its occurrence in a vent rather than at surface (Dennis, 1972, p. 451). Apophyses of tuffisite in the sedimentary wall rock can be seen occasionally in drill core, but are rare in outcrop. These "veins" suggest that the system was fluidized during eruption (Ollier, 1967, p. 60).

4. Thermal Metamorphism of Country Rocks

Sedimentary rocks surrounding the diatreme have been relatively unaffected by its intrusion. Hematitic sediments in contact with the diatreme have been bleached, and their contained iron has been reduced, so that the rocks are green in color. These alteration zones are only a few centimetres in width.

The virtual absence of metamorphic effects adjacent to the diatreme is consistent with the dissipation of thermal energy in doing the work of fluidization (Hatch, Wells and Wells, 1972, p. 456).

5. Attitude of Peripheral Sediments

It is evident from Map 2 that the majority of the sediments immediately adjacent to the diatreme tend to dip in towards its centre.

The inward dipping attitude of these sediments is attributed to two principle causes.

(i) Outcrops representing the Ogilvie and McLeod Formations have been interpreted as large blocks of wallrock from up section, which have entered the system (this thesis, p. 55). Because these blocks are too large to be fluidized, they sink and hence occur beneath their original stratigraphic level (Lorenz et al, 1975, p. 31). Subsidence of these blocks occurs when their terminal velocity exceeds that of the system (op. cit., p. 40).

(ii) Small outcrops of sediment adjacent to the diatreme belong to the Akaitcho Formation, and presumably occur at their original stratigraphic level. The attitude of these blocks is attributable to the withdrawal of magmatic support in the waning stages of volcanic activity.

B. The Role of Groundwater

Although the gas phase plays a major role in the formation of diatremes, little is known concerning its composition and origin. Three principle sources of gas have been proposed (Lorenz et al, 1975, p. 17).

1. Non-magmatic sources, comprising mainly water vapor generated when rising magma comes in contact with groundwater. Eruptions brought about in this way are termed phreatomagmatic if they expel essential ejecta, and phreatic if they do not (Ollier, 1974, p. 292).

2. Absorption by magma of water vapor, CO_2 and other gases, and their subsequent release.

Groundwater in the pores and cracks of sedimentary wall rocks is an important source of water vapor.

When these rocks are detached from the walls, and comminuted within the pipe, the water is absorbed into the magma and supplements magmatic gases (Lorenz et al, 1975, p. 22).

$CO_2(g)$ may be derived through assimilation of carbonate wall rocks (op. cit., p. 23).

3. Juvenile gases of magmatic origin.

In most eruptions, all three of the above sources are probably involved, but in widely different proportions (op. cit., p. 17). The gas originates by exsolution from the magma, or by contact of the magma with water-bearing wall rocks. Geochemical studies indicate that water derived from the walls is generally the major constituent of volcanic gases and far outweighs the contribution of juvenile water from greater depths (op. cit., p. 22).

The precise nature of the gas phase responsible for formation of the BBX diatreme cannot be determined. There is a strong suggestion however, that the diatreme formed by a phreatomagmatic mechanism. This is evidenced by the presence in the diatreme of accretionary lapilli, base surge bed forms, and fragments of sideromelane (op. cit., pp. 18 and 47). In addition, structures in the diatreme and in the adjacent sediments suggest that its origin was explosive. This is consistent with a phreatic origin for the diatreme, as such eruptions generally involve extreme violence (American Geological Institute, 1962, p. 379).

Features suggestive of a phreatomagmatic origin for the diatreme are described and discussed below.

1. Base Surge Deposits (?)

In the vicinity of trenches 1 and 2, towards the southeast margin of the diatreme, a variety of curved surfaces are recognizable upon close examination (Plate 24). These surfaces are generally gently curved and open downwards. They do not intersect, but rather, define a series of overlapping moundlike bodies of agglomerate. These surfaces resemble bed forms in base surge deposits (Fisher and Waters, 1970, p. 165, Plate 3).

Base surges are high velocity density currents which spread outward from the base of a vertically rising ejecta column (op. cit., p. 158). They deposit dune-like bed forms and thinly bedded, fine

Plate 24 Trench 1, showing base surge bed forms (?). A possible base surge deposit is indicated by the moundlike bodies of agglomerate (by hammer). A dune-like bed form of greater amplitude can be seen at the upper right (arrow). Note strong potassium alteration (light brown), malachite stain (light green) and limonite (orange).

to coarse grained tuffs (op. cit., p. 157). These deposits originate from phreatomagmatic eruptions.

2. Accretionary Lapilli (?)

Accretionary lapilli consist of a core of lithic or juvenile material surrounded by one or many concentric or slightly eccentric layers of ash (Lorenz et al, 1975, p. 46). Their origin is a matter of some debate, but they are generally ascribed to adhesion due to absorbed water (op. cit., p. 46). It has been proposed that the concentric structure is due to downslope rolling of lapilli on damp ash, or to accretion when raindrops fall through the ash cloud (Walker and Croasdale, 1970, p. 308). A much more plausible origin however, appears to be their formation in eruption clouds associated with the development of volcanic vents (Lorenz et al, 1975, p. 46). The eruption clouds are rich in water vapour, especially in phreatic eruptions of basaltic ash (Moore and Peck, 1962, p. 190).

Accretionary lapilli are not well-defined in the BBX diatreme. Occasionally however, basaltic lapilli are surrounded by relatively thick featureless rims of rock flour. These lack a concentric structure, but this may be due in part to extensive carbonitization which has obscured original textures.

Where several of these rimmed fragments occur together, their interstices are filled with more coarsely crystalline carbonate, suggestive of crystallization in open spaces. These factors imply that prior to the introduction of carbonate, rock flour adhered to the ejecta. It is difficult to envisage a mechanism other than that described above, by which this would occur.

The postulated presence of accretionary lapilli in the diatreme holds two implications with respect to its origin.

(i) That the rock enclosing the lapilli is extrusive (Moore and Peck, 1962, p. 191).

(ii) Although accretionary lapilli are not by themselves diagnostic, their occurrence with fragments of sideromelane (this thesis, p. 93) and base surge bed forms is suggestive of a phreatomagmatic origin (Lorenz et al, 1975, p. 47).

3. Structures Indicative of an Explosive Eruption

An unusual but well-defined cone-like structure occurs in the agglomerate in trench 2 and is shown in Plates 25 and 26. The structure comprises at least seven concentric layers, some of which are discontinuous. The cone opens to the west, and its axis is oriented at approximately 290° - 18°. The south part of the cone is truncated by a joint plane (strike 314°, dip 84° SW).

The visible portion of the structure is 30 inches in length, and opens to a width of 15 inches from approximately 5 inches at the apex. Two observations have some bearing on its origin and significance.

(i) The conical fractures truncate "bed forms", but are themselves truncated by late joints.

(ii) Accidental fragments of granite in the agglomerate are parted along these conical surfaces.

Plate 25 Trench 2, showing shattercone (?); diagonal view. Note truncation of the cone by a joint plane immediately to the left of the hammer. Note malachite (light greenish blue), limonite (orange) and wad (black).

Plate 26 Trench 2 showing shattercone (?); view along axis. Note malachite (light greenish blue), limonite (orange) and wad (black).

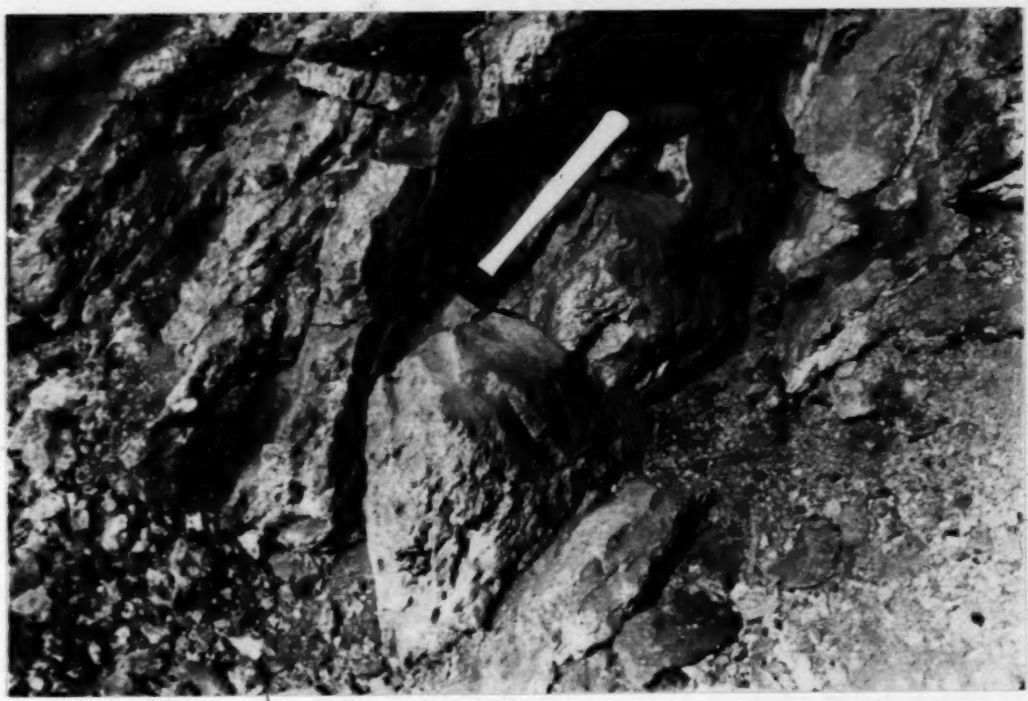

In loosely consolidated conglomerates, shear fractures tend to cut indiscriminantly across pebbles, while tension fractures break around the pebbles (Billings, p. 169). In view of this observation, the conical fractures in trench 2 are interpreted as shear planes, and the structure itself is interpreted as a shattercone.

If this interpretation is correct, then it can be inferred that the diatreme was formed by an explosive mechanism such as would be expected in phreatomagmatic eruptions. This postulate is supported by the observation that the axis of the cone is roughly perpendicular to the diatreme axis and parallels fractures in the adjacent sediments which have already been related to its formation (this thesis, p. 144). Both of these features are consistent with an explosive event in which force was exerted more or less perpendicular to the axis of the diatreme. The fact that the cone opens to the west is consistent with this postulate, as the structure outcrops west of the central axis of the vent.

The truncation of "bed forms" in the diatreme, by the shattercone, suggests that it postdates them, and indicates that more than one pulse of volcanism was involved in formation of the diatreme. The high initial velocity and turbulent flow of base surges results in high shear stress on the surface beneath the flow (Fisher and Waters, 1970, p. 159). It is interesting to note that the shattercone occurs "beneath" the postulated base surge deposits in outcrop. It can be suggested from this that the shattercone is the result of a late phreatomagmatic eruption and its associated base surge.

C. The Significance of Textural Varieties of Lava

Three lava types have been distinguished in the diatreme (this thesis, p. 88). These volcanics have been termed black lava, pumiceous lava, and light colored lava. The possible significance of these groups is discussed below.

(1) Black Lava

Although black lava is not abundant in the diatreme, it is apparent from petrographic studies that it represents juvenile magmatic material. This lava commonly occurs in elongate sinuous forms and engulfs accidental volcanic, sedimentary and granitic fragments. Feldspar phenocrysts in the lava exhibit a trachytic texture, with their long axes parallel to elongation of the lava or to the perimeter of the included fragment. These features are consistent with the behavior of molten lava in a fluidized system, and suggest that fluidization of liquid and solid materials by gas has taken place (Lorenz et al, 1975, p. 34).

Accidental fragments engulfed by juvenile volcanic matter have been noted from diatremes in several locations, including southwest Germany, Montana and Missouri (op. cit., p. 34). These features have been attributed to rapid exsolution of the gas phase, which sprayed the liquid phase (magma) and the solid phase (phenocrysts and chips of wall rock) into open spaces. The hot liquid coalesced around the solid particles to form free surfaces. Surface tension and spinning of the ejecta in the gas phase, produced rounded and ovoid droplets of magma with a solid nucleus. Trachytic textures in the juvenile lava have also been attributed to rotation of the fragments in the gas phase.

(2) Pumiceous Lava

Vesicular lava, pumiceous lava and glass shards occur occasionally in the diatreme. These features are formed by the expansion of gases in the lava (Williams, Turner and Gilbert, 1954, p. 23). The presence of granulated sideromelane in the diatreme has already been noted (this thesis, p. 93). Sideromemelane forms from the drastic chilling of basaltic magma, and suggests that abundant water was present in the system (Fisher and Waters, 1970, p. 180).

A continuum exists between lava containing occasional vesicles, and glass shards and clusters of fragments exhibiting a vitroclastic texture (Plates 15 and 16). These fragments are presumably formed by comminution due to effervescence of viscous magma (Williams, Turner and Gilbert, 1954, p. 153). Where glass shards are abundant, they tend to be supported in a matrix of comminuted rock debris, subsequently carbonatized. This suggests that because these fragments are more delicate, they are more readily abraded during fluidization.

Tabular fragments of vitric tuff occur occasionally in the diatreme. These have been interpreted as indurated fragments of a pre-existing volcanic pile which has been intruded by the diatreme.

(3) Light-Colored Lava

This is a diverse group and is the main volcanic constituent of the diatreme. It is slightly more coarsely crystalline than other lava types, occurs as rounded to irregular grains, and shows no alignment of feldspar phenocrysts. While it is clearly a different phase than the black lava, its precise significance cannot be determined. Its coarser grain size suggests that it cooled more slowly than the black lava, and the absence of a trachytic texture indicates that it was unaffected by flow during formation of the diatreme. These features, and the irregular rather than elongate shape of the fragments may be interpreted in two ways:

(i) That they represent a less viscous phase of juvenile lava.

(ii) That they are derived from a pre-existing volcanic pile intruded by the diatreme.

The fact that fragments of light colored lava are engulfed by black lava (this thesis, p. 99) suggests that the fragments represent an earlier pulse of volcanic activity.

The amount of juvenile magmatic material among the pyroclastic ejecta of diatremes ranges from close to zero to nearly 100% (Lorenz et al, 1975, p. 53). The difficulty in distinguishing juvenile from accidental and accessory volcanic material in the BBX diatreme is evident from the above discussion. It is clear however, that the black lava and at least some of the pumiceous lava is juvenile. Assuming that fragments of "light-colored lava" are accidental, juvenile lava is thought to represent a relatively small proportion of the total, possibly less than 25%.

D. Venting of the Diatreme and Level of Intrusion

The BBX diatreme is an exhumed volcanic vent which has been eroded well below its original level of intrusion. That the diatreme was originally vented at the surface can be inferred from the following considerations.

1. The presence of spherical lapilli (this thesis, p. 163).
2. The presence of accretionary lapilli (this thesis, p. 170).

3. The presence of glass shards and sideromelane (this thesis, p. 93).

4. Martitization of basaltic ejecta (this thesis, p. 116).

The stratigraphic level at which the diatreme vented at the surface can be inferred from the following considerations.

1. Sedimentary Fragments in the Diatreme

The following observations are relevant if it is assumed that the process of fluidization reached maturity, and therefore that the vent contents have been homogenized (this thesis, p. 158). Implicit in this assumption is that sedimentary fragments seen in outcrop and in drill core derive not only from immediately adjacent sedimentary horizons, but also from those above and below the present level of erosion.

(i) The abundance of red hematitic sediments in the diatreme presumably reflects the dominant horizons through which it passed. These sediments are not present above the McLeod Formation (Table 7).

(ii) The Pethei Group (Table 7) consists entirely of carbonates. Carbonate fragments are relatively rare in the diatreme. They are generally small and include featureless carbonate and light grey dolomitic marlstone.

The relationship between diatremes and alkaline ultramafic and carbonatite magmas has been noted (this thesis, p. 120). According to Lorenz et al (1975, p. 23), calcite may be abundant among the pyroclastic ejecta of diatremes. While some of the carbonate in the BBX diatreme may be attributable to a juvenile source, the marlstone definitely derives from existing rocks intruded by the diatreme. The fact that carbonate fragments are relatively rare in the diatreme, suggests that it intruded only the relatively thin basal formations of the Pethei Group.

2. Pressure Gradients

Pressure gradients of compressible gases flowing in long narrow conduits are not linear. Instead, pressures drop only slightly throughout most of the length then fall rapidly close to the outlet as the gas accelerates (Lorenz et al, 1975, p. 38). Although the relevance of these observations to volcanic vents is complicated by variations in the configuration of the pipe, wall effects, and internal friction, it can be assumed that the highest pressure drop within diatremes is near the surface (op. cit., p. 38). For this reason, most large blocks of wall rock are derived from near-surface levels where gas velocities are the highest. This suggests that large blocks of sediment belonging to the Ogilvie and McLeod Formations originated close to the original surface of eruption. No large blocks of carbonate have been encountered in the diatreme.

While this is clearly a tentative conclusion, the above observations suggest that the diatreme intruded the Sosan and Kahochella Groups, and the basal part of the Pethei Group. This is consistent with the geological setting of other diatremes in Hearne Channel, which intrude at least to the level of the McLeod Formation (this thesis, p. 43). If this interpretation is correct, it can be assumed that the seven (?) Seton basalt pipes in Hearne Channel are coeval, but that the BBX diatreme is more deeply eroded (this thesis p. 43).

E. Relationship Between the Diatreme and the Diabase

The relative ages of the diatreme and the diabase are not known with certainty. According to Lorenz et al, 1975, p. 12), diatreme activity often closes with the intrusion of magma as plugs and dikes. While it can be suggested from this that the diabase plug represents this late magmatic pulse, the following evidence is to the contrary.

(1) The diatreme contains occasional fragments of medium crystalline porphyritic and diabasic intrusive. These resemble the border phases of the diabase plug.

(2) The diatreme contains numerous xenocrysts of twinned plagioclase having the same composition (An 38) as the diabase plug (this thesis, p. 87). Moreover, these xenocrysts exhibit lamellar twinning as do those in the diabase, whereas the juvenile lava in the diatreme contains untwinned plagioclase microlites.

These features suggest that the diatreme intrudes a mafic body similar in texture and composition to the diabase plug. It is tempting to suggest that the diatreme has incorporated border phases of the diabase, and therefore that it plunges steeply to the north. While other evidence exists to support this conclusion (this thesis, p. 185), it must be noted that the configuration of the diabase at depth is unknown, and it may in fact represent a local plug related to a more deep-seated sill or laccolith.

Two conclusions arise from this discussion.

(1) The diatreme intrudes and therefore postdates a pre-existing mafic intrusion of which the diabase plug is a part.

(2) The juvenile lava in the diatreme has a considerably different plagioclase composition than the diabase (An 53 versus An 38), and the intrusions are therefore not genetically related.

F. Orientation of the Diatreme

Three observations suggest that the diatreme may be inclined steeply to the north.

(1) Doming of Sediments

While the majority of sediments adjacent to the diatreme dip in towards its centre, those at the northeast end appear to dip away (Map 2). This doming is consistent with the possibility that the diatreme is not vertical. An inclined diatreme migrating to the surface would exert a vertical pressure on the hanging wall, and cause doming. Sediments on the footwall would be relatively unaffected, except on cessation of volcanic activity, when they would tend to sag in towards the vent.

(2) Potassium Alteration and Mineralization

The highest grades of mineralization intersected to date occur in the vicinity of trenches 1 and 2 at the south-southwest end of the diatreme (this thesis, p. 9). This mineralization is associated with intense potassium alteration. Other outcrops of agglomerate are generally unmineralized and only weakly altered. These features are consistent with an inclined conduit in which hydrothermal fluids migrated along the footwall.

(3) Diabase Inclusions in the Diatreme

The incorporation of fragments and xenocrysts from the diabase into the diatreme has been discussed above. It is evident from Map 2 that if the diatreme plunged to the north, it would encounter the diabase plug at depth.

III. Origin of the Diatreme

It is apparent from the above discussion that the BBX diatreme has had a complex eruptive history, involving at least 2 pulses of volcanism. The presence of textures indicative of phreatomagmatic eruptions, suggests that water vapor was probably an important constituent of the gas phase. The role played by gases other than water vapor cannot be determined, but it seems probable that they were involved, at least initially in formation of the conduit.

A model explaining the origin of the diatreme must take into account two principle considerations.

A. In their simplest form, phreatomagmatic eruptions involve the intrusion of an igneous body into weak water-saturated sediments at a depth of a few hundred metres (Lorenz et al, 1975, p. 18). When the water in the overlying sediments is heated sufficiently, the system becomes unstable and erupts (op. cit., p. 19).

It has been shown that the emplacement of the diatreme into the Proterozoic succession was controlled by a shear fracture related to compressional folding at deep levels (this thesis, p. 146). It is unlikely that this type of plastic deformation could occur in weak water-saturated sediments. The phreatomagmatic model must therefore be modified to take this into consideration.

The Sosan and Kahochella Groups comprise a substantial stratigraphic thickness deposited over a considerable period of time. It is conceivable therefore, that sediments in the lower parts of this sequence were in the advanced stages of diagenesis and lithification, while those higher in the section were water-saturated, loosely consolidated, and possibly submerged in a shallow sea. Hence, the lower parts of the sequence would behave plastically during deformation, and give rise to the shear fractures which controlled emplacement of the diatreme. Water-saturated sediments in the upper part of the sequence would not be similarly affected. This suggests that the water necessary to cause the phreatomagmatic eruption was not available at depth and therefore, that another mechanism must have been involved in the initial formation of the pipe.

B. The pressure gradient of compressible gases flowing in long narrow conduits is non linear (this thesis, p. 182). Because of this, the high gas velocities necessary to erode a channel are unlikely to be achieved by steam or volcanic gas rising along fractures, except in a short interval very near the surface (Lorenz et al, 1975, p. 27). Regional stratigraphic evidence suggests that the diatreme rose through a considerable thickness of sedimentary strata, on the order of 1000 metres (Figure 7), and is therefore unlikely to be a phreatomagmatic eruption in the classical sense. This again suggests that a mechanism other than a phreatomagmatic eruption must have been involved in the initial formation of the conduit.

The rise of alkaline magma along deep-seated basement fractures was probably related to orogenesis in the Great Slave Basin (for a more detailed discussion, refer to Chapter 2, p. 39). In view of the above considerations the formation of the diatreme may have been brought about by one or a combination of the following mechanisms. In each case, it is assumed that the shear fracture controlling the diatreme was opened, if only briefly, by tectonic stresses.

A. Seepage of seawater into the fracture, and its contact with magma at depth.

B. The rise of magma along the shear fracture, and its ultimate contact with water-saturated sediments or seawater.

C. Drilling of a conduit by high pressure gases exsolved from the underlying magma. Fluid inclusion studies of olivine crystals in alkali basalts indicate that CO_2 under extreme pressure is available at great depths (Lorenz et al, 1975, p. 23). Exsolution of this CO_2 from the magma could be brought about by decreased pressure resulting from opening of the shear fracture. This high pressure CO_2 would escape violently and erode its way to the surface. This initial conduit could then act as a locus for movement of magma and surface water.

There is good evidence to suggest that the diatreme vented at a stratigraphic level equivalent to at least the basal part of the Pethei Group, but has subsequently been eroded to the level of the Akaitcho Formation. Regional stratigraphy suggests that the eroded interval is considerable, and may be approximately 500 metres (Figure 7). In view of this, the presence of base surge textures, accretionary lapilli and sideromelane at the present level of exposure seems anomalous. These features can be explained by one or a combination of the following mechanisms.

A. Subsidence

The withdrawal of magmatic support in the waning stages of volcanic activity may result in caldera-like subsidence of both vent fillings and adjacent wall rocks. The walls themselves, or newly formed cyclinrical or conical fractures function as ring faults (Lorenz et al, 1975, p. 41). Subsidence may result in volcanics originally present at surface, occurring at depths of as much as 1 kimometre in volcanic pipes (op. cit., p. 52). Kimberlite pipes in Montana contain inward-dipping tuff beds broken by unconformities, as deep as 1280 metres below the original surface. This has been accounted for by repeated eruptions, alternating with subsidence (op. cit., p. 51).

B. Homogenization of Vent Contents

The various processes involved in fluidization can conceivably result in mixing of vent contents so that they may occur beneath their original level of deposition. While this may account for the presence of accretionary lapilli and sideromelance at depth, it does not explain the presence here of major features such as base surge deposits.

C. Reactiviation of an Early Volcanic Vent

Mafic tuffs outcrop to the northeast of the diatreme. These are thought to represent part of a pre-exisitng volcanic pile cut by the diatreme. It can be suggested that the base surge structure outcropping in the diatreme is related to an early phase of volcanism which deposited these tuffs. Implicit in this model is that the volcanism was followed by deposition of a thick sequence of sedimentary strata prior to reactiviation of the vent and formation of the present diatreme.

IV. Conclusions

The process of fluidization is essentially non-explosive (Ollier, 1974, p. 307). The evidence that fluidization was an important formative process in the diatreme must therefore be resolved with the evidence of explosive activity. It can be suggested from the foregoing discussion that the formation of the diatreme involved an early phase of volcanism in which fluidization played an important role, and a late phreatomagmatic phase characterized by explosive activity. The complex textures and structures in the diatreme, and the seemingly random distribution of "bed forms" and matrix-supported lapilli, can be attributed to this periodic volcanism and to the complexities of the fluidization process. Subsidence and collapse within the vent in the waning stages of volcanic activity have further complicated these textures.

SECTION III

GEOCHEMISTRY

PREFACE

The BBX deposit has had a complex history characterized by repeated pulses of hydrothermal activity. It will be demonstrated in this and the following section that the mineralizing fluids active in forming the deposit had diverse origins.

In this section, the chemistry and source of the fluid responsible for depositing late-stage quartz veins will be discussed on the basis of fluid inclusion and oxygen isotope studies. While these late-stage fluids deposited only minor amounts of chalcopyrite, evidence exists to suggest that the main mineralizing phase had a similar chemistry and derivation.

CHAPTER 7

FLUID INCLUSION STUDY

I. General Remarks

The formation of a majority of ore deposits is ascribed to crystallization of metalliferous and gangue-minerals from solutions rich in volatiles and soluble salts (Roedder, 1979, p. 684). The deposition of minerals from these solutions is brought about by encounters with appropriate physical or chemical environments, and the solutions themselves generally pass out of the system. Hence, although they are of fundamental importance to our understanding of ore-forming processes, these fluids are generally not available for study except in rare cases (e.g. Red Sea and Salton Sea brines). Traces of these solutions that do remain in the system are thought to be represented by fluid inclusions, which generally comprise aqueous liquid plus vapor, trapped as an homogeneous fluid in irregularities in a crystal. Studies of these inclusions make it possible to place certain limitations on the conditions under which a mineral deposit formed.

The purpose of the present study is to determine the nature of the fluid responsible for mineralizing the BBX diatreme, and on this basis to speculate on the origin and affinity of the mineralization. In particular, on the basis of temperature of formation and chemistry, it is possible to tentatively determine if the deposit formed by magmatic hydrothermal or by other processes (Roedder, 1976, p. 100).

II. Instrumentation

This study was carried out on a television-equipped Chaixmeca VT 2120 heating-freezing microscope stage (Poty et al, 1976). This device is capable of an accuracy of ± 0.1°C in the temperature ranges determined in this study.

III. Selection of Samples and Sample Descriptions

The mineralization in the BBX diatreme is generally unsuitable for fluid inclusion studies. The main metalliferous minerals are opaque and hence of no use in freezing and heating experiments. The only minerals which are potentially suitable for study are quartz, carbonate and barite, and the almost complete lack of vuggy cavities associated with these minerals precludes the selection of optimum specimens for study (Roedder, 1976, p. 77).

A total of 30 specimens were selected from the diatreme and adjacent areas in order to provide a representative sample from mineralized and unmineralized zones and from quartz-carbonate veins. Polished thick sections of these specimens were prepared and examined under a petrographic microscope, with the following results.

A. Carbonate is unsuitable for study as it generally contains abundant impurities, and is not sufficiently transparent.

B. Barite occurs as clean, very tranparent grains in the diatreme. Unfortunately, only three fluid inclusions could be found, and these were too small for heating and freezing experiments (i.e. $\leq$ 5 microns).

C. Quartz is present in at least 2 modes; as gangue associated directly with the mineralization, and as late-stage quartz-carbonate veins. Although quartz which occurs as gangue in the main mineralized zones tends to be quite clean and transparent, it is present in such small quantities that suitable fluid inclusions are difficult to find. Several primary fluid inclusions were located, but all were too small for heating and freezing studies (i.e. $\leq$ 5 microns).

Quartz which occurs in late-stage veins is far more abundant and more coarsely crystalline and hence more amenable to study. Quartz in these veins tends to contain abundant impurities and to be highly fractured. Hence, although fluid inclusions are numerous, they are difficult to see clearly, and the vast majority are secondary. Nevertheless, a total of 107 apparently primary fluid inclusions were located for study. Of these, experimental data could only be obtained from 38 (Table 9).

IV. Problems and Sources of Error

The major problem in this study arises from the small size of the fluid inclusions (this chapter, p. 203). Although the inclusions could be seen clearly under the petrographic microscope, the poorer resolution of the heating lens precluded the use of many of these inclusions for high temperature studies. Moreover, precise homogenization temperatures of the larger inclusions were often obscured as a result of poor resolution.

The above features account for the fact that in certain cases, it was not possible to determine both T_h and T_f for a given inclusion (Table 9).

Errors reported in this study have been taken as one standard deviation from the mean.

TABLE 9

FLUID INCLUSION DATA

Sample No.	Type	Major Axis (μ)	Minor Axis (μ)	Vapour Bubble Area (%)	T_h(°C)	T_f(°C)	Daughter Crystal
N3B	Giant Quartz Vein	27	13.5	13.3	----	+30.0	
		15	9.0	10.0	147.2	-18.9	
		16.5	15.0	7.4	157.3	----	
		18.0	9.0	12.5	137.2	+27.0	
		10.8	3.6	16.7	143.0	----	halite
45B	Giant Quartz Vein	30.0	12.0	10.1	143.0	+6.2	
		27.0	6.0	20.0	----	+8.2	
		12.0	9.0	8.9	----	+4.9	
		45.0	15.0	8.1	147.2	+3.2	
31B	Giant Quartz Vein	21.0	6.0	14.3	139.5	----	halite in adjacent 4 inclusions
		16.5	12.6	8.8	----	+33.2	
		14.4	7.5	7.7	----	+27.8	
		9.6	6.0	11.8	----	-21.5	
		18.0	12.0	9.3	----	+5.8	
		15.0	12.0	7.6	----	+1.8	halite
		12.0	7.5	12.5	149.4	----	
		18.0	12.0	7.3	----	+5.0	halite
		24.0	15.0	6.5	----	+12.0	halite
		12.0	12.0	8.7	159.0	----	halite
		19.5	13.5	6.9	----	+13.4	halite
		33.0	24.0	4.7	----	+9.6	
		33.0	27.0	5.7	152.3	----	halite

Continued ....

TABLE 9 (cont'd)

FLUID INCLUSION DATA

Sample No.	Type	Major Axis (μ)	Minor Axis (μ)	Vapour Bubble Area (%)	T_h(°C)	T_f(°C)	Daughter Crystal
267-10	Quartz-carbonate vein-depth of 267 feet in DDH 76-1	12.6	8.4	8.3	137.2	+28.8	halite
		24.0	6.0	9.1	118.2	----	halite, sylvite(?)
		28.8	9.6	6.0	----	+11.0	halite
		24.6	21.0	5.8	151.4	+19.0	halite
		18.0	9.6	9.7	143.1	----	halite
		22.8	10.8	14.8	137.0	----	
		63.6	48.0	4.6	----	+5.9	halite sylvite(?)
		27.0	15.6	10.0	----	+22.8	halite
		12.0	6.0	9.3	149.5	----	
		12.0	7.2	11.1	146.6	----	
		12.0	7.2	6.7	151.8	----	halite
302	Quartz Vein -depth of 302 feet in DDH 76-1	42.0	18.0	5.6	147.0	----	halite
		48.0	15.0	7.1	160.5	----	halite, sylvite(?)
		22.5	13.5	6.7	----	-22.4	
362-6	Quartz-carbonate vein -depth of 362 feet in DDH 76-1	18.0	10.8	7.3	----	+11.0	halite
		21.0	12.6	7.4	142.0	+3.5	
	Total Population:	38	38	38	21	24	
	Mean:	22.5	12.6	9.2	145.7		
	1 Standard Dev.:	11.7	7.7	3.4	9.3		

V. Fluid Inclusion Petrography (Plates 27 and 28)

The fluid inclusions are all apparently primary as determined from the criteria outlined by Roedder, 1976 (p. 74). The inclusions exhibit a considerable range of shapes, and can be described as elongate, equant, triangular and irregular. Nevertheless, many of the inclusions have at least one linear boundary, which may suggest that they are related to growth planes within the host mineral. In addition, curved boundaries occur in some inclusions, although none approach sphericity. This curvature indicates that limited recrystallization of the host mineral has occurred in order to reduce the high surface energy of the system and suggests that the host mineral (quartz) is soluble in the included fluid (Roedder, 1979, p. 701). Inclusions exhibiting necking textures or obvious pinching of boundaries were avoided.

The major axes of the fluid inclusions (as seen in two dimensions) range from 9.6 microns to 63.6 microns, with a mean of 22.5 ± 11.7 microns. The minor axes range from 3.6 to 48.0 microns, with a mean of 12.6 ± 7.7 microns (Table 9).

Plate 27 Photomicrograph showing a typical three phase fluid inclusion from a late-stage quartz vein (phase IV). Phases are liquid (l), vapour (v) and daughter crystal (halite, d). (Transmitted light.)

Plate 28 Photomicrograph showing a typical three phase fluid inclusion from a late-stage quartz vein (phase IV). Phases are liquid (l), vapour (v) and daughter crystal (halite, d). (Transmitted light.)

v
d
l
20 μ

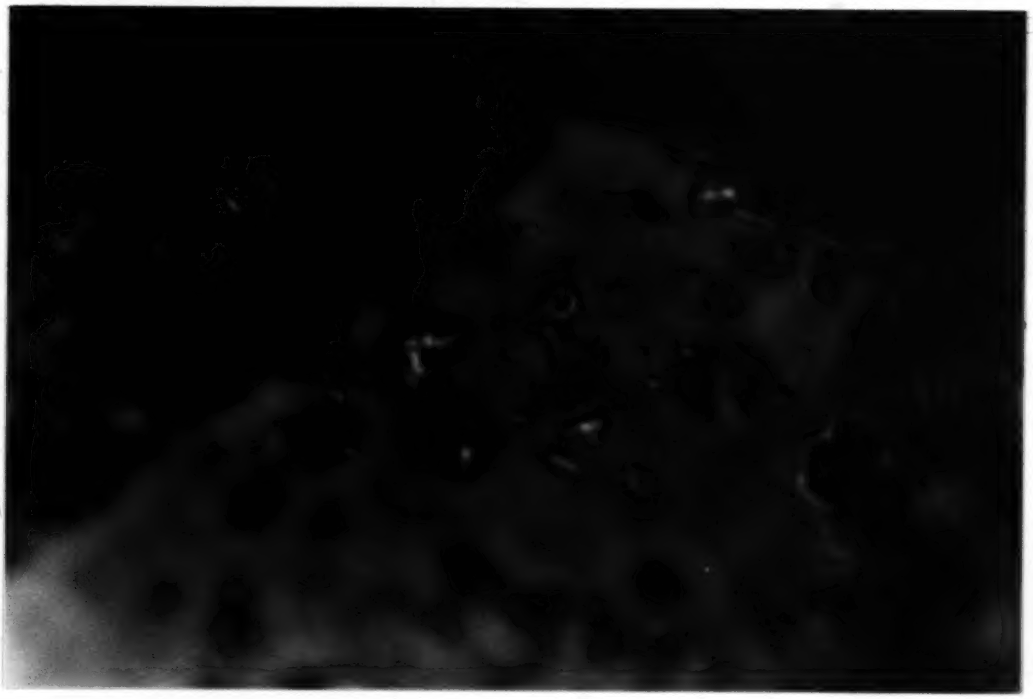

The fluid inclusions contain two principle visible phases; an aqueous liquid phase, and a vapour phase. The vapour phase averages 9.2 ± 3.4% of the area of the inclusion.[1] In addition to liquid and vapour phases, approximately half of the inclusions studied contain a single visible daughter crystal (Table 9). The cubic habit and isotropic nature of these crystals suggest that they are halite. Three of the inclusions listed in Table 9 contain two cubic daughter crystals. Because of the very small distances in fluid inclusions, water soluble daughter crystals generally have time to reach minimum surface energy. Hence the number of daughter mineral phases is generally equal to the number of crystals (Roedder, 1967, p. 541). This suggests that both halite and sylvite are present in these inclusions, although both are cubic and cannot be distinguished with certainty on the basis of morphology.

---

[1] Areas were determined visually from sketches of the fluid inclusions drawn to scale on graph paper, and are therefore approximate.

Daughter crystals of anhydrite (?) were tentatively identified in two inclusions on the basis of their anisotropy and elongate habit. These same inclusions contain halite daughters but are extremely small and could not be used for heating and freezing experiments.

VI. Low Temperature Studies

A. Introduction

Low temperature studies of fluid inclusions are undertaken primarily to determine the composition of the mineralizing fluid. Interpretation of freezing temperature (T_f) data is contingent on a sound understanding of the problems and limitations of the data gathering process and the complexities of the system being studied. While it is evident from the present study that the fluids responsible for mineralizing the BBX diatreme are both variable and complex, a rigorous interpretation of available data is not possible for the following reasons.

1. Clathrate Compounds

In most cases, the solid formed during freezing of inclusions was found to persist on thawing to temperatures well in excess of 0°C. The existence of solid phases at temperatures significantly higher than the freezing point of pure water, indicates that clathrate hydrates have formed, and suggests that gases such as CO_2 and CH_4 are present in the system.

Clathrates are non-stoichiometric crystalline compounds in which an expanded ice lattice forms cages that contain gas molecules (Miller, 1974, p. 151). They resemble ice in appearance and form both below and above the freezing point of water under specific P-T conditions (Hitchon, 1974, p. 195). The encaged molecules do not interact chemically with the water molecules, but serve to stabilize the water lattice by filling cavities. As this function is independent of the composition of the gas, mixed hydrates will form where more than one gas is present in an inclusion (Collins, 1979, p. 1442). The interpretation of clathrate melting temperatures is complicated by the following:

i. A number of geologically important gases, including CO_2, CH_4, H_2S, SO_2, N_2, various hydrocarbons and rare gases form hydrates with the same unit cell structure (Hollister and Burruss, p. 165). Hence, the identification of specific clathrates on the basis of form and habit is extremely difficult. Moreover, complete multicomponent solid solutions are possible amongst all of these clathrates (Hollister and Burruss, 1976, p. 165). Stability data pertaining to tentatively identified clathrates must therefore be used with caution.

ii. The stability of gas hydrates is dependent not only on pressure and temperature, but varies according to the salinity of the aqueous solution (Collins, 1979, p. 1442, Fig. 1). As will be discussed later, determination of salinity in the presence of gas hydrates is extremely difficult except under the most ideal conditions.

2. Availability of Stability Data

While abundant information is currently available on clathrates, their presence in fluid inclusions is a special case requiring special consideration, and is not well documented. Recent papers by Collins (1979) and Hollister and Burruss (1976) provide useful information on CO_2 and CH_4 clathrates in fluid inclusions and discuss the effect of salinity on the stability of these compounds. To this author's knowledge, a similar treatment of other geologically important gases and mixtures of gases is not currently available. The data that are available are based on studies of CO_2-H_2O-NaCl and CH_4-H_2O-NaCl systems. While NaCl is known to be the dominant salt, significant quantities of Ca, K, Mg and B are well documented in fluid inclusions (Roedder, 1976, p. 98). Moreover, the chemistry of the inclusions in the present study is known to be more complex than the systems mentioned above. Interpretation of the the chemistry of these inclusions using published stability diagrams for pure systems is therefore subject to some error.

3. Metastable Phenomena

The existence of metastable phenomena in fluid inclusions is well documented and arises from the fact that the inclusions represent very small systems, even from an atomic viewpoint. Consequently, failure to nucleate new stable phases is often a problem (Roedder, 1967, p. 533).

Metastability has also been documented in the case of clathrate compounds, where small amounts of the compound persist after dissociation conditions of pressure and temperature have been established (Deaton and Frost, 1946, p. 10). In some cases, metastable compounds may persist for a considerable period of time. Hence, measurements of dissociation temperatures of these compounds, taken as they are allowed to warm up to room temperature, may be anomalously high.

4. Optical Difficulties

The effectiveness of the present study was severely limited by the small size of the inclusions and by poor resolution at high magnification. In a recent study by Collins (1979), most of the inclusions examined were of the order of 50 to 100 microns (largest dimension). According to Collins (1979, p. 1437), some of the detailed observations regarding phase changes were not possible on inclusions less than 20 microns (largest dimension), depending on experimental conditions. Moreover, in the case of the CO_2 hydrate, measurement of decomposition temperatures is exceptionally difficult because of the similarity in refractive index between hydrate and aqueous solution (Collins, 1979, p. 1437). The above difficulties all but precluded the observation of subtle phase changes and details of petrography which are necessary to the accurate interpretation of complex fluid inclusion systems.

B. Behavior upon Freezing

The following observations were made during freezing of the inclusions.

1. In all cases, fluid inclusions had to be supercooled to well below their actual freezing temperatures before visible freezing occurred. Generally, inclusions were cooled to less than -100°C. In some cases, temperatures as low as

-160°C were achieved. This supercooling was necessary in order to overcome metastability.

Freezing of inclusions was observed in only a few cases. Where it was observed, inclusions became cloudy, and generally, but not necessarily, underwent an abrupt shrinkage of the vapor bubble. Frequently, inclusions remained clear and their frozen state became apparent only with the development of a crystal mush on thawing. Freezing occurred at temperatures of approximately -80°C, often following extreme supercooling. In several cases, inclusions froze at -78 to -80°C after warming from supercooled temperatures of below -100°C.

2. In several instances, cooling of fluid inclusions resulted in the appearance of a dark border surrounding the vapour bubble. This border, which appeared to increase the size of the vapour bubble, disappeared abruptly at -80°C on warming.

3. First melting temperatures[1] could not always be recognized. In some cases however,

---

[1] First melting temperature is defined as the approximate temperature during warming, at which liquid in appreciable amounts is formed in the inclusions (Roedder, 1962, p. 1054).

temperatures as low as -56°C to -60°C were noted.

4. Freezing temperatures[2] were generally greater than 0°C because of the presence of gases and clathration. In several cases, clathrates persisted to temperatures in excess of 40°C. This data was discarded as being due to metastable equilibria.

C. Statistical Treatment of Data

Freezing temperature data is summarized in Table 9 and treated statistically in Table 10 and Figure 19. Because of the small population involved, the lack of a well-defined gaussian distribution, and the possibility of metastable equilibria, interpretation of this data is clearly subjective. Nevertheless, freezing temperatures appear to fall into three groups having mean values of -20.9 ± 1.8°C, 7.3 ± 3.6°C and 26.9 ± 4.7°C. The possibility that population 2 is skewed towards higher values may be interpreted as the result of metastable equilibria, in which case a mean of 7.3°C is

---

[2] Freezing temperature is defined as the temperature at which the last crystal, usually ice, melts in the inclusion under reversible equilibrium conditions (Roedder, 1962, p. 1055). Because of the presence of hydrates in the system, the term is used somewhat loosely, and here includes "decomposition temperature" of hydrates (Collins, p. 1436).

TABLE 10

STATISTICAL TREATMENT OF FREEZING TEMPERATURE DATA

T_f(°C)	Frequency	% Frequency
(-)24-(-)22.1	1	4.17
(-)22-(-)20.1	1	4.17
(-)20-(-)18.1	1	4.17
0-(+) 1.9	1	4.17
2- 3.9	2	8.33
4- 5.9	4	16.67
6- 7.9	1	4.17
8- 9.9	2	8.33
10- 11.9	2	8.33
12- 13.9	2	8.33
14- 15.9	--	--
16- 17.9	--	--
18- 19.9	1	4.17
20- 21.9	--	--
22- 23.9	1	4.17
24- 25.9	--	--
26- 27.9	2	8.33
28- 29.9	1	4.17
30- 31.9	1	4.17
32- 33.9	1	4.17
	24	100.02

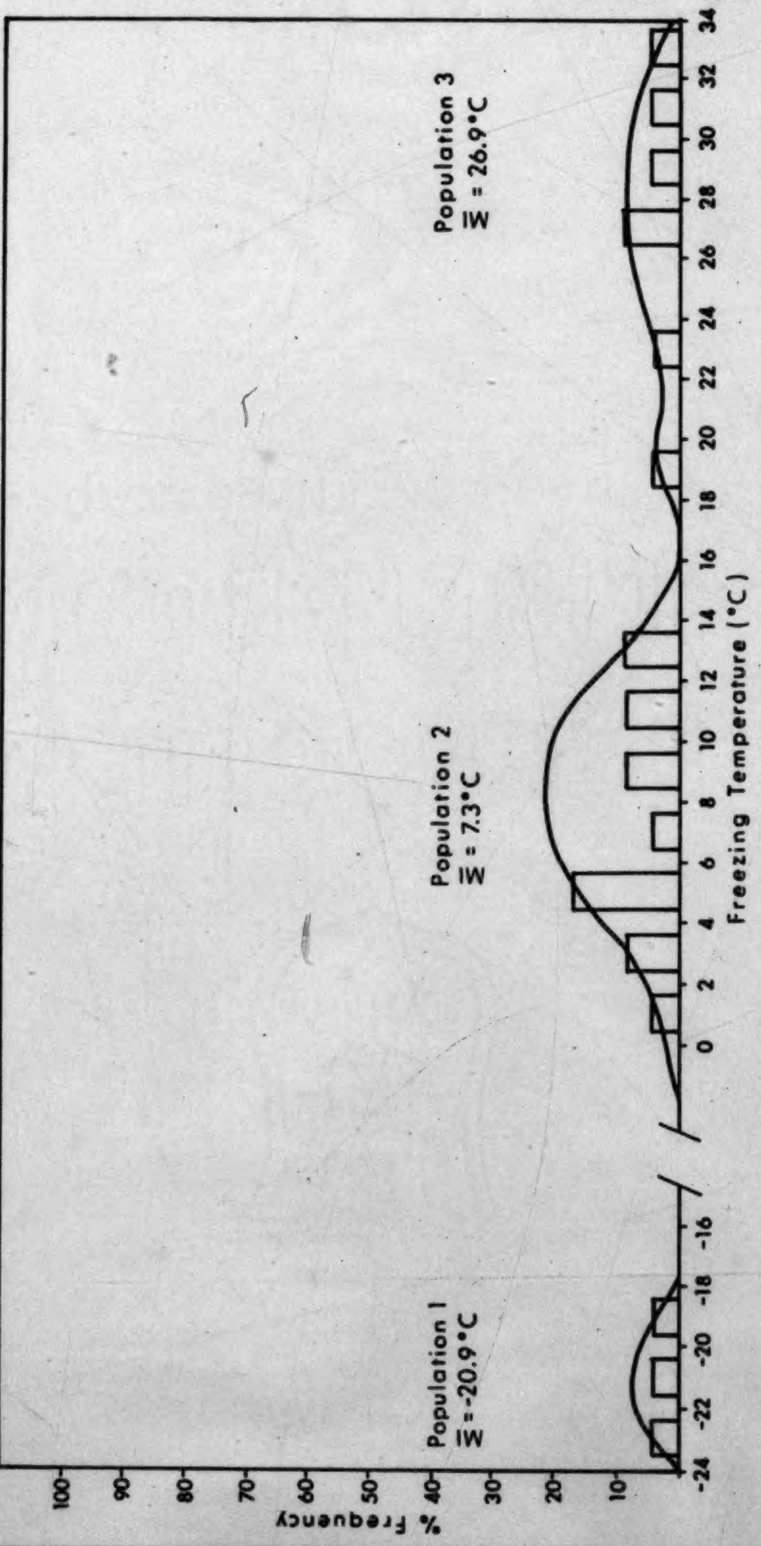

Figure 19 Histogram of Freezing Temperature VS % Frequency for Quartz

slightly high. While it can be suggested that population 3 is entirely the result of metastability in population 2, this is not felt to be the case. These populations appear to be relatively distinct, with a spread of almost 20°C between their mean values, and do not overlap within experimental error.

D. Discussion of Results

1. Determination of Salinity

The behavior during freezing of fluid inclusions in which gas is a constituent is complex. Gas hydrates form in fluid inclusions prior to freezing of the remaining aqueous solution to ice. During their formation, water is removed from the aqueous phase, and salts such as NaCl are rejected. These salts concentrate in the residual aqueous phase and increase its salinity. Consequently, salinity estimates based on the depression of the freezing point of water by salts will be anomalously high and may be in error by as much as 50% (Collins, 1979, p. 1443).

The addition of NaCl or a similar electrolyte decreases the chemical potential of water and thereby lowers the temperature of formation of hydrates (Hollister and Burruss, 1976, p. 166). Because hydrate freezing temperatures are salinity dependent, a knowledge of freezing temperatures can be used to determine the salinity of the aqueous solution indirectly, provided the chemistry of the inclusion is well understood (Collins, 1979, p. 1441). In the present case the complex chemistry of the inclusions and uncertainties regarding the composition of the gas phase make such a determination impossible. Nevertheless, a variety of useful information can be gleaned from the foregoing studies.

i. In the three cases in which clathrate compounds did not form and daughter crysstals were not present, freezing took place between -18.9°C and -22.4°C, with a mean of -20.9 ± 1.8°C. If we assume that these are relatively simple 2 phase inclusions of the system NaCl-H_2O, then a salinity of 23 wt % NaCl equivalent is indicated (Roedder, 1962, Figure 4, p. 1059). As pure NaCl can only depress T_f to -21.1°C (op. cit., Figure 4), the presence of other salts is indicated in at least one instance.

ii. First melting temperatures as low as -56°C to -60°C (this Chapter, p. 214) appear to suggest a complex solution, presumably with a significant calcium component (Roedder, 1963, p. 178).

iii. Daughter crystals were present in 10 of the 24 inclusions for which freezing data are available. Moreover, of the 38 inclusions examined in this study as a whole, 19 (50%) contained halite daughters and are therefore saturated with respect to NaCl (Roedder, 1967, p. 533).

In view of the tentative identification of sylvite and sulphate daughter crystals in some inclusions, high concentrations of KCl and $CaSO_4$(?) must be considered a possibility, at least in some instances. According to Roedder (1967, p. 533), salt crystals generally nucleate, even in very small inclusions, but other phases present in smaller amounts may fail to form daughter crystals because of metastability. This lends some credence to the idea that high concentrations of potassium and sulphate are present in all inclusions, but that daughter crystals of sylvite and anhydrite failed to nucleate in all but a few. To some extent, this is supported by the fact that two of three sylvite(?) daughters tentatively identified in this study were found in relatively large inclusions (Table 9).

2. Clathrate Chemistry

The formation of clathrates in the inclusions during freezing has been well established, and is a useful indicator of the presence of even small amounts of gases dissolved in the aqueous solution (Collins, 1979, p. 1440). Unfortunately, the complex chemistry of clathrates discussed earlier, makes precise identification of these gases all but impossible. In spite of these limitations however, several tentative observations can be made.

Freezing temperatures greater than 0°C have been shown to fall into two reasonably distinct groups. It is evident from Table 9 that clathrates in different inclusions in a given specimen may decompose within either of the above temperature ranges. It is reasonable to assume that inclusions in a given specimen, separated by distances of perhaps a few microns, were trapped at the same pressure. Therefore, if we assume that salinity is also constant, this difference in decomposition temperature may be attributable to a variation in the gas composition and appears to suggest that the fluid chemistry varied somewhat with respect to gas content, even over short intervals.

Although the composition of the gases forming the clathrates cannot be determined with certainty, it seems probable that $CO_2(g)$ is present in at least some of the inclusions. In support of this conclusion are the following observations:

i. CO_2 is the commonest gas found in fluid inclusions (Stanton, 1972, p. 167). Unfortunately, its presence is not always easy to detect. According to Roedder (1963, p. 195), unless the gas bubble is squeezed very flat, even 10% liquid CO_2 can be missed optically because it clings to the interface between the gas bubble and water, and is hidden by total reflection. Moreover, if the CO_2 pressure in inclusions is not high, a separate liquid CO_2 phase may fail to develop, even on cooling slightly below the critical point for CO_2(+31°C) (Roedder, 1963, p. 188). In some cases, the development of a liquid CO_2 phase on rapid cooling can only be detected by a slight darkening of the borders and a rigorous motion of the gas bubble (Roedder, 1963, p. 195). In the present study, a slight darkening of the border, and apparent enlargement of the gas bubble on rapid cooling has been noted (this Chapter, p. 213), and may suggest the presence of a liquid CO_2 phase. The sudden disappearance of this phase at -80°C may be interpreted as a masking effect due to freezing of water in the inclusions at this temperature. In inclusions where this darkening was not noted, the possibility that CO_2 is present as a dissolved gas in the aqueous solution must be considered.

ii. Of the major geologically important gases, H_2S is readily detectable by its strongly sulphurous odour, even in very minute quantities. Crushing of specimens used in this study did not reveal the presence of $H_2S(g)$ and it is therefore eliminated as a possibility.

iii. The abundance of carbonate in the diatreme suggests that CO_2 was present, at least during certain phases of hydrothermal activity.

Although the presence of CO_2 has been tentatively established in these inclusions, evidence suggests that the low temperature clathrates are probably hybrid compounds of H_2O and at least two gases, one of which may be CO_2. Figure 20 shows phase relations for the system H_2O-CO_2 and indicates that while clathrates of pure H_2O and CO_2(g) can exist up to +10°C, pure CO_2 clathrates in equilibrium with a saturated solution of NaCl such as that postulated in this study, cannot exist above approximately -10°C, regardless of pressure. Although the chemistry of this system is clearly more complex than is indicated by Figure 20, a decomposition temperature of +7.3°C in a saturated NaCl solution is not consistent with pure CO_2 clathrates.

Next to CO_2, CH_4 is the most common gas occurring in fluid inclusions (Collins, 1979, p. 1442), and the CH_4 clathrate is completely miscible with the CO_2 clathrate (Hollister and Burruss, 1976, p. 165). Although the presence of CH_4 cannot be conclusively demonstrated, its addition into the CO_2-H_2O system shifts the decomposition isochore to higher temperatures and pressures, and effectively counteracts the influence of NaCl in the solution (Collins, 1979, p. 1442). A hybrid CO_2-CH_4 clathrate in a saturated NaCl solution can therefore exist at temperatures greater

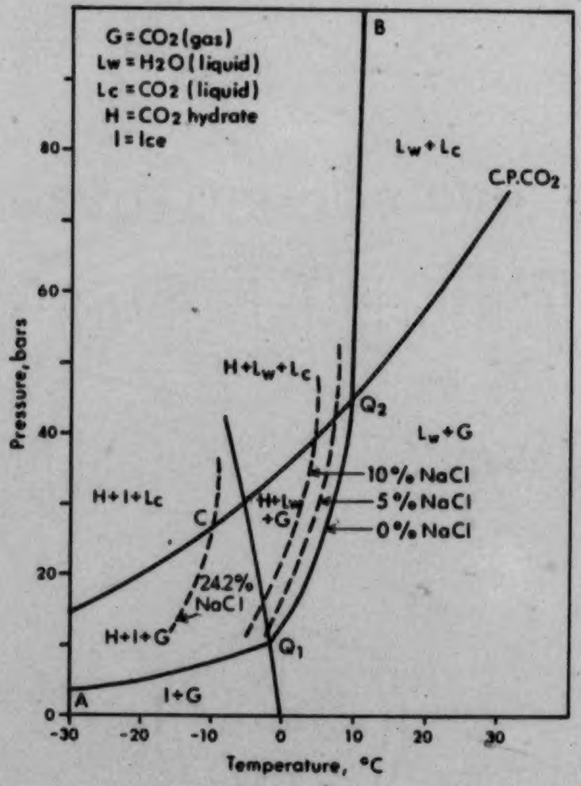

Phase Diagram for the System H_2O-CO_2 The Dashed lines indicate the shift to lower Temperatures of the decomposition of CO_2 hydrate in equilibrium with 5 mass %, 10 mass % and saturated Nacl solutions (24.2 mass %)

(after Collins, Fig. 1, p.1436)

Figure 20

than -10°C, although exact dissociation conditions of such a compound are not known.

The pure methane clathrate can exist in a highly saline solution at a temperature of +7.25°C (45°F), though at a relatively high pressure (Figure 21).

In light of the above discussion, the identity of the clathrates is a matter of speculation. Although CO_2 is present in the system, it is unlikely to occur in large amounts because its solubility in salt solutions is heavily dependent on the concentration of salt, and decreases rapidly as salinity increases. It is unlikely therefore, that a large quantity of CO_2 would dissolve in a hydrothermal solution saturated or very nearly saturated with NaCl (Takenouchi and Kennedy, 1965, p. 451). Moreover because of the high salinity of the inclusions, clathrates of pure CO_2 cannot exist at temperatures greater than 0°C. Therefore, it is tentatively concluded that the low temperature clathrates (T_f = 7.3°C) are hybrid compounds of H_2O, $CO_2(g)$ and another gas, possibly methane.

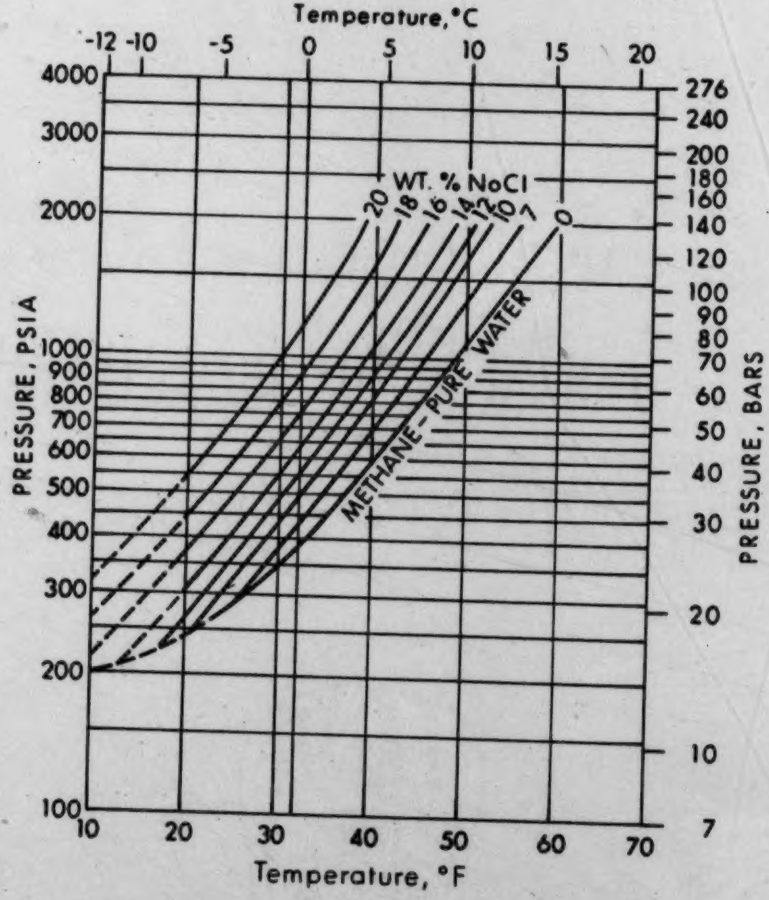

Methane Hydrate Decomposition
Conditions for various Sodium
Chloride Brine Concentrations

(after Kobayashi et al, fig. 3, p. 29)

Figure 21

The possibility that the range in clathrate decomposition temperatures in closely spaced inclusions within a given specimen is the result of variations in gas content has already been discussed. In view of the potential for solid solution amongst gases forming clathrates, such a variation in decomposition temperature could be the result of small fluctuations in the relative concentrations of CO_2 and CH_4(?) in a given inclusion. This postulated variation in gas content is supported by the observation that those inclusions having a mean T_f of -20.9°C (Figure 19) appear to contain no gas whatsoever. Conceivably, a wide range in gas composition may exist between the pure end members CH_4(?) and CO_2.

Those clathrates having a mean decomposition temperature of 26.9°C (80.6°F) are somewhat more problematic. While metastability may have had some effect on the decomposition temperature of these compounds, statistical considerations suggest that this relatively high temperature population is real. Even if it is assumed that metastability has resulted in an apparant T_f several degrees higher than the actual T_f, the composition of these clathrates remains speculative.

The pure methane hydrate is stable up to +21.4°C (Roedder, 1963, p. 193). Reference to Figure 21 however, suggests that for highly saline inclusions, this temperature is considerably lower. Moreover, extrapolation of Figure 21 suggests that even for a decomposition temperature as low as 20°C (68°F) in a 20 wt % NaCl solution, corresponding pressures would be extremely high and unrealistic (see "Geobarometry, this Chapter, p. 229).

Although this is in apparent contradiction to the foregoing discussion, Hollister and Burruss (p. 165) have stated that at a given pressure, the CO_2-CH_4 clathrate melts at a higher temperature than for the pure CH_4 clathrate. The magnitude of this effect is unknown however.

According to Collins (1979, p. 1443) gas hydrate melting above 10°C may be a useful indicator of the presence of hydrocarbons in fluid inclusions, and these must be considered a viable possibility in this instance. Unfortunately, available data do not justify further speculation.

3. Geobarometry

Because clathrates are pressure-temperature dependent, the decomposition temperature can be used in conjunction with phase diagrams to determine the pressure within the fluid inclusion. Assuming that the inclusion has remained a closed system, this pressure should be equivalent to the pressure on the fluid at the time it was trapped.

In the present case, uncertainties as to the composition of the clathrates makes such pressure determinations difficult. Nevertheless, by making certain assumptions, it is possible to establish broad limits on the pressure regime under which the quartz veins formed.

Reference to Figure 20 indicates that pure CO_2 clathrates in equilibrium with a saturated solution of NaCl cannot exist above approximately -10°C, regardless of pressure. However, pure CO_2 clathrates in equilibrium with pure H_2O can exist up to approximately +10°C. The addition of methane into the CO_2-H_2O system shifts the decomposition isochore to higher temperatures and pressures, and counteracts the effect of NaCl in the solution (this Chapter, p. 224). Hence if we assume that the low temperature clathrates are CO_2-CH_4 hybrids, Figure 20 can be used to determine a minimum pressure on the system, using the 0% NaCl isochore (Q_1Q_2B).

Using a mean decomposition temperature of 7.3°C, a pressure of approximately 30 bars (435 psi) is indicated. Assuming an average overburden pressure of 565 psi/1000 feet, this corresponds to a minimum depth of formation of 770 feet (235 metres).

The possibility that at least some clathrates are pure CH_4-H_2O compounds, makes it possible to determine a maximum pressure for the system. Extrapolation of Figure 21 indicates that a decomposition temperature of 7.3°C corresponds approximately to a pressure of 4000 psi (276 bars) in highly saline (i.e. 20 wt %) NaCl inclusions. Using an average overburden pressure of 565 psi/1000 feet, a depth of 7080 feet (2158 metres) is indicated.

As the composition of the gas is not known with certainty and the chemistry of the aqueous solution is somewhat more complex than that shown in Figures 20 and 21, the above pressure determinations are clearly subject to some error. Nevertheless, a pressure range of 435 psi to 4000 psi (235 m to 2158 m) while considerable, is in accordance with independent evidence which suggests an intermediate to shallow depth of formation as follows:

i. The absence of boiling phenomena, and the presence of gases in the inclusions suggests that the system was not vented and was therefore probably not a surface phenomenon.

ii. The postulated control of quartz-carbonate veins by joint planes related to tectonic unloading (this thesis, p. 150), and the dilatant nature of many of the smaller veins, particularly along bedding planes, suggests that the event was relatively near surface.

iii. The presence of barite in the diatreme may suggest near-surface deposition, as barium in solution commonly migrates to the region of sulphate stability and thus is often bound to a narrow zone close to the earth's surface (Fischer and Puchelt, 1978, p. 56-F-2).

iv. Consideration of the regional stratigraphy (Figure 7) suggests that these veins which now cut the Akaitcho Formation, could have been overlain by a maximum of 1000 metres of sedimentary and volcanic cover; probably substantially less.

VII. High Temperature Studies

A. Introduction

The use of fluid inclusions as geothermometers is based on the homogenization temperature (T_h) determined by heating the inclusions until liquid and vapour phases homogenize. Unfortunately, T_h can only be considered a minimum temperature of formation (Smith and Little, 1959, p. 380). Determination of the true formation temperature requires the application of a pressure correction which can usually only be estimated, and hence limits the usefulness of fluid inclusions as geothermometers.

B. Statistical Treatment of Data

Fluid inclusions homogenized in the liquid phase on heating.

Homogenization temperatures determined in this study are listed in Table 9, and are treated statistically in Table 11 and Figure 22. On the basis of this data, there appears to be no well- defined difference between homogenization temperatures in giant quartz veins, and those in quartz-carbonate veins, and they are therefore treated as a single population. The mean homogenization temperature for this population is 145.7 ± 9.3°C.

C. Pressure Correction and Temperature of Formation

The application of a pressure correction is contingent on a knowledge of the depth at which the deposit formed, and assumes that the total pressure on the system is equal to the lithostatic pressure. While the magnitude of this correction is well known for aqueous NaCl solutions (Potter, 1977), the presence of CO_2 or other gases in the inclusions complicates the correction somewhat (Smith and Little, 1959, p. 385). Unfortunately, published information pertaining to pressure corrections for the system H_2O-NaCl-CO_2 do not appear to be available. The situation is further complicated by the postulated presence of CH_4, the effect of which is not known.

TABLE 11

STATISTICAL TREATMENT OF HOMOGENIZATION TEMPERATURE DATA

T_h (°C)	Frequency	% Frequency
115-119.9	1	4.76
120-124.9	--	--
125-129.9	--	--
130-134.9	--	--
135-139.9	4	19.05
140-144.9	4	19.05
145-149.9	6	28.57
150-154.9	3	14.29
155-159.9	2	9.52
160-164.9	1	4.76
	21	100.00

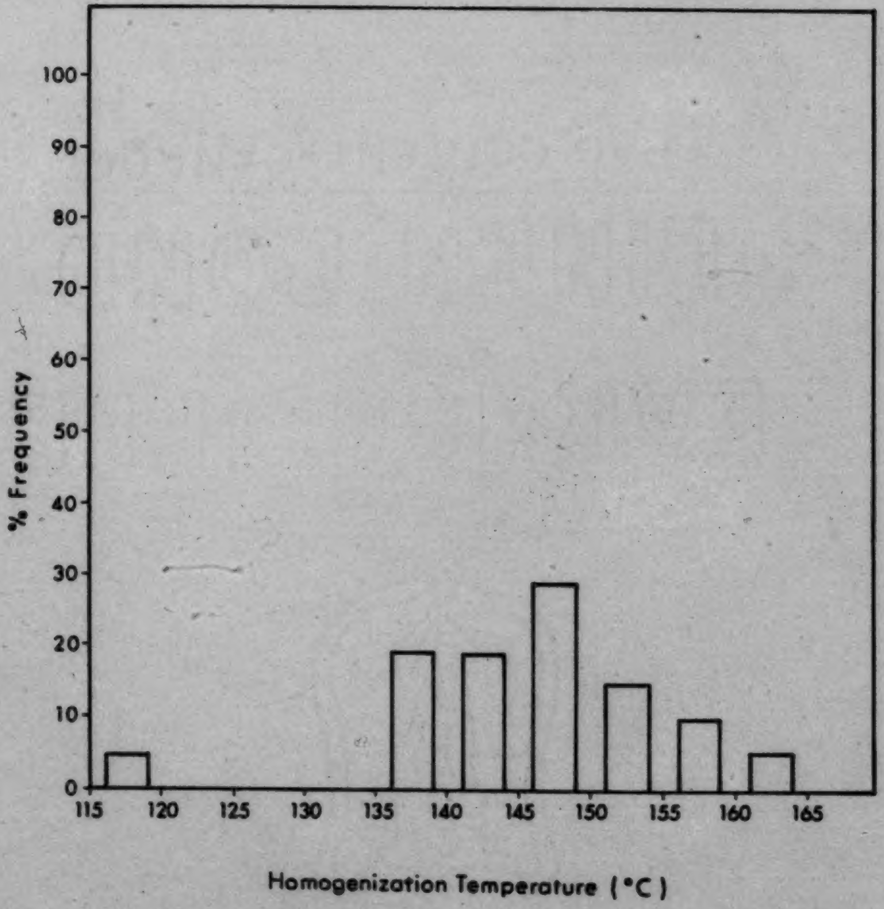

Figure 22 Histogram of Homogenization Temperature VS % Frequency for Quartz

In spite of these limitations, an approximate temperature of formation can be obtained from the data of Potter (Figures 5 and 6). Although gases are known to be present in the inclusions, the fact that they were not visible, suggests that the gas pressure is relatively low and that gases are a minor constituent. Therefore, their effect on the homogenization temperature of the inclusions is felt to be relatively minor, and a pressure correction for the system $NaCl-H_2O$ is tentatively assumed to closely approximate that required for the system presently under study.

In determining the pressure correction (ΔT), it is assumed that the fluid is saturated with NaCl (i.e. 23.3 wt % NaCl).

(i) Minimum Pressure Correction

$P = 30$ bars, $\Delta T_{min} = 4.7 \pm 3°C$

Minimum temperature of formation =

$(145.7 \pm 9.3°C) + (4.7 \pm 3°C)$

$T_{min} = 150.4 \pm 12.3°C$[1]

---

[1] ΔT values have an uncertainty of ± 3°C (Potter, 1977, p. 603). This uncertainty has been added to the error already determined for T_h.

(ii) Maximum Pressure Correction

$$P = 276 \text{ bars}, \ \Delta T_{max} = 33.4 \pm 3°C$$

Maximum temperature of formation =

$$(145.7 \pm 9.3°C) + (33.4 \pm 3°C)$$

$$T_{max} = 179.1 \pm 12.3°C.$$

VIII. Implications

A considerable volume of fluid inclusion data is available from deposits of diverse origins. On the basis of this data, generalizations can be made regarding the nature of various types of mineralizing fluids. In particular, Roedder (1976, p. 87-95) has been able to distinguish tentatively between magmatic hydrothermal and Mississippi Valley-type fluids, on the basis of fluid inclusion characteristics such as temperature, gross salinity and density.

A. Temperature

Homogenization temperatures of inclusions in Mississippi Valley-type deposits range from 100°C to 150°C and rarely as high as 200°C, whereas magmatic hydrothermal deposits range from 100°C to more than 500°C and frequently show a range of more than 100°C for minerals in a single deposit. In the present study, the relatively low homogenization temperature (146°C) and narrow temperature range are consistent with Mississippi Valley-type fluids.

B. Gross Salinity

The salinity of inclusions from Mississippi Valley-type deposits is seldom less than 15 wt % NaCl equivalent, and frequently exceeds 20 wt %. Moreover, analyses of these inclusions indicate that the salts consist mainly of Na and Ca chlorides, with Cl-Na-Ca-K-Mg and B in order of decreasing wt % (Roedder, 1976, p. 98). Magmatic hydrothermal deposits generally have salinites of less than 10 wt % NaCl equivalent. The very high NaCl content and the inferred presence of Ca and K in the inclusions in this study is consistent with the composition of Mississippi Valley-type fluids.

C. Density

Most Mississippi Valley-type fluids have densities very close to or slightly greater than 1 gm/cc. Magmatic fluids on the other hand are generally significantly less than 1 gm/cc.

The density of the fluid in this study was found to be 1.23 gm/cc (Appendix 2). This is an approximate density because of uncertainties regarding the composition of the liquid, and the volume occupied by the vapour bubble. Also, the presence of gas in the inclusions would reduce this figure slightly. In spite of these uncertainties however, the density of the fluid is felt to be slightly greater than 1 gm/cc, which is consistent with Mississippi Valley-type fluids.

On the basis of the above considerations, the mineralizing fluid examined in this study appears to be consistent with Mississippi Valley-type fluids, although the possibility of a magmatic hydrothermal origin cannot be eliminated with certainty.

The term "Mississippi Valley-type deposit" includes a highly diverse assemblage of mineral deposits. The origin of these deposits is a matter of some debate, but most appear to result from one or more processes in which an ore element is dissolved from a dilute source area, transported to the future site of the mineral occurrence, and deposited in a concentrated form (Roedder, 1976, p. 68). Proposed sources of ore elements include sea water, leaching from sedimentary, metamorphic and igneous rocks, expulsion from recrystallizing metamorphic minerals and recrystallizing magmas, and volcanic exhalations (Roedder, 1976, p. 68). Meteoric water, sea water, connate and decomposition fluids in sediments, and metamorphic and magmatic waters have all been proposed as sources of mineralizing fluids.

The precise origin of the fluid in this study, and implications regarding the sources of the mineralization are discussed in the following chapters.

CHAPTER 8

OXYGEN ISOTOPE STUDY

I. Introduction

In the previous chapter, the temperature and chemistry of the hydrothermal fluid responsible for the formation of late-stage quartz veins were determined. On the basis of these data it was concluded that the fluid was not of magmatic hydrothermal origin, but its precise derivation could not be defined. The purpose of this study is to combine the above data with the results of oxygen isotope work, and so determine as nearly as possible, the origin of this fluid.

II. Theoretical Background

Water is the principle constituent of hydrothermal fluids and a knowledge of its origin is essential to any theory on the formation of a mineral deposit. As oxygen isotopes are geochemical parameters based on the water molecules themselves, they are an ideal source of information on the genesis of hydrothermal fluids. Because of isotopic fractionation during natural chemical and physical processes, natural waters of different origins show systematic differences in their ^{18}O contents. These differences are sufficiently well understood that the $\delta^{18}O$

value of the water can be used as an indicator of its source. According to White (1974, p. 955), six major types of water are active in the formation of ore deposits; meteoric water, ocean water, connate water, metamorphic water, magmatic water and juvenile water. Each of these may be altered isotopically and chemically by migration into new physical and chemical environments. Indeed, the formational history of many ore deposits is sufficiently complex that more than one of the above types of water may have been involved at some point (op. cit., p. 971). The $\delta^{18}O$ values of hydrothermal waters determined for a given ore deposit are interpreted in terms of the above considerations.

III. Methodology

$\delta^{18}O$ values have been determined for five specimens of quartz for which homogenization temperatures are known (Chapter 7, Table 9). The $\delta^{18}O$ values of water in equilibrium with this quartz at a given temperature have been determined using the following isotope thermometry equation for the quartz-water system (Knauth and Epstein 1976):

$$\delta^{18}O_W = \delta^{18}O_Q - [3.09 \times 10^6/T^2 - 3.29]$$

where T = equilibrium temperature in °K

W = water

Q = quartz

The calculation of $\delta^{18}O_w$ was performed twice for each sample in order to take into consideration the range in temperatures resulting from the application of pressure corrections. The temperatures used are the maximum temperature of formation ($T_h + \Delta T_{max}$) and the minimum temperature of formation ($T_h + \Delta T_{min}$) (this thesis, p. 237). The results of these calculations are summarized in Table 12.

IV. Discussion

The following observations are based on Table 12.

A. The range of $\delta^{18}O_w$ values between the five samples is small and suggests that quartz from both quartz-carbonate veins and giant quartz veins crystallized from solutions which were isotopically similar. Fluid inclusion studies suggest that the chemistry of these fluids was also similar, at least with respect to dissolved salts.

The fact that the $\delta^{18}O_w$ value of quartz from quartz-carbonate veins is slightly more positive than that of quartz from giant quartz veins is due to a mass balance effect between quartz and carbonate, as the latter is enriched in ^{18}O.

TABLE 12

OXYGEN ISOTOPE DATA FOR QUARTZ

Sample[1] No.	$\delta^{18}O_Q$	T_h(°C)	I T_{min}(°C)	I $\delta^{18}O_w$	II T_{max}(°C)	II $\delta^{18}O_w$
N3B	+13.09	146.2	150.9	-0.82	179.6	+1.30
45B	+12.67	145.1	149.8	-1.33	178.5	+0.80
31B	+11.82	150.0	154.7	-1.78	183.4	+0.28
267-10	+14.22	138.0	142.7	-0.37	171.4	+1.86
362-6	+14.21	142.0	146.7	-0.04	175.4	+2.13
			mean:	-0.87	mean:	+1.27

I $\delta^{18}O_w$ calculated using minimum temperature of formation

$T_{min} = T_h + T_{min}$, where $\Delta T_{min} = 4.7°C$

II $\delta^{18}O_w$ calculated using maximum temperature of formation

$T_{max} = T_h + \Delta T_{max}$, where $\Delta T_{max} = 33.4°C$.

---

[1] Samples from Quartz and Quartz-carbonate veins cutting the BBX diatreme and adjacent sediments

B. The range in $\delta^{18}O$ values which does exist suggests either that the fluid evolved slightly with time, and/or that the system was closed. In an open system with an infinite reservoir of water, $\delta^{18}O_w$ would be expected to be the same in all cases. The possibility that T_h values are slightly in error must also be considered.

C. The $\delta^{18}O$ value of the hydrothermal fluid ranges from slightly negative to slightly positive, depending on whether T_{min} or T_{max} was used in the calculation. The $\delta^{18}O$ value of the fluid can be assumed to lie somewhere between these two extremes. The arithmetic mean of the 10 values listed in Table 12 is +0.20‰ SMOW.

It can be concluded from this that the mineralizing fluid was definitely not of primary magmatic or of metamorphic origin (Taylor, 1974, pp. 850, 851, 855). Seawater and connate formation remain as possibilities.

1. Seawater

The isotopic composition of present day seawater is very uniform at $\delta^{18}O = 0$ (Taylor, 1974, p. 850). If it is assumed that the isotopic composition of the ocean has remained constant through time, it is reasonable to suggest that the fluid in question is seawater.

2. Connate Formation Water

Connate water is initially ocean water which has been trapped in marine sediments and has been out of contact with the atmosphere for at least an appreciable part of a geologic period (White, 1974, p. 955). According to Taylor (1974, p. 852), these waters show a very wide range in both $\delta^{18}O$ and salinity. Isotopic evidence cited by Taylor (1974, p. 853) suggests that meteoric waters are a major constituent of these brines (especially "Oil Field Brines") in the mid-continent region of North America.

V. Conclusions

It is clear from the above that the precise origin of the hydrothermal fluid cannot be resolved on the basis of oxygen isotope work alone. While the isotopic composition of the fluid is strongly suggestive of seawater, the presence of trapped gases and the absence of boiling phenomena in the fluid inclusions suggest that the deposit formed at some depth, and therefore rules out seawater per se as the mineralizing fluid.

It is concluded therefore, that the mineralizing fluid contained connate formation water as its principle component. The possible slightly negative $\delta^{18}O$ of this solution may imply a small meteoric component. It is conceivable that the very high salinity of the brine is in part original (from seawater) and in part due to the solution of evaporites or to shale membrane filtration (Taylor, 1974, p. 852). Water which has undergone these chemical and isotopic changes is referred to as "evolved connate water" (White, 1974, p. 955), and the fluid is a stratafugic brine originating within the sedimentary pile.

Closing Remarks to Section III

I. The quartz veins which have been studied in the previous two chapters represent a very late phase of hydrothermal activity, and contain only minor amounts of mineralization (mainly chalcopyrite). Two principle lines of evidence suggest that certain earlier phases of hydrothermal activity responsible for the deposition of substantial quantities of copper and lead mineralization, (Phase II, Chapter 10), and of barite (Phase III, Chapter 10) may have had a similar chemistry, and also originated as connate brines within the sedimentary pile.

1. Fluid Inclusion Evidence

Quartz occurs as a gangue mineral in equilibrium with galena and chalcopyrite in the main mineralized zones. Barite is associated in some instances. Fluid inclusions in quartz and barite from these zones were found to be extremely small, and therefore unsuitable for heating and freezing studies. In spite of the small size however, a variety of qualitative information was obtained from petrograhic studies. Filling ratios in fluid inclusions in both quartz and barite suggest low to moderate temperatures of homogenization. In addition, the presence of halite daughter crystals in many inclusions suggest that the fluid was saturated with respect to NaCl. As many as four daughters were observed in a single inclusion in both quartz and barite. Based on the habit of these crystals, sylvite and anhydrite were tentatively identified in addition to halite. In two instances, a small droplet of unidentified immiscible liquid was observed adjacent to the vapour bubble in inclusions from barite.

These features suggest a relatively low temperature, highly saline, chemically complex solution containing a third fluid phase in some instances, and are consistent with data obtained from late-stage quartz-carbonate veins.

2. Chemistry of Alteration Assemblages

Highly mineralized zones in the diatreme are characterized by pronounced potassium alteration. Small amounts of lithium are associated with muscovite in these zones (this thesis, p. 106). It is clear from studies of hydrothermal alteration (this thesis p. 108) that K and Li have been introduced hydrothermally into the diatreme. The abundance of K and Li in various sediments and natural waters is summarized in Table 13. It is evident from this table that both K and Li are significantly more abundant in formation water (brines) than in either seawater or "hydrothermal water".

TABLE 13[1]

a. Abundance of Lithium and Potassium in Natural Waters

	Li (ppm)	K (ppm)
River	23	6.5
Seawater	0.19	392
Formation Water (Brines)	26	1441
Hydrothermal Water	8.2	116

b. Abundance of Lithium and Potassium in Common Sediments and Sedimentary Rocks Types

	Li (ppm)	K_2O(wt.%)
Soils	26	1.68
Sands and Sandstone	38	1.48
Argillaceous Sediments	66	2.81
Marine Shales	76	
Fresh Water Shales	67	
Shales		2.45
Limestone		0.31
Dolomite	15.2	0.68

---

[1] Data from Cocco et al, "Lithium" and "Potassium".

While this evidence is indirect, it supports the postulate that the main mineralizing fluid was a connate brine.

II. The mineralogy and paragenesis of the BBX deposit is complex (Chapter 10). It must be noted that the main mineralizing event and the event responsible for depositing late-stage quartz veins were probably separated by a considerable time interval. Therefore, although they may both be related to connate brines, at least subtle differences in chemistry are to be expected. This is evidenced in part by the fact that the early phase is associated with substantial amounts of mineralization, while the late-stage quartz veins are relatively barren.

III. It has been suggested from studies of structural geology that the late-stage quartz veins were deposited following a period of uplift and tectonic unloading (this thesis, p. 150). Implicit in this model is that the quartz veins were deposited relatively closer to the surface than the main phase of mineralization. Homogenization temperatures in fluid inclusions in these veins would therefore require a smaller pressure correction than those in quartz from the main mineralized zones. Because homogenization temperatures appear to be similar in each case, it is suggested that the main phase of mineralization was deposited at a higher temperature than is indicated for the late-stage quartz veins studied in the previous chapters.

IV. The mineralogy and geological environment of the BBX deposit preclude its classification as a "Mississippi Valley-type" deposit in the classical sense. Nevertheless, it is suggested from the above that the late-stage quartz veins and possibly the main phase(s) of mineralization (phases II and III, chapter 10) were deposited from circulating connate brines which leached metallic elements out of the sedimentary pile and deposited them in concentrated form in the diatreme. This model is supported by lead isotope studies (Chapter 9), and is discussed in greater detail in Chapter 10.

SECTION IV

ECONOMIC GEOLOGY

PREFACE

In the following chapters, the nature and occurrence of mineralization in the BBX diatreme and immediately adjacent areas is discussed. In order to facilitate interpretation of the economic geology of the deposit, eight samples of varying mineralogy were selected from mineralized zones, both on surface and at depth. The major and accessory element chemistry of these samples was determined by quantitative XRF analysis, and is shown in Tables 14 and 15. These analyses represent the whole rock chemistry of highly altered and mineralized volcanics. Because of the late addition and depletion of certain elements, and the inhomogeneous nature of the breccia initially, these analyses cannot be used to determine detailed chemical trends, or for chemical classification. They are of some use however, in outlining broad trends, and can be used to help interpret the mineralogy of the deposit. Data pertinent to the interpretation of these analyses are shown in Table 16. The major element chemistry of unaltered basalts of various types is shown for comparative purposes in Table 17.

The following points should be noted regarding these analyses.

1. The major element chemistry shown in Table 14 does not total 100% because of the abundance of carbonate (hence CO_2) which is not detected by the analytical technique. Moreover, the samples contain substantial quantities of mineralization (Table 15) which are not shown in Table 14.

2. Table 15 is a selective analysis of the samples and does not reflect all elements present. Cobalt for instance may occur in significant quantities (Table 2) but cannot be detected by XRF analysis.

Interpretations based on these chemical analyses are discussed in the following chapters.

TABLE 14

MAJOR ELEMENT CHEMISTRY OF SELECTED SAMPLES FROM MINERALIZED ZONES IN THE BBX DIATREME (XRF QUANTITATIVE ANALYSES - REPORTED IN WT.%)[1]

	SAMPLE NUMBERS							
ELEMENT	A	B	C	D	E	284	288	297
SiO_2	37.80	32.49	42.51	41.74	36.37	47.33	33.31	46.54
Al_2O_3	10.09	7.35	16.97	15.22	9.70	21.50	12.95	21.34
Fe_2O_3	2.21	7.86	11.98	11.88	6.33	10.81	21.93	9.94
MgO	0.32	10.32	1.64	3.26	9.63	2.38	2.33	1.85
CaO	0.10	18.62	1.69	4.50	17.65	0.81	0.51	1.19
Na_2O	0.02	0.02	0.02	0.04	0.03	0.06	0.03	0.04
K_2O	4.20	5.59	8.74	8.06	6.45	8.45	3.98	8.96
TiO_2	0.96	1.27	2.13	2.01	1.82	2.44	1.20	2.32
MnO	0.01	0.42	0.05	0.09	0.42	0.02	0.01	0.02
S	7.11	0.25	6.52	5.48	0.14	2.11	4.00	3.48
P_2O_5	00.17	0.11	00.23	0.23	0.15	0.14	0.11	0.37
H_2O	3.61	3.53	3.00	3.71	1.70	3.48	2.53	3.64
TOTAL (%)	66.60	87.83	95.48	96.20	90.41	99.53	82.89	99.69

---

[1] Analysis by Dr. R.G. Holland, University of Newcastle Upon Tyme; Phillips PW 1212 XRF

TABLE 15

ACCESSORY ELEMENT CHEMISTRY OF SELECTED SAMPLES FROM MINERALIZED ZONES IN THE BBX DIATREME (XRF QUANTITATIVE ANALYSES - REPORTED IN PPM)[1]

ELEMENT	SAMPLE NUMBERS							
	A	B	C	D	E	284	288	297
Ba	467	562	911	1 271	498	627	64 600	1 087
Nb	8	15	26	24	21	36	10	35
Zr	330(?)	56	100	95	85	136	53	126
Y	27	24	10	13	19	17	5	19
Sr	<1	32	8	24	30	20	904	23
Rb	139	26	176	152	147	229	77	240
Zn	6	<1	<1	<1	2	<2	<2	<2
Cu	6 546	2 643	57 592	46 295	581	12 932	7 900	18 000
Ni	207	4 776	2 455	696	2 202	103	33	46
Cr	209	227	437	399	323	609	257	520
La	3	5	41	11	12	15	5	19
Ce	212	113	63	59	51	24	33	36
U	<2	151	<2	<2	20	17	<2	11
Th	2 247	63	58	22	52	5	<2	11
Pb	42 320	21 867	17 818	14 344	8 185	186	<2	81

---

[1] Analyses by Dr. R.G. Holland, University of Newcastle Upon Tyme; Phillips PW 1212 XRF

TABLE 16

PERTINENT INFORMATION ON CHEMICALLY ANALYZED SAMPLES FROM MINERALIZED ZONES

SAMPLE NO.	LOCATION	ALTERATION	COMMENTS
A	Trench 1	Potassic-intense	Abundant galena, minor chalcopyrite
B	Trench 1	Potassic-intense	Little visible mineralization, abundant erythrite stain, "heavy".
C	Trench 1	Potassic-intense	Abundant chalcopyrite, minor erythrite
D	Trench 1	Potassic-intense	Abundant chalcopyrite
E	Trench 1	Potassic-intense	Slightly radioactive (2.5 x background), abundant erythrite
284	DDH 76-1, 284 ft.	Potassic-strong	Abundant chalcopyrite
288	DDH 76-1, 288 ft.	Potassic-moderate	Abundant specularite and barite
297	DDH 76-1, 297 ft.	Potassic-strong	Abundant chalcopyrite

TABLE 17

MAJOR ELEMENT CHEMISTRY OF RELATIVELY UNALTERED BASALTIC ROCKS[1]

Element	Glassy to Microcrystalline Basalt	Labradorite Olivine Basalt	Labradorite Alkali Basalt	Basaltic Pumice	Basalt
SiO_2	49.80	47.13	48.00	50.21	50.87
Al_2O_3	14.88	12.54	17.42	13.36	12.92
Fe_2O_3	1.55	4.72	6.17	1.39	2.85
FeO	10.24	6.26	4.64	9.88	13.19
MgO	6.74	13.19	4.55	8.34	5.40
CaO	10.72	10.17	9.60	10.81	9.02
Na_2O	2.91	2.25	4.00	2.34	2.46
K_2O	0.24	0.65	1.30	0.55	0.76
H_2O^+	0.54	0.35	0.42	0.11	0.17
H_2O^-	0.06	0.30	0.15	0.00	0.04
TiO_2	2.20	1.84	3.20	2.63	2.95
P_2O_5	0.28	0.36	0.54	0.27	--
MnO	0.21	0.19	0.13	0.17	0.26
CO_2				0.01	
Cl				0.02	
F				0.04	
	100.19	99.95	100.12	100.11	100.89

---

[1] Data after Mueller and Saxena, Table 15-1, p. 334.

CHAPTER 9

LEAD ISOTOPE STUDY

I. General Remarks

The application of lead isotopes to the problems of ore genesis has been reviewed by Doe and Stacey (1974). The major use of these isotopes is in defining the provenance of lead and in determining the age of mineralization (op. cit., p. 757).

In the present study, the age of mineralization has been determined by the model lead method as outlined by Faure (1977, pp. 227-266). The origin and history of the mineralization has been interpreted on this basis.

II. Methodology

Thirteen sets of lead isotope data have been determined from mineralized samples in the BBX diatreme, and are shown in Table 18. The samples studied correspond to those for which chemical analyses are available (Tables 14 and 15). Samples A to E are from the main surface showing (Trench 1). Samples 284, 288 and 297 are from the subsurface in DDH 76-1 (Table 16).

The lead analyzed from sample A (specimens 1 to 6) is from hand picked specimens of galena. Lead in the remaining samples has been separated from whole-rock pulps in ion exchange columns. In samples B, C, D and E, which contain substantial amounts of lead (Table 15), but no visible

TABLE 18

LEAD ISOTOPE DATA, BBX DEPOSIT

Sample Number	206/204	207/204	208/204
A(1)	16.312	15.502	35.847
A(2)	16.334	15.520	35.900
A(3)	16.481	15.519	35.949
A(4)	16.293	15.519	35.918
A(5)	16.305	15.493	35.816
A(6)	16.271	15.496	35.827
B	32.464	17.165	40.598
C	20.874	15.894	39.649
D	16.679	15.560	36.204
E	34.379	16.890	40.894
284	50.700	19.295	40.806
288	61.409	20.268	45.758
297	94.710	24.317	50.503

galena (Table 16), lead is thought to be derived from anglesite developed after galena in the oxidized zone of the deposit. According to Faure (1977, p. 227), the isotopic composition of lead in secondary minerals such as anglesite is usually similar to that of lead in galena with which they are associated.

Lead is a very minor constituent of samples from depth (samples 284, 288 and 297) and its source mineral is unknown.

Lead isotope analyses were carried out on an Aldermaston MM30 solid-source mass spectrometer.

III. Discussion of Results

Lead isotope data for the BBX deposit are plotted in figures 23 and 24. Best fitting straight lines for these plots were calculated by the method of Cumming et al, (1972). The following observations are based on these diagrams.

A. A well-defined four point isochron in figure 23 defines an age of 1870 ± 15 m.y. for the lead mineralization. Although the mantle growth curve is not shown on this plot, this isochron intersects the growth curve at 1887 m.y., with an upper time limit of 1830 m.y., and a lower time limit of 1939 m.y. It also intersects the mantle growth curve at -35 m.y.,

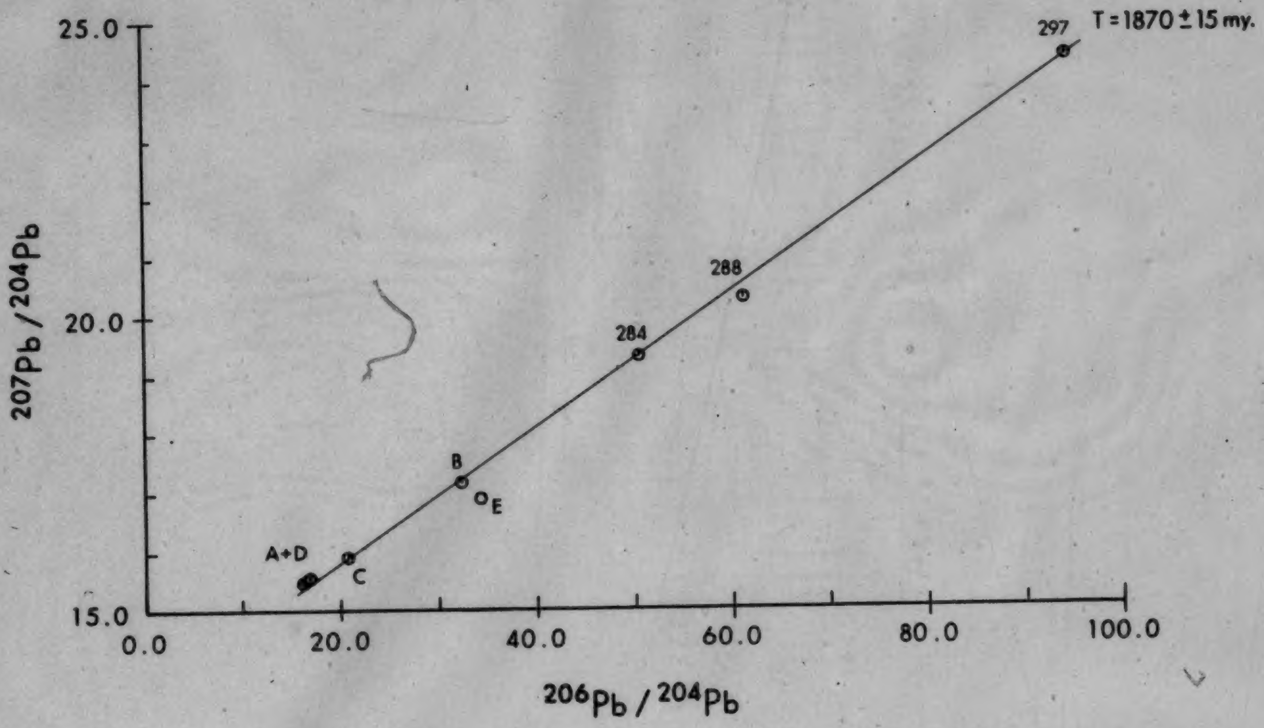

Figure 23: Plot of 207Pb/204 Pb vs. 206Pb/204Pb for the BBX deposit, All Data.

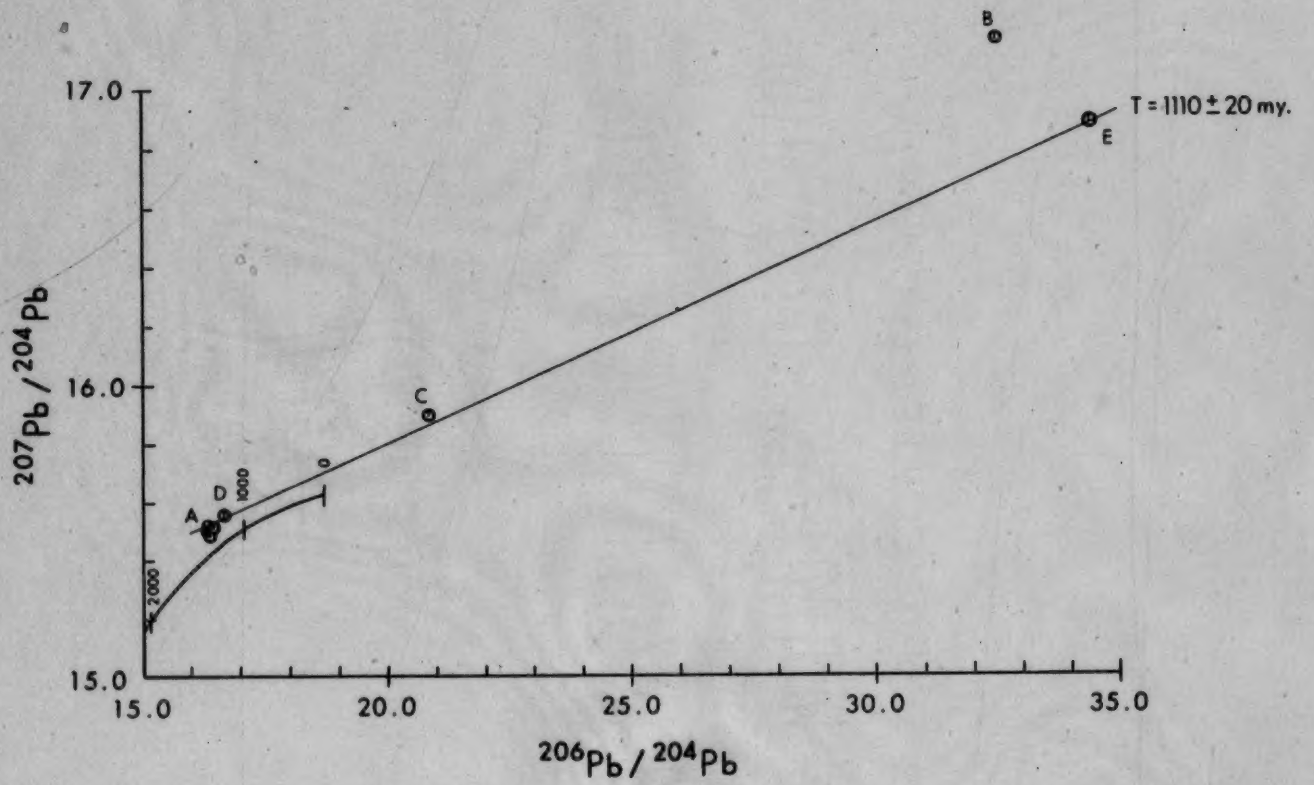

Figure 24: Plot of 207 Pb / 204 Pb vs. 206 Pb/204 Pb for the BBX deposit, Expanded Scale.

with an upper time limit of 73 m.y., and a lower time limit of -138 m.y. Within the limits of error therefore, the 1870 m.y. isochron intersects the mantle growth curve at T = 1870 m.y. and at T = 0 m.y. The implications of this are discussed in the following section.

B. Points A, D, E and possibly 288 do not lie on the 1870 m.y. isochron, and suggest that more than one mineralizing event has occurred. Unfortunately, available data are insufficient to determine a reliable age for this event. Figure 24 shows these data on an expanded scale, plotted with reference to the Stacey and Kramer mantle growth curve. Two possible tentative interpretations can be made.

1. Points A, D and E define an isochron having an age of 1110 ± 20 m.y. The concentration of the data at the two extremes of this isochron however, limits the reliability of this interpretation.

2. The cluster of points related to sample A has an isochron age of approximately 1550 m.y.

IV. Implications

A. The Seton Volcanics and Mineralization

The intersection of the 1870 m.y isochron with the mantle growth curve at 1870 m.y. is consistent with a two stage model for lead evolution. In the first stage, the lead isotopic composition evolved from uranium by radioactive decay in the mantle. At 1870 m.y., the $^{238}U/^{204}Pb$ ratio was changed into a variety of values resulting in a secondary isochron (Doe and Stacey, 1974, p. 763) having an age of 1870 m.y. This change is associated with the introduction of this mantle-derived material into the crust.

According to Badham (1978a, p. 1474), three separate periods of intrusive magmatic activity are recognized in the East Arm; early Aphebian ($\approx$2100 m.y.), middle Aphebian ($\approx$1870 m.y.) and late Aphebian ($\approx$1790 m.y.). An isochron age of 1870 m.y. for the lead mineralization at BBX corresponds to the middle Aphebian phase of magmatism of which the Seton volcanics are the major expression (op. cit., p. 1481). This serves to confirm that the BBX diatreme is in fact related to Seton volcanism, although an age of

1870 m.y. is somewhat older than ages determined in previous studies (i.e. 1833 m.y., 1804 m.y. and 1805 m.y., this thesis, p. 41). Implicit in this model is the probability that at least some lead and perhaps other mineralization was approximately coeval with and related to Seton volcanism. The possibility that this initial mineralizing event was magmatic hydrothermal in origin must be considered. A deep-seated (mantle) source is indicated for both the volcanics and the uranium-lead mineralization.

B. Late Hydrothermal Activity

Late hydrothermal activity again introduced lead into the system. Possible ages for this activity are 1110 ± 20 m.y. and 1550 m.y. (Helikian). An age of 1110 m.y. corresponds roughly with the ages of the diabase dykes and sills which intrude the Et-Then Group (this thesis, p. 42). Ages of 1550 m.y. are not well documented for the East Arm. Uranium mineralization occurring in conglomeratic sandstones of the Hornby Channel Formation however, has been dated at 1510 ± 9 m.y. by the U-Pb method (Bloy, 1979, pp. 7 and 50). This age is thought to represent an update or a date of epigenetic mineralization much younger than the host rock (op. cit., p. i).

The origin of this late-stage lead can be tentatively inferred from its isotopic composition. The 207/204 ratio of lead from Sample A is higher than that of the Seton volcanics (Cumming, 1980), and hence this lead is not related to the mafic parent magma of the diatreme. Moreover, the fact the the 207/204 ratios are higher than those of the mantle growth curve, may suggest that this lead is of crustal origin and was derived from sediments in Great Slave Basin (Cumming, personal communication). While this is a tentative conclusion, it is consistent with fluid inclusion and oxygen isotope evidence which suggests that late hydrothermal activity was not magmatic, but rather, involved the deposition of mineralization from connate brines (this thesis, Section III).

The fact that the 1110 m.y. date corresponds with a known magmatic event in the East Arm may imply a causitive relationship which is discussed in Chapter 10 (p. 324), and chapter 11 (p. 342).

C. Zonation

The lead from samples 284, 288 and 297 is considerably more radiogenic than that from samples A to E. This suggests that the initial U:Pb ratio was higher in these samples and implies a crude primary zonation with a higher U:Pb ratio at depth. Sample 297 is very radiogenic. Although a reliable quantitative determination is not possible, this suggests that a considerable amount of uranium was present in the system early in its history.

CHAPTER 10

THE MINERALIZATION

I. General Remarks

The complex mineralogy and paragenesis of the BBX deposit are attributable to a series of mineralizing events which span a considerable time interval comprising much of the geological history of Great Slave Basin. The mineralization derives both from magmatic hydrothermal fluids related to mid-Aphebian intrusive activity, and from connate brines which leached metals from basin sediments. The complex origin of the deposit is attributable to the relative porosity and permeability of the diatreme and to its control by a major structure extending to basement. Hence, the diatreme acted repeatedly as a conduit for movement of hydrothermal fluids of diverse origins.

II. Mineralogy and Paragenesis

The mineralogy of the BBX deposit has been determined primarily through microprobe analysis (semiquantitative), supplemented by ore microscopy. Minerals which have been identified in the diatreme are listed alphabetically with comments in Table 19. The paragenetic sequence of the deposit has been determined through ore microscopy, and in consideration of the results of lead isotope work (Chapter 9), and fluid inclusion and oxygen isotope studies (Chapters

TABLE 19
EPIGENE MINERALS IDENTIFIED IN THE BBX DIATREME
Key

1. Identification Technique(ID):
P = Microprobe, semiquantitative
X = Xray diffraction
M = Ore microscopy
V = Visual Megascopic Identification
W = Wet chemistry
S = Staining Technique

2. Abundance(Ab):
A = Abundant
O = Occasional
M = Minor
Tr = Trace

3. Phase(Ph):
1 = Primary
O - Oxidation Zone

Mineral	Published Formula	ID by	Ab	Ph	Comments
Acanthite	Ag_2S	P	Tr	1	intergrown with jalpite
Anglesite	$PbSO_4$	P	O	O	alteration product of galena
Arseniosiderite	$Ca_{a_3}Fe^{3+}_4 (OH)_6(H^2O)_3 (AsO_4)_4$	P	Tr	O	alteration product of arsenopyrite
Arsenopyrite	FeAsS	P	M	1	may contain minor cobalt
Azurite	$Cu_3(CO_3)_2(OH)_2$	V	O	O	
Barite	$BaSO_4$	P,X	A	1	
Bravoite	(Fe,Ni,Co) S_2, complete solid solution, FeS_2-CoS_2-NiS_2	P	Tr	O	Fe, Co, Ni content varies widely-alteration product of Pentlandite
Calcite	$CaCO_3$	V,S	A	1	
Chalcopyrite	$CuFeS_2$	M	A	1	
Covellite	CuS	M,P	M	O	alters from chalcopyrite, digenite, jalpaite. Commonly associated with anglesite

... Continued ...

Table 19 (cont'd)

Mineral	Published Formula	ID by	Ab	Ph	Comments
Digenite	$Cu_{1.765}S$ to $Cu_{1.79}S$, may contain some Ag	P	M	1	silver-bearing
Dolomite, Ferroan	$CaMg(CO_3)_2$, with sub-substitution of Fe^{2+} for Mg	P,X,S	A	1	
Dyscrasite	Ag_3Sb	P	Tr	1	"silver-bearer" associated with galena
Erythrite	$Co_3(AsO_4).8H_2O$	X	O	O	
Galena	PbS	M,P	A	1	contains tiny grains of dyscrasite
Gersdorffite	(Ni,Co,Fe)AsS, ratio As:S may vary	P	O	1	Complex diadochy between elements. Varying Co,Ni, Fe,S,As content
Glaucodot	(Co,Fe)AsS, with Co>9 wt %	P	M	1	
Jalpaite(?)	Ag_3CuS_2	P	Tr	1	intergrown with acanthite
Limonite	Hydrous Fe oxides	P,V	A	O	
Malachite	$Cu_2(CO_3)(OH)_2$	V	A	O	
Manganiferous calcite	$CaCO_3$, with substitution of Mn^{2+} for Ca	X	Tr	1	occurs with calcite and trace barite and pyrite in vuggy cavity lined with chlorite. Suggests minor remobilization
Marcasite	FeS_2	P,M	M	O	alteration product of pyrrhotite

... Continued ...

Table 19 (cont'd)

Mineral	Published Formula	ID by	Ab	Ph	Comments
Millerite	NiS	P	Tr	O	alteration product of siegenite
Pentlandite	$(Fe,Ni)_9S_8$	P,M	Tr	1	forms exsolution intergrowth with pyrrhotite; presence inferred-now altered to bravoite
Potassium Feldspar	$KAlSi_3O_8$	P,X,S	A	1	
Pyrite	FeS_2	P,M	O	1	may contain minor cobalt
Pyrrhotite	$Fe_{1-X}S$	P,M	Tr	1	presence inferred, now altered to Marcasite
Quartz	SiO_2	P,X	A	1	
Rutile(?) (TiO_2 phase)	TiO_2	P	M	1	precise polymorph of TiO_2 unknown
Siegenite	$(Co,Ni)_3S_4$	P	Tr	1	presence inferred-now altered to Millerite
Silver, native	Ag	P	Tr	1	
Specularite	Fe_2O_3	V,M	O	1	
Sphalerite	ZnS	P	Tr	1	
Wad	Complex hydrous Mn oxide may contain BaO, CuO, K_2O, Na_2O, CoO, Fe_2O_3, Al_2O_3, PbO_2, LiO_2	V,W	O	O	predominantly MnO, also contains Cu, Fe

7 and 8).

Four main phases of mineralizing activity have been recognized, each differing in mineralogy and in economic importance (Table 20).

A. Phase I Ag, Co-Ni Mineralization

1. Introduction

Phase I is characterized by a series of complex Fe-Co-Ni sulfides and sulfarsenides probably deposited at elevated (magmatic) temperatures. Minor amounts of rutile, native silver, and possible chalcopyrite and galena are associated. Quartz and carbonate are present as gangue. The presence of U and Pb has been inferred from lead isotope studies. Th, REE, Bi, Sn and W occur in minor quantities in the diatreme, and may also be associated with this phase of mineralization.

2. Mineralogy

The nature of phase I mineralization is illustrated in the following discussion.

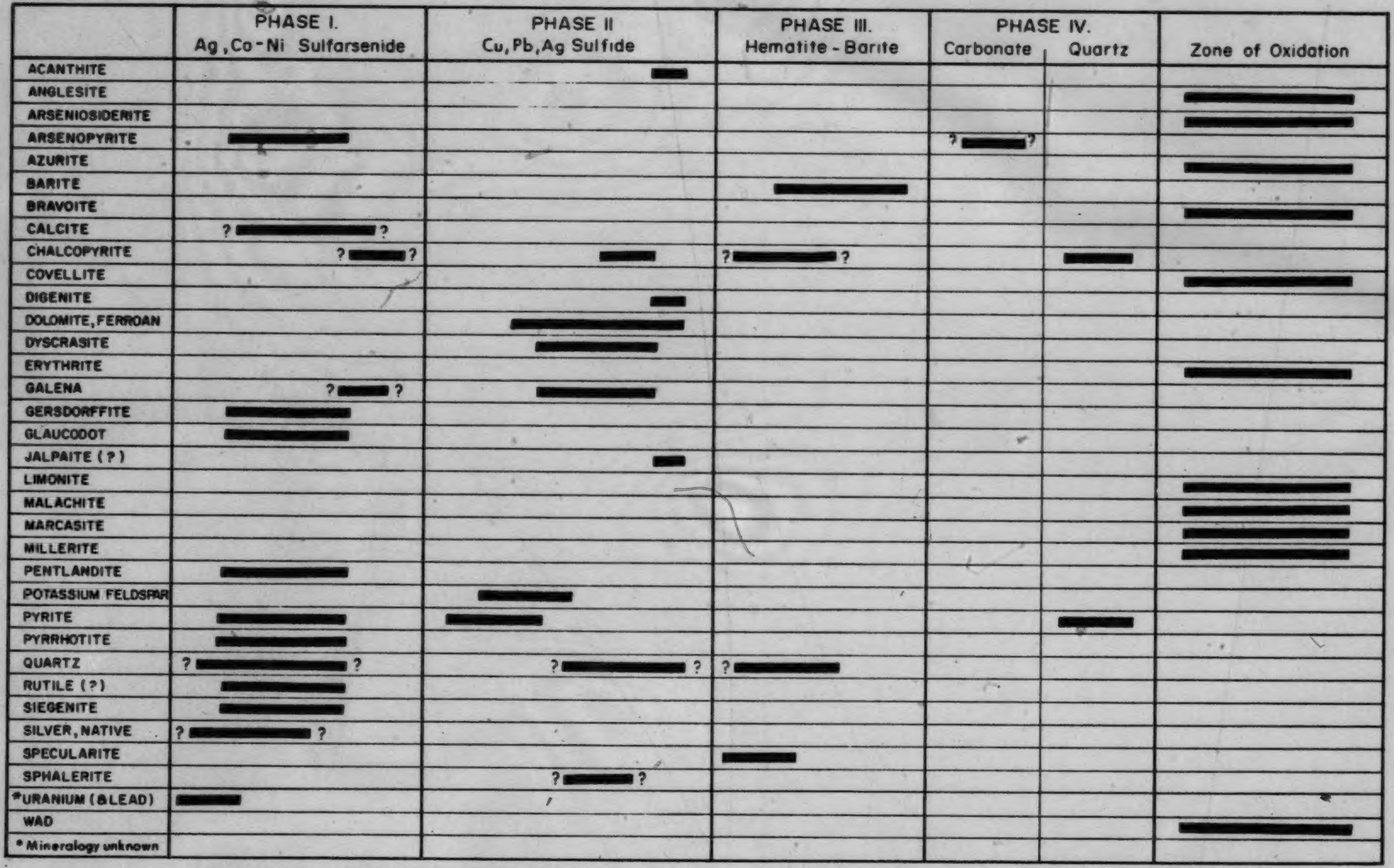

	PHASE I. Ag, Co-Ni Sulfarsenide	PHASE II Cu, Pb, Ag Sulfide	PHASE III. Hematite - Barite	PHASE IV.		Zone of Oxidation
				Carbonate	Quartz	
ACANTHITE		▬				
ANGLESITE						▬
ARSENIOSIDERITE						▬
ARSENOPYRITE	▬			?▬?		
AZURITE						▬
BARITE			▬			
BRAVOITE						▬
CALCITE	?▬?					
CHALCOPYRITE	?▬?	▬	?▬?		▬	
COVELLITE						▬
DIGENITE		▬				
DOLOMITE, FERROAN		▬				
DYSCRASITE		▬				
ERYTHRITE						▬
GALENA	?▬?	▬				
GERSDORFFITE	▬					
GLAUCODOT	▬					
JALPAITE (?)		▬				
LIMONITE						▬
MALACHITE						▬
MARCASITE						▬
MILLERITE						▬
PENTLANDITE	▬					
POTASSIUM FELDSPAR		▬				
PYRITE	▬	▬			▬	
PYRRHOTITE	▬					
QUARTZ	?▬?	?▬?	?▬			
RUTILE (?)	▬					
SIEGENITE	▬					
SILVER, NATIVE	?▬?					
SPECULARITE			▬			
SPHALERITE		?▬?				
*URANIUM (& LEAD)	▬					
WAD						▬
* Mineralogy unknown						

TABLE 20 PARAGENETIC SEQUENCE OF MINERALIZATION IN BBX DIATREME

(i) Gersdorffite is the principle Co-Ni-bearing phase. Arsenopyrite and glaucodot occur as minor constituents. Both gersdorffite and glaucodot exhibit considerable variation in the ratio Fe:Co:Ni:As:S as noted in Table 19. Arsenopyrite may contain minor amounts of Co.

(ii) Pyrrhotite and pentlandite are rare minerals in the diatreme and have undergone pervasive alteration to marcasite and bravoite respectively, in the zone of oxidation. Their former presence has been inferred from microprobe analyses and textural considerations. Pyrrhotite occurs as narrow exsolution spindles in pentlandite, apparently along octahedral parting planes (Plate 29).

(iii) Native silver was identified in only one instance and occurs as tiny grains randomly distributed within siegenite (?). This suggests that it precedes siegenite in the paragenetic sequence (Plate 30).

(iv) Siegenite (?) has been completely altered to millerite in the zone of oxidation (Plate 30)(this Chapter p. 311).

Plate 29 Photomicrograph showing pyrrhotite-pentlandite exsolution intergrowth. Minerals are pyrrhotite (po, now altered to marcasite), pentlandite (pn, now altered to bravoite), galena (gn) and chalcopyrite (cp). (Reflected light.)

Plate 30 Photomicrograph showing siegenite (light yellow) being replaced along crystallographic directions by chalcopyrite (dark yellow). Siegenite has altered to millerite in the zone of oxidation. Disseminated bright white grains are native silver. (Reflected light.)

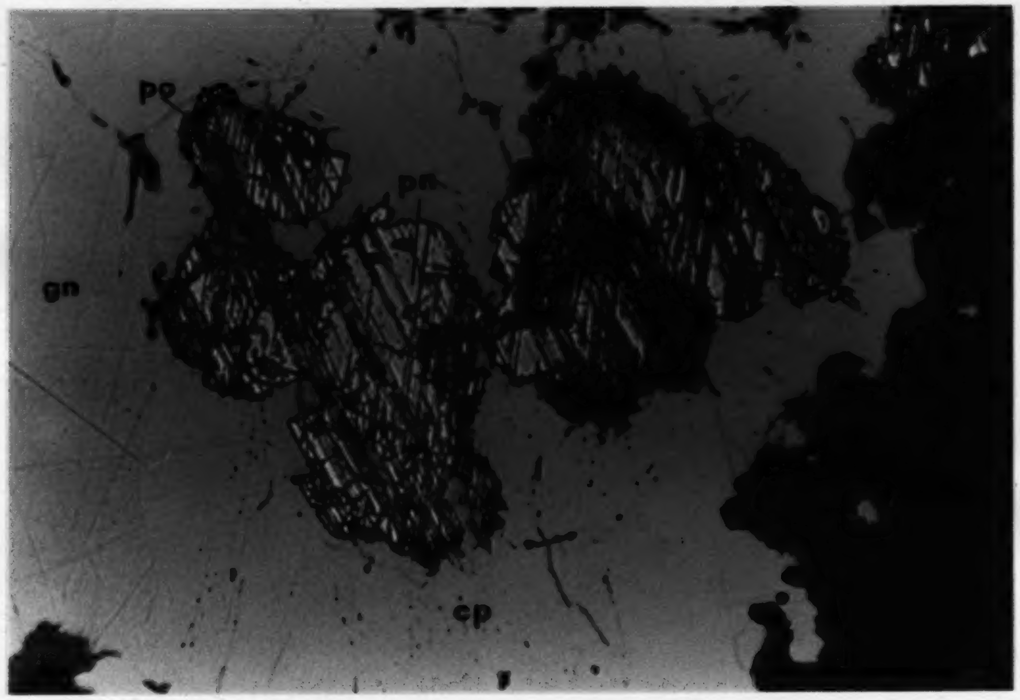
po
pn
gn
cp

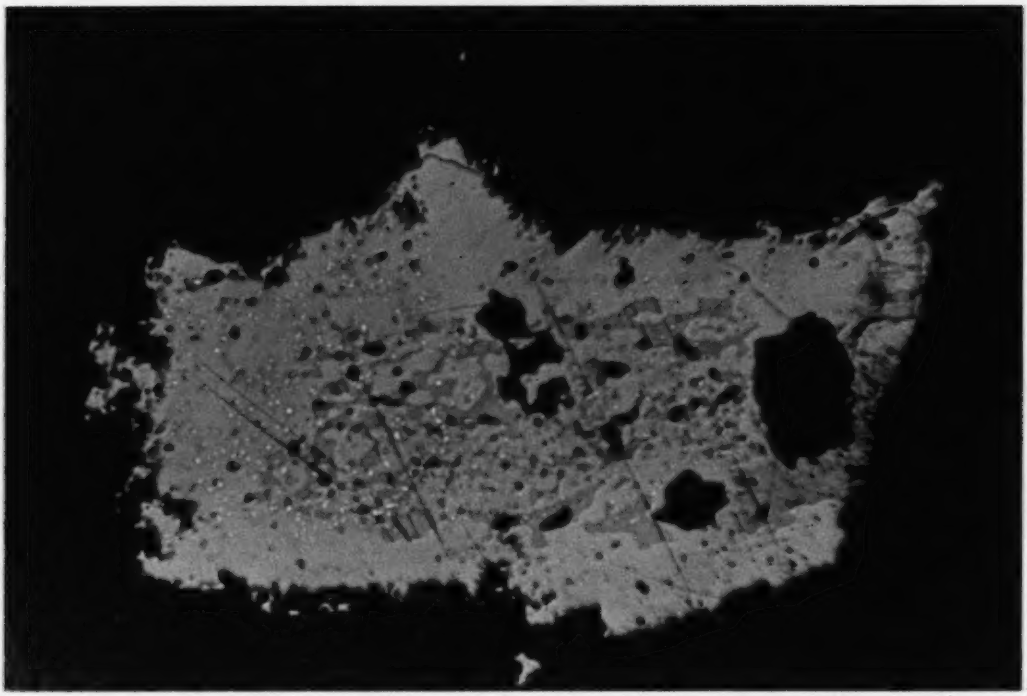

(v) Rutile occurs occasionally as tiny subhedral to euhedral grains, commonly associated with glaucodot and pyrite.

3. Mode of Occurrence of Mineralization

Phase I mineralization exhibits a variety of interesting textures. These are described below, and their possible significance is discussed.

(i) Co-Ni minerals (especially glaucodot, gersdorffite and bravoite) and rutile, galena and chalcopyrite occasionally occur in layered intergrowths, which in some cases have a concentric structure (Plate 31). The significance of these features is not known. They may be interpreted as accretionary structures or as colloform structures. Their presence is consistent with Ag, Co-Ni arsenide ores in general, in which zonal, accretionary and colloform textures are commonly developed (Stanton, 1972, pp. 603, 607). It should be noted that the significance of "colloform" textures is debatable, and that they do not necessarily suggest colloidal deposition (Park and MacDiarmid, 1970, p. 129).

Plate 31 Photomicrograph showing layered intergrowth of chalcopyrite (yellow), glaucodot (white) and galena (greyish white). Greenish grey phase is limonite (L). (Reflected light.)

Plate 32 Photomicrograph showing a fine grained intergrowth of glaucodot (white) and rutile (light grey). (Reflected light.)

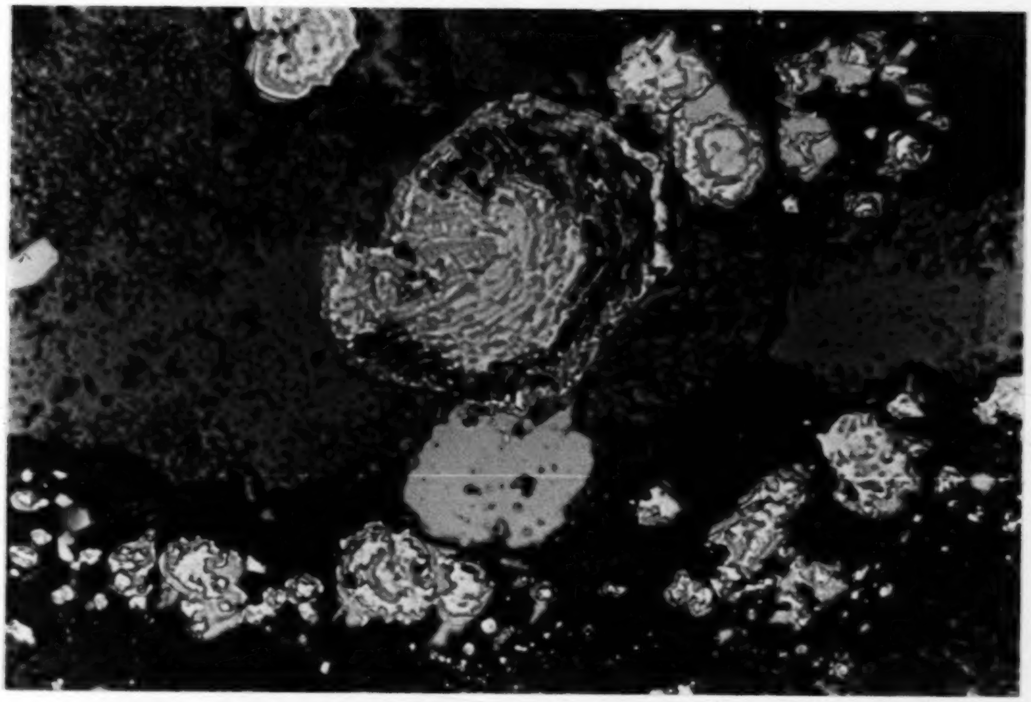

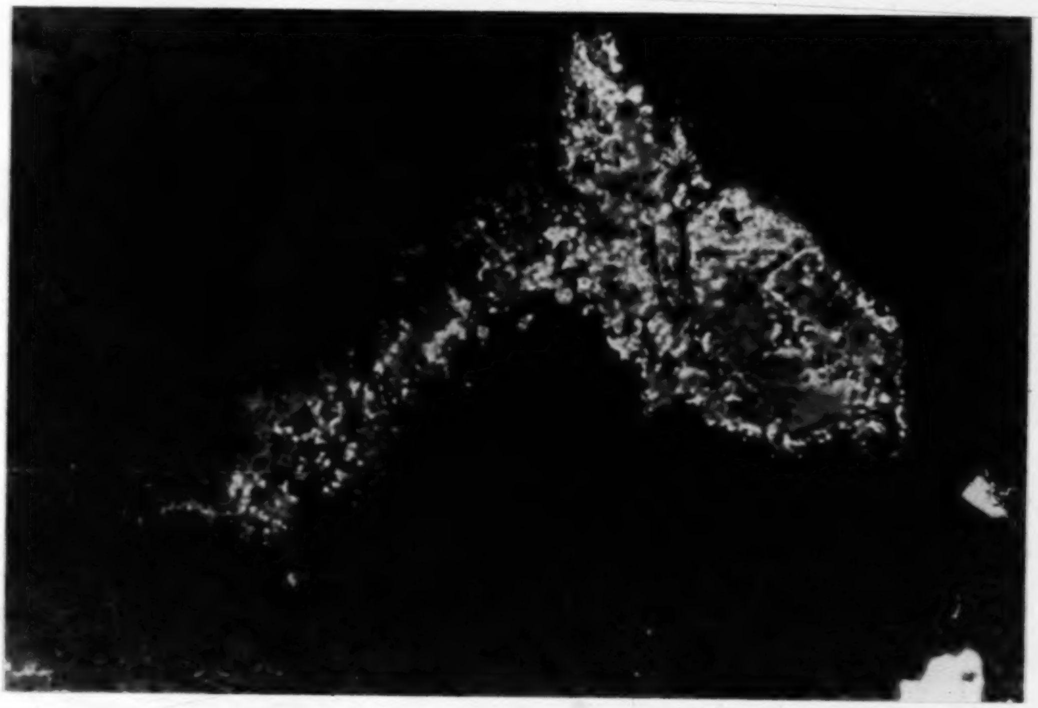

(ii) Fine grained clusters of glaucodot and rutile occur rarely in the diatreme (Plate 32). Chalcopyrite is intimately intergrown with glaucodot in these masses. These clusters resemble the "framboidal spherules" described by Park and MacDiarmid (p. 133), but their origin is not well understood.

(iii) Gersdorffite, and to a lesser extent arsenopyrite, glaucodot and pyrite, commonly occur as finely disseminated grains in chalcopyrite and occasionally in galena (Plates 33 and 34). These grains vary from anhedral to euhedral. As gersdorffite is not known to form exsolution intergrowths with chalcopyrite and galena, these emulsion textures (Ramdohr, 1969, p. 113) have two possible origins.

(a) They may be undigested replacement relics. To some extent, this interpretation is supported by the occasional occurrence of gersdorffite as crystal skeletons in galena (Plate 35).

(b) They may represent an original "framboidal" cluster which has been

Plate 33 Photomicrograph showing emulsion texture with gersdorffite (high relief, dark yellow) in chalcopyrite (light yellow). (Reflected light.)

Plate 34 Photomicrograph showing emulsion texture, with gersdorffite (white to pale pink) in chalcopyrite (yellow). (Reflected light.)

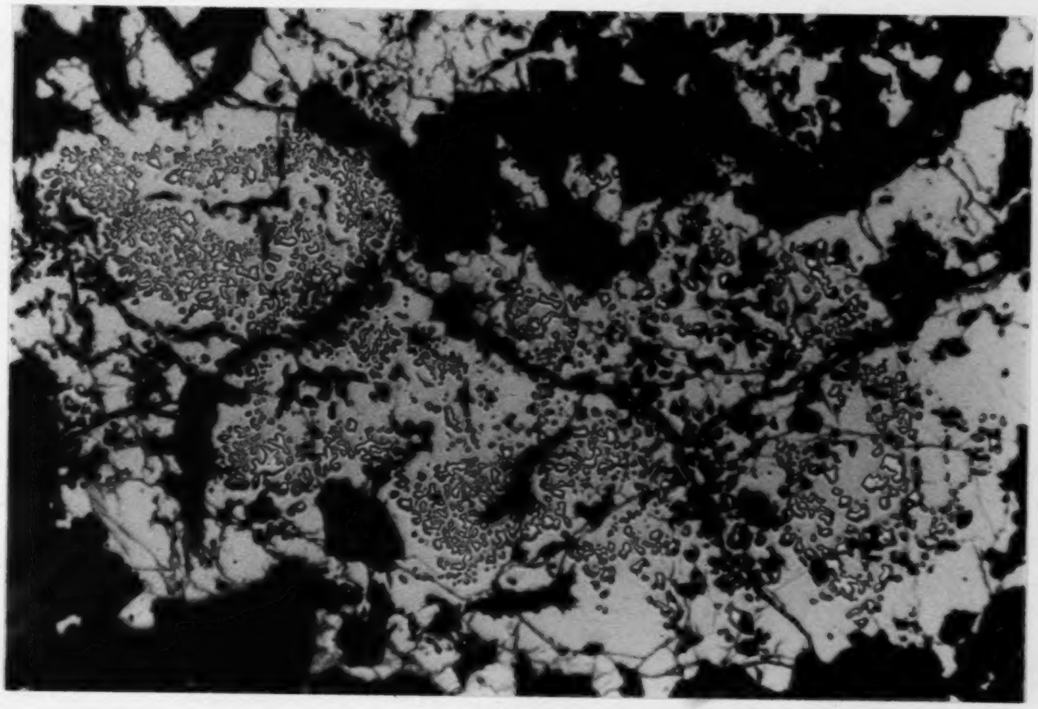

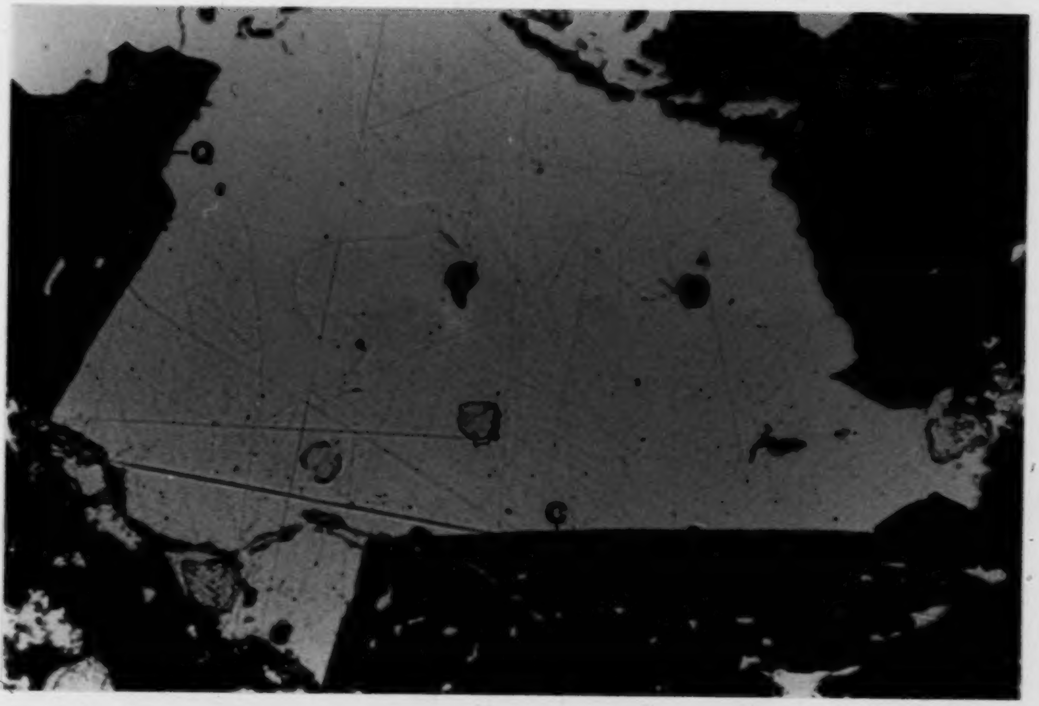

Plate 35 Photomicrograph showing skeletal crystals of gersdorffite (pale pink) in galena (greyish-white). Other phases are chalcopyrite (yellow), quartz (Q) and ferroan dolomite (C). (Reflected light.)

subsequently infilled and enclosed by later sulfide mineralization.

(iv) Fe-Co-Ni sulfides and sulfarsenides also occur as fine grained disseminations in the matrix of basalt fragments and around the perimeter of vacuoles.

(v) Accretionary (colloform?) structures occasionally appear to have undergone slight cataclasis (Plate 30). This is consistent with Ag, Co-Ni arsenide deposits in general, in which accretionary structures are commonly slightly disrupted, permitting late-stage veins to develop in earlier ore and gangue minerals (Stanton, 1972, p. 607).

4. Paragenesis

Because Ag, Co-Ni phases are a relatively minor constituent of the mineralization in the BBX deposit, their exact paragenesis is difficult to determine. It is suggested by lead isotope studies however, that U (and Pb) are early.

Textural relationships suggest that native silver is also an early phase. Fe-Co-Ni minerals are generally late, but their precise relationships are indeterminable. In one instance, pyrite was found to be zoned, with Co, Ni and As relatively enriched in the core and absent from the rim. This may suggest that Co-Ni-As phases were early, and Fe-sulfide phases late. This is consistent with the general paragenesis of this assemblage as illustrated by the Silverfields deposit at Cobalt, Ontario (Stanton, 1972, p. 607, Figure 17-13).

Chalcopyrite and galena are occasionally intimately intergrown with Fe-Co-Ni phases (this Chapter, p. 283, also Plate 31). Textural relationships suggest that these minerals are late to form, and that chalcopyrite postdates galena. Because these minerals are important constituents of Phase II, their association with Phase I is uncertain and difficult to demonstrate. The suggestion that they are related to Phase I is tentatively based on the following observations.

(i) Chalcopyrite commonly forms delicate layered intergrowths with gersdorffite, even in the absence of significant concentrations of Phase II mineralization. It seems unlikely that Phase II sulphides, which probably postdate Phase I mineralization by hundreds of millions of years (Chapter 9), would so selectively and delicately replace isolated Fe-Co-Ni phases.

(ii) The association of Pb with Phase I mineralization has been demonstrated through Pb isotope studies. The postulated presence of chalcopyrite late in Phase I, suggests that the conditions necessary for sulfide formation (i.e. galena) existed at this time. This is also consistent with the paragenesis suggested by pyrite zonation as described above.

5. Economic Significance

Co-Ni sulfides and sulfarsenides constitute a relatively minor part of the mineralization, and their occurrence in the diatreme is sporadic. Phase I minerals have not been recognized outside of the main surface showing (trenches 1 and 2). Although Co, Ni and Ag may be relatively concentrated in this zone (Table 2), their sporadic distribution in the diatreme makes Phase I of very little economic value. Moreover, it is probable that these silver values are attributable mainly to the considerably more abundant silver sulfide minerals associated with Phase II. Chalcopyrite and galena are thought to be relatively minor constituents of Phase I.

B. Phase II Cu-Pb Sulphides

1. Introduction

Phase II is characterized by the deposition of sulfide mineralization at moderate temperatures (T_h>146°C, this thesis, p. 234 and 254). This mineralization consists primarily of chalcopyrite, with lesser galena, and relatively minor silver-bearing phases including digenite, dyscrasite, jalpaite (?) and acanthite. Sphalerite occurs in exceedingly trace quantities. Quartz, ferroan dolomite and possibly other carbonates occur as gangue.

This phase of mineralization is associated with moderate to intense potassium alteration (Plates 23 to 26). The potassium enrichment associated with this event is illustrated in Tables 14 and 18 which show a substantially higher K:Na ratio in mineralized basalts (Table 14) relative to unaltered basalts (Table 18).

2. Mineralogy and Paragenesis

The paragenetic sequence of phase II mineralization is shown in Table 20. The following remarks pertain to this mineralization.

(i) Potassium alteration and the formation of ferroan dolomite, precede the deposition of sulfide phases. Potassium feldspar and carbonate often occur along the perimeter of mineralized zones.

(ii) Chalcopyrite is the principal mineral in this phase, and occurs in discrete zones throughout the diatreme. Galena is apparently restricted to the main surface showing (trenches 1 and 2) where it is relatively abundant but is almost completely altered to anglesite. Trace quantities of sphalerite detected by microprobe analysis are assumed to be coeval with the deposition of chalcopyrite and galena.

The precise relationship between chalcopyrite and galena is uncertain. Although chalcopyrite generally replaces and therefore postdates galena, the reverse is occasionally true. This is consistent with the complex paragenesis of lead mineralization suggested by lead isotope studies.

(iii) Silver-bearing phases are relatively rare. Dyscrasite occurs in trace amounts as a "silver-bearer" associated with galena. Acanthite and jalpaite occur in minor amounts and are commonly intergrown, with jalpaite forming narrow veinlets in acanthite (Plate 36). Digenite, which contains minor quantities of silver, appears to preferentially replace pyrrhotite (Plate 37). Textural relationships suggest that silver-bearing sulfide phases generally postdate the deposition of chalcopyrite and galena. Nevertheless, they appear to exhibit an affinity for lead mineralization and are present only in samples containing galena and/or anglesite.

Plate 36 Photomicrograph showing acanthite-jalpaite intergrowth. Minerals are acanthite (Ac; the light green color is an oxidation product), jalpaite (Jl; light blue veinlets, altering to covellite (dark blue) in the zone of oxidation), chalcopyrite (yellow) and galena (greyish-white). (Reflected light.)

Plate 37 Photomicrograph showing digenite (Dg) preferentially replacing pyrrhotite spindles. Digenite is altering to covellite (light and dark blue) in the zone of oxidation. Other minerals are bravoite (white; after pentlandite) and chalcopyrite (yellow). (Reflected light.)

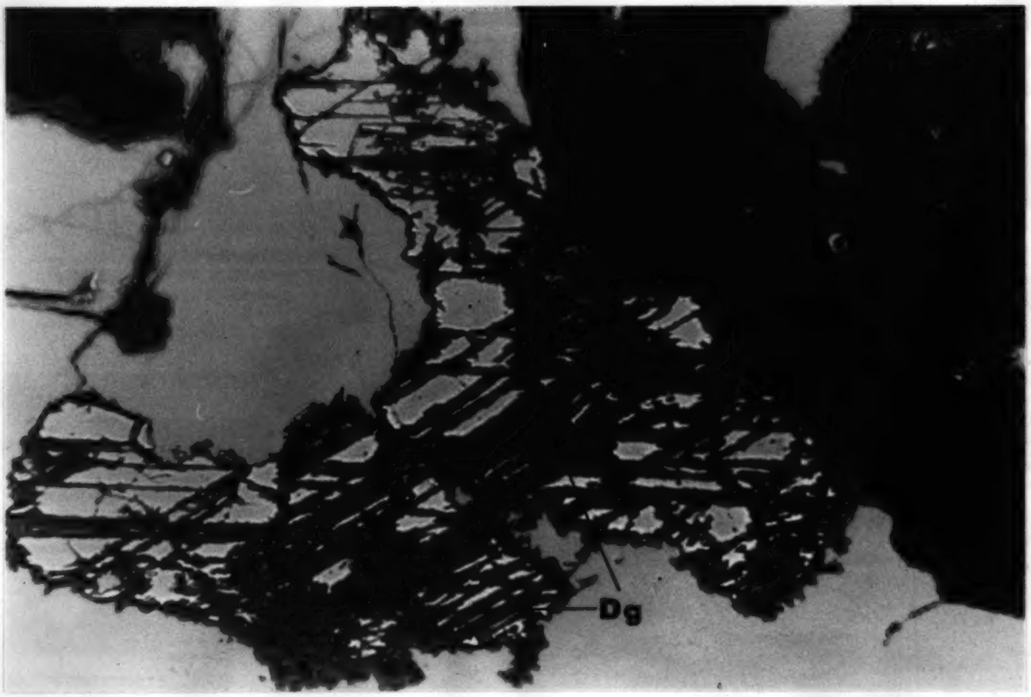

Dg

(iv) Pyrite is relatively common, both as part of the potassium alteration assemblage, and as primary euhedral grains which are commonly replaced by galena (Plate 38).

3. Controls of Mineralization

Phase II mineralization occurs principally in massive fine grained form in the matrix and to a lesser but significant extent in veinlets cutting both the matrix and breccia fragments.

The sulfides appear to exhibit a marked affinity for hematitic sedimentary rock fragments which they can be seen rimming and replacing internally. Fragments of oolitic and pisolithic hematite particularly, very frequently contain at least trace amounts of disseminated chalcopyrite (and locally galena).

Replacement of basalt fragments by sulfides is limited. Where it does occur however, it is associated particularly with serpentine pseudomorphs of olivine. To a lesser extent, it occurs in very fine grained form throughout the basalt fragments. In one rather spectacular case,

Plate 38 Photomicrograph showing pyrite (light yellow) being replaced by galena (white). The pale greenish-grey veinlets are anglesite (A; after galena). (Reflected light.)

Plate 39 Photomicrograph showing preferential replacement of glass shards by galena (white). The yellow mineral is chalcopyrite. (Reflected light.)

galena appears to have preferentially replaced glass shards (Plate 39).

4. Economic Significance

Phase II represents a major pulse of hydrothermal activity, and is thought to be responsible for the bulk of mineralization deposited in the diatreme. The economic potential of Phase II mineralization is limited however, by the following considerations.

(i) Galena and silver-bearing sulfides are apparently restricted to the vicinity of trenches 1 and 2.

(ii) Chalcopyrite occurs both at surface and at depth in the diatreme but is restricted to relatively discrete zones (see for example Table 3). The nature and significance of these zones is discussed at a later point in this chapter (VIII "Deposition of Mineralization").

C. Phase III Barite-Specularite

1. Introduction

Phase III mineralization comprises predominantly barite and specularite. Quartz and possibly chalcopyrite are associated. Fluid inclusion studies suggest that this phase of mineralization was deposited at low to moderate temperatures. These minerals occur in the matrix between breccia fragments, in narrow veinlets, and to a small extent replace breccia fragments. Hence the locus of mineralization is the same as that for chalcopyrite and galena (phase II). Moreover, barite and specularite appear to be restricted to zones of sulfide mineralization, and are therefore associated with potassium alteration.

2. Mineralogy and Paragenesis

The following remarks characterize Phase III mineralization.

(i) Specularite and barite may occur together or separately. Where they are intergrown, it is evident that barite postdates specularite. An example of this relationship occurs in DDH 76-1, where bladed crystals of specularite occur along fractures. Barite has later infilled these fractures, resulting in rather striking barite-specularite veins up to 1 cm in width (Plate 40).

(ii) Barite is orange in color, possibly due to the presence of abundant finely divided iron oxides. It occurs occasionally in narrow veinlets with quartz. These veinlets are extremely fine grained, relatively hard (quartz) and may be mistaken for narrow veinlets of potassium feldspar which also cut the volcanics.

(iii) The association of chalcopyrite with phase III mineralization is uncertain. Occasionally however, chalcopyrite occurs with specularite on the perimeter of barite veins (Plate 41). Specularite also occurs on the perimeter of chalcopyrite veinlets. These features suggest a paragenetic sequence for phase III mineralization, with specularite (early), followed by chalcopyrite (intermediate) and barite (late)(Table 20). Barite exhibits well-defined replacement textures with chalcopyrite.

Plate 40 Photomicrograph showing a barite (white)-specularite (black) vein. (Transmitted light.)

Plate 41 Photomicrograph showing a barite-chalcopyrite-specularite intergrowth. Barite (medium grey); chalcopyrite (yellow); specularite (light greyish blue, bladed crystals). (Reflected light.)

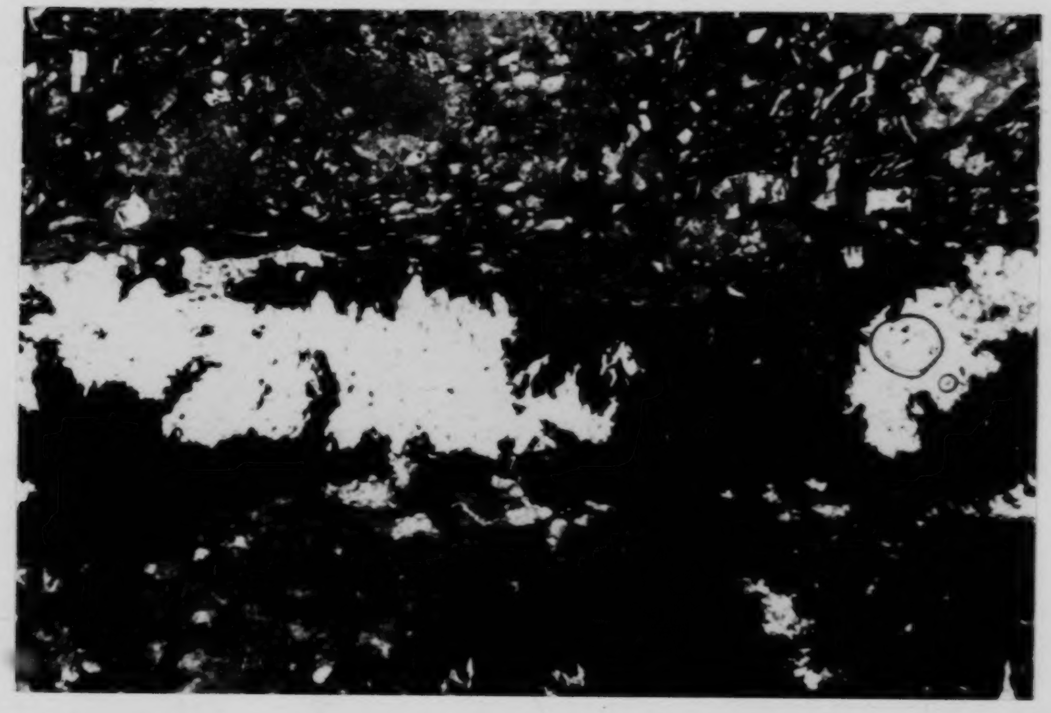

3. Economic Significance

Although barite and specularite may occur in substantial quantities in the diatreme (Tables 1 and 15), they have no economic value. Chalcopyrite is felt to be a relatively minor constituent of Phase III and has little economic significance.

D. Phase IV Carbonate-Quartz

Phase IV is characterized by the deposition of substantial quantities of carbonate and quartz. The early stages of this hydrothermal event were non-mineralizing, and resulted in widespread carbonatization of the diatreme. Later quartz-carbonate veins and quartz veins contain traces of mineralization, particularly chalcopyrite and pyrite. In the vicinity of Great Slave Lodge, pyrite in these quartz veins was found by microprobe analysis to contain trace quantities of cobalt. Carbonate-rich veins occasionally contain minor quantities of a white sulfarsenide (?) along cleavage planes and fractures. This mineral has not been positively identified but may be arsenopyrite. Silicification is the main alteration type associated with this later quartz-carbonate veining. Crosscutting relationships in these veins suggest that several pulses of hydrothermal activity, alternating with brecciation, were associated with this phase [for a more detailed discussion, refer to Chapter 5, especially "Quartz-Carbonate Veins and Stockworks" (p. 147) and "Chronology" (p. 150)].

III. Remobilization of Hydrothermal Mineralization

A minor amount of remobilization has been brought about by late tectonic events in the East Arm. These events resulted in small-scale shearing in the diatreme, and in the formation of numerous chlorite slips (this thesis, p. 118). Chalcopyrite is smeared out along these slips, which suggests that it formed prior to shearing. This stress also resulted in slight deformation of galena, as indicated by curved crystal surfaces, and of quartz, which occasionally exhibits undulose extinction.

A minor amount of remobilization of existing hydrothermal phases appears to be associated with this deformation. This is suggested by the following observations.

A. Pyrite and unidentified sulfarsenides (?) form crustlike masses along chlorite slips, which suggests growth subsequent to shearing.

B. Colorless barite, red manganiferous calcite and pyrite were noted in one instance as very fine grained euhedral crystals growing into narrow cavities lined by chlorite.

C. Large pyrite grains occur occasionally in mineralized zones, particularly in association with galena. These crystals are generally subhedral to euhedral, with somewhat rounded edges, and contain numerous inclusions of galena and non-metalliferous minerals. This is tentatively interpreted as a poikiloblastic texture, and the pyrite crystals are thought to be porphyroblasts formed by recrystallization.

The formation of pyrite porphyroblasts is not uncommon (Ramdohr, p. 65), and may result from dynamic, contact or pure load metamorphism (op. cit., p. 71). In the present case, it is probably the result of shearing (dynamic metamorphism).

Remobilization is attributed principally to heat generated during shearing, which resulted in "sweating out" of the relatively more mobile constituents. The process was presumably facilitated by minor quantities of water present in the diatreme.

IV. Changes in the Zone of Oxidation

A pronounced gossan is associated with the mineralization at the main surface showing (trenches 1 and 2). This gossan contains malachite, azurite, limonite, erythrite and wad as its principle visible phases (Plates 23 to 26). In addition to their presence on the outcrop surface, these minerals are developed along joints, fractures, "bedding surfaces", and occasionally around the perimeter of fragments in the agglomerate. In addition to the above, numerous other minerals formed in the zone of oxidation, have been identified by microprobe analysis. Secondary minerals of particular interest are discussed briefly below.

A. Anglesite occurs very commonly as an alteration product of galena (Plate 38). Occasionally, the relic cubic structure of galena is visible. The economic importance of anglesite is suggested from Tables 15 and 16, which show substantial quantities of lead in several samples containing no visible galena.

B. Arseniosiderite was tentatively identified in only one instance. This mineral, which is a low temperature oxidation product of arsenopyrite, may range in color from golden yellow to reddish brown and brownish black (Moore, 1974, p. 57).

C. Bravoite (Plate 29) is a minor phase and is tentatively interpreted as an alteration product of pentlandite (this Chapter, p. 280).

D. Covellite is a relatively minor phase, and is preferentially associated with galena, chalcopyrite, and particularly with anglesite. The association of covellite with copper-free minerals is not unusual, and has been documented from other deposits. According to Ramdohr, (1969, p. 642), covellite is often precipitated on galena in deposits rich in copper, sometimes in the zone of oxidation, but normally in the zone of cementation.

It is interesting to note that where galena and anglesite are absent, covellite is generally not developed, even in the presence of chalcopyrite. This suggests that the chemistry of galena and anglesite is conducive to the formation of covellite in this deposit. It is beyond the scope of this study however, to speculate further on this association.

Covellite is also developed (in the presence of galena) on minor copper-bearing phases such as digenite (Plate 37) and jalpaite (Plate 36).

E. "Limonite" denotes a mixture of fine grained undetermined oxides of iron, after the usage of Bateman (p. 252). Limonite in the BBX deposit is preferentially associated with chalcopyrite, and is presumably altering from this mineral along fractures and grain boundaries (Plate 42). The complex chemistry of the deposit, and the variety of elements liberated in the zone of oxidation, suggest that various trace elements may be associated with this oxide.

F. Marcasite (Plate 29) is a minor phase, and has tentatively been interpreted as an alteration product of pyrrhotite (this Chapter, p. 280).

G. Millerite is chiefly a product of incipient weathering of Ni-rich sulfides (Ramdohr, p. 619). This mineral (Plate 30) was positively identified in only one instance, and was found by microprobe analysis to contain traces of Fe and Co. The presence of these elements suggests that millerite is after a member of the linnaeite group, probably siegenite (op. cit., p. 686).

H. Wad is a complex hydrous manganese oxide (Berry and Mason, p. 375) and is black in color (Plates 23, 25 and 26). It may contain a variety of other metallic oxides as noted in Table 19. The detailed chemical

Plate 42 Photomicrograph showing alteration of chalcopyrite (yellow) to limonite (light greyish-green) along grain boundaries and fractures. The white mineral intergrown with chalcopyrite (upper right) is an unidentified Fe-Co-Ni phase, possibly gersdorffite. (Reflected light.)

composition of this oxide in the BBX deposit has not been investigated. Limited chemical tests however, have shown that it contains Fe and Cu in addition to Mn. In view of the complex chemistry of the deposit, and the strong oxidation, the presence of a variety of other elements listed in Table 19 may be anticipated.

V. Geochemical Inferences

A variety of elements occur in trace quantities in the diatreme (Tables 1 and 15). Because some of these elements may substitute into the lattices of common rock forming minerals, speculation on their possible relationship to hydrothermal phases must be made with caution. The following is an attempt to account for some of the more common elements on the basis of chemical analyses and other considerations.

A. Sr probably substitutes for Ba in the mineral barite (Berry and Mason, 1959, p. 427). This can be inferred from Table 15 which shows a dramatic increase in Sr content corresponding to an increase in Ba between sample 288 and other samples analyzed.

B. A relatively high Th content in sample A corresponds to a relatively high Zr content (Table 15). This may suggest that Th has substituted for Zr in the mineral zircon (Berry and Mason, 1959, p. 561). Rare earth elements (REE) (Table 15), may also substitute into the zircon lattice (op. cit., p. 561).

C. Cr varies sympathetically with Ti (Tables 14 and 15). This is consistent with the chemistry of titaniferous magnetite, which is an important constituent of basalt. Cr substitutes for Fe^{3+} in magnetite (Berry and Mason, 1959, p. 354). The presence of V may also be accounted for in this manner.

D. Nb varies sympathetically with Ti (Tables 14 and 15) and is probably associated with rutile (Berry and Mason, 1959, p. 370). It is uncertain whether this phase is hydrothermal in origin or is an original constituent of the basalt.

E. Ag, Ni-Co arsenide mineralization is often spatially coincident with earlier Sn-W-tourmaline mineralization (Badham, 1976, p. 564). This is consistent with the occurrence of Sn and W in the diatreme, although these elements occur only in trace quantities (Table 1). Because Sn may also be a constituent of rutile (Deer, Howie and Zussman, 1970, p. 416), its precise origin is uncertain.

F. Bi (Table 1) is a common constituent of Co-Ni arsenide ores (Stanton, 1972, p. 603). However, it is produced largely as a by-product of ores of other metals, particularly copper and lead (Rathjen and Wyche, 1975, p. 147). Hence Bi may be associated with Phase I and/or Phase II mineralization. Its precise origin remains uncertain.

VI. Zonation

Because of limited diamond drilling and geochemical analyses, it is not possible to discern zonation patterns with certainty. The limited data that are available show no horizontal or concentric trends in mineralogy, chemistry or hydrothermal alteration. The deposit does however appear to exhibit a crude vertical zonation primarily associated with Phase I mineralization. This zonation is suggested by the following observations.

A. Pb isotope studies (Chapter 9) suggest that lead at depth in the diatreme is more radiogenic than that at surface. This implies that the original U:Pb ratio was higher at depth.

B. Samples from the main surface showing contain from 0.8 to 4.2% lead, whereas those at depth contain almost no lead (Table 15). Taken in consideration with the lead isotope data cited above, this may indicate that during Phase I, uranium was deposited preferentially at depth, and lead preferentially at higher levels. At least some of this lead however is related to Phase II (this Chapter, p. 293).

C. Nickel is common in samples from trenches 1 and 2 but is a very minor constituent in samples from depth (Table 15). Although cobalt has not been analyzed for, it can be assumed to vary more or less directly with nickel content (Tables 1 and 2). This again suggests a zonation, with Co-Ni mineralization deposited preferentially at higher levels.

VII. Origin of Mineralization

The mineralization in the BBX diatreme is ascribed to two principle sources.

A. Mineralization Related to Emplacement of the Diatreme

Phase I mineralization includes U-Pb-Co-Ni-Ag-Ti and possibly Th, REE, Sn-W, Bi and Cu. Lead isotope evidence suggests that lead and uranium were deposited in the diatreme coincident with its formation. It can be assumed that the formation of the diatreme involved relatively high (magmatic) temperatures. Moderate to high temperatures of formation are characteristic of arsenopyrite, glaucodot, gersdorffite, siegenite, pyrrhotite and pentlandite (Ramdohr, 1969). This suggests that these minerals are related in some way to the formation of the diatreme. The precise mechanism by which Phase I mineralization was concentrated and deposited, can only be speculated upon.

Ag, Co-Ni arsenide mineralization is associated with each of the three periods of intrusive magmatic activity in the East Arm (this thesis, p. 269). The origin of these deposits has been discussed by Badham (1978a, p. 1488). Based on studies of the mineralization associated with the Easter Island Dyke, he suggested that the arsenide fluids were generated at depth in the dyke by hydrothermal breakdown of olivine, and possibly also clinopyroxene and primary sulfide phases. He postulated a convective recirculation of water which leached Ag, Ni, Co, Fe, As, Sb and Bi to form a metalliferous fluid depleted in reduced sulfur species.

The paragenetic sequence in the BBX deposit is similar to that described for late Aphebian (≈ 1790 m.y.) Co-Ni mineralization in the East Arm (Badham, 1978a, p. 1488). It has been suggested that magnetite-apatite-actinolite mineralization with associated REE and U is related to fluids derived from late highly volatile phases of calc-alkaline diorites. Silver-arsenide fluids were relatively late to escape into fractures and dilatant joints within the intrusions.

Whatever the precise mode of origin, the association in the BBX deposit of Ag, Co-Ni arsenide mineralization with mafic igneous rocks is consistent with the geology of such deposits elsewhere (Stanton, 1972, p. 609). Ag, Co-Ni mineralization is probably related to leaching of the mafic volcanics and underlying magma by late-stage hydrothermal fluids.

The presence of U (and possibly Th and REE) early in the paragenetic sequence may be attributable to fluids derived from late highly volatile phases of the magma as described above. That the diatreme and the uranium have a deep-seated (i.e. mantle) origin however, has been inferred from studies of structural geology and lead isotopes. This is consistent with the postulate that mantle de-gassing is a principal means of radioelement transfer to the crust, and that this transfer is effected through diatreme formation (Gabelman, 1977, p. 31). It is possible therefore that this early phase of mineralization (U ± Th, REE) is the result of gaseous transfer from the mantle.

B. Mineralization Related to Connate Brines

1. Source of Mineralization

Oxygen isotope, lead isotope and fluid inclusion studies suggest that later phases of mineralization (phases IV and possibly phases II and III) were deposited from hydrothermal fluids consisting predominantly of evolved connate water. The term "evolved" denotes that significant chemical and isotopic changes have taken place relative to the original connate fluid (White, 1974, p. 955). These changes include increased salinity, and the addition of various ore-forming elements leached from adjacent rocks.

In addition to evidence from the above sources, this model is supported by considerations of the chemistry of sedimentary rocks and modern day connate brines.

(i) Li and K

The relatively high concentrations of

these elements in formation waters has already been noted (this thesis, p. 251). Lithium is an important constituent of many modern subsurface brines, and is recovered economically from these brines in some instances (Vine, 1975, p. 479). Table 13b indicates that K and Li are relatively more concentrated in shales and argillaeous sediments than in other types of sedimentary rock.

(ii) Pb and Ba

Many subsurface brines contain from 1 to nearly 6000 PPM dissolved Ba (Hanor, 1979, p. 158), whereas magmatic hydrothermal fluids generally do not contain significant concentrations of this element (Fischer and Puchelt, 1978, p. 56-F-2). Metal rich oil field brines containing up to 92 mg/l Pb have been recorded (Hanor, 1979, p. 156).

Pb and Ba can both substitute for K in feldspars and mica's (op. cit., p. 139). The highest concentration of lead in crustal rocks (80 PPM) is in deep sea clays (Faure, 1977, p. 199).

(iii) Cu

Cu and Pb may be derived from andesite and shale at elevated temperatures in saline solutions (Ellis, 1979, p. 658).

The above observations suggest that the connate brine may have derived its metal content primarily from argillaceous sediments and possibly to a small extent from mafic volcanics in the basin. Leaching experiments with shales indicate that abundant calcium, the presence of sulfate, and increased temperature, can all enhance the extraction of metals such as Cu, Pb, Zn and Mn compared to the extraction achieved by an NaCl brine (Hitchon, 1977, p. 15). These three features are found in fluid inclusions in the BBX deposit (Section III). The sulfur species necessary for the extraction of metals and for their precipitation in the diatreme could be derived from evaporites in the basin (Dunsmore and Shearman, 1977, p. 197). Dissolved salts in the fluid may also derive from evaporites, or they may be the result of shale membrane filtration (this thesis, p. 249).

2. Movement of Mineralizing Fluids

Factors resulting in the movement of hydrothermal brines into the diatreme from the basin can be inferred from the following considerations.

(i) Temperature

Temperatures on the order of 150°C to 175°C have been postulated for these mineralizing events (Section III). The average geothermal gradient in older sedimentary basins is 15°C to 40°C/km (Hanor, 1979, p. 143). Using 40°C/km, and a maximum thickness of platform sediments of 1.4 km (Figure 7), a temperature of 56°C could be generated by normal geothermal gradients. Significantly higher temperatures determined in this study sugggest either that the fluids originated from deep within the basin, and/or that an external source of heat (i.e. magmatic) is required.

(ii) Structural Control of Mineralization

The presence of galena and chalcopyrite (Phase II), barite-specularite (Phase III) and carbonate-quartz (Phase IV) in narrow veins cross-cutting the diatreme, implies that these mineralizing events postdated or were related to tectonism in the basin.

(iii) Lead Isotope Data

Late hydrothermal events have been tentatively dated at 1110 m.y. and possibly 1550 m.y. (this thesis, p. 270). While the relative importance of these events cannot be determined, it is interesting to note that an age of 1110 m.y. corresponds roughly with late magmatic activity in the East Arm (this thesis, p. 42).

It can be suggested from the above that tectonism and associated magmatic activity in Great Slave Basin, were responsible for initiating the movement of hydrothermal fluids into appropriate sites of deposition, and that this may have occurred on more than one occasion (i.e. 1550 m.y., 1110 m.y.). The mechanism by which this occurred cannot be precisely determined.

Faulting of a sedimentary basin can provide a permeable conduit for the movement of fluids from depth under conditions where hydrostatic pressure is exceeded by pressures at depth (Hanor, p. 165). With a greater degree of tectonic deformation, particularly uplift, deep brines can be driven towards sites of mineral deposition (op. cit., pp. 165-166). This is consistent with the structural history of the East Arm, and with the postulate that late quartz-carbonate veins were deposited following a period of uplift (this thesis, p. 150).

Magmatic activity results in an increased geothermal gradient, and provides a potential means for inducing fluid flow (Hanor, 1979, p. 167). Sufficient thermal expansion of a brine permits a convective current to be established, provided that permeability is adequate (White, 1974, p. 969). The elevated temperature of this fluid, and its movement through the basin, would promote leaching of metals from the country rocks.

Evidence indicates that mineralizing fluids migrated from depth into relatively porous and permeable zones, including the diatreme and the south margin of the diabase plug (this thesis, p. 154). The control of these features and of quartz-carbonate stockworks by major shear fractures presumably extending to basement, raises the possibility that the fluids migrated from deep basinal areas, along the Archean-Proterozic contact. If this was the case, the deposits can be characterized as hypogene in origin, and a lateral secretion hypothesis per se does not appear to be valid.

Dewatering is not considered to be an important factor in initiating the movement of the hydrothermal fluids. Studies have shown that most of the water trapped during slow deposition of sediments is flushed out within the upper kilometre of burial (Hanor, 1979, p. 165), and that seventy five percent of the water in shales is normally expelled during shallow burial from 0 m to 100 m (op. cit., p. 141). These observations are not consistent with the relatively late age of the mineralization (1110 m.y.?) which considerably postdates deposition of the Great Slave Supergroup. Moreover, the temperatures and salinities of these waters are generally much lower than those of sedimentary waters known to contain high concentrations of metals, and of fluid inclusions from main-stage mineralization in Mississippi Valley-type deposits (op. cit., p. 165).

VIII. Deposition of Mineralization

A. Introduction

The complex mineralogy of the BBX deposit is the result of four separate phases of mineralizing activity. These phases are characterized by different mineralogy, chemistry and possibly temperature, and in some cases are derived from widely different sources. It is somewhat surprising therefore, that the minerals ascribed to these individual events are generally spatially related. The main surface showing for example, contains substantial quantities of mineralization from Phases I to IV. Immediately outside of this zone however, none of these phases appear to be represented.

With the possible exception of Phases II and III, this spatial association is felt to be largely coincidental. Phase I mineralization is apparently restricted to the main surface showing. The fact that Phase II mineralization has subsequently occupied the same zone, cannot be judged as significant on the basis of the limited data available. Phase IV quartz-carbonate veins are structurally controlled and are dependent on existing fractures in the diatreme. Their occasional association with earlier mineralization therefore, is fortuitous.

The purpose of this section is to devise a workable model which will explain the distribution of mineralization in the diatreme, and the factors controlling its deposition. The discussion is concerned mainly with Phase II mineralization because of its relative abundance and greater economic potential. The deposition of Phase III mineralization is discussed briefly.

B. Theoretical Background

Modern theories on the transport of metals in aqueous systems suggest that metallic elements travel in solution as complex ions; particularly as chloride complexes and bisulfide-polysulfide complexes (Stanton, 1972, p. 153). According to Barnes (1979, p. 438), the chemical efficiencies of each of these complexes are similar. but factors influencing their stabilities, particularly oxidation state and pH, may have opposite effects. The relative geological importance of these complexes which are described briefly below, has not been established.

Chloride complexes develop in the presence of high concentrations of chloride ion supplied by compounds such as HCl, NaCl and KCl (Stanton, 1972, p. 153). Conditions under which this mechanism will operate are an abundance of the chloride ion, moderately elevated temperatures, and a slightly acid pH (op. cit., p. 154). One of the most effective mechanisms of precipitation from these complexes, is to increase the pH (Barnes, 1979, p. 436). As most hydrothermal fluids are weak acids, extraction of hydrogen ions tends to reduce the stability of chloride complexes, and leads to mineral precipitation. The hydrolysis of feldspars and micas is one of the most effective reactions consuming hydrogen ions. The alteration of plagioclase to sericite is an example of such a reaction.

The view that metals travel mainly as sulfide complexes has been proposed by Barnes and Czamanske. These authors suggest (p. 368) that current data do not favor transport of ore metals as chloride complexes, at least at low temperatures. They conclude that the transport of base metals as bisulfide or sulfide complexes is feasible at temperatures up to at least 250°C (op. cit., p. 377). Transport would take place in alkaline solutions in the presence of abundant sulfide (Stanton, 1972, p. 154). Above 250°C, chloride complexes may become more important because compounds such as HCl and KCl become highly associated in aqueous solutions at elevated temperatures. Certain metal-chloride complexes may also become more stable with increasing temperature (Barnes and Czamanske, 1967, p. 368).

Of the more than 30 possible sulfur-containing species, only SO_4^{2-}, H_2S and HS^- appear to be reasonable as complexing agents (op. cit., p. 345). Deposition of metals carried as sulfide complexes can be brought about by decreasing the activities of sulfide species in the solution. This in turn will decrease the solubility of metallic complexes (op. cit. p. 374). The most effective reactions chemically, but not necessarily geologically, are brought about by oxidation of the ore-forming solution through exposure to rocks or fluids containing oxidized species (e.g. magnetite, hematite and other ferric minerals)(op. cit., p. 374.)

The activities of sulfide complexes may also be decreased by lowering the pH of the solution. To some extent, oxidation and lowering of the pH may be related. In the following equations, the complexing of aqueous sulfide species with oxygen liberates H^+ and consequently lowers the pH, except where the principal species is S^{2-} (Barnes and Czamanske, 1967, p. 375).

$$H_2S + 2O_2 \rightarrow SO_4^{2-} + 2H^+$$
$$HS^- + 2O_2 \rightarrow SO_4^{2-} + H^+$$
$$S^{2-} + 2O_2 \rightarrow SO_4^{2-}$$

The liberated H^+ may react with the ionized species as follows:

$$S^{2-} + H^+ \rightarrow HS^-$$
$$HS^- + H^+ \rightarrow H_2S(g)$$

The formation of $H_2S(g)$ in this way reduces the activities of the stronger complexing agents and brings about the deposition of metallic minerals. Hydrogen ions may also react with the wall rock to form micas and clay minerals. An example of this reaction is the alteration of chlorite to sericite.

C. Occurrence and Affinity of Mineralization

The factors which control the distribution of mineralization in the diatreme are not well-defined. Nevertheless, mineralized zones exhibit certain broad features of texture and lithology which when contrasted with those of unmineralized zones, provide some insight into the factors controlling mineralization. These features are as follows.

1. Wall Rock Alteration

Basaltic fragments in mineralized zones have undergone moderate to intense potassium alteration. In general, the concentration of mineralization varies directly with the intensity of alteration. It should be noted however, that zones exhibiting strong potassium alteration are occasionally unmineralized.

2. Packing of Breccia Fragments

Volcanic fragments in mineralized zones are relatively tightly packed. The matrix in these zones rarely comprises more than 15% of the rock, and generally substantially less. These zones correspond to "volcanic bed forms" discussed in Chapter 6 of this thesis.

3. Affinity for Oxidized Species

The sulfides appear to exhibit a marked affinity for breccia constituents containing oxidized species. Fragments of oolitic and pisolithic hematite particularly, frequently contain at least trace amounts of disseminated chalcopyrite (and locally galena). Replacement of basalt fragments by sulfides is limited. Where it does occur however, it has three principal habits.

(i) Replacing serpentine pseudomorphs of olivine. During the alteration of olivine to serpentine, iron oxides such as magnetite and in some cases goethite are formed (this thesis, p. 64).

(ii) Fine disseminations in the matrix of basalt fragments. These fragments contain abundant finely divided oxidized species, particularly magnetite. The possibility that basalt fragments were hematitized during formation of the diatreme (this thesis, p. 116), suggests that abundant hematite was present prior to the hydrothermal event.

(iii) Replacing glass shards (Plates 17 and 39). Altered volcanic glasses such as palagonite are amorphous mineraloids and contain numerous oxides including Fe_2O_3 (Kerr, 1977, p. 424).

D. Discussion

The association of mineralization with tightly packed zones suggests that its deposition was induced by factors related to the restriction of fluid movement. This restriction would provide greater time for reaction with the wall rock. Moreover, the greater surface area in these zones would facilitate chemical exchange with the wall rock, and would also foster heat loss from the hydrothermal fluid into the relatively cooler rocks of the diatreme. The sympathetic variation of wall rock alteration with mineralization however, suggests that it is a chemical rather than a thermal exchange which is significant.

Potassium alteration, as illustrated in the sericitization of chlorite, involves the addition of Al, Si, K and H from the hydrothermal fluid (this thesis, p. 109). Of these elements, only hydrogen may have an effect on the stability of metal complexes in hydrothermal fluids. Changes in the concentration of H^+ in the system can bring about precipitation of metals whether they are carried as chloride or as sulfide complexes. Potassium alteration per se therefore, is somewhat incidental and develops only because of the relatively high concentration of potassium in the fluid. Changes in the pH of the solution, and the associated loss of H (and K) to form sericite are the principal factors controlling the precipitation of mineralization.

The possibility that metals were carried as chloride complexes is supported only by the relatively high salinity of the fluid (this thesis, p. 218). Such a saturated fluid would presumably be relatively efficient at transporting metals.

The complexing of metals with sulfur species appears to be a more viable alternative and is consistent with the following features.

1. Relatively low temperatures of formation (150°C - 175°C).
2. The affinity of mineralization for oxidized species.

It is proposed therefore that metals were carried in solution as bisulfide-polysulfide complexes, and that their deposition was brought about by oxidation of the fluid, which resulted in a change in its pH. This model solves the problem of finding an external source of sulfur to combine with metallic elements to form sulfides. The fact that no H_2S was detected in fluid inclusions is not felt to be particularly significant as those inclusions which were tested were from relatively barren late-stage quartz veins (Phase IV). Moreover, it is conceivable that sulfide species were consumed in the formation of sulfides or were removed from the system.

This model has two important implications.

1. H^+ liberated by oxidation could remain in the fluid and recombine with sulfur species to reduce the activities of complexing agents and bring about the deposition of mineralization. Conversely, it could migrate into the wall rock and be used in the formation of sericite. This would explain the fact that some zones exhibiting strong potassium alteration are unmineralized. These may also be interpreted as alteration haloes adjacent to mineralized zones however.

2. The breakdown of sulfide complexes would result in a gradual enrichment of SO_4^{2-} in the fluid. In the presence of Ba, barite would precipitate. This is consistent with the presence of barite as a relatively late mineral in the paragenetic sequence. An alternate possibility is discussed in the following section.

IX Implications

It has been suggested (this thesis, p. 150) that late-stage quartz-carbonate veins (Phase IV) were deposited following a period of uplift. It is conceivable therefore, that Phases II, III and IV of the mineralization may have been deposited in stages as the diatreme was brought nearer to the surface by tectonic unloading. Although the fluids responsible for each of these phases have been interpreted as connate brines, it is possible that they evolved somewhat as unloading proceeded.

Sulfide-depositing solutions generally have a reducing influence (Ramdohr, 1969, p. 907) and it is suggested that they were active at depth. This is consistent with the presence of sulfide mineralization relatively early in the paragenetic sequence. As the host rocks were brought closer to the surface, the fluids would gradually come under the influence of oxygenated surface waters. This is is consistent with the geochemistry of barite which is commonly deposited by fluids with high oxidation potential where sulfur is present as sulfate. Such conditions occur close to the earth's surface (Fischer and Puchelt, 1978, p. 56-F-2). Phase IV quartz-carbonate veins were deposited relatively near the surface where overburden pressures were sufficiently low to allow dilatant bedding joints to form (this thesis, p. 150).

It is conceivable that the chemical changes in these fluids were accompanied by a gradual decrease in temperature as the system neared the surface. To some extent, this is consistent with fluid inclusion and structural data (this thesis, p. 253).

SECTION V

CLOSING REMARKS

CHAPTER 11

SUMMARY AND CONCLUSIONS

I. Summary

The BBX diatreme is one of seven Seton volcanic centres occurring in the vicinity of Taltheilei Narrows and Hearne Channel. These diatremes are controlled principally by a major basement fault, as indicated by their occurrence in a linear belt (18° az), and by the presence of granitic fragments in the vent agglomerate. Within the Proterozoic succession however, the emplacement of these diatremes was controlled by zones of structural weakness in the roof rocks. The BBX diatreme is controlled by one of a set of shear fractures related to compressional folding.

The diatreme consists primarily of mafic volcanic fragments, with lesser amounts of sedimentary and granitic country rock, all set in a matrix of finely comminuted rock debris. This "rock flour" is now present only occasionally in unaltered form. Generally, it has undergone pervasive chloritic and carbonate alteration. The volcanics themselves are thought to be predominantly accidental fragments from a pre-existing volcanic pile. Juvenile volcanic matter is felt to be a relatively minor constituent of the agglomerate, possibly less than 25%.

The volcanics were originally hematitized by oxidation during formation of the diatreme. Subsequent deuteric processes have altered the volcanics to a propyllitic assemblage. Potassium alteration is intimately associated with mineralization and occurs intermittently in the diatreme. Late hydrothermal fluids have resulted in strong carbonatization, and occasionally silicification of the agglomerate.

Lead isotope studies suggest that the juvenile fraction of the BBX volcanics is mantle-derived, and that the diatreme was emplaced at 1870 ± 15 m.y. This corresponds to the middle Aphebian phase of intrusive magmatic activity in the East Arm.

It has been suggested that the complex mineral assemblage in the diatreme is the result of several periods of mineralizing activity which are summarized below .

Phase I

A. U-Pb: These phases may have been introduced by gaseous transfer from the mantle during formation of the diatreme.

B. Fe-Co-Ni: These phases were deposited as high temperature sulfides and sulfarsenides from hydro-

> thermal fluids associated with mid-Aphebian magmatism. The metals probably derive from the mafic parent magma of the BBX diatreme, and were incorporated into the fluid by hydrothermal leaching.

Phases II, III and IV.

> Chalcopyrite, galena, barite and specularite may have been deposited from circulating connate brines. The change from reducing (sulfide) fluids to those with high oxidation potential (barite, specularite) may be related to tectonic unloading, and mixing of the fluids with oxygenated surface (meteoric) waters. This change in chemistry may have been accompanied by a decrease in temperature. Late magmatic activity in the East Arm (1110 ± 20 m.y.) may have provided the thermal energy necessary to drive these hydrothermal systems.

The fact that the BBX diatreme hosts mineralization of such diverse origins is attributable to its relatively high original porosity and permeability, and to its control by a major structure extending to depth.

II. Implications

The implications of this study regarding the geologic history of the East Arm and the economic geology of the deposit are discussed below.

A. Geotectonics

In view of the limited scope of this study, it would be inappropriate to discuss in detail the relationship between the BBX diatreme and the tectonic history of the East Arm. The following observations however, arise from this study and should be noted.

1. Structural studies suggest that the emplacement of the diatreme was controlled by a shear fracture related to compressional folding. It can be assumed that this folding is associated with the compressional stage of structural evolution of the East Arm (this thesis, p. 38). This compression postdated deposition of the Great Slave Supergroup, and represents a late stage in the structural evolution of the geosyncline.

   An age of 1870 ± 15 m.y has been determined for the BBX diatreme (this thesis, p. 269). In consideration of the above, it can be suggested that deposition of the Great Slave Supergroup was completed by 1870 m.y.

This is supported by the observation that alkaline diorites dated at between 1845 and 1630 m.y. were intruded contemporaneously with, or after deposition of the Christie Bay and Pethei Groups, and are overlain unconformably by the Et-Then Group (Hoffman, 1969, p. 444, this thesis, p. 41).

2. It has been suggested in Chapter 6 (p. 183) that the BBX diatreme intruded the Proterozoic succession as far as the basal portion of the Pethei Group. This implies that the formation of the diatreme occurred shortly after a change in the sedimentary regime (Table 5, p. 35). The change from the Flysch (Kahochella Group) to the to the Calc-Flysch (Pethei Group) phase of sedimentation is related to the tectonic evolution of Great Slave Basin. In particular, it reflects the change from pre-orogenic to syn-orogenic sedimentation in the Coronation geosyncline (this thesis, p. 37).

The above observations indicate on the one hand, that the diatreme postdated deposition of the Great Slave Supergroup (point #1), and on the other hand that it considerably preceded deposition of the entire Great Slave Supergroup. These two points are clearly incompatible. The dilemma can be partially resolved if the compressional stage of deformation commenced during, rather than after deposition of the Great Slave Supergroup.

A more difficult problem to resolve is the relationship of the diatreme to the tectonic cycle in the Coronation Geosyncline and Great Slave Basin. It has been suggested above (point #1), that the diatreme was emplaced at a late stage in the structural evolution of the geosyncline. This is inconsistent with the inference of point #2, that the diatreme formed at a very early stage in the structural evolution of the geosyncline.

Because of the narrow scope of this study, the tentative nature of the above observations, and the lack of detailed knowledge of the tectonic history of the area, further speculation is not warranted.

B. The Mineralizing Events

1. Badham (1976) has suggested that the complex polymetallic Ag, Co-Ni arsenide ore type is part of a spectrum of late and post-orogenic deposits. These often include earlier Sn-W mineralization, and later Ag, Bi sulphosalt and sulfide veining (op. cit., p. 559). The Ag, Co-Ni arsenide mineralization in the Aristifats deposit is consistent with this model if it is assumed that the emplacement of the diatreme postdated compressional folding (late orogenesis, see above).

2. According to Badham (1976, p. 564), the Ag, Co-Ni arsenide ore association is characterized by a complex paragenesis that usually takes the following form.

Stage 1: U-quartz
Stage 2: Ag, Ni, Co, As ± Bi + carbonates
Stage 3: Sulfides, Ag + Bi sulphosalts, fluorite, barite, carbonates, quartz.

Consideration of Table 20 (this thesis, p. 279) shows that the mineralization in the Aristifats deposit closely follows this paragenesis. It is not however, a typical Ag, Co-Ni arsenide deposit. According to Badham (1976, p. 566), the major problem with Ag, Co-Ni arsenide ore genesis is in the origin of the mixture of "felsic" (Sn-W, and sulphides) and "basic" (Co-Ni) elements. He proposes (p. 566) that the deposits form by means of a series of coincidental orogenic events which result in the admixture of remnant granitic hydrothermal solutions and newly generated hydrothermal fluids related to basic magmas. While this model may be valid for the Ag, Co-Ni association in general, it appears to be inapplicable in the present case. Studies have indicated with a reasonable degree of certainty, that the "basic" association (Co-Ni) does in fact derive from hydrothermal fluids related to mafic magmas. The "felsic" association however (sulfides, barite) has been tentatively shown to have been deposited from hydrothermal fluids consisting predominantly of connate formation water. The metal content of these brines has been leached from argillaceous sediments in the basin which contain a variety of metallic elements in trace quantities. The possibility that lateral secretion may account for the "felsic" association has been noted by Badham (1976, p. 566) but was not felt to be applicable to the deposits he studied. While the mechanism of lateral secretion may be operative under appropriate conditions, the mineralizing fluids responsible for the BBX deposit (Phases II to IV) probably originated in distal deep-basinal sediments, and their flow was controlled by fractures and zones of structural weakness.

C. Economic Considerations

1. It is beyond the scope of this study to discuss the economic potential of the BBX deposit in detail. Should this be undertaken in the future however, the following points should be considered.

(i) The mechanism by which diatremes form, discussed in Chapter 6, suggests that the vent pinches considerably with depth. Its horizontal cross-sectional area may therefore be considerably smaller at depth than at the surface. This reduces the potential volume of mineralized rock, and also makes drilling to depth within the diatreme difficult. This difficulty is compounded by possible irregularities in the vent wall, by late structural modifications (tilting, shearing), and by the possibility that the diatreme is not vertical (this thesis, p. 185).

ii) The relatively more valuable constituents of the mineral assemblage, particularly Ag, Co and Ni, occur in significant quantities only in the vicinity of trenches 1 and 2. They have not been encountered elsewhere.

(iii) Phase II mineralization (chalcopyrite and galena) locally reaches significant concentrations. The economic importance of this phase however is limited by its intermittent occurrence, and by the fact that galena appears to be restricted to the vicinity of trenches 1 and 2.

Exploration for Phase II mineralization is complicated by the following considerations.

(a) Deposition of the mineralization is brought about by chemical exchange with the wall rock in tightly packed zones interpreted as "volcanic bed forms". The complex origin of the diatreme (Chapter 6), and the apparently random distribution of these bed forms makes it all but impossible to predict the locations of potential zones of interest.

(b) "Bed forms" in some cases exhibit only weak potassium alteration. This suggests that the mineralizing fluid did not migrate throughout the diatreme, but rather followed relatively discrete pathways.

The possibility that the vent is inclined and that mineralizing fluids migrated preferentially along the footwall (this thesis, p. 185) must be considered.

Unfortunatley, this model does not explain the locations of some of the more significant copper showings encountered in DDH 76-1

2. Hoffman et al (1977, p. 123) have suggested that if the basalt pipes on the BBX and JDA groups, which are mineralized, are the same age as those to the south in Hearne Channel, they are more deeply eroded. They inferred from this that the southern pipes may be mineralized at depth. The possibility that phase II mineralization was deposited at relatively deep levels lends some credence to this inference, but its validity cannot be adequately assessed on the basis of this study alone. The following observations however, do have some bearing on the matter.

(i) Although both the BBX and JDA diatremes are mineralized, it is important to understand the nature and significance of this mineralization. On the JDA group, it comprises minor amounts of chalcopyrite and pyrite associated with localized quartz-carbonate veining. These narrow veins, which form an anastomosing network, are evidently controlled by a vertical east-west shear zone and are not associated with visible wall rock alteration. Although the veins exhibit rather pronounced malachite staining, they have no economic potential, and are interpreted as belonging to the same phase of hydrothermal activity responsible for late quartz-carbonate veins on the BBX property (phase IV). Trace amounts of chalcopyrite associated with quartz-carbonate veins were also noted from one of the southerly diatremes in Hearne Channel.

It does not appear valid therefore to distinguish the two northerly diatremes from those farther south, on the basis of the presence or absence of mineralization.

(ii) A large subcrop of sandstone south of the JDA group (Map 1) has been interpreted as representing the basal part of the Akaitcho Formation (this thesis, p. 54). This must be resolved with drill hole data from the BBX deposit which shows Akaitcho sediments to depths of as much as 800 feet. This suggests either that a fault exists between the JDA and BBX groups, or that the affiliation of these sediments has been misinterpreted. Assuming that a fault does exist, it can be suggested that the JDA diatreme is more deeply eroded than that on the BBX property.

III. Suggestions for Further Work

The purpose of this study has been to document the geology of the Aristifats (BBX) deposit, and to speculate on the nature, origin and affinity of both the diatreme and the associated mineralization. To a large degree this objective has been achieved. Future studies would benefit from two principle avenues of investigation.

A. Much of the discussion on the origin of the diatreme was predicated on the assumption that sedimentary rocks at depth on the BBX property belong to the Akaitcho Formation. As noted in Chapter 3, there is some question as to whether these sediments are in fact part of the Akaitcho Formation. In particular, pisolithic sediments do not appear to be consistent with published descriptions of the Akaitcho Formation, and strikingly similar rocks outcropping in Hearne Channel have been assigned to the Ogilvie Formation (this thesis, p. 55). The successful resolution of this problem would have some bearing on the origin of the diatreme, and may be of some use in resolving the question of whether the southerly pipes in Hearne Channel are mineralized at depth.

B. Sulfur isotope studies carried out on minerals such as chalcopyrite, galena and barite may be successful in determining the source(s) of sulfur in the ore-forming fluid, particularly with respect to phases II and III. This would provide useful information on the origin of the deposit, and hopefully would lend support to the views expressed herein.

References Cited

American Geological Institute, Dictionary of Geological Terms. Garden City, New York: Doubleday and Company, Inc. (Dolphin Books), 1962.

Argy, G.H., and Siega, L.J., 1971, "Geological Report on The BBX Mineral Claims, Taltheilei Narrows - Great Slave Lake, Northwest Territories". Report prepared for the BBX Syndicate. D.I.A.N.D. files, Yellowknife, N.W.T.

Baadsgaard, H., Morton, R.D., and Olade, M.A.D., 1973, "Rb-Sr Isotopic Age For the Precambrian Lavas of the Seton Formation, East Arm of Great Slave Lake, Northwest Territories", Can. J. Earth Sci., V.10, pp. 1579-1581.

Badham, J.P.N., 1976, "Orogenesis and Metallogenesis with Reference to the Silver-Nickel, Cobalt Arsenide Ore Association", Metallogeny and Plate Tectonics, Strong, D.F., editor. Geological Association of Canada, Special Paper Number 14, pp. 559-571.

Badham, J.P.N., 1978a, "Magnetite-Apatite-Amphibole - Uranium and Silver-Arsenide Mineralizations in Lower Proterozoic Igneous Rocks, East Arm, Great Slave Lake, Canada", Econ. Geol., V.73, pp.1474-1491.

Badham, J.P.N., 1978b, "The Early History and Tectonic Significance of the East Arm Graben, Great Slave Lake, Canada", Tectonophysics, V.45, pp. 201-215.

Badham, J.P.N., 1979, "Geology and Petrochemistry of Lower Aphebian (2.4-2.0 Ga) Alkaline Plutonic and Hypabyssal Rocks in the East Arm of Great Slave Lake, Northwest Territories", Can. J. Earth Sci., V.16, No. 1, pp. 60-72.

Badham, J.P.N. and Stanworth, C.W., 1977, "Evaporites from the lower Porterozoic of the East Arm, Great Slave Lake", Nature, V.268, No. 11, pp. 516-517.

Barnes, H.L., 1979, "Solubilities of Ore Minerals", Geochemistry of Hydrothermal Ore Deposits, Second Edition, Barnes, H.L., editor. New York: John Wiley and Sons, pp. 404-454.

Barnes, H.L. and Czamanske, G.K., 1967, "Solubilities and Transport of Ore Minerals", Geochemistry of Hydrothermal Ore Deposits, Barnes H.L., editor. New York: Holt, Rinehart and Winston, Inc., pp. 334-378.

Barnett, E. deBarry, and Wilson, C.L., Inorganic Chemistry: A Textbook for Advanced Students, Second Edition. London: Longmans Green and Co., 1958.

Bateman, A.M., Economic Mineral Deposits, Second Edition. New York: Wiley, 1950.

Bell, R.T., 1978, "Breccia's and Uranium Mineralization in the Wernecke Mountains, Yukon Territory - A Progress Report", Geol. Surv. Can. Paper 78-1A, pp. 317-322.

Bell, Robert, 1900, "Summary Report on the Operations of the Geological Survey for The Year 1899", Geol. Surv. Can. Annual Report, V. XII.

Berry, L.G., and Mason, Brian, Mineralogy, Concepts, Descriptions, Determinations. San Francisco: W. H. Freeman and Company, 1959.

Billings, Marland P., Structural Geology, Third Edition. Englewood Cliffs, New Jersey: Prentice-Hall, Inc., 1972.

Blackadar, D.W., and McInnis, M.D., 1976, "BBX Property - East Arm Great Slave Lake, Mackenzie Mining Division", Great Plains Development Company of Canada, Ltd., Mining Exploration Department Project Yearend Report (Inhouse).

Bloy, Graeme, R., 1979, "U-Pb Geochronology of Uranium Mineralization in the East Arm of Great Salve Lake, N.W.T." Unpublished MSc. Thesis, University of Alberta, Edmonton.

Cocco, G., Fanfani, L., Zanazzi, P.F., Heier, K.S., Billings, G.K., and Steinnes, E., 1978, "Lithium", Handbook of Geochemistry, v. II-1, Wedepodl, K.E. editor. Heidelberg: Springer-Verlag, pp. 3-A-1 to 3-O-1.

Cocco, G., Fanfani, L., Zanazzi, P.F., Heier, K.S., Billings, G.K., and Steinnes, E., 1978, "Potassium", Handbook of Geochemistry, v. II-2, Wedepohl, K.E., editor. Heidelberg: Springer-Verlag, pp. 19-A-1 to 19-M-N-1.

Collins, Peter, L.F., 1979, "Gas Hydrates in CO_2- Bearing Fluid Inclusions and The Use of Freezing Data for Estimation of Salinity", Econ. Geol. v. 74, pp. 1435-1444.

Cumming, G.L., 1980, "Pb Isochron Dating of the Seton Formation, East Arm of Great Slave Lake, Northwest Territories", Can J. Earth Sci. v. 17. No. 11, pp. 1591-1593.

Cumming, G.L., Rollett, J.S., Rossotti, F.J.C. and Whewell, R.J., 1972, "Statistical Methods for the Computation of Stability Constants. Part 1. Straight -line Fitting of Points with Correlated Errors", Jour. Chem. Soc. Lond., Dalton Trans., pp. 2652-2658.

Deaton, W.M., and Frost, E.M., 1946, "Gas Hydrates and Their Relation To The Operation of Natural Gas Pipelines", U.S. Department of the Interior, Bureau of Mines, Monograph 8.

Deer, W.A., Howie, R.A., and Zussman, J., An Introduction To The Rock-Forming Minerals. London: Longman Group Limited, 1970.

Dennis, John G., Structural Geology. New York: Ronald Press Co., 1972.

Doe, B.R. and Stacey, J.S., 1974, "The Application of Lead Isotopes to the Problems of Ore Genesis and Ore Prospect Evaluation: A Review", Econ. Geol. v. 69, pp. 757-776.

Dunham, Robert J., 1969, "Vadose Pisolite in the Capitan Reef (Permian), New Mexico and Texas", Depositional Environments in Carbonate Rocks-A Symposium, Friedman, Gerald M., editor. Society of Economic Paleontologists and Mineralogists, Special Publication No. 14. Tulsa, Oklahoma, March, 1969, pp. 182-191.

Dunsmore, H.E., and Shearman, D.J., 1977, "Mississippi Valley-type lead-zinc orebodies: a sedimentary and diagenetic origin" Proceedings of the Forum on Oil and Ore in Sediments, Imperial College, London, March, 1975, pp. 189-201.

Ellis, James A., 1979, "Explored Geothermal Systems", Geochemistry of Hydrothermal Ore Deposits, Second Edition. Barnes, H.L., editor. New York: John Wiley and Sons, pp. 632-683.

Faure, Gunter, Principles of Isotope Geology. New York: John Wiley and Sons, 1977.

Fischer, K., and Puchelt, H., 1978, "Barium", Handbook of Geochemistry, v. II-4. Wedepohl, k.E., editor. Heidelberg: Sringer-Verlag, pp. 56-A-1 to 56-O-2.

Fisher, Richard V., and Waters, Aaron, C., 1970, "Base Surge Bed Forms in Maar Volcanoes", American Journal of Science, V. 268, pp. 157-180.

Gabelman, John, W., 1977, "Migration of Uranium and Thorium-Exploration Significance", Studies in Geology No. 3. Tulsa: A.A.P.G.

Goff, S.P., and Scarfe, C.M., 1978, "Preliminary Report on The Volcanic Suites of the East Arm, Great Slave Lake, N.W.T.", Mineral Industry Report, 1975, Northwest Territories, EGS 1978-5, pp. 129-134.

Hanor, Jeffrey, S., 1979, "The Sedimentary Genesis of Hydrothermal Fluids", Geochemistry of Hydrothermal Ore Deposits, Second Edition. Barnes, H.L., editor. New York: John Wiley and Sons, pp. 137-172.

Hatch, F.H., Wells, A.K. and Wells, M.K. Petrology of the Igneous Rocks, Thirteenth Edition. London: George Allen and Unwin, Ltd., 1972.

Hathaway, John C., Flow Chart for Phyllosilicate identification, USGS Sedimentary Mineralogy Laboratory.

Hitchon, Brian, 1974, "Occurrence of Natural Gas Hydrates in Sedimentary basins", Natural Gases in Marine Sediments. Kaplan, Isaac, R., editor. New York: Plenum Press, pp. 195-225.

Hitchon, Brian, 1977, "Geochemical links between oilfields ore deposits in sedimentary rocks", Proceedings of the Forum on Oil and Ore in Sediments, Imperial College, London, March 1975, pp. 1-34.

Hoffman, P.F., 1968, "Stratigraphy of The Lower Proterozoic (Aphebian) Great Slave Supergroup, East Arm of Great Slave Lake, District of Mackenzie", Geol. Surv. Can. Paper 68-42.

Hoffman, P.F., 1969, "Proterozoic Paleocurrents and Depositional History of the East Arm Fold Belt, Great Slave Lake, Northwest Territories", Can. J. Earth Sci. v. 6, pp. 441-462.

Hoffman, P.F., 1973, "Evolution of an Early Proterozoic Continental Margin: the Coronation Geosyncline and Associated Aulacogens of the Northwestern Canadian Shield", Phil. Trans. R. Soc. Lond. A., V. 273, pp. 547-581.

Hoffman, P.F., 1977, "Preliminary Geology of Proterozic Formations in the East Arm of Great Slave Lake, District of Mackenzie", Geol. Surv. Can., Open File 475, 1:50,000, 16 maps.

Hoffmann, P.F., Bell, I.R., Hildebrand, R.S., and Thorstad, L., 1977, "Geology of The Athapuscow Aulacogen, East Arm of Great Slave Lake, District of Mackenzie", Geol. Surv. Can. Paper 77-1A, pp. 117-129.

Hoffman, P.F., Dewey, John F., and Burke, Kevin, 1974, "Aulacogens and Their Genetic Relation to Geosynclines, with a Proterozoic Example from Great Slave Lake, Canada", Modern and Ancient Geosynclinal Sedimentation. Dott, R.H., Jr. and Shaver, Robert H., editors. Society of Economic Paleontologists and Mineralogists, Special Publication No. 19. Tulsa, Oklahoma.

Hoffman, P.F., and Henderson J.B., 1972, "Archean and Proterozoic Sedimentary and Volcanic Rocks of the Yellowknife -Great Slave Lake Area, Northwest Territories", International Geological Congress, twenty-fourth Session, Canada, 1972, Field Excursion A28, Guidebook.

Hollister, Lincoln S., and Burruss, Robert C., 1976, "Phase Equilibria in Fluid Inclusions from the Khtada Lake Metamorphic Complex", Geochemica et Cosmochimica Acta, V. 40, pp. 163-175.

Kerr, Paul F., Optical Mineralogy, Fourth Edition. New York: McGraw-Hill Book Company, 1977.

Knauth, L.P. and Epstein, S., 1976, "Hydrogen and Oxygen Isotope Ratio's in Nodular and Bedded Cherts", Geochim. Cosmochim. Acta., V. 40, pp. 1095-1108.

Kobayashi, Riki, Withrow, Harold J., Williams G. Brymer, and Katz, Donald L., 1951, "Gas Hydrate Formation with Brine and Ethanol Solutions", Natural Gasoline Association of America, Proceedings, pp. 27-31.

Lloyd, John, 1971, "A Report on A Time Domain Induced Polarization Survey for Milner Resources Limited by Eagle Geophysics Limited, Vancouver, B.C.", D.I.A.N.D. Files, Yellowknife, N.W.T.

Lorenz, Volker, McBirney, Alexander R., and Williams, Howel, 1975, An Investigation of Volcanic Depressions Part III Maars, Tuff Rings, Tuff-Cones and Diatremes, NASA Progress Report (NGR-38-003-012) Houston, Texas (Clearing House for Federal Scientific and Technical Information Springfield, Va., NASA CR-115236).

Loveridge, Age of Seton Volcanics, Geol. Surv. Can. (Unpublished).

Meyer, Charles and Hemley, J. Julian, 1967, "Wall Rock Alteration", Geochemistry of Hydrothermal Ore Deposits. Barnes, H.L., editor. New York: Holt, Rinehart and Winston, Inc., pp. 166-235.

Miller, S.L., 1974, "The Nature and Occurrence of Clathrate Hydrates", Natural Gases in Marine Sediments. Kaplan, Isaac, R., editor. New York: Plenum Press, pp. 151-177.

Moore, James, G., and Peck, Dallas, L., 1962, "Accretionary Lapilli in Volcanic Rocks of The Western Continental United States", Journal of Geology, V.70, pp. 182-193.

Moore, Paul Brian, 1974, "III Isotypy of Robertsite, Mitridatite and Arseniosiderite, Am. Min, V. 59, pp. 48-59.

Moorehouse, W.W., The Study of Rocks in Thin Sections. New York: Harper and Row, 1959.

Mueller, Robert, F., and Saxena, Surendra, K., Chemical Petrology. New York: Springer-Verlag, 1977.

Nickerson, D., 1970, "Report on The BBX Claims, Taltheilei Narrows, Great Slave Lake, N.W.T.", D.I.A.N.D. Files, Yellowknife, N.W.T.

Nickerson, D., 1972, "Results of the Diamond Drill Program, BBX Claims, Taltheilei Narrows, N.W.T., August, 1972", D.I.A.N.D. Files, Yellowknife, N.W.T.

Nutter, D.E., and Sawyer, D.A., 1975, "BBX Copper Prospect", Great Plains Development Company of Canada, Ltd., inhouse report.

Olade, M.A.D., and Morton, R.D., 1972, "Observations on the Proterozoic Seton Formation, East Arm of Great Slave Lake, Northwest Territories", *Can. J. Earth. Sci.*, V. 9, No. 9, pp. 1110-1123.

Ollier, C.D., 1967, "Maars, Their Characteristics, Varieties and Definition", *Bull. Volcanol.*, V. 30-31, pp. 45-75.

Ollier, C.D., 1974, "Phreatic Eruptions and Maars", *Developments in Solid Earth Geophysics*. Civetta, Gasparini, Luongo, Rapolla, editors. New York: Elsevier Scientific Publishing Company, pp. 289-311.

Olson, r.A., 1972, "Report on the BBX Claim Group, East Arm Fold Belt, Great Slave Lake, Northwest Territories", D.I.A.N.D. Files, Yellowknife, N.W.T.

Park, C.F., and MacDiarmid, R.A., *Ore Deposits*, Second Edition. San Fransisco: W.H. Freeman and Company, 1970.

Potter, Robert W., 1977, "Pressure Corrections for Fluid Inclusion Homogenization Temperatures Based on the Volumetric Properties of the System NaCl-H_2O", *Jour. Research*, U.S. Geol. Survey, V. 5, No. 5, Sept.-Oct. 1977, pp. 603-607.

Poty, B.P. Leroy, J.R., and Jachimowicz, L., 1976, "Un Nouvel Appareil Pour la Mesure des Temperatures Sons le Microscope: L'installation de Micro-Thermometric Chaixmeca"; *Bull. Soc. Fr. Mineral. Cristallogr.*, V.99, pp. 182-186.

Ramdohr, Paul, *The Ore Minerals and Their Intergrowths*. Braunschweig: Pergamon Press, 1969.

Rathjen, John, and Wyche, Charlie, 1975, "Bismuth", *Mineral Facts and Problems*, Bicentennial Edition. U.S. *Bureau of Mines, Bulletin* 667, U.S. Department of the Interior.

Roedder, Edwin, 1962, "Studies of Fluid Inclusions: I. Low Temperature Applications of a Dual Purpose Freezing and Heating Stage", *Econ. Geol.*, V. 57, pp. 1045-1061.

Roedder, Edwin 1963, "Studies of Fluid Inclusions. II: Freezing Data and Their Interpretation", *Econ. Geol.* V. 58, No. 2, pp. 167-211.

Roedder, Edwin, 1967, "Fluid Inclusions as Samples of Ore Fluids", Geochemistry of Hydrothermal Ore Deposits. Barnes, H.L., editor. New York: Holt, Rinehart and Winston, Inc., pp. 515-574.

Roedder, Edwin, 1976, "Fluid Inclusion Evidence on the Genesis of Ores in Sedimentary and Volcanic Rocks", Handbook of Stratabound and Stratiform Ore Deposits, V. 2, Geochemical Studies. New York: Elsevier Scientific Publishing Company, pp. 67-110.

Roedder, Edwin, 1979, "Fluid Inclusions as Samples of Ore Fluids", Geochemistry of Hydrothermal Ore Deposits, Second Edition. Barnes, H.L., editor. New York: John Wiley and Sons, pp. 684-737.

Smith, F.G., and Little, W.M., 1959, "Filling Temperatures of H_2O-CO_2 Fluid Inclusions and Their Significance in Geothermometry", Canadian Mineralogist, V. 6, pp. 380-388.

Stacey, J.S., and Kramers, J.D., 1975, "Approximation of Terrestrial Lead Isotope Evolution by a Two-Stage Model". Earth and Planetary Science Letters, V. 26, pp. 207-221.

Stanton, R.L., Ore Petrology. New York: McGraw-Hill Book Company, 1972.

Takenouchi, Sukune, and Kennedy, George C., 1965, "The Solubility of Carbon Dioxide in NaCl Solutions at High Temperatures and Pressures", American Journal of Science, V. 263, pp. 445-454.

Taylor, Hugh P., 1974, "The Application of Oxygen and Hydrogen Isotope Studies to Problems of Hydrothermal Alteration and Ore Deposition", Econ. Geol., V. 69, pp. 843-883.

Turner, Francis, J., Metamorphic Petrology, Mineralogical and Field Aspects. New York: McGraw-Hill Book Company, 1968.

Vine, J.D., 1975, "Lithium in Sediments and Brines - How, Why and Where to Search", Jour. Research, U.S. Geol. Survey, V. 3, No. 4, pp. 479-485.

Walker, G.P.L. and Croasdale, R., 1970, "Characteristics of Some Basaltic Pyroclastics" Bull. Volcanol., V. 35, pp. 303-317.

White, Donald E., 1974, "Diverse Origins of Hydrothermal Ore Fluids", Econ. Geol., V. 69, pp. 954-973.

Williams, Howel, Turner, Francis J., and Gilbert, Charles, M., Petrography, An Introduction to the Study of Rocks in Thin Sections. San Fransisco: W.H. Freeman and Company, 1954.

Winkler, Helmut, G.F., Petrogenesis of Metamorphic Rocks, Fifth Edition. Berlin: Springer-Verlag, 1979.

Wyder, J.E., 1974, "A Geophysical Report on An Induced Polarization and Magnetometer Survey on the BBX claims, Great Slave Lake, N.W.T., For Great Plains Development Company of Canada, Ltd.", Great Plains Development Company of Canada, Ltd., inhouse report.

Appendix 1

Summary of Mining Exploration on the BBX Property

The following chronical summarizes mining exploration carried out on the BBX property to date. The review is based on inhouse reports of Great Plains Development Company of Canada, Ltd., and on assessment records available at the Department of Indian Affairs and Northern Development in Yellowknife, N.W.T. This appendix is intended only as a brief review of the extent of mining exploration on the property, and of the results which have been achieved. While it is of general interest as a complement to Map 3 which shows the location and orientation of drill holes, it does not provide detailed information on mineralized zones and grades of mineralization.

1948 (November) - BBX 1 & 2 staked by G. Wonnacott. These claims which are now retained as leases lie east of Aristifats Lake. BBX 2 contains the main surface showing. The adjoining property has since been staked under a variety of names, but remains today as shown in figure 3.

1949 - Diamond Drilling - three diamond drill holes totalling 228 feet were drilled on BBX 2(?). The exact location of these drill holes is not known, but it is presumed that they were collared in the vicinity of the main surface showing. Drill logs and assays are not available for these holes.

1950 (May/June)
- Diamond Drilling - three diamond drill holes totalling 242 feet were collared in the vicinity of the main surface showing. Although drill logs are available, they are very brief and of little use except as a general indication of the presence or absence of mineralization. Drill cores and assays are not available. These holes all intersected agglomerate, and significant amounts of galena and chalcopyrite were noted as follows:

Hole No.	Footage	Length	Description
1	27-59 ft.	32 ft.	"Vein zone-evenly disseminated galena and chalcopyrite - 25% mineralization".
2	48-78 ft.	30 ft.	"Vein zone-chalcopyrite and disseminated galena-30% mineralization.

- Trenching (2 Trenches) - These are assumed to be trenches 1 and 2 covering the main surface showing.

1952 - Diamond Drilling for J. McAvoy (?) - two diamond drill holes totalling 676 feet were drilled in the vicinity of the main surface showing. Both holes intersected mineralization within the agglomerate, but its concentration was not noted, and assays are not available. Chalcopyrite, galena, pyrite, manganese stain and erythrite were noted.

1956 - BBX Property optioned by Preston East Dome Mines Limited.

1957 - Diamond Drilling - between January and March, 1957, 2083 feet of diamond drilling, in 13 holes, was carried out by Preston East Dome Mines. Agglomerate was intersected in all but two of these holes (#9 & #11). At least some mineralization was intersected in all holes, both within the diatreme and in quartz-carbonate veins in the surrounding sediments". Significant mineralized horizons, referred to as "vein zones" on the logs, were intersected as follows:

Hole No.	Footage	Length
3	48 - 68 ft.	20 ft.
4	188 -194 ft.	6 ft.
5	70 - 86 ft.	16 ft.
6	75 - 80 ft.	5 ft.
7	46 - 49 ft.	3 ft.

The prominent mineral in these zones is chalcopyrite, but bornite, azurite, niccolite, millerite(?) and cobalt minerals were also described.[1]

The concentration of this mineralization was not noted however, and if assays were carried out, the results are not available.

1958 - Rio Tinto Canadian Exploration Limited briefly took over exploration of the property from Preston East Dome Mines. Drill core was re-examined and re-assayed, but the option was allowed to lapse.

1965 - Trenching - one rock trench, assumed to be TR-4 (map 2).

1970 - Geological report on the BBX claims for J. McAvoy(?) (Nickerson, 1970).

1971 - A geological examination of the property was carried out on behalf of the BBX Syndicate (Argy, and Siega). This examination was supplemented by a Time Domain Induced Polarization Survey for Milner Resources Limited of Edmonton, Alberta, by Eagle Geophysics Limited of Vancouver, B.C. (Lloyd, John). [2]The conclusions of this report are quoted below (Lloyd, p. 10).

(1) "The main mineralized zone carrying significant values in copper and silver is relatively small, as demonstrated by the weak IP response directly adjacent to the trenches and the lack of IP response in the interpreted direction of strike".

---

[1] Mineral identifications were based on hand specimen examination and hence may be in error. In particular, niccolite and bornite were not detected by ore microscopy or semiquantitative microprobe analysis in the present study.

[2] Presumably, Milner Resources was part of the BBX Syndicate

(2) "The vein-shears in the shale-sandstone sequence give strong IP responses. Insufficient data was collected over these occurrences to determine accurately their width, depth, strike direction and length. These zones however, carry only minor and sporadic values in copper."

1972 (April)

- Report on the BBX Claim Group, East Arm fold Belt Great Slave Lake, N.W.T. (Olson, R.A., 1972)
- Soil Geochemistry Survey - indicates a possible oval shaped anomaly (Nutter and Sawyer, 1975, p. 80).

1972 (August)

- Between August 9 and August 26, 1100 feet (7 holes) of diamond drilling was carried out on behalf of Colby Mines (Nutter and Sawyer, 1975, p. 67) and is described by Nickerson (1972). Agglomerate was intersected in all holes except No.'s 72-1 and 72-7. Diamond drill hole 72-4 intersected significant concentrations of copper in the agglomerate with an average grade of 1.63% between 75 and 85 feet. Minor cobalt, and traces of gold, lead, and zinc were also detected. Other diamond drill holes were relatively unmineralized.

1973 (May)

- BBX property geologically mapped by Great Plains Development Company of Canada, Ltd. (Nutter and Sawyer, 1975).

1974 (January)

- BBX property optioned by Great Plains Development Company of Canada, Ltd.

1974 (June)

- Geophysics - Induced polarization and magnetometer surveys were carried out on the property for Great Plains Development Company of Canada, Ltd. by Kenting Exploration Services Limited (Wyder, J.E.)

(i) Induced Polarization

A Huntec Mark III Induced Polarization System was used, with electrodes arranged in both gradient and pole-dipole arrays. Significant I.P. anomalies were found to be associated with the known copper mineralization in trenches 1 and 2. Similar I.P. anomalies outlined elsewhere within the diatreme were proposed as potential mineralized zones.

(ii) Magnetometer

A McPhar M700 fluxgate magnetometer was used to test whether magnetics could be used to outline the boundaries of the diatreme. The survey was unsuccessful and did not reflect any particular geologic model.

1975 (February-April)

- Diamond Drilling - A seven hole 2859 foot diamond drilling program was carried out by Great Plains Development. Five of these holes were drilled to test I.P. anomalies defined during the 1974 survey. Two additional holes (75-6, 75-7) were drilled to test the possible extensions of copper mineralization intersected in DDH 75-5. Of the seven holes, significant copper values were encountered only in DDH 75-5, which contained 7 relatively discrete mineralized zones. Copper concentrations ranged from 0.84% over 14 feet to 2.0% over 26 feet.

1976 (September)

- Diamond Drilling - One vertical hole was drilled to a depth of 800' in order to test the possible extensions of mineralized zones intersected in DDH 75-5. The hole intersected five discrete mineralized zones within the diatreme with copper values ranging from 1.23% over 9 feet to 2.24% over 38 feet (table 3, this thesis).

Appendix 2

Density Calculation for Mineralizing Fluid Based on Fluid Inclusion Data

Fluid density is given by

$$\rho_T = \rho_W + \rho_V$$

at STP

ρ_T = total density

ρ_W = density of aqueous phase
= density of water (1 g/cc) + density of NaCl (21.5 g/cc) weighted according to weight %. It is assumed that the solution is saturated with respect to NaCl (23.3 wt % NaCl)

ρ_V = density of vapour phase (water vapour) = 0.0008 g/cc = 0.00 g/cc.

Now: Vapour phase occupies 9.2% of the area of the incluision (p.206 this thesis). This is converted to volume % by assuming that the inclusions are spherical. The vapour phase therefore occupies 2.8 volume % of the inclusion. The aqueous phase occupies (100 - 2.8) = 97.2% of the inclusion by volume.

$$\rho_T = [2.78(0) + .233\ (97.2)(2.16) + .767\ (97.2)(1)]\ \text{g/cc}/100$$

$$= [0 + 48.92 + 74.57]/100\ \text{g/cc}$$

$$\underline{\rho_T = 1.23\ \text{g/cc}}$$

Conditions

The calculation of fluid density is approximate for the following reasons:

(1) The area of the inclusion occupied by the vapour phase is an approximate value based on sketches of the inclusions made to scale on graph paper. This approximation is compounded by assuming that the inclusions are spherical when calculating volume % of the inclusion occupied by the vapour phase. This assumption is necessary however, as the configuration and depth of inclusions in the third dimension cannot be readily determined.

(2) For the purpose of this calculation, the inclusions were assumed to be saturated with NaCl. This is clearly an over simpliciation as concentrations of kCl and $CaSO_4$(?) have also been inferred for these inclusions.

(3) The presence of small quantities of gases such as CO_2 and CH_4 in the inclusions has not been taken into consideration in this calculation, as their exact composition and concentration is unknown. The presence of these gases would decrease the density of the inclusions slightly however.

1 OF

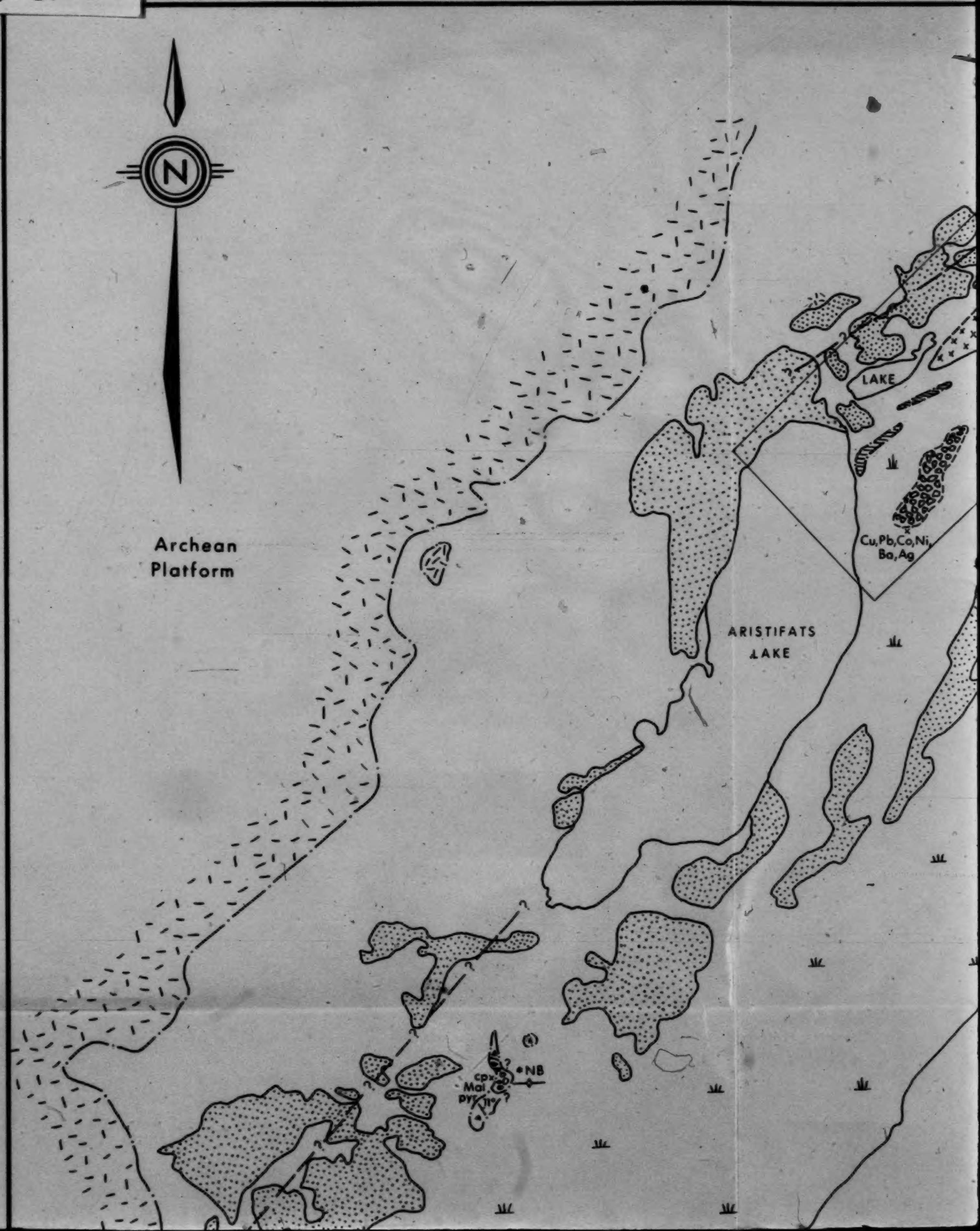
N
Archean
Platform
LAKE
Cu,Pb,Co,Ni,
Ba,Ag
ARISTIFATS
LAKE
?
NB
cpx
Mal
py

2 OF

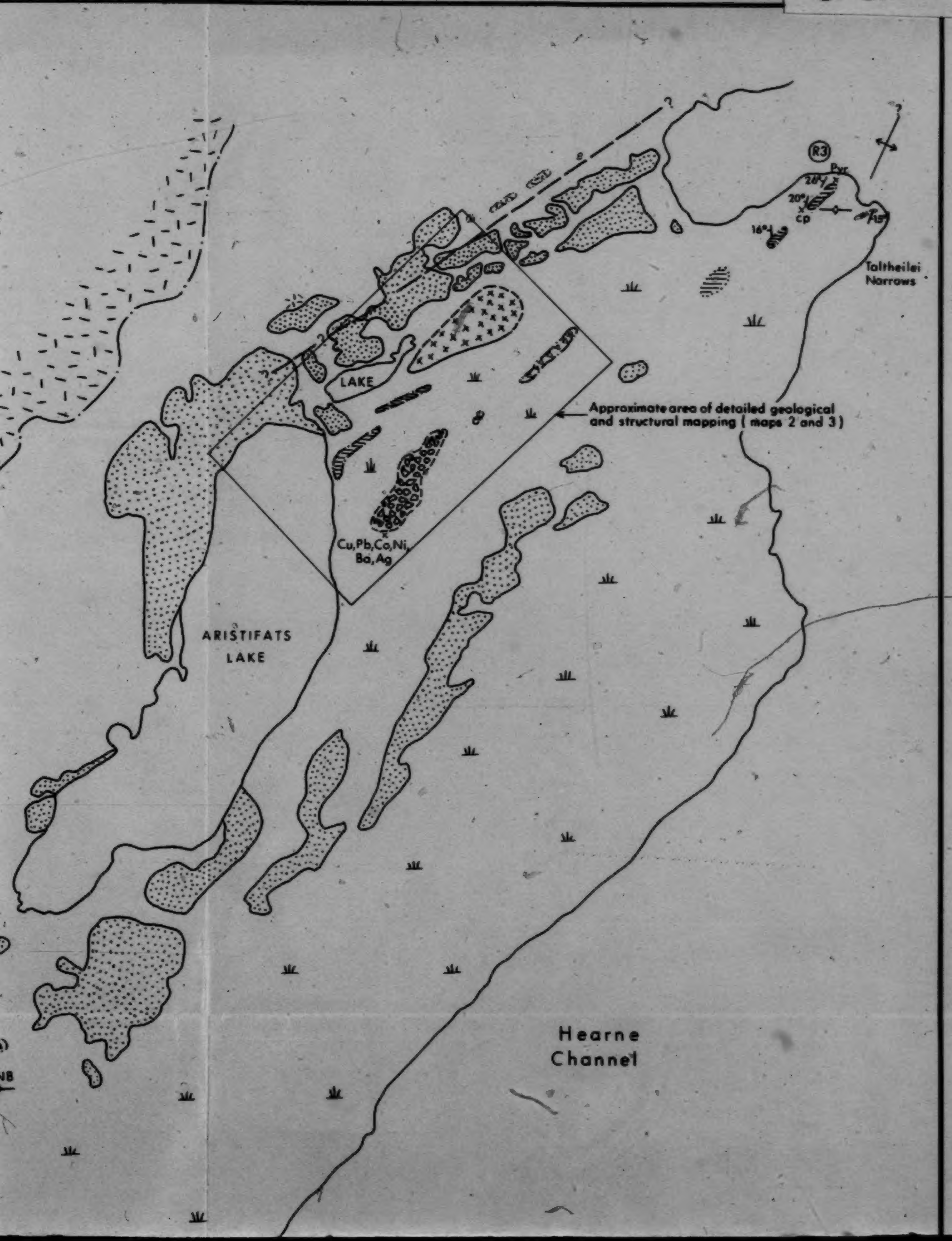
R3
Pyr
28°
20°
cp
16°
15°
Taltheilei Narrows
LAKE
Cu,Pb,Co,Ni,
Ba,Ag
ARISTIFATS LAKE
Hearne Channel
NB

Approximate area of detailed geological and structural mapping (maps 2 and 3)

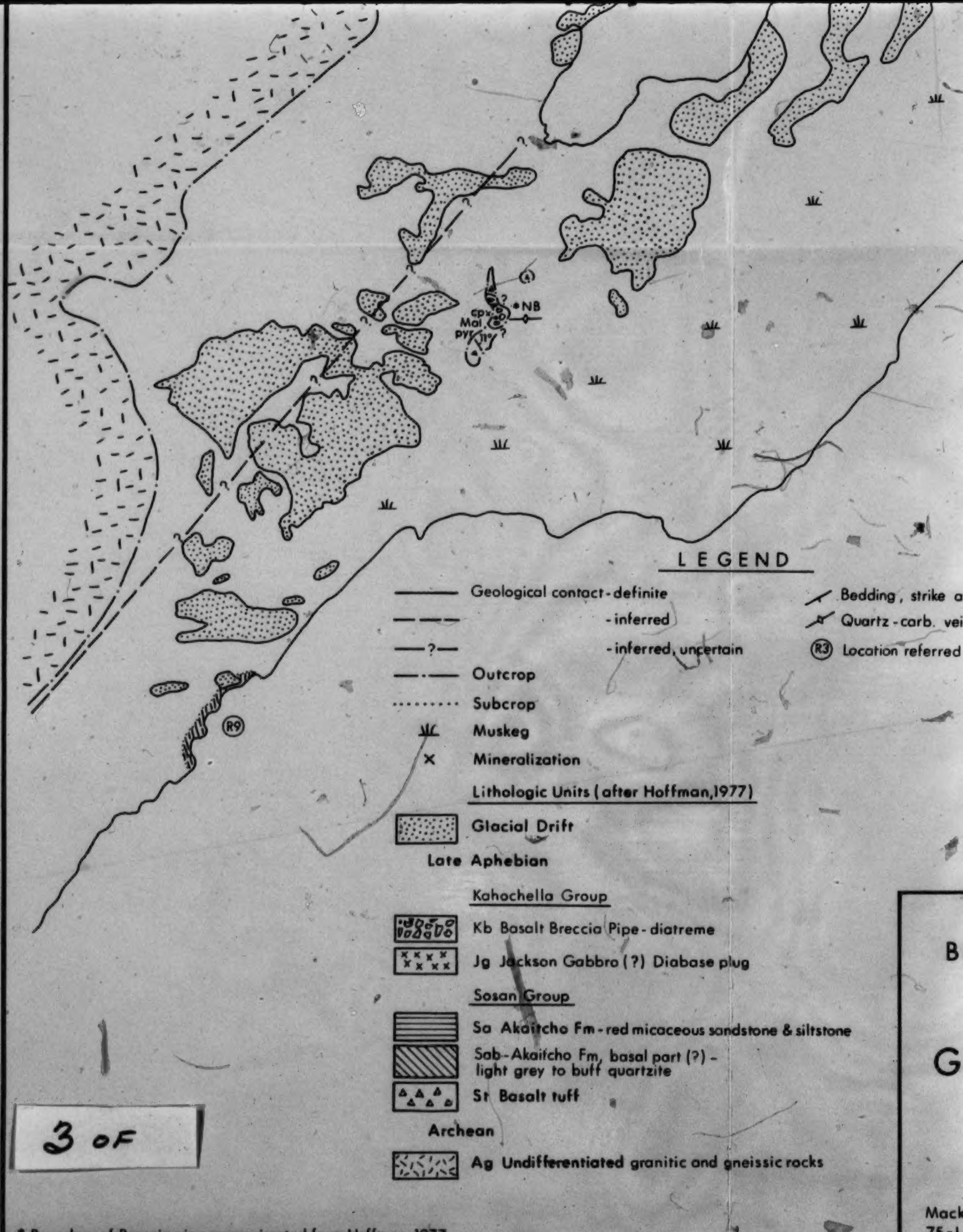
?
?
?
?
?
(4)
?
cpx
NB
Mal
pyr
?
R9
LEGEND
Geological contact - definite
- inferred
—?—
- inferred, uncertain
Outcrop
Subcrop
Muskeg
Mineralization
Lithologic Units (after Hoffman, 1977)
Glacial Drift
Late Aphebian
Kahochella Group
Kb Basalt Breccia Pipe - diatreme
Jg Jackson Gabbro (?) Diabase plug
Sosan Group
Sa Akaitcho Fm - red micaceous sandstone & siltstone
Sab - Akaitcho Fm, basal part (?) - light grey to buff quartzite
St Basalt tuff
Archean
Ag Undifferentiated granitic and gneissic rocks
Bedding, strike a
Quartz - carb. vei
R3 Location referred
B
G
Mack
75-L

3 OF

* Boundary of Breccia pipe approximated from Hoffman, 1977

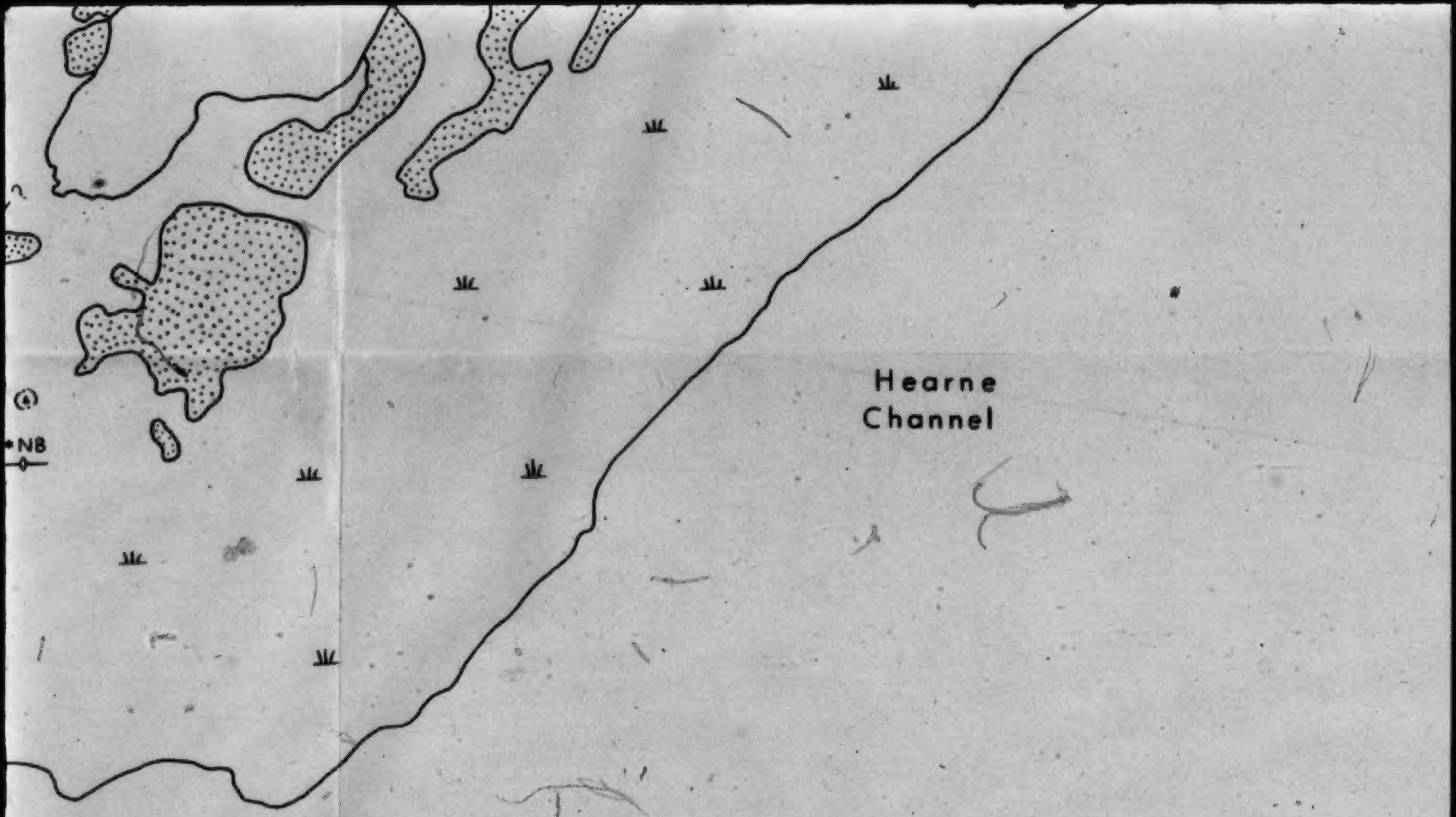

LEGEND

gical contact - definite
- inferred
- inferred, uncertain
rop
rop
eg
alization

Bedding, strike and dip
Quartz - carb. vein, vertical
(R3) Location referred to in thesis

logic Units (after Hoffman, 1977)

al Drift

bian

chella Group

salt Breccia Pipe - diatreme

ckson Gabbro (?) Diabase plug

Group

kaitcho Fm - red micaceous sandstone & siltstone

Akaitcho Fm, basal part (?) - grey to buff quartzite

salt tuff

ndifferentiated granitic and gneissic rocks

MAP 1

BBX PROPERTY AND ADJACENT AREAS
NORTHWEST TERRITORIES
GEOLOGICAL COMPILATION

0 1
KILOMETRES

Mackenzie M. D.
75-L-12

June, 1980

4 of 4

1 OF

2 OF

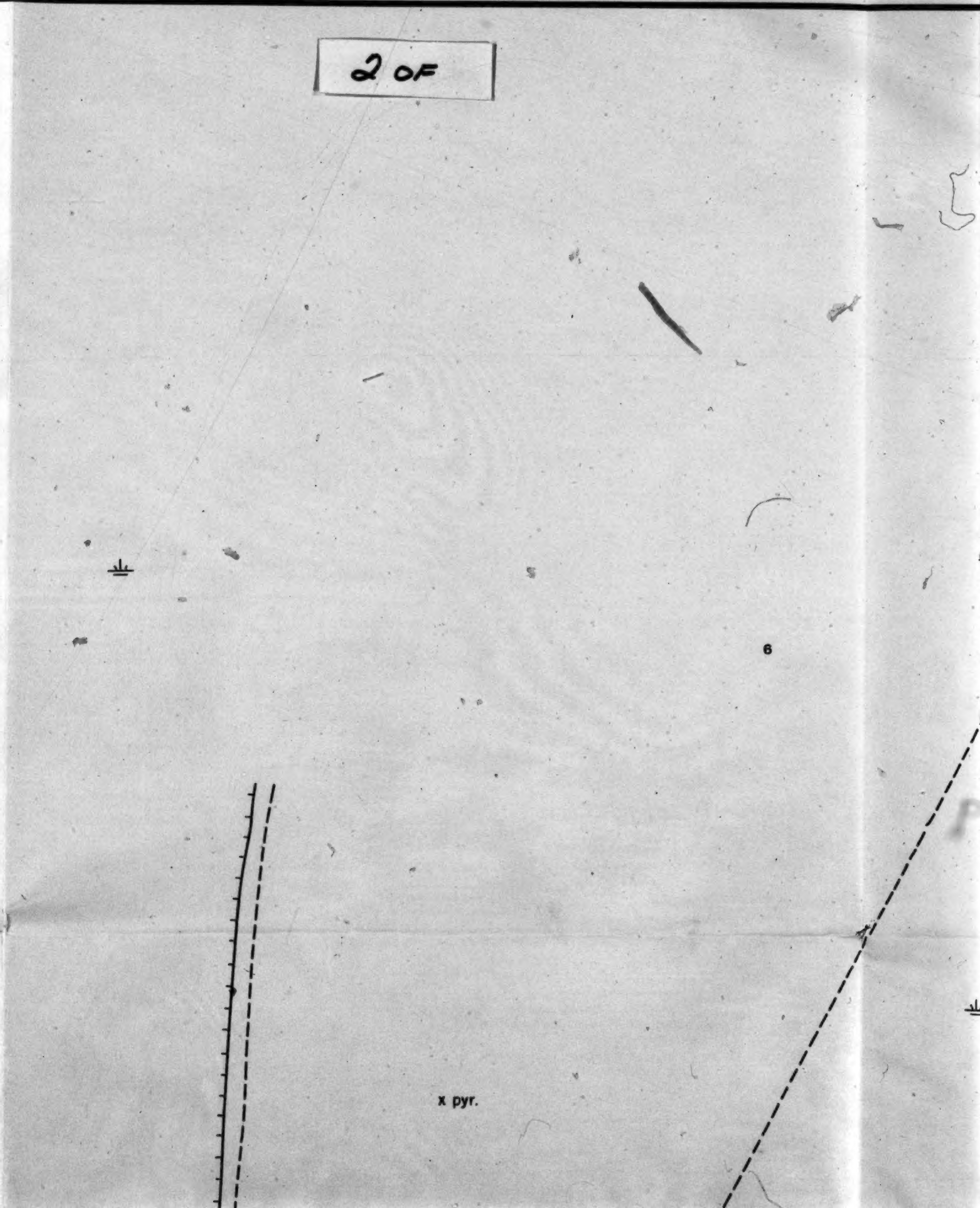

3 OF

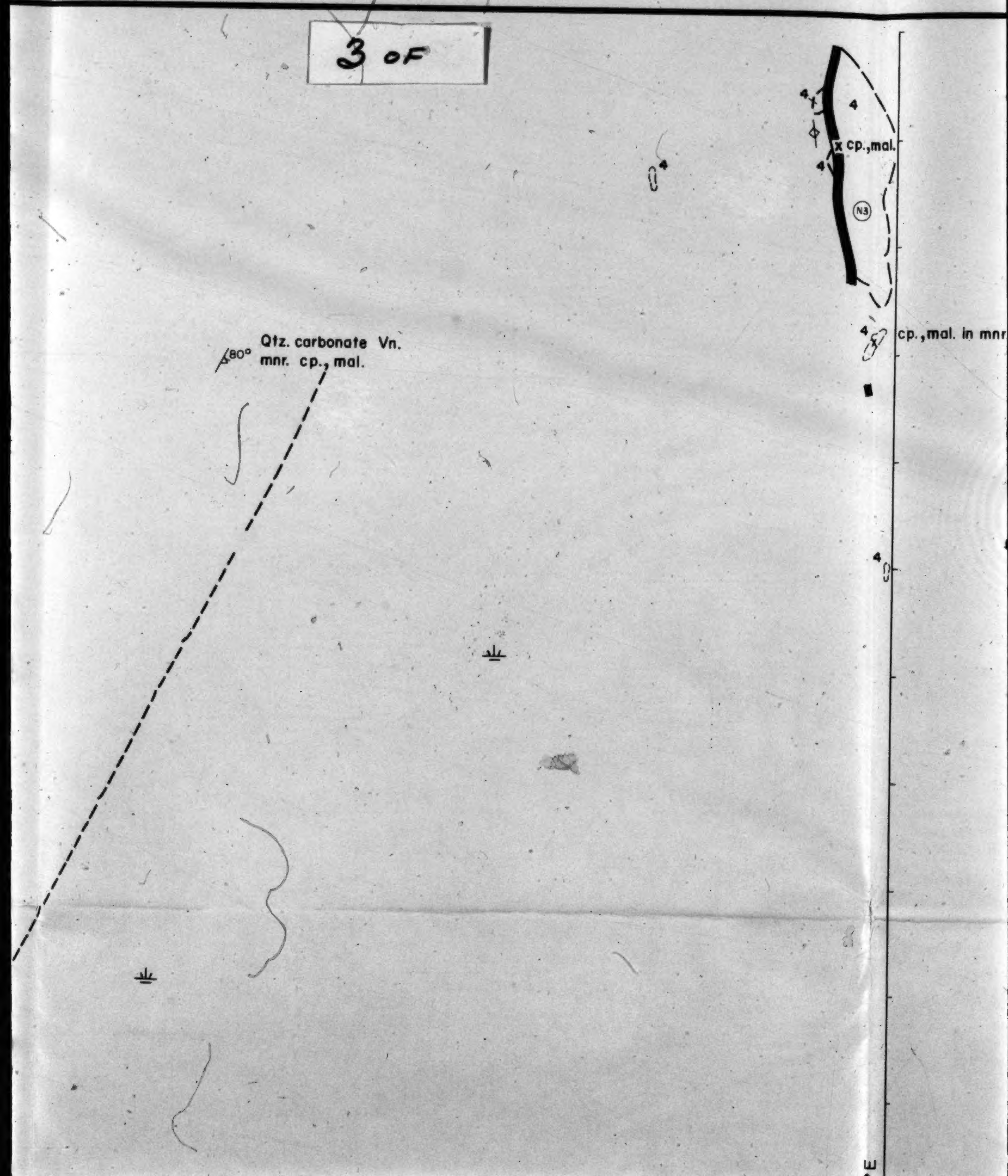
4
4
x cp., mal.
4
4
N3
Qtz. carbonate Vn.
80°
mnr. cp., mal.
4
cp., mal. in mnr
4
E

4 OF

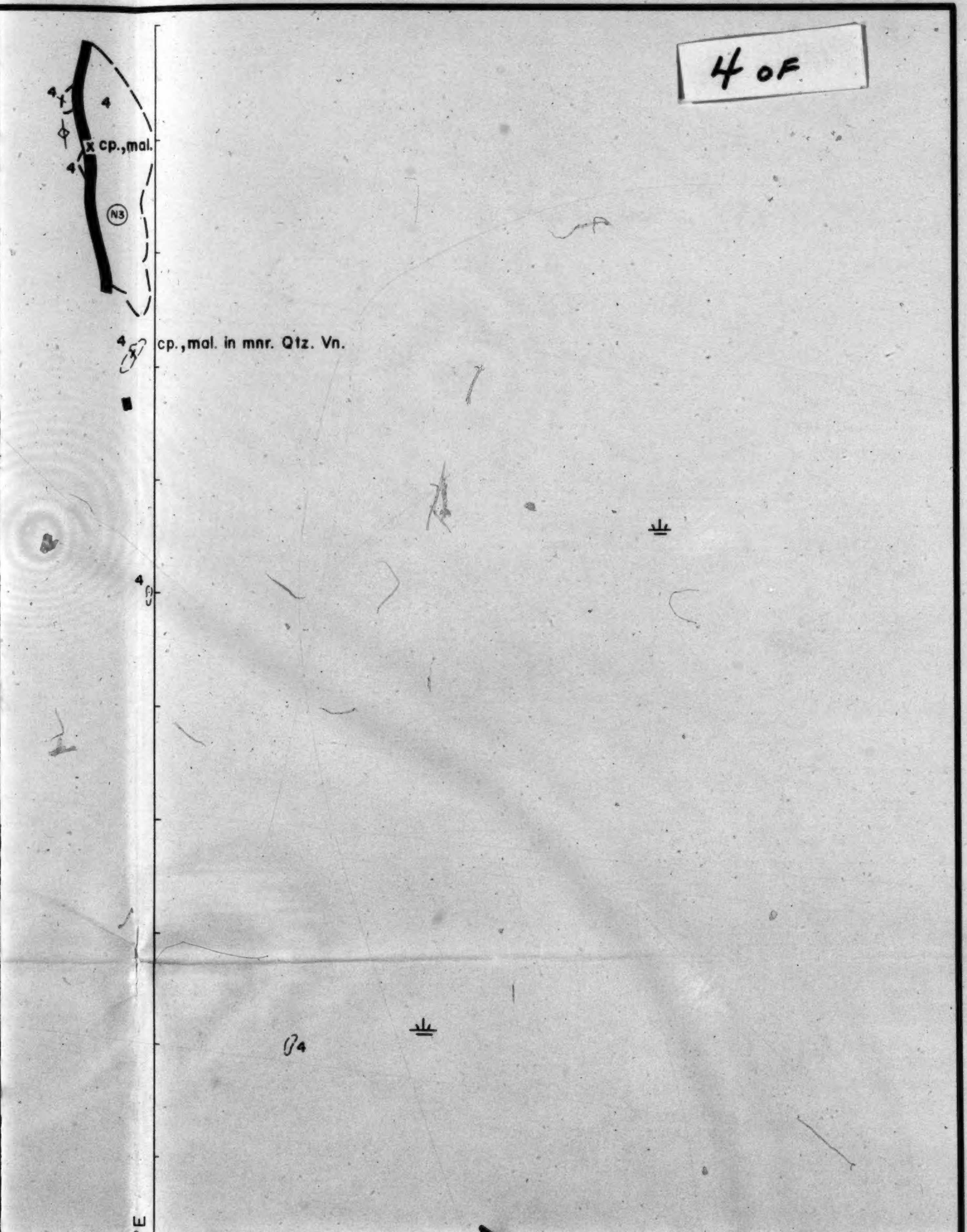
4
4
x cp., mal.
4
N3
4
cp., mal. in mnr. Qtz. Vn.
4
4
E

5 OF

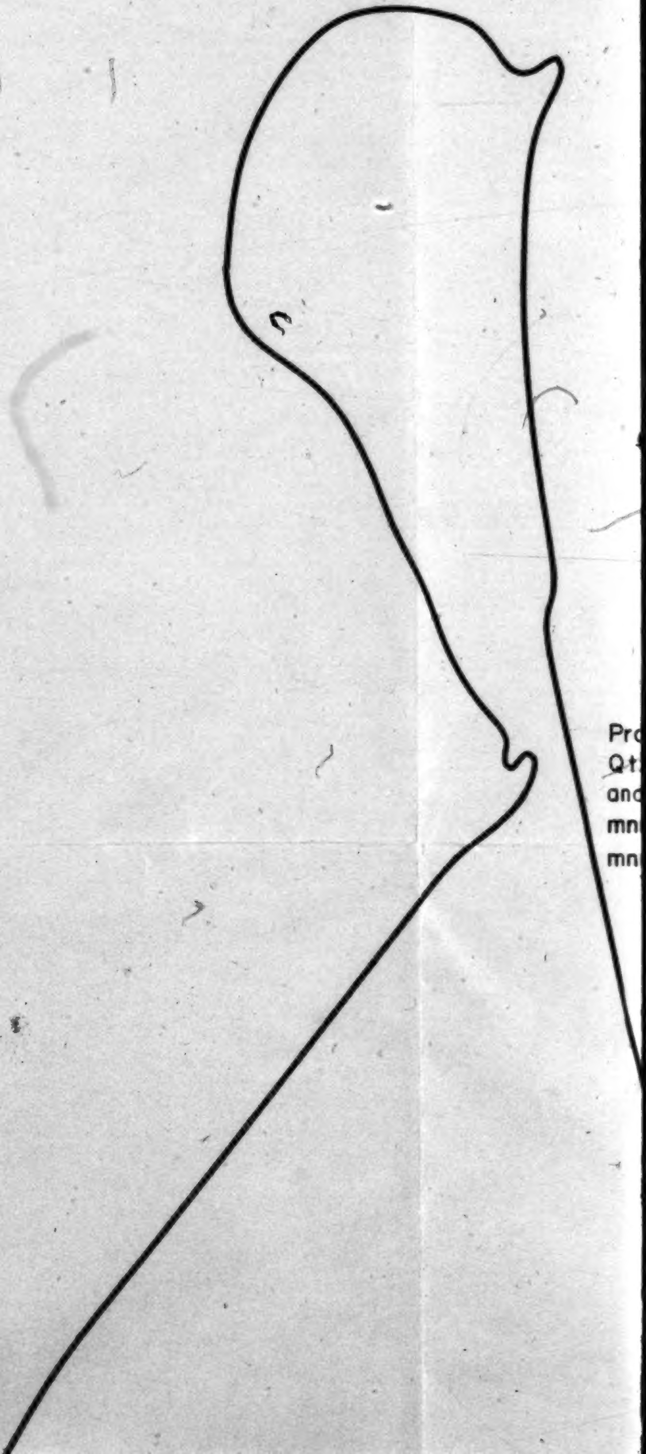
Pro
Qt
and
mn
mn

6 OF

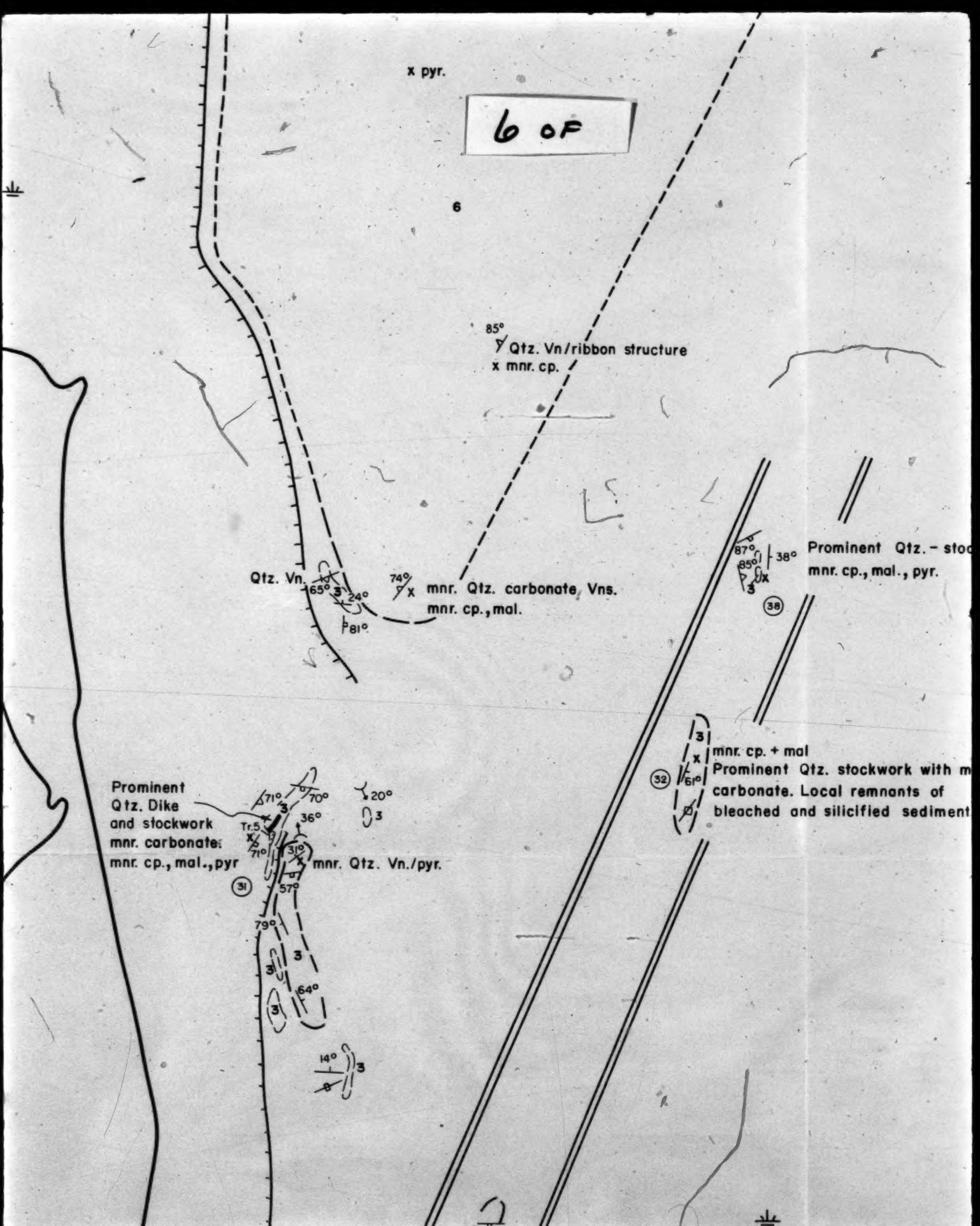
x pyr.
6
85°
Qtz. Vn/ribbon structure
x mnr. cp.
Qtz. Vn.
65°
3
24°
81°
74°
x mnr. Qtz. carbonate Vns.
mnr. cp., mal.
87°
85°
38°
3
x
Prominent Qtz. - sto
mnr. cp., mal., pyr.
38
3
x
mnr. cp. + mal
32
61°
Prominent Qtz. stockwork with m
carbonate. Local remnants of
bleached and silicified sediment
Prominent
Qtz. Dike
and stockwork
mnr. carbonate.
mnr. cp., mal., pyr
71°
70°
20°
3
3
36°
Tr. 5
x
71°
31°
x
mnr. Qtz. Vn./pyr.
31
57°
79°
3
3
64°
3
14°
3

7 OF

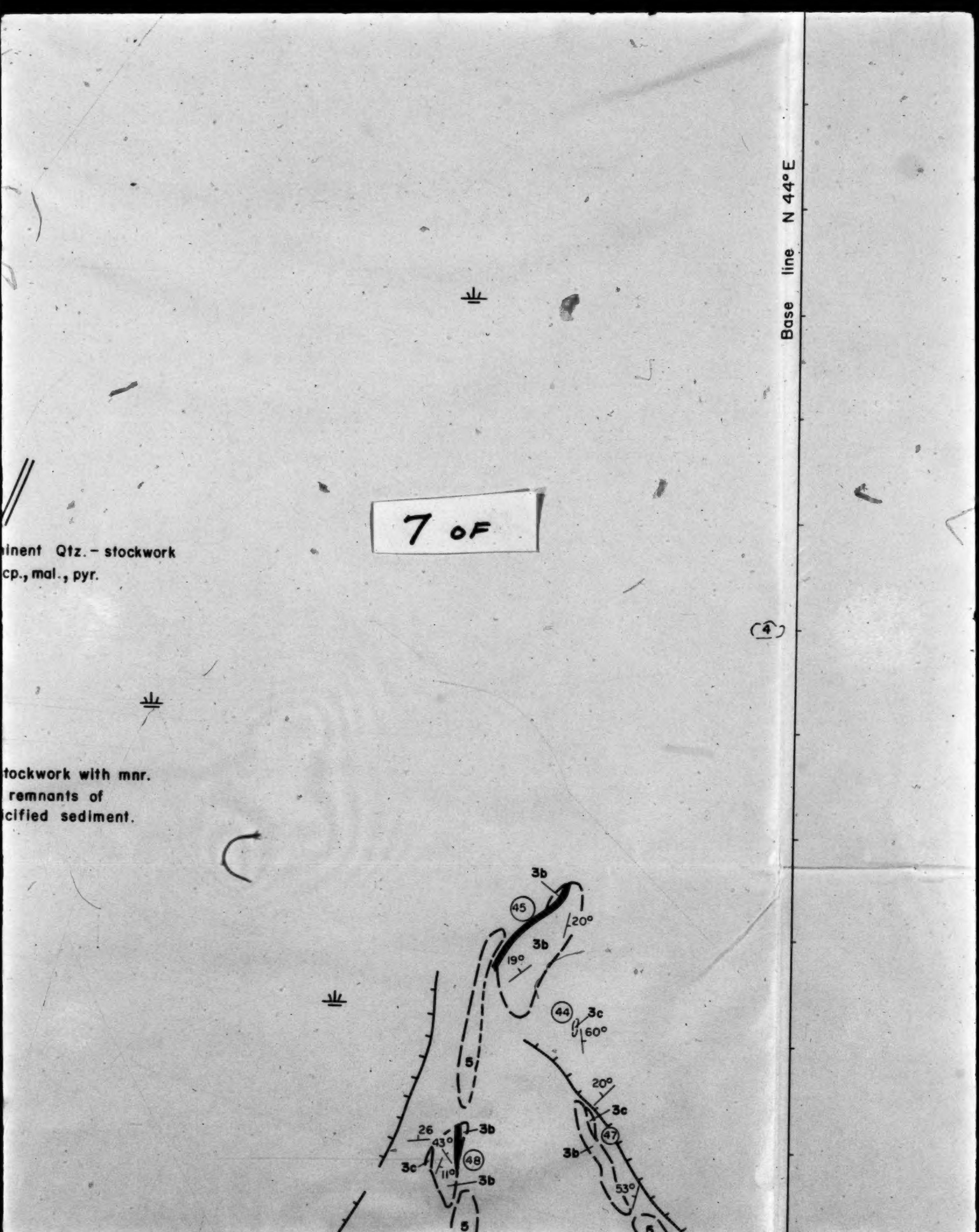

Base line N 44°E
inent Qtz. - stockwork
cp., mal., pyr.
tockwork with mnr.
remnants of
icified sediment.
4
3b
45
20°
3b
19°
44
3c
60°
5
20°
3c
47
3b
53°
5
26
43°
3b
48
3c
11°
3b
5

8 OF

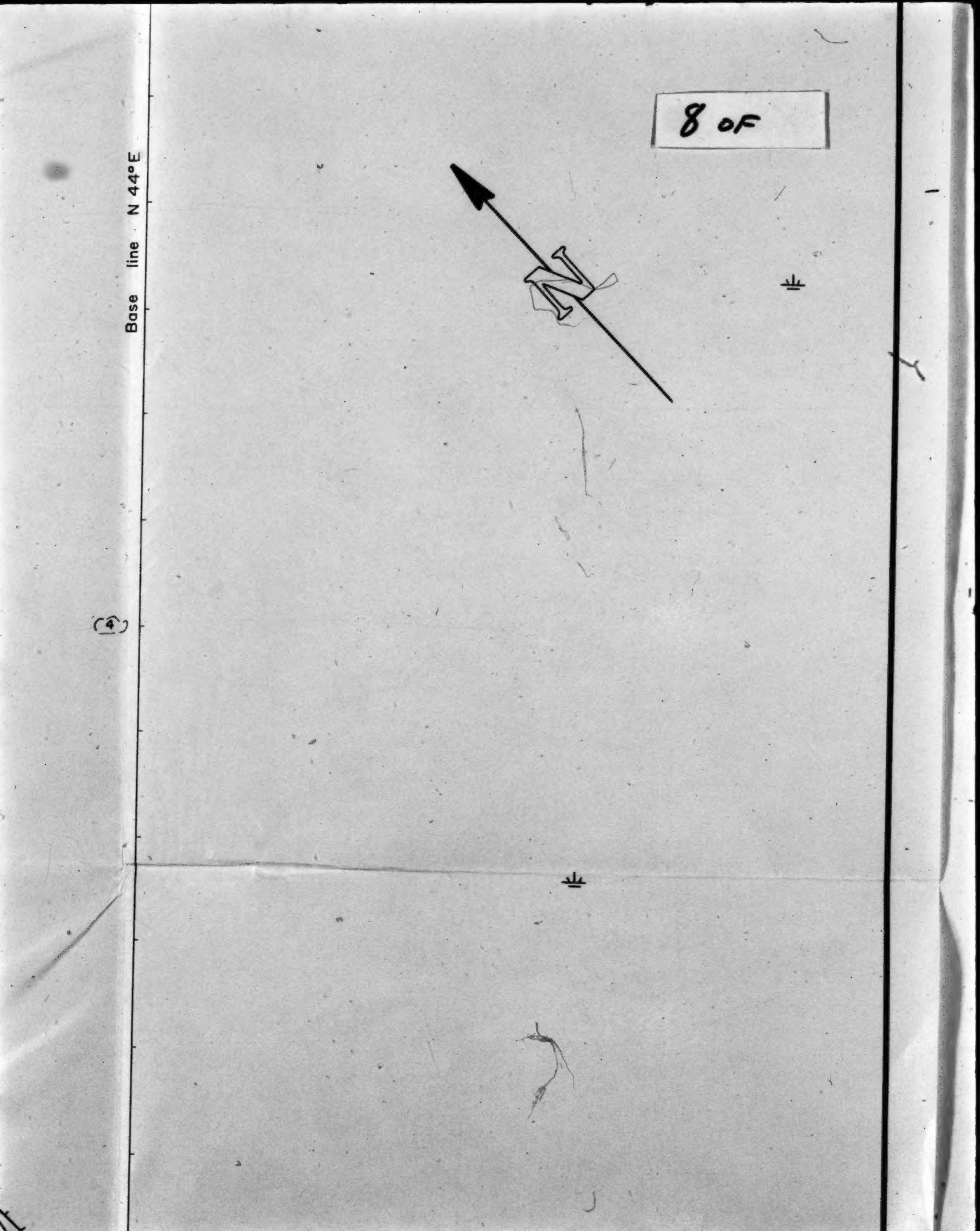
N
Base line N 44°E
4

9 OF

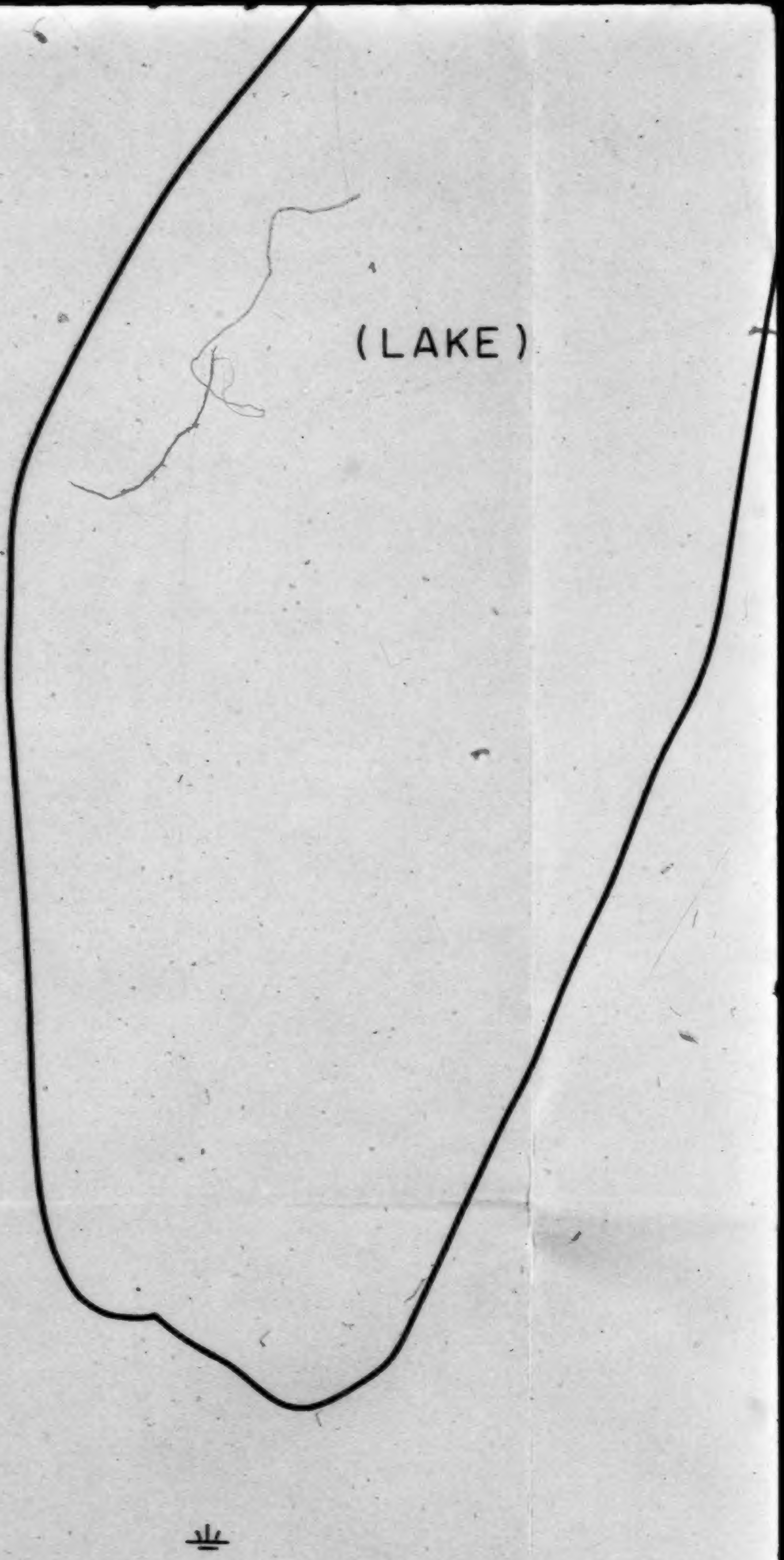

10 OF

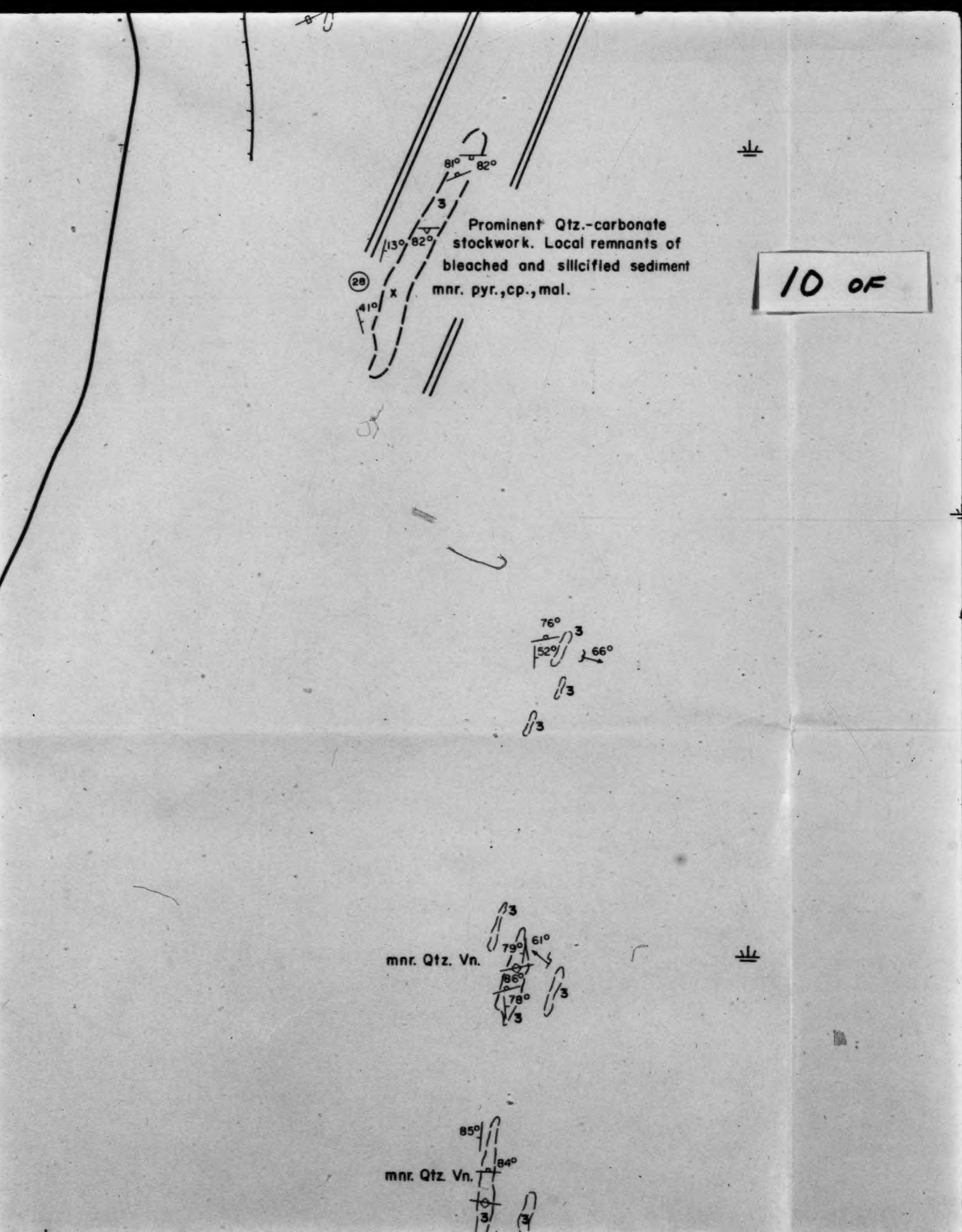
81°
82°
3
Prominent Qtz.-carbonate stockwork. Local remnants of bleached and silicified sediment mnr. pyr., cp., mal.
13°
82°
28
x
41°
76°
3
52°
66°
3
3
3
61°
79°
mnr. Qtz. Vn.
86°
78°
3
3
85°
84°
mnr. Qtz. Vn.
3
3

11 OF

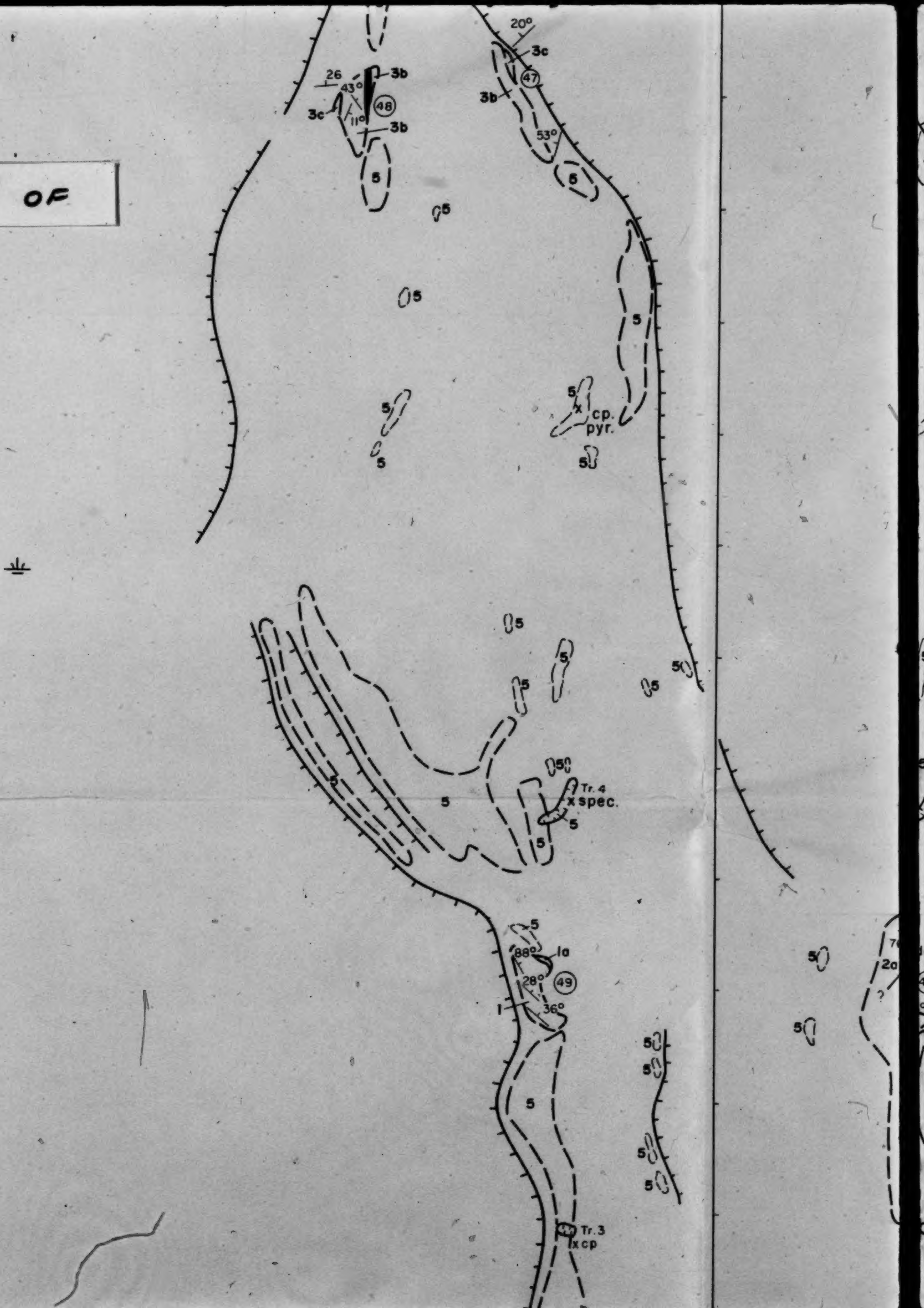

20°
3c
47
3b
53°
26
43°
3b
48
3c
11°
3b
5
cp.
pyr.
Tr. 4
x spec.
5
1a
88°
28°
49
1
36°
Tr. 3
x cp
2a
?

12 OF

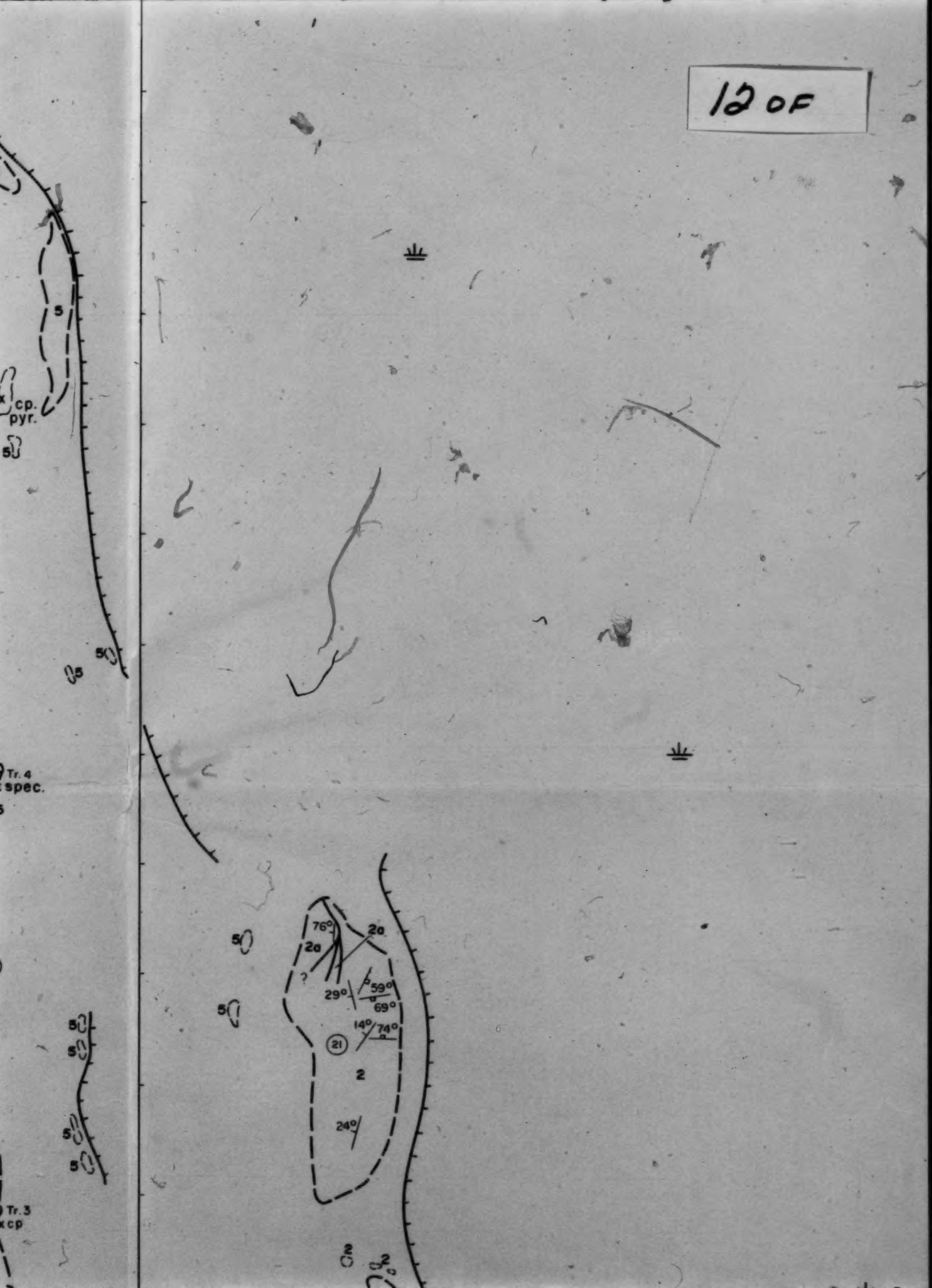

5
x
cp.
pyr.
5
5
5
Tr. 4
spec.
5
5
5
5
5
5
5
5
Tr. 3
xcp
76°
2a
2a
?
29°
59°
69°
14°
74°
㉑
2
24°
2
2

13 OF

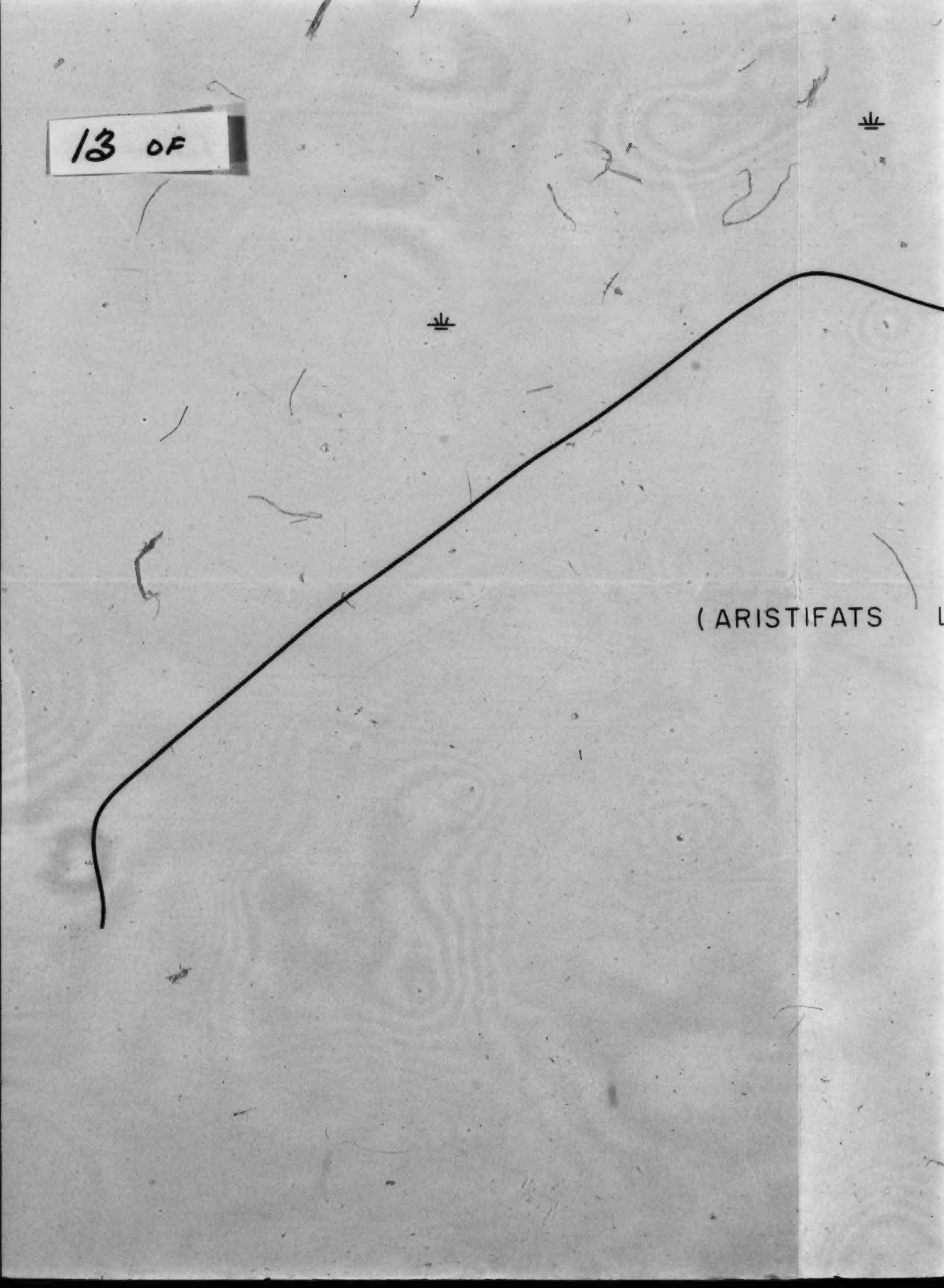
(ARISTIFATS L

14 OF

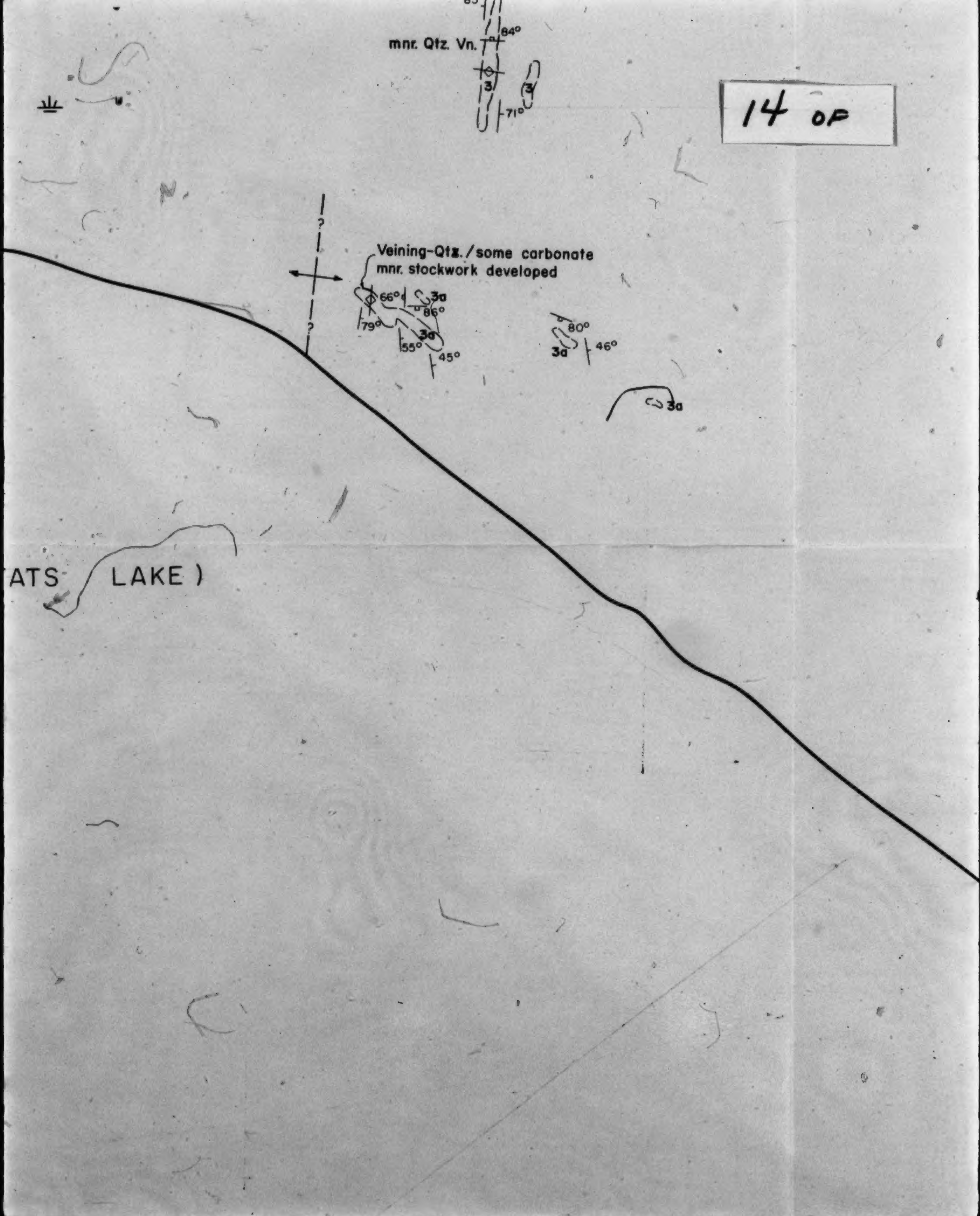
mnr. Qtz. Vn.
84°
3
3
71°
?
?
Veining-Qtz./some carbonate
mnr. stockwork developed
66°
3a
86°
79°
3a
55°
45°
80°
3a
46°
3a
ATS LAKE)

15 OF

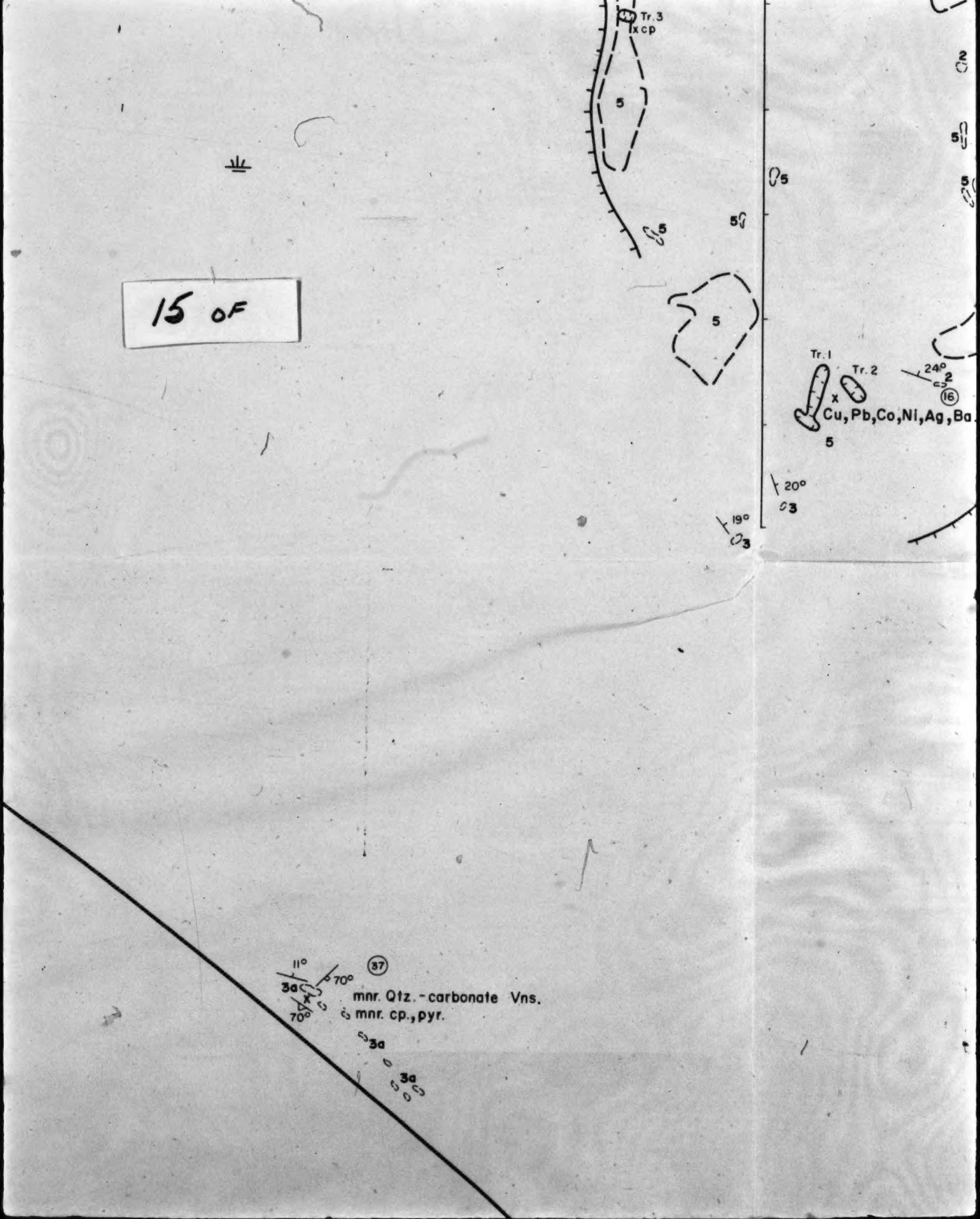
Tr. 3
x cp
5
5
5
5
5
5
2
5
5
Tr. 1
Tr. 2
24°
2
⑯
x
Cu, Pb, Co, Ni, Ag, Ba.
5
20°
3
19°
3
㊲
11°
70°
3a
x
70°
mnr. Qtz.-carbonate Vns.
mnr. cp., pyr.
3a
3a

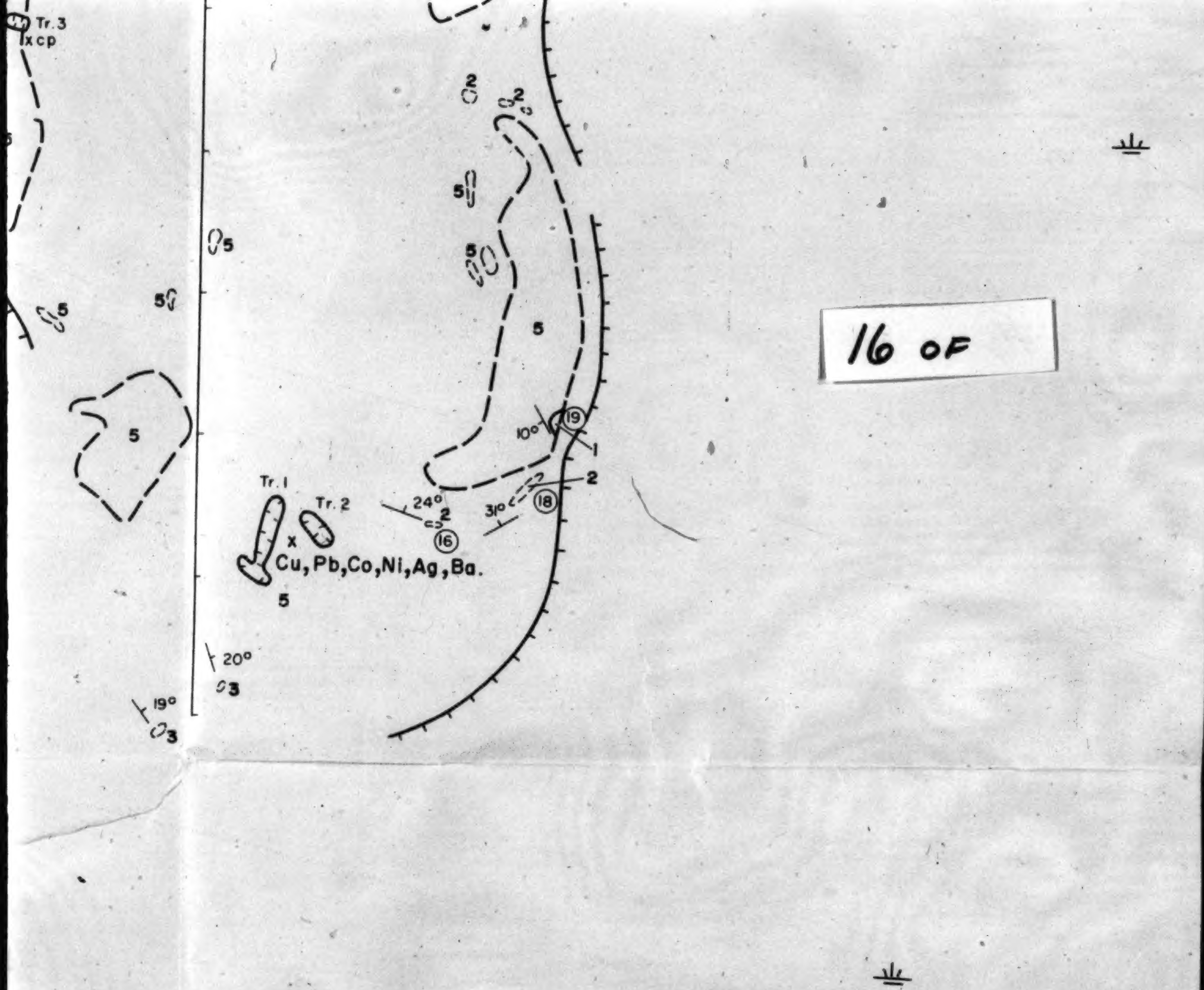
Tr. 3
x cp
5
5
5
5
2
2
5
5
5
5
10°
19
1
2
18
24°
2
31°
16
Tr. 1
Tr. 2
x
Cu, Pb, Co, Ni, Ag, Ba.
5
20°
3
19°
3

16 OF

LITHOLOGIC UNITS

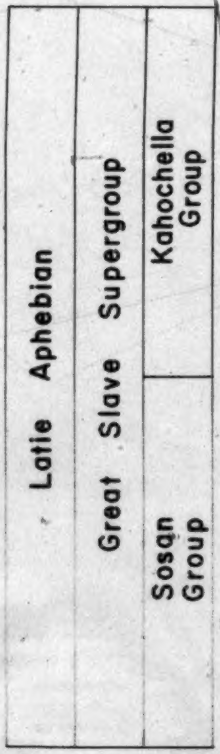

1 (Km) Mc Leod Fm (?) - Shale, red, in part silty, in part with massive irregular bedding and shale concretions, in part thinly bedded and fissile, with ripple marks and desiccation cracks.

(a) Grey shale

2 (Ko) Ogilvie Fm (?) - Shale, medium grey, thinly bedded and very fissile, grading into micaceous siltstone and shale

(a) Shale, red, massive.

3 (Sa) Akaitcho Fm - Siltstone, red, hematitic, slightly to moderately micaceous, thinly bedded, grading into shale and very fine grained sandstone.

(a) Sandstone, red, very fine grained, quartzose. Comprises hematite-rich bands with quartz and glauconite in hematite cement, and hematite-poor bands.

(b) Shale, red, in part silty, slightly hematitic.

(c) Shale, medium grey, with ripple marks and desiccation cracks.

* 4 (St) Basalt tuff - Green, vitric-lithic airfall and lapilli tuff.

Intrusive Rocks

* 5 (Kb) Basalt breccia pipe (diatreme) - unbedded, irregularly intrusive, locally contains exotic clasts, poorly sorted.

6 (Jg) Jackson gabbro (?) - Olivine diabase.

Hydrothermal Veins

■ Large quartz veins up to 1 meter wide, bearing minor chalcopyrite and pyrite.

17 OF

1. Formation names after Hoffman 1977, "Table of Forma

2. Outcrops of red concretionary shale and grey fissile shale the diatreme are tentatively assigned to these formatio (see text, chapter 3, pt 1.)
These rocks are interpreted as blocks of sediment fro section which subsided in the diatreme during its format

* Rock descriptions from Hoffman 1977, "Table of Form

sive
n part
ks

y fissile,

tely
hale and

zose.
artz

ic.
nd

ff.

,
rted.

yrite

"Table of Formations."

grey fissile shale bordering
o these formations

of sediment from up
during its formation.

"Table of Formations."

18 OF

LEGEND

⊂⊃	Outcrop Boundary.
═	Geological trend.
----	Inferred Geological Contact.
/ 20°	Bedding, Strike and Dip.
/ 40°	Joints, Strike and Dip (Ve
/ 80°	Veins, Strike and Dip (ø
60°	Axial Trends of small Folds
Z 40°	shape of Fold in profile.
x x	Anticline, Existence uncerta
⬭	Trench, to scale.
x Cu	Mineralization.
⏚	Muskeg
/	Prominent Break in Slope.
3a	Lithologic Unit
⑰	Locations referred to in thesis
▯	Dock

LEGEND

Boundary.
l trend.
Geological Contact.

Strike and Dip.
rike and Dip (⅋ Vertical.)

rike and Dip (ø Vertical.)
nds of small Folds - patterns show
Fold in profile.
, Existence uncertain.

o scale.
tion.

Break in Slope.
Unit.
eferred to in thesis

19 OF

G

3

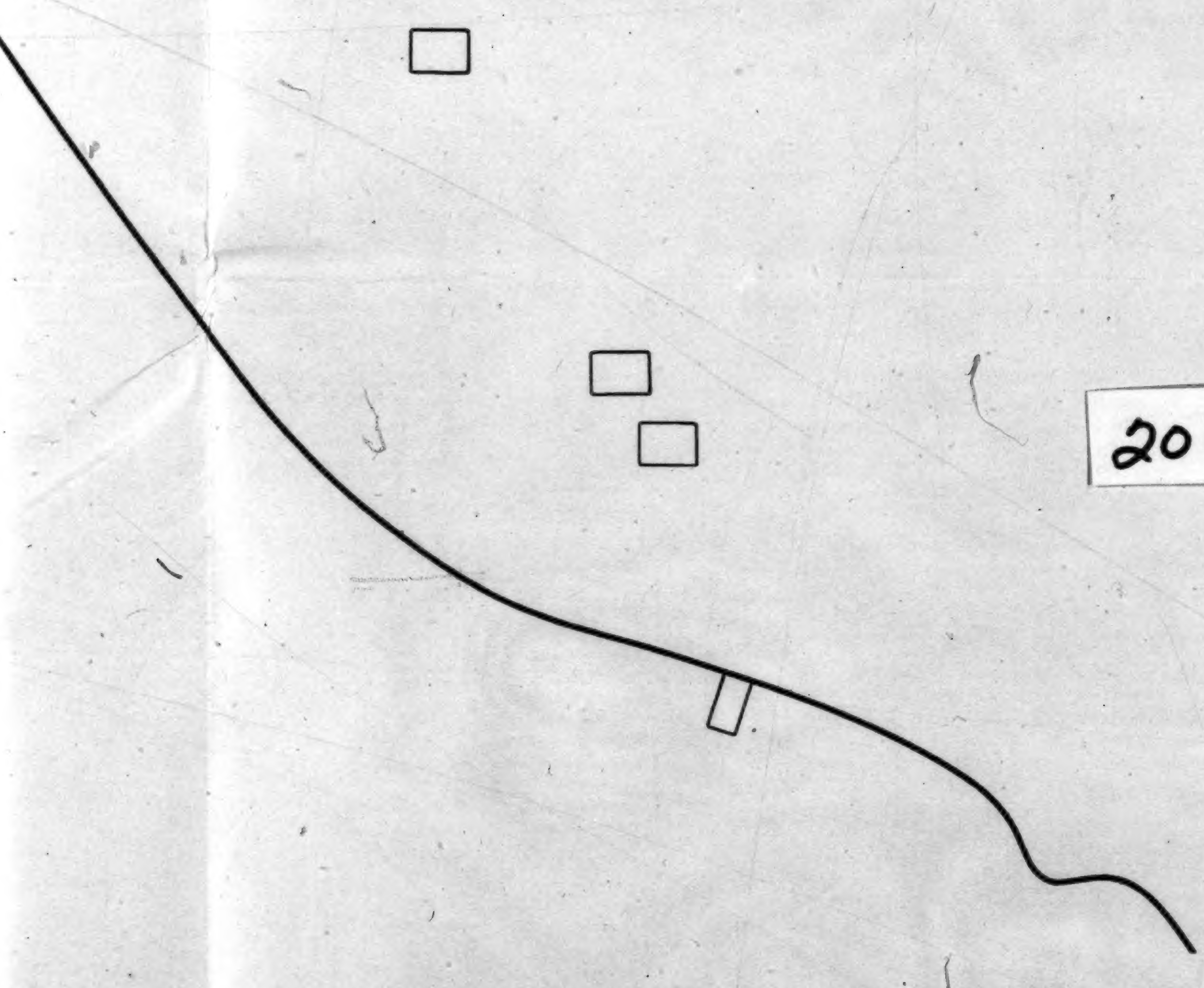

20 OF

MAP 2

BBX CLAIMS

NORTHWEST TERRITORIES

GEOLOGY AND STRUCTURE

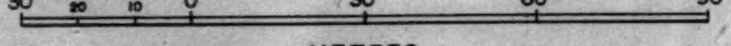
30
20
10
0
30
60
90

METRES

LITHOLOGIC UNITS

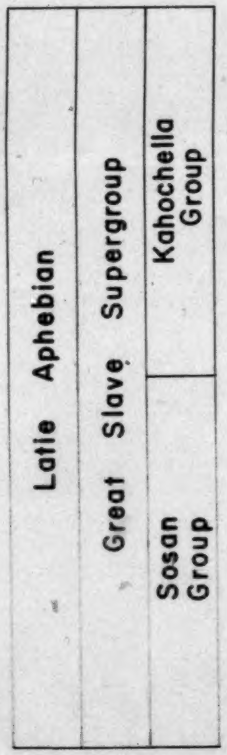

1 (Km) Mc Leod Fm (?) - Shale, red, in part silty, in part with massive irregular bedding and shale concretions, in part thinly bedded and fissile, with ripple marks and desiccation cracks.
(a) Grey shale

2 (Ko) Ogilvie Fm (?) - Shale, medium grey, thinly bedded and very fissile, grading into micaceous siltstone and shale
(a) Shale, red, massive.

3 (Sa) Akaitcho Fm - Siltstone, red, hematitic, slightly to moderately micaceous, thinly bedded, grading into shale and very fine grained sandstone.
(a) Sandstone, red, very fine grained, quartzose. Comprises hematite-rich bands with quartz and glauconite in hematite cement, and hematite-poor bands.
(b) Shale, red, in part silty, slightly hematitic.
(c) Shale, medium grey, with ripple marks and desiccation cracks.

* 4 (St) Basalt tuff - Green, vitric-lithic airfall and lapilli tuff.

Intrusive Rocks

* 5 (Kb) Basalt breccia pipe (diatreme) - unbedded, irregularly intrusive, locally contains exotic clasts, poorly sorted.

6 (Jg) Jackson gabbro (?) - Olivine diabase.

Hydrothermal Veins

■ Large quartz veins up to 1 meter wide, bearing minor chalcopyrite and pyrite.

1. Formation names after Hoffman 1977, "Table of For
2. Outcrops of red concretionary shale and grey fissile sh the diatreme are tentatively assigned to these format (see text, chapter 3, pt 1.) These rocks are interpreted as blocks of sediment f section which subsided in the diatreme during its form

* Rock descriptions from Hoffman 1977, "Table of For Other descriptions refer to actual outcrops in study a

21 OF

nassive
s, in part
narks

very fissile,
ale

lerately
o shale and

artzose.
quartz
nd

atitic.
ks and

tuff.

sive,
sorted.

copyrite

77, "Table of Formations."

and grey fissile shale bordering
d to these formations

cks of sediment from up
ne during its formation.

77, "Table of Formations".
utcrops in study area

22 OF

LEGEN

◌	Outcrop Boundary.
═	Geological trend.
----	Inferred Geological Co
20°	Bedding, Strike and Di
40°	Joints, Strike and Dip (
80°	Veins, Strike and Dip
60°	Axial Trends of small
Z 40°	shape of Fold in pro
✕	Anticline, Existence un
◌	Trench, to scale.
x Cu	Mineralization.
⏚	Muskeg
∕	Prominent Break in Sl
3a	Lithologic Unit
⑰	Locations referred to in th
▯	Dock
▭	Cabins

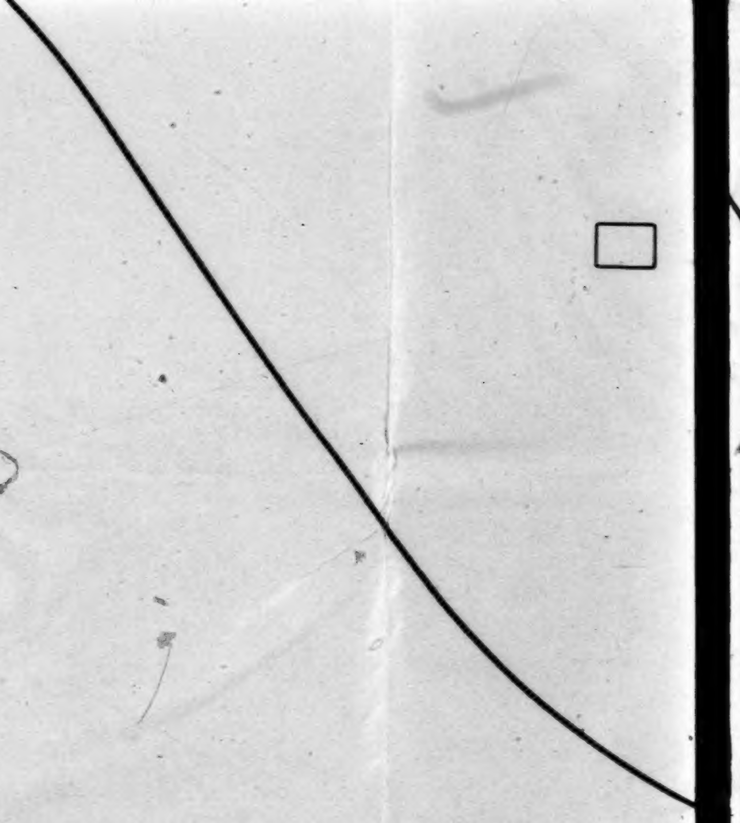

LEGEND

Boundary.
trend.
Geological Contact.

Strike and Dip.
ike and Dip (✕ Vertical.)

ike and Dip (0 Vertical.)
ds of small Folds - patterns show
Fold in profile.
Existence uncertain.

scale.
ion.

Break in Slope.
Unit
eferred to in thesis

23 OF

G

MACKENZI
N.T.S. 75 -

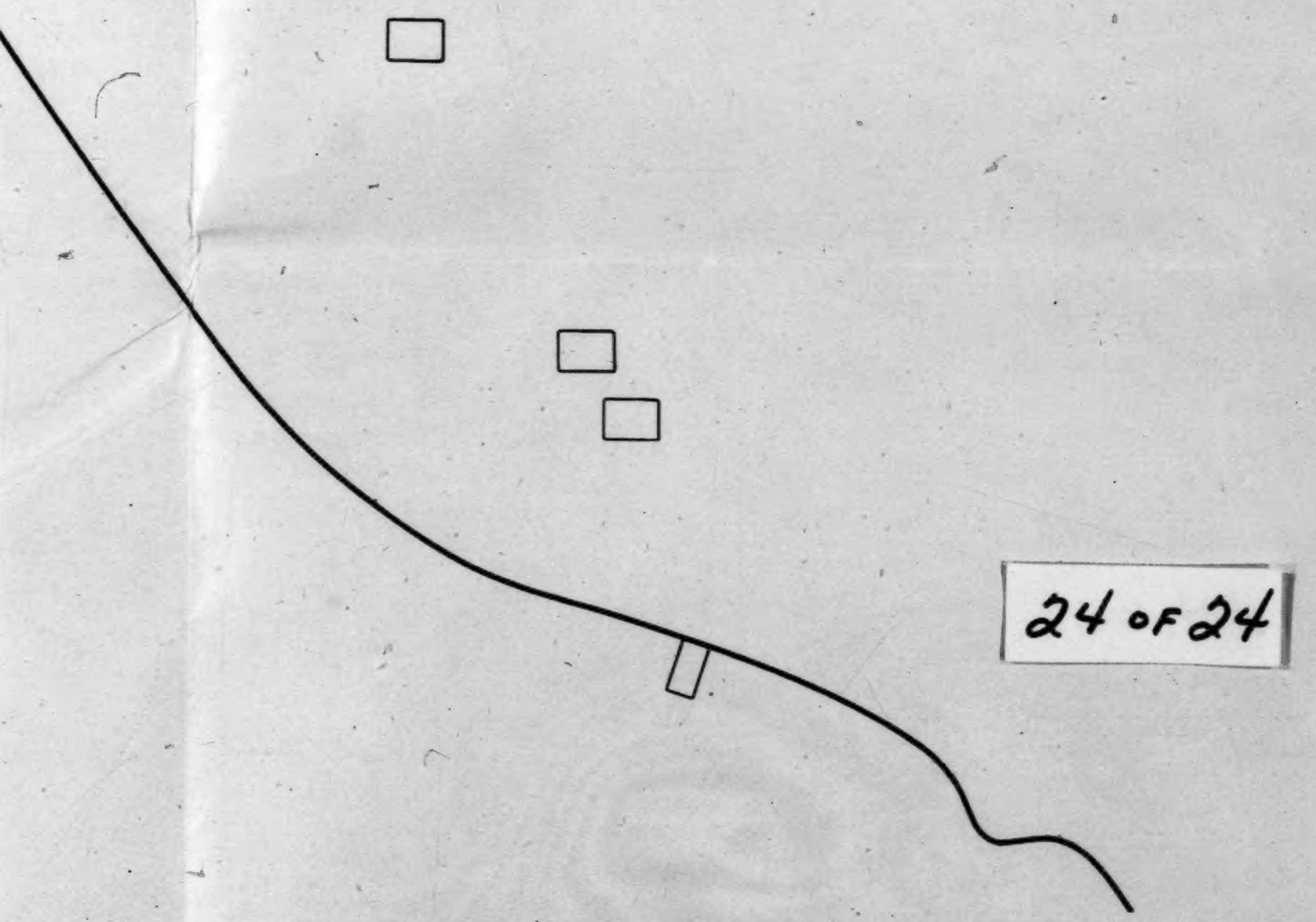

24 OF 24

MAP 2

BBX CLAIMS

NORTHWEST TERRITORIES

GEOLOGY AND STRUCTURE

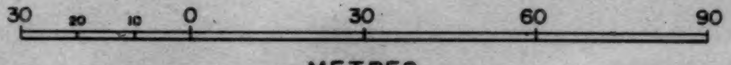
30
20
10
0
30
60
90
METRES

MACKENZIE M.D.
N.T.S. 75-L-12

D. BLACKADAR
1980

1 OF

KEY TO DIAMOND DRILL

DIAMOND DRILL HOLES

◉ 75-2 Great Plains Development (1975 and 1976)

● 7 Colby Mines (1972)

■ 12 Preston East Dome Mines (1957)

(~) Location Approximate

DRILL SECTIONS VERTICAL HOLES

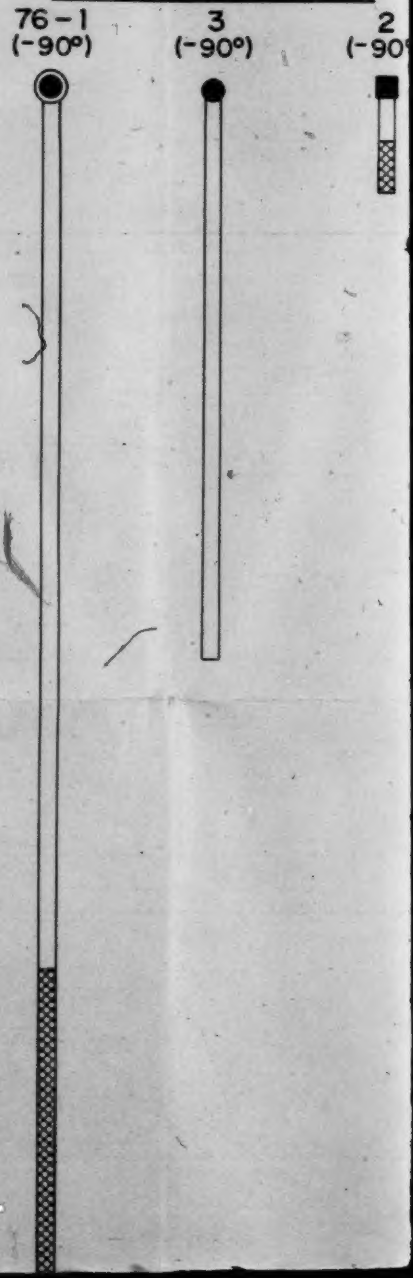

2 OF

OND DRILL HOLES

SECTIONS
AL HOLES

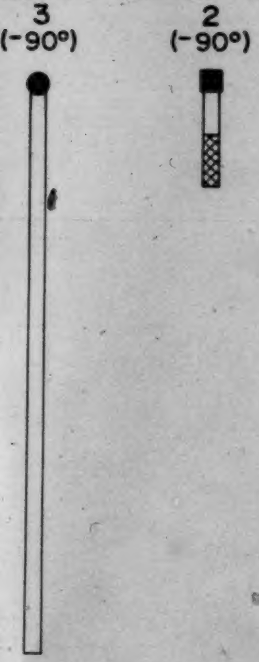

DRILL HOLE	INCLINATION AT COLLAR
76-1	-90°
75-1	-45°
75-2	-45°
75-3	-45°
75-4	-45°
75-5	-45°
75-6	-45°
75-7	-45°
72-2	-45°
72-3	-90°
72-4	-42°
72-5	-42°
72-6	-43°
72-7	-60°
57-1	-45°
57-2	-90°
57-3	-38°
57-4	-75°
57-5	-41.5°
57-6	-55°
57-7	-40°

3 OF

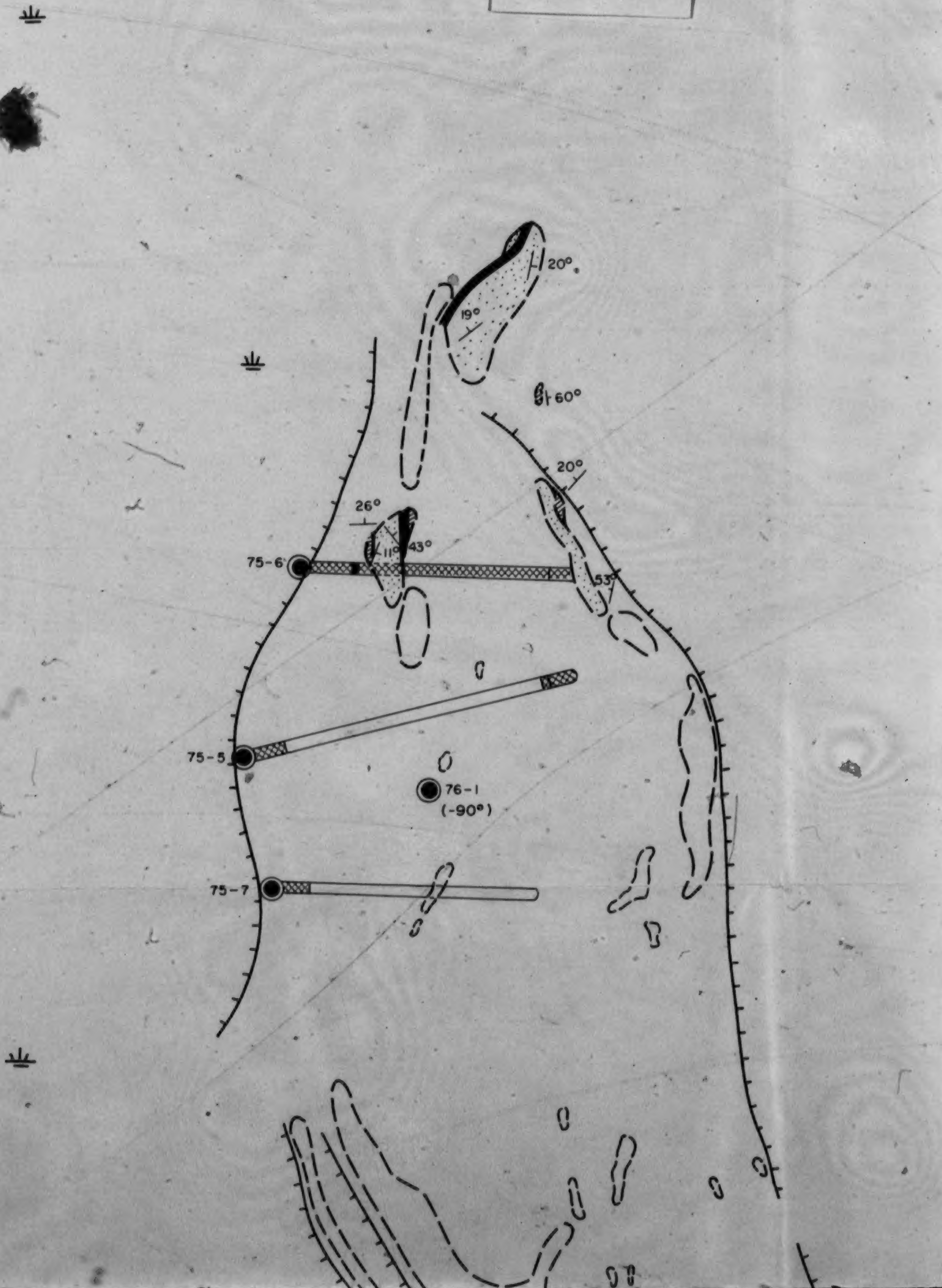
20°
19°
60°
20°
26°
11°
43°
75-6
53°
75-5
76-1
(-90°)
75-7

4 OF

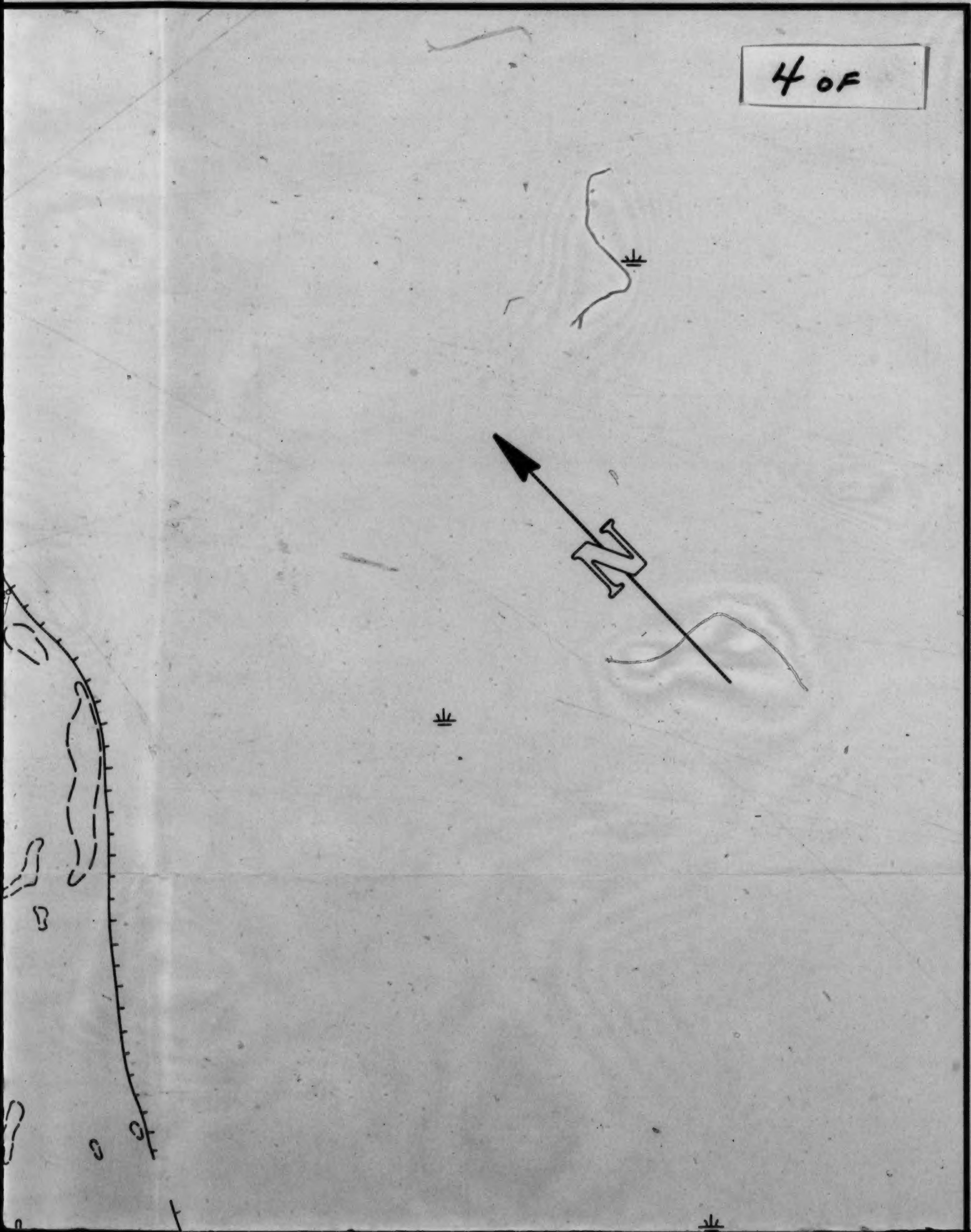

5 OF

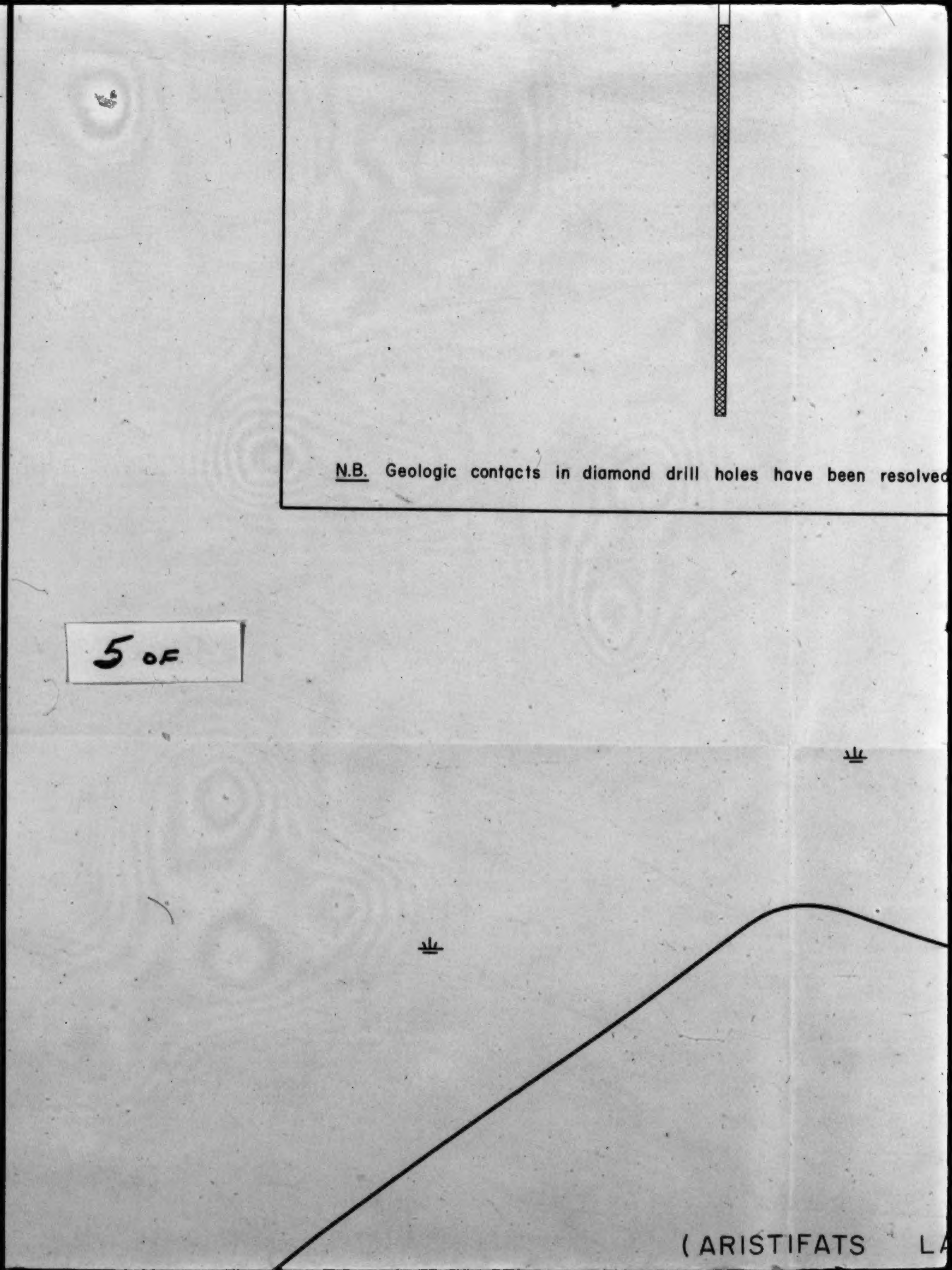

N.B. Geologic contacts in diamond drill holes have been resolved

(ARISTIFATS LA

6 OF

57-2	-90°
57-3	-38°
57-4	-75°
57-5	-41.5°
57-6	-55°
57-7	-40°
57-8	-45°
57-9	-40°
57-10	-40°
57-11	-45°
57-12	-45°
57-13	-45°

ave been resolved to horizontal before plotting on this map.

7 OF

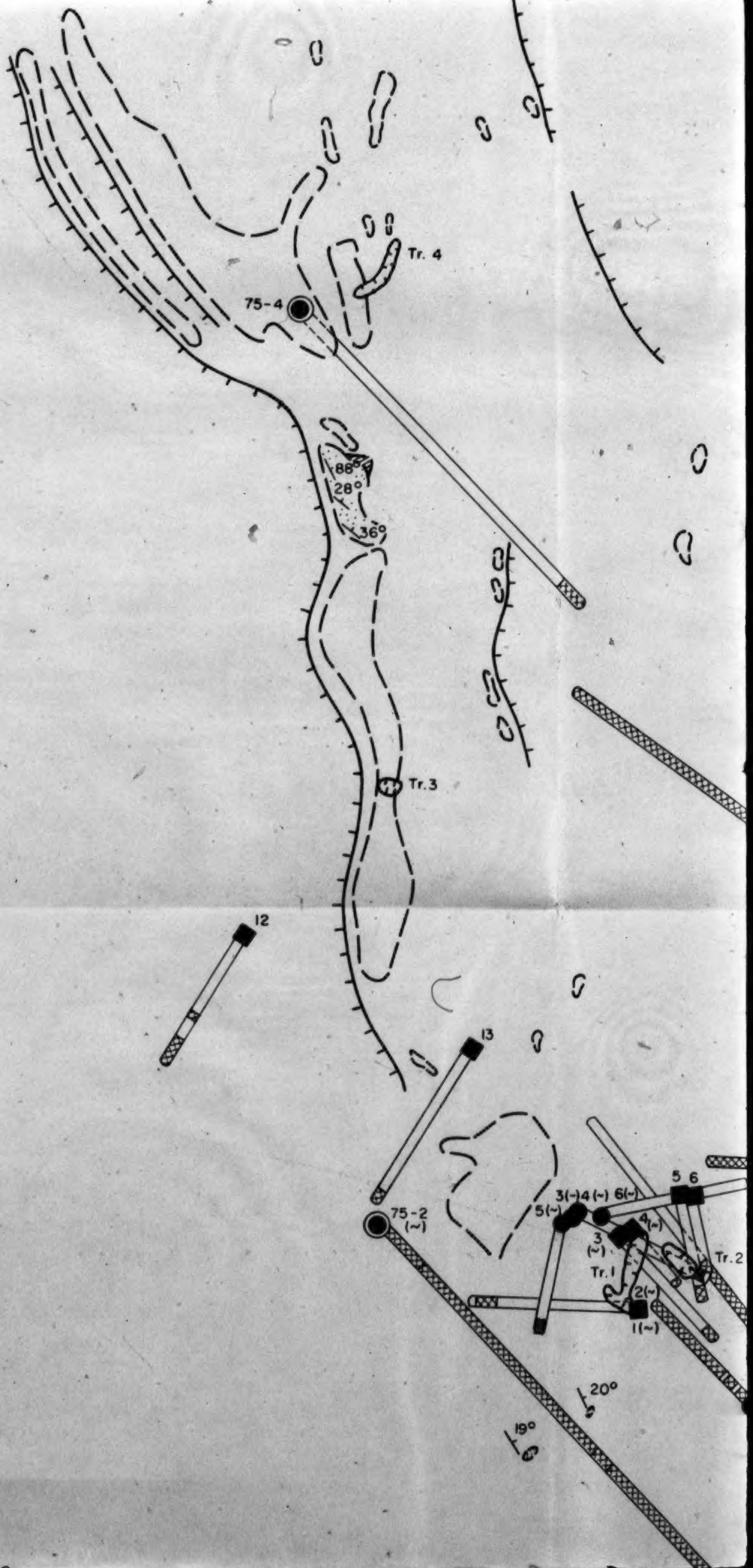
Tr. 4
75-4
88°
28°
36°
Tr. 3
12
13
75-2
(~)
3(~)4(~)
6(~)
5 6
5(~)
4(~)
3
(~)
Tr. 1
Tr. 2
2(~)
1(~)
20°
19°

8 OF

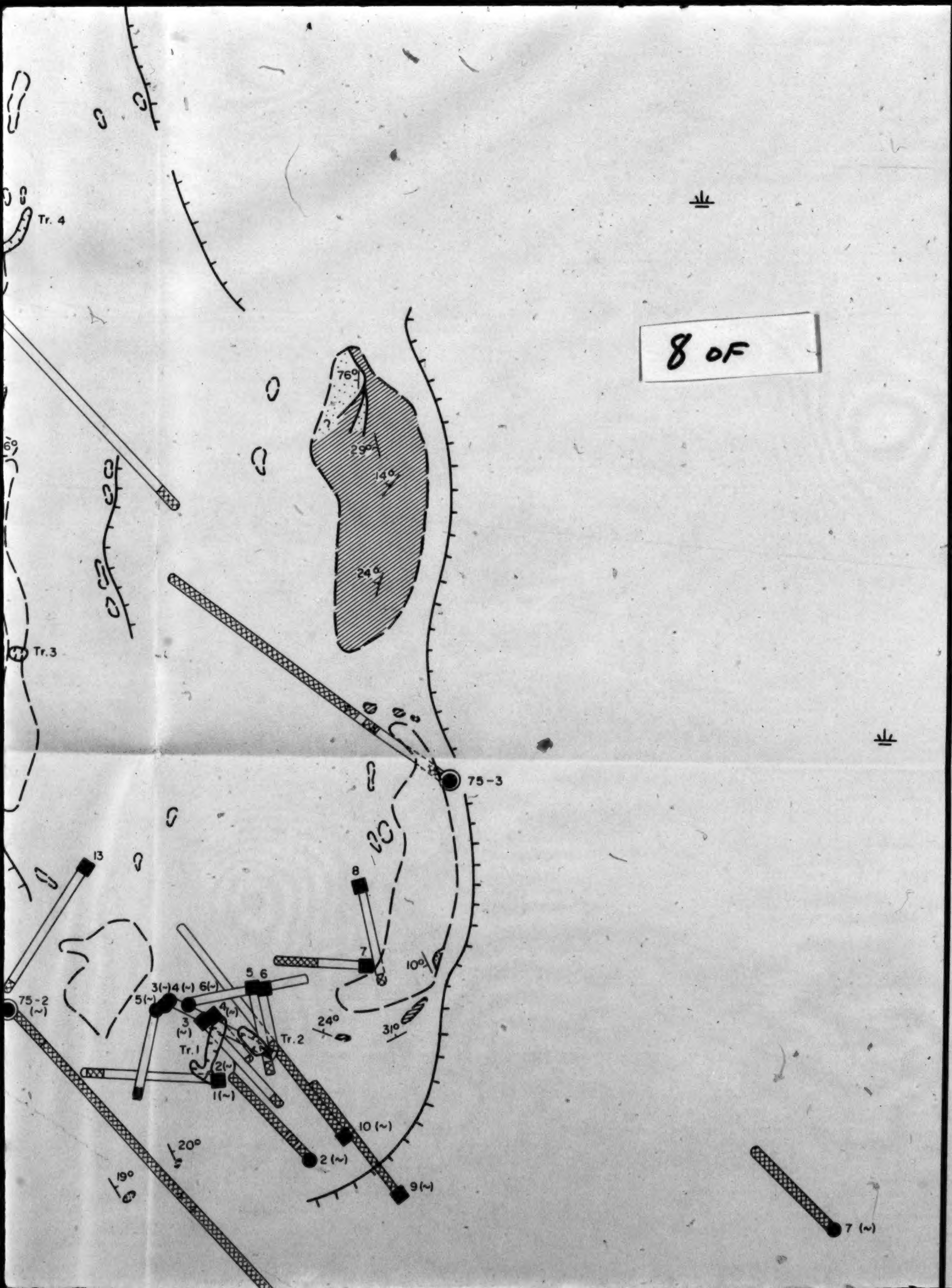
Tr. 4
6°
Tr. 3
76°
?
29°
14°
24°
75-3
13
8
7
10°
5
6
3(~)
4(~)
6(~)
5(~)
75-2
(~)
3
(~)
4(~)
Tr. 1
Tr. 2
2(~)
1(~)
24°
31°
10 (~)
2 (~)
9(~)
20°
19°
7 (~)

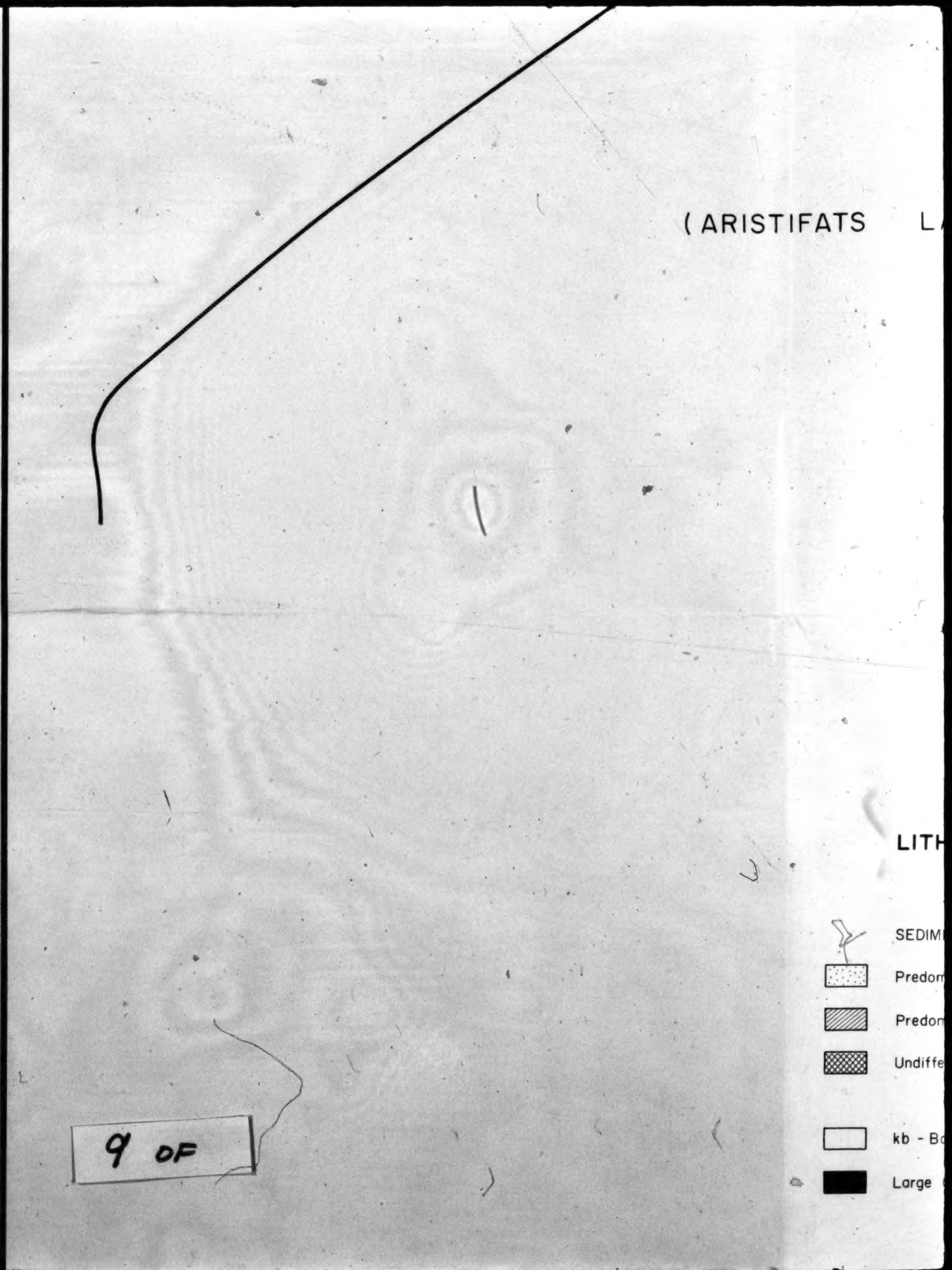

(ARISTIFATS L
LITH
SEDIM
Predom
Predom
Undiffe
kb - Bo
Large

9 OF

LITHOLOGIC UNITS

SEDIMENTARY ROCKS

░	Predominantly Red.
▨	Predominantly Grey
▩	Undifferentiated (in drill core)
☐	kb - Basalt Breccia Pipe (Diatreme)
■	Large Quartz Veins with mnr cp., pyr.

LEGEND

⬭	Outcrop Boundary.
/20°	Bedding, Strike and Dip.
⬯	Trench, to scale.
⏚	Muskeg
⟋	Prominent Break in Slope

10 OF

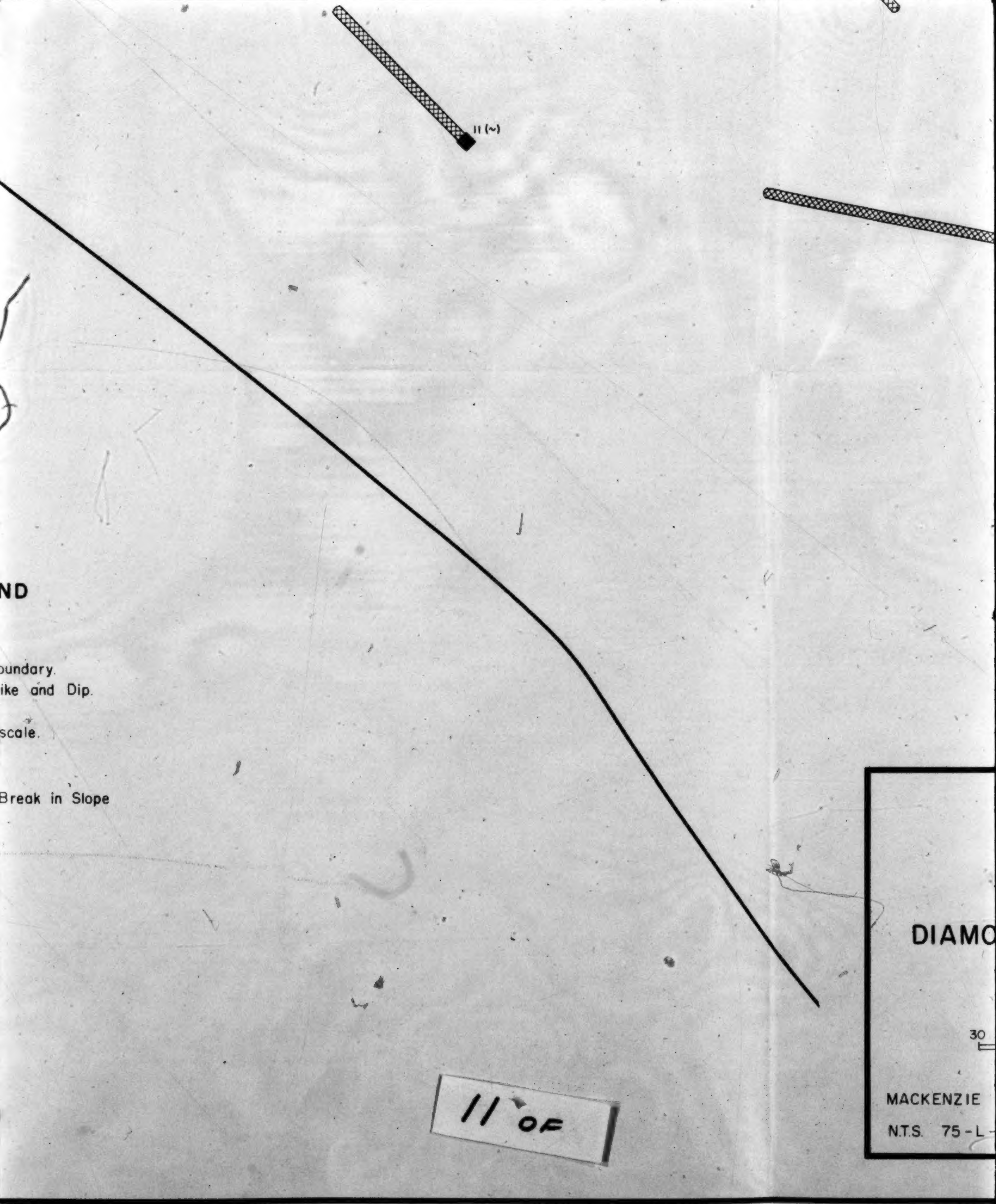
11 (~)
ND
oundary.
ike and Dip.
scale.
Break in Slope
DIAMO
30
MACKENZIE
N.T.S. 75-L-

11 OF

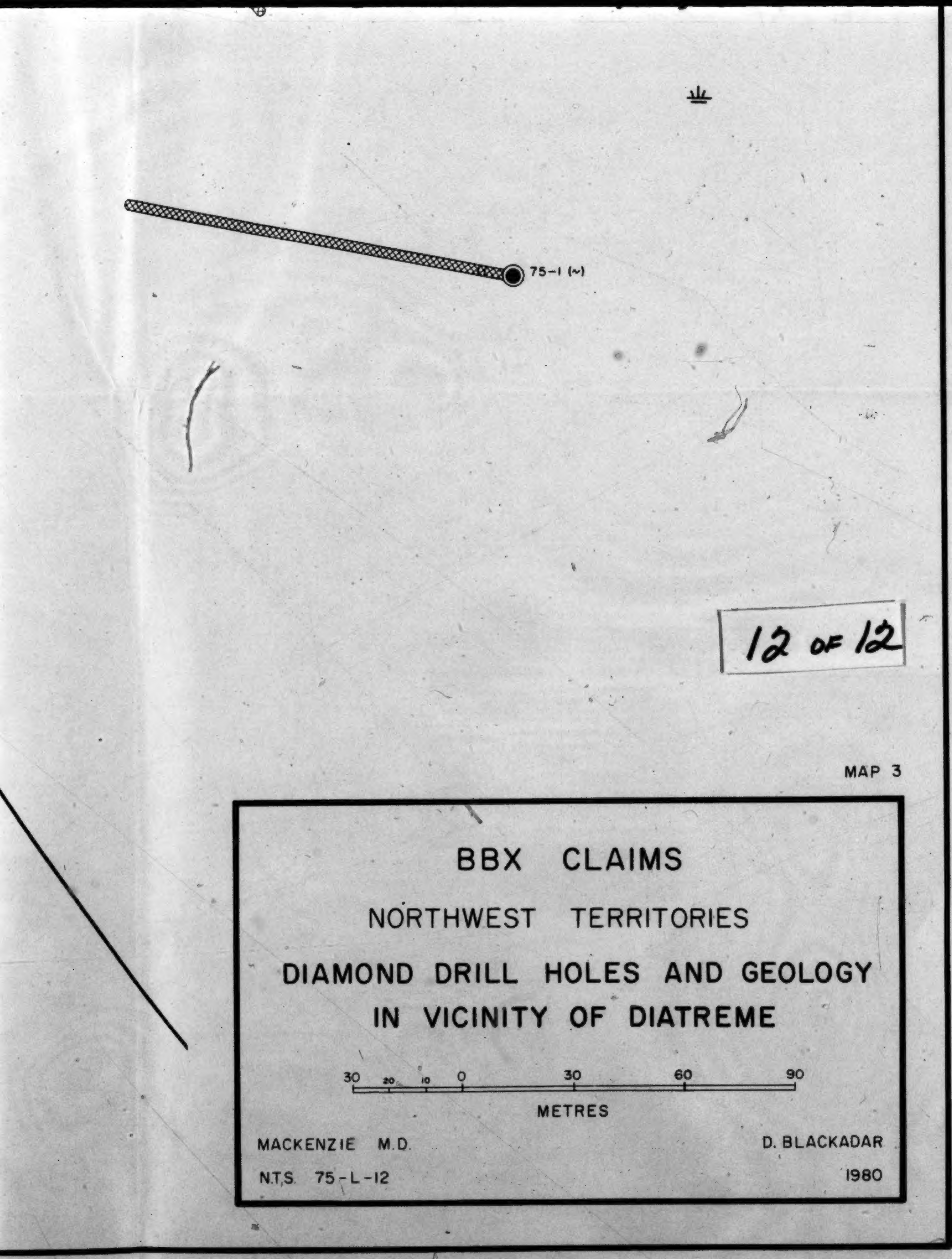
75-1 (~)

12 OF 12

MAP 3

BBX CLAIMS

NORTHWEST TERRITORIES

DIAMOND DRILL HOLES AND GEOLOGY IN VICINITY OF DIATREME

30
20
10
0
30
60
90
METRES

MACKENZIE M.D.
N.T.S. 75-L-12

D. BLACKADAR
1980